Volume 71A
Number 1
Jan.–Feb. 1967

Physics and Chemistry

U.S. DEPARTMENT OF COMMERCE

SECTION A

JOURNAL OF RESEARCH

NATIONAL BUREAU OF STANDARDS

Journal of Research

of the

National Bureau of Standards

A. Physics and Chemistry

Jan.–Feb. • 1967

VOLUME • 71A

NUMBER • 1

Editor: C. W. Beckett

Associate Editors: D. D. Wagman
J. M. Richardson

Publication dates:
Feb. 1, Apr. 1, June 1, Aug. 1, Oct. 1, Dec. 1, 1967

JOURNAL OF RESEARCH

The National Bureau of Standards Journal of Research reports research and development in the fields of activity shown at right. Also included from time to time are survey articles on topics closely related to the Bureau's scientific and technical program.

The Journal is published in three separate sections as follows:

A. Physics and Chemistry

Contains papers of interest primarily to scientists working in these fields. Issued six times a year. Annual subscription: domestic, $5.00; foreign, $6.00. Single copy, $1.00.

B. Mathematics and Mathematical Physics

Presents studies and compilations designed mainly for the mathematician and the theoretical physicist. Issued quarterly. Annual subscription: domestic, $2.25; foreign, $2.75. Single copy, 75c.

C. Engineering and Instrumentation

Reports research and development results of interest chiefly to the engineer and the applied scientist. Issued quarterly. Annual subscription: domestic, $2.75; foreign, $3.50. Single copy, 75c.

The National Bureau of Standards is a principal focal point in the Federal Government for assuring maximum application of the physical and engineering sciences to the advancement of technology in industry and commerce. Its responsibilities include development and maintenance of the national standards of measurement, and the provision of means for making measurements consistent with those standards; determination of physical constants and properties of materials; development of methods for testing materials, mechanisms, and structures, and making such tests as may be necessary, particularly for government agencies; cooperation in the establishment of standard practices for incorporation in codes and specifications; advisory service to government agencies on scientific and technical problems; invention and development of devices to serve special needs of the Government; assistance to industry, business and consumers in the development and acceptance of commercial standards and simplified trade practice recommendations; administration of programs in cooperation with United States business groups and standards organizations for the development of international standards of practice; and maintenance of a clearinghouse for the collection and dissemination of scientific, technical and engineering information. The scope of the Bureau's activities is suggested in the following listing of its three Institutes and their organizational units.

Institute for Basic Standards. Applied Mathematics. Electricity. Metrology. Mechanics. Heat. Atomic Physics. Physical Chemistry. Laboratory Astrophysics.* Radiation Physics. Radio Standards Laboratory.* Radio Standards Physics & Radio Standards Engineering. Office of Standard Reference Data.

Institute for Materials Research. Analytical Chemistry. Polymers. Metallurgy. Inorganic Materials. Reactor Radiations. Cryogenics.* Materials Evaluation Laboratory. Office of Standard Reference Materials.

Institute for Applied Technology. Building Research. Information Technology. Performance Test Development. Electronic Instrumentation. Textile and Apparel Technology Center. Technical Analysis. Office of Weights and Measures. Office of Engineering Standards. Office of Invention and Innovation. Office of Technical Resources. Clearinghouse for Federal Scientific and Technical Information.**

*Located at Boulder, Colo. 80302.
**Located at 5285 Port Royal Road, Springfield, Va. 22151.

U.S. DEPARTMENT OF COMMERCE
Alexander B. Trowbridge, Acting Secretary

NATIONAL BUREAU OF STANDARDS
A. V. Astin, Director

Order all publications from the Superintendent of Documents
U.S. Government Printing Office, Washington, D.C. 20402

Use of funds for printing this publication approved by the Director of the Bureau of the Budget (June 22, 1966).

Dedication of the New NBS Laboratories

On November 15, 1966, Secretary of Commerce John T. Connor dedicated the new ultra-modern facilities of the National Bureau of Standards at Gaithersburg, Md. This $120 million laboratory complex serves as the nerve center of the Nation's measurement and standardization activities. With three Institutes devoted to Basic Standards, Materials Research, and Applied Technology, the Bureau's new home has been designed to meet the needs of today and the challenges of the future in the physical sciences.

Dedication ceremonies were held in a courtyard between the Bureau's new library and one of the laboratory buildings. In the center of the courtyard is an apple tree descended from the tree under which Sir Isaac Newton was sitting when, according to the story, an apple fell on his head, leading him to conceive the law of universal gravitation.

Surrounding this tree was an audience of 2500, including distinguished guests from government, industry, and the world scientific community. The Reverend Edward G. Latch, Chaplain of the House of Representatives, gave the invocation and the benediction. Introduced by Dr. A. V. Astin, Director of the National Bureau of Standards, Secretary Connor said:

"It is no accident of history that the establishment of NBS in 1901 coincided with the beginning of America's transformation into the industrial giant of the twentieth century. . . . Today the demands made upon the Bureau and the nature of its program reflect the complexity of our atomic and space-age world."

The Secretary began his remarks with a message from President Johnson. The President noted that throughout its 65 years' existence the Bureau had advanced the frontiers of measurement in pace with the demands of science and industry; he extended his congratulations and best wishes for continuing achievement.

Secretary Connor stated that at age 65 the Bureau had significant accomplishments behind it and a future promising even greater contributions to the Nation. He noted that the new facilities are a symbol of the Bureau's future, but that the germ of future achievement lies in the members of the Bureau's staff.

In connection with the dedication, the Secretary sponsored a Symposium on Technology and World

Eleven stories high, the Administration Building at the National Bureau of Standards' new site near Gaithersburg, Md., towers above the other buildings in the laboratory complex. The building houses the Director and his staff as well as other NBS activities not requiring laboratory space.

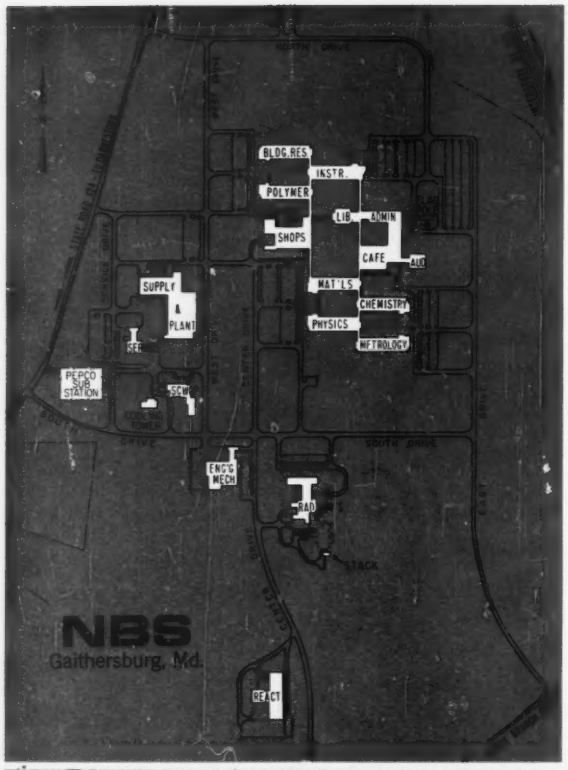

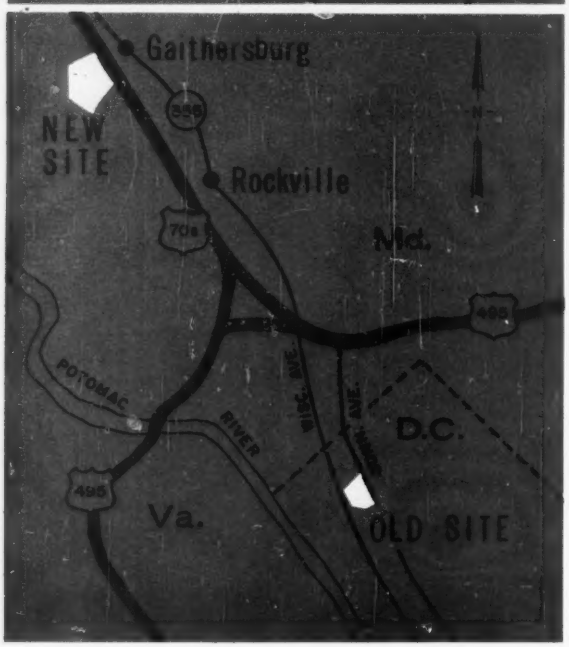

The new NBS site is 20 miles northwest of the old Washington site, at the Darnestown exit of Interstate Highway 70S. It borders and is west of 70S and Gaithersburg, Md. The plan view shows the layout of existing buildings.

Trade which was held at the Bureau during the two days following the dedication. It featured as speakers experts from industry, government, and education of many countries, attracting an attendance of nearly 500.

Following the dedication ceremonies, the invited guests were given a tour of the installation. On Saturday, November 19, the general public was invited to visit the new facilities and to view over 100 laboratories and demonstrations. In an eight-hour period over 20,000 people roamed the site. Some of the things they saw were a 100-ft linear accelerator which produces one of the world's most intense electron beams; a recently completed high-flux research reactor; a 12-million pound capacity hydraulic testing machine; the NBS Museum containing historical instruments, equipment, standards, and materials pertaining to the Bureau's activities during its 65-year history; a vault containing the national measurement standards—or parts symbolizing those standards; a demonstration of glass blowing techniques used to make highly unusual, and precise apparatus; and many of the Bureau's laboratories in the fields of metrology, electricity, mechanics, heat, atomic physics, radiation physics, analytical chemistry, physical chemistry, polymers, metallurgy, and building research.

By the close of 1966, transfer of the Bureau's Washington (D.C.) laboratories to the Gaithersburg site will be largely completed and most of the 2700 staff members will be relocated in 15 major buildings at the site. Of about 300 persons remaining at the Washington site, most will be relocated in new special-purpose laboratories now under construction at Gaithersburg. In addition, the Bureau will continue to maintain a staff of about 600 in Boulder, Colo., for work in radio standards and cryogenics, and a staff of about 300 at the Clearinghouse for Federal Scientific and Technical Information at Springfield, Va., as well as small groups of employees at widely scattered field stations.

Although the Bureau is located 20 miles northwest of its old site, the mailing address remains: National Bureau of Standards, Washington, D.C. 20234. The new telephone number is (Area Code 301) 921–1000. To reach the Bureau by car, use the Darnestown exit on Interstate Highway 70S.

JOURNAL OF RESEARCH of the National Bureau of Standards—A. Physics and Chemistry
Vol. 71A, No. 1, January–February 1967

Electric Fields Produced in Cubic Crystals by Point Defects

A. D. Franklin* and D. J. Sparks[1]

Theoretical Physics Division, U.K.A.E.A., Harwell, England

(October 8, 1966)

Charged point defects in crystals polarize the surrounding ions. These induced dipoles contribute to the electric field in the crystal. In this paper, lattice sums for the calculation of this contribution are given for the NaCl, CsCl, CaF_2, and ZnS structures. Various positions for the defect are chosen, and the field evaluated near lattice sites in the vicinity of the defect, with radial (with respect to the defect) displacements of ± 20 percent of the cation-anion distance allowed away from each lattice site. The lattice sums are expressed in power series, including terms up to cubic in the displacements, and the coefficients tabulated.

Key Words: Electric fields, ionic crystals, lattice sums, point defects, polarization, NaCl, CsCl, CaF_2, ZnS.

Electric Fields From Defects in Cubic Crystals

Impurities and other point defects in ionic crystals polarize the ions around them. The electric field produced at a neighboring ion is the sum of the field due to the charge on the defect plus the fields due to dipoles (electronic and displacement) induced upon all the other surrounding ions. In the dielectric continuum model of Mott and Littleton,[2] the induced dipole on the ith ion is

$$\mathbf{m}_i = (\Delta q)\frac{r_0^3 M_{\pm}\mathbf{r}_i}{r_i^3} \tag{1}$$

where $\mathbf{r}_i$ is the vector from the defect to ith ion, Δq is the difference between the charge on the defect and that normally associated with the site occupied by the defect, r_0^3 is the volume of crystal containing one molecule M_aX_b, and

$$M_{\pm} = \frac{\alpha_{\pm}}{a\alpha_+ + b\alpha_-}\frac{K-1}{4\pi K}$$

with $\alpha_{\pm}$ the polarizability of the $\begin{Bmatrix}\text{cation}\\ \text{anion}\end{Bmatrix}$ and K the static dielectric constant of the crystal.

If the vector from the ith to the jth ion be designated $\mathbf{r}_{ij}$, then the field at the jth ion due to the induced dipoles on all the other ions is

$$\mathbf{F}_j = \sum_{i\neq j}\left\{\frac{3(\mathbf{m}_i\cdot\mathbf{r}_{ij})\mathbf{r}_{ij}}{r_{ij}^5} - \frac{\mathbf{m}_i}{r_{ij}^3}\right\}. \tag{2}$$

If the defect is taken as the origin, and with $\mathbf{r}_j/|r_j| = \boldsymbol{\eta}_j$ and the vectors expressed as

$$\mathbf{r} = a(h\mathbf{x} + k\mathbf{y} + l\mathbf{z}) \tag{3}$$

where $\mathbf{x}$, $\mathbf{y}$, and $\mathbf{z}$ are the coordinate axes, eq (2) can be written as

$$\mathbf{F}_j\cdot\boldsymbol{\eta}_j = \frac{\Delta q r_0^3}{a^5}\{M_+S_{jC} + M_-S_{jA}\}. \tag{4}$$

The quantities S_{jC} and S_{jA} are lattice sums over the cation and anion sites respectively, and have the form

$$S_j = \sum_i \frac{2P_{ji}P_{jj} - 3P_{ii}P_{jj} - P_{ji}^2 + 2P_{ii}P_{ji}}{P_{jj}^{1/2}P_{ii}^{3/2}[P_{jj} - 2P_{ji} + P_{ii}]^{5/2}}$$

with

$$P_{jj} = h_j^2 + k_j^2 + l_j^2$$

$$P_{ji} = h_jh_i + k_jk_i + l_jl_i$$

$$P_{ii} = h_i^2 + k_i^2 + l_i^2.$$

The sum does not include the origin nor the evaluation point j, but does include in principle all other lattice sites. The evaluation point j need not be at a lattice site; by taking nonintegral values of h_j, k_j, and l_j, the sums appropriate to other positions may be found.

The lattice sums have been evaluated by computer for several cubic structures, with the defect occupying various lattice sites and with the evaluation of the field also at or near several different lattice sites. The evaluation point was allowed to move away from the lattice site a distance and direction specified in each case by a single parameter X. This parameter is so

*Work done while on temporary attachment from the National Bureau of Standards, Washington, D.C.

[1] Present address, Trinity College, Cambridge, England.

[2] N. F. Mott and M. J. Littleton, Trans. Far. Soc. **34**, 485 (1938).

defined that if **r** is the radius vector from the defect at the origin to the lattice site, $(1+AX)$ **r** is the radius vector of the evaluation point, with A chosen to make the displacement of the evaluation point from the lattice site approximately a/10 when $X=1$. The sums were evaluated near a given lattice site with X equal to -2, -1, 0, 1, and 2. From these five values for S_j, the coefficients in the interpolation formula

$$S_j = S_j^\circ + XS_j' + X^2S_j'' + X^3S_j''' \qquad (5)$$

were found by making the series agree exactly with the calculated sums at $X=-1$, 0, and 1, and fit approximately, by least squares, at $X=-2$ and 2. The values of S_j at $|X|=2$ are accurate to about 1 percent. Convergence in the calculated fields was assumed to have been achieved when the total contribution from a given set of ions, with the same numerical values of h, k, l, was less than the total from all ions included divided by 10^5.

TABLE 1a. *Sets of coefficients for use in eq* (5)

Set	S°	S'	S''	S'''
A	−5.8952	0.6078	0.2513	−0.01102
B	−1.2153	−.5796	−.0599	.00930
C	−2.3713	.2846	−.0107	−.00091
D	−0.3880	−.0538	.0012	.00011
E	−1.9650	−.1714	.0593	.00755
F	−2.2874	.5183	.0530	.00171
G	−1.3537	.1015	.0020	−.00066
H	−0.7302	−.0820	.0050	−.00019
I	−.2467	−.0305	.00006	.00016
J	−8.2036	1.2307	−.0110	−.01745
K	−0.4697	−0.1865	−.0336	−.00298
L	−7.1106	.0282	.1914	−.00173
M	−11.5685	2.3025	−.0697	−.03626
N	−0.0614	−0.3048	−.0935	−.00829
O	−2.3529	−.2252	.0605	.00766
P	−2.0496	.8115	−.1610	.02028
Q	−2.6663	−.1731	.0557	.00189
R	−0.9769	−.1125	.0050	.00003
S	−2.3570	.3536	−.0255	.00042
T	−0.5922	−.0733	−.0068	.00072
U	−5.8465	.8771	.0145	−.01787
V	0.1222	−.1132	−.0404	−.00370

TABLE 1b. *Electric fields in cubic crystals from dipoles induced by point defects, using eqs 4 and 5 and the coefficients in table 1a*

Structure	Distance denoted by "a" (eq 3)	Defect site	Evaluation point	Anions			Cations		
				Inside	Same Shell	Outside	Inside	Same Shell	Outside
NaCl	Cation-anion	Cation [anion at (0, 0, 1)]	$(1+0.1X)(\frac{1}{2}, \frac{1}{2}, \frac{1}{2})$			A			B
			$(1+0.08X)(0, 0, 1)$		C	D			E
			$(1+0.05X)(0, 1, 1)$	F		H		G	I
CsCl	Cation-cation	Cation [anion at $(\frac{1}{2}, \frac{1}{2}, \frac{1}{2})$]	$(1+0.1X)(\frac{1}{2}, \frac{1}{2}, \frac{1}{2})$		J	K			L
			$(1+0.08X)(0, 0, 1)$	M		N		C	O
			$(1+0.05X)(0, 1, 1)$	P		Q	F	G	R
CaF_2	Anion-anion	Cation [anion at $(\frac{1}{2}, \frac{1}{2}, \frac{1}{2})$]	$(1+0.1X)(\frac{1}{2}, \frac{1}{2}, \frac{1}{2})$		J	K			B
			$(1+0.8X)(0, 0, 1)$	M		N			E
			$(1+0.05X)(0, 1, 1)$	P		Q		G	I
		Empty cube center [Anion at $(\frac{1}{2}, \frac{1}{2}, \frac{1}{2})$]	$(1+0.1X)(\frac{1}{2}, \frac{1}{2}, \frac{1}{2})$		J	K			A
			$(1+0.08X)(0, 0, 1)$	M		N		C	D
			$(1+0.05X)(0, 1, 1)$	P		Q	F		H
		Anion [cation at $(\frac{1}{2}, \frac{1}{2}, \frac{1}{2})$]	$(1+0.1X)(\frac{1}{2}, \frac{1}{2}, \frac{1}{2})$			L		S	T
			$(1+0.08X)(0, 0, 1)$		C	O	M/2		N/2
			$(1+0.1X)(\frac{1}{2}, \frac{1}{2}, -\frac{1}{2})$			L		U	V
Zinc-blende	(Cation-cation)/$\sqrt{2}$	Anion [cation at $(\frac{1}{2}, \frac{1}{2}, \frac{1}{2})$]	$(1+0.1X)(\frac{1}{2}, \frac{1}{2}, \frac{1}{2})$			B		S	T
			$(1+0.08X)(0, 0, 1)$			E	M/2		N/2
			$(1+0.1X)(\frac{1}{2}, \frac{1}{2}, -\frac{1}{2})$			B		U	V
		Midpoint of unit cell edge [cation at $(\frac{1}{2}, \frac{1}{2}, \frac{1}{2})$ [anion at (1, 0, 0)]	$(1+0.1X)(\frac{1}{2}, \frac{1}{2}, \frac{1}{2})$			A		S	T
			$(1+0.08X)(0, 0, 1)$		C	D	M/2		N/2
			$(1+0.1X)(\frac{1}{2}, \frac{1}{2}, -\frac{1}{2})$			A		U	V

The results, in the form of the coefficients in the power series, are given in table 1. Each set of coefficients occurs several times, so for the sake of economy these sets are listed together in table 1a and given symbols. In table 1b, these symbols are used to indicate the set of coefficients appropriate to the situation described in the first four columns of the table.

With the defect at the origin, the ions in the crystal can be divided into three groups: those on the shell that includes the lattice site around which the evaluation is being performed ("same shell"), all those within this shell ("inside"), and all those outside of it ("outside"). In the last six columns, the contributions to S_j from anions and cations in these three groups are listed separately. Values for S° symbolized by D, E, T, and V have already been given by Mott and Littleton (see footnote 2).

(Paper 71A1–428)

JOURNAL OF RESEARCH of the National Bureau of Standards—A. Physics and Chemistry
Vol. 71A, No. 1, January–February 1967

Heat Capacity and Thermodynamic Properties of Beryllium 1:3-Aluminate, $BeO \cdot 3Al_2O_3$, from 15 to 390 °K

George T. Furukawa and William G. Saba

Institute for Basic Standards, National Bureau of Standards, Washington, D.C. 20234

(September 9, 1966)

The heat capacity of beryllium 1:3-aluminate, $BeO \cdot 3Al_2O_3$, was determined from 15 to 380 °K and the thermodynamic properties calculated from 0 to 390 °K. The entropy at 298.15 °K was found to be 175.55 J deg^{-1} mol^{-1} (41.96 cal deg^{-1} mol^{-1}).

Key Words: Beryllium 1:3-aluminate, enthalpy, entropy, Gibbs energy, heat capacity, low temperature calorimetry, thermodynamic properties.

1. Introduction

The results of the heat-capacity measurements on beryllium 1:3-aluminate,[2] $BeO \cdot 3Al_2O_3$, from 15 to 380 °K presented herein have been obtained as a part of the program at the National Bureau of Standards to provide accurate thermodynamic data on "light-element" compounds. Earlier measurements on the BeO—Al_2O_3 system that have been reported from this laboratory are aluminum oxide (corundum), Al_2O_3[3],[3] and beryllium 1:1-aluminate (chrysoberyl), $BeO \cdot Al_2O_3$ [6]. Measurements on beryllium oxide, BeO, of relatively small cyrstal size have recently been completed [4] and will be reported in a future paper.

2. Sample

Lang et al. [9], reported "practically all $BeO \cdot 3Al_2O_3$" and "all $BeO \cdot 3Al_2O_3$" for the results of petrographic and x-ray examinations, respectively, on a sample prepared by fusing a mixture of 1 to 3 molal ratio of BeO to Al_2O_3. Semi-Elements, Inc. prepared, on request, the sample accordingly for the heat-capacity measurements presented. The preparation procedure was as follows: stoichiometric amounts of dried BeO and Al_2O_3 powder were thoroughly mixed and fused in an arc furnace. To avoid contamination a fused mass was formed within a relatively large charge of the mixture so that the unfused mixture would serve as the container for the fused portion of the material. The fused material was cooled to room temperature in about three hours, freed of any unfused material, and crushed and sieved to collect particle sizes between 0.3 and 2 mm (10 and 50 mesh) on the edge.

Some of the particles in the sample that was received appeared gray, presumably from occlusion of traces of carbon from the graphite electrodes used in the arc fusion preparation. Qualitative spectrochemical analysis of the material by the Spectrochemical Analysis Section of the National Bureau of Standards showed the limits of impurities given in table 1.

TABLE 1. *Spectrochemical analysis of beryllium 1:3-aluminate* ($BeO \cdot 3Al_2O_3$) [a]

Element	Percentage limit	Element	Percentage limit
Ag	< 0.0001	Mg	0.001–0.01
B	0.001–0.01	Mn	0.0001–0.001
Ca	0.001–0.01	Na	0.01–0.1
Cu	< 0.0001	Si	0.01–0.1
Fe	0.01–0.1	Zr	0.001–0.01

[a] Analyzed by Elizabeth K. Hubbard, Spectrochemical Analysis Section.

A petrographic (microscopic) examination of the $BeO \cdot 3Al_2O_3$ sample was made in the Crystallography Section of the National Bureau of Standards. The crystal size was found to be on the average about 300 μ.

[1] This work was sponsored by the United States Air Force Office of Scientific Research, under Order No. OAR-ISSA-65-8.
[2] The numbers indicate base to acid anhydride ratio.
[3] Figures in brackets indicate references listed at the end of this paper.

Since the sample was ground for the microscopic examination, the crystal size of the original 10 to 50 mesh polycrystalline material on which the heat-capacity measurements were made is considered to be larger than 300 μ. The crystals were clear with some voids and growth defects resulting probably from too rapid cooling. There was some evidence of another phase being present, possibly up to about 5 percent. No BeO phase was detected.

X-ray diffraction examination of the $BeO \cdot 3Al_2O_3$ sample was also made in the Crystallography Section of the NBS. The pattern obtained is in agreement with published values for $BeO \cdot 3Al_2O_3$ [1, 2, 7] with some possible impurity lines close to $BeO \cdot Al_2O_3$ and α-Al_2O_3 but without presence of all strong lines of these substances. A few unidentified lines were also found. The patterns corresponding to graphite, BeO, and $3BeO \cdot Al_2O_3$ were absent.

Optical properties of $BeO \cdot Al_2O_3$ and $BeO \cdot 3Al_2O_3$ have been found to be very similar [2, 7, 9, 10]. It seems, therefore, that the impurity phase observed petrographically in the sample investigated is probably not $BeO \cdot Al_2O_3$. If the undetectable $BeO \cdot Al_2O_3$ is present, then the excess Al_2O_3 should be observed as α-Al_2O_3 or there is an unidentified compound of BeO and Al_2O_3 of ratio greater than 1 to 3. The x-ray pattern obtained does not definitively indicate the presence of α-Al_2O_3.

Distinctive x-ray diffraction patterns have been reported for $BeO \cdot Al_2O_3$ and $BeO \cdot 3Al_2O_3$ [1, 2, 7]. Lang et al. [9], observed an unidentified phase of high refractive index in mixtures that have been heated to melting temperatures, having compositions between $BeO \cdot Al_2O_3$ and Al_2O_3. These investigators also found another unidentified phase in x-ray diffraction patterns of fused mixtures of composition between $BeO \cdot Al_2O_3$ and BeO. The major *d*-spacings observed for the latter impurity phase cannot be identified with the *d* values reported for the more recently found $3BeO \cdot Al_2O_3$ phase [7]. Lang et al. [9], could not determine the presence of both of the unidentified phases in the same specimen or any similarity, if any, in the phases. They were not able to identify either phase in the same specimen by both petrographic and x-ray methods. These results seem to indicate that yet unidentified phases exist in the $BeO—Al_2O_3$ system or additional careful study of the known phases is needed.

Young [13] observed from x-ray measurements some disproportionation of $BeO \cdot 3Al_2O_3$ to $BeO \cdot Al_2O_3$ and Al_2O_3 after heating for two weeks at 1150 °C. This suggests that $BeO \cdot 3Al_2O_3$ is metastable in the range of the heat-capacity measurements obtained. Earlier, Foster and Royal [2] found $BeO \cdot 3Al_2O_3$ to have a stronger tendency toward crystal growth than $BeO \cdot Al_2O_3$ and found no evidence for $BeO \cdot 3Al_2O_3$ to disproportionate. The relatively rapid cooling during the preparation of the sample used in the measurements presented here has apparently preserved the material mostly, if not all, in the $BeO \cdot 3Al_2O_3$ phase.

Chemical analysis of the $BeO \cdot 3Al_2O_3$ sample was performed in the Analysis and Purification Section of the NBS. Two 0.5 g samples were dissolved in hydrochloric acid by heating the mixture sealed in tubes at 250 °C for 16 hr. The treatment of the resulting solution and the analysis for Be and Al were essentially the same as those described for $BeO \cdot Al_2O_3$ [6]. The results of the chemical analysis, summarized in table 2, show the beryllium and aluminum composition to have the theoretical stoichiometric ratio within the precision of the analytical method. The amount of graphite impurity was considered insignificant, and the sample was taken to be 100 percent $BeO \cdot 3Al_2O_3$ in the processing of the heat-capacity data obtained.

TABLE 2. *Chemical analysis of beryllium 1:3-aluminate* ($BeO \cdot 3Al_2O_3$)

Sample	Percentage by weight[a]		Mol ratio
	Al	Be	Al_2O_3/BeO
1	48.96	[b] 2.71	3.017
		[b] 2.74	2.984
2	48.93	2.72	3.004
Theoretical	48.92	2.72	

[a] Analysis by E. J. Maienthal, Analysis and Purification Section.
[b] Duplicate aliquots.

Although $BeO \cdot 3Al_2O_3$ is considered to be inert, the sample was handled and poured into the calorimeter vessel in a controlled-atmosphere box containing dry argon gas (dew-point of about −80 °C). The calorimeter vessel was provided with a screw-cap and gasket closure and a "pump out" tube with a valve previously described [5]. The vessel containing the sample was pumped to a high vacuum and purged with dry helium gas several times and finally sealed with 60.5 torr pressure of helium gas. The mass of sample investigated was 252.1429 g.

3. Apparatus and Method

The heat-capacity measurements on $BeO \cdot 3Al_2O_3$ were made in an adiabatic calorimeter similar in principle and design to that described previously [11]. The calorimeter, sample container, and the adjuvant instruments were the same, except for the bridge, as those used for the recently published measurements on $BeO \cdot Al_2O_3$ [6]. Description of methods and procedures used for the measurements of temperature, power, and time interval of heating, and the calibration information on the temperature scale and electrical instruments are given in the reference.

An automatic Mueller bridge, capable of resistance measurements up to almost 500 Ω to the nearest 0.00001 Ω, was used with the platinum-resistance thermometer for most of the temperature measurements. The performance of this automatic bridge was found comparable to the high-precision manually

operated Mueller bridge used exclusively in the measurements with $BeO \cdot Al_2O_3$ [6]. The bridge readings were automatically recorded on punch cards and subsequently processed on the high-speed digital computer to obtain the temperatures associated with each heating interval.

The 1961 atomic weights based on carbon 12 were used for converting the mass of sample investigated to gram formula weight basis [8]. The energy measurements were made in terms of the MKSA unit of energy, the joule. Wherever conversion to calorie was made, the following relation was used:

1 defined calorie = 4.1840 J.

4. Heat-Capacity Measurements and Results

Measurements totaling 147 heat-capacity "points" were obtained on the calorimeter vessel plus sample from about 15 to 390 °K and 87 points were obtained subsequently on the empty vessel in the same temperature range. Smoothed values of heat capacity at closely and regularly spaced integral temperatures were calculated for the two series of measurements using high-speed digital computer methods. The heat capacity of the sample was then obtained by differencing the smoothed values from the two series of measurements at the corresponding regular temperatures. The values of heat capacity for the $BeO \cdot 3Al_2O_3$ below 15 °K were obtained by extrapolating the smoothed experimental values at the lower temperatures in accordance with a T^3 relation.

Briefly, the procedures used in analyzing the experimental observations were as follows. Since the data could not be adequately represented over the complete temperature range in terms of a single heat-capacity equation, a number of polynomials of varying degrees of complexity were fitted by the method of least squares to the data over different temperature ranges. To avoid curvature corrections the analysis was formulated according to the relation:

$$Q_{T_2,T_1} = H(T_2) - H(T_1) = \int_{T_1}^{T_2} C(T)\,dT,$$

where Q_{T_2,T_1} is the input energy, T_1 and T_2 the corresponding initial and final temperatures, respectively, for each of the points, and $C(T)$ is the polynomial for which the coefficients were obtained by the least-squares method. Three or four polynomials were selected from the group on the basis of their fit over the complete temperature range of observations and for their agreement where the temperatures overlap. The polynomials were evaluated at closely spaced regular temperatures and joined at temperatures where the values of heat capacity and their first and second derivatives showed the best agreement. A numerical smoothing analysis was performed on these tabular values using the computer to test the smoothness of the joining process. Since the values were adequately smooth, they were changed insignificantly by the computer smoothing program.

The deviations of the observed values of heat capacity for the calorimeter-vessel-plus-sample and for the empty-vessel measurements from the final smoothed tabular values for the two series of measurements are plotted in figures 1 and 2, respectively. Except below about 50 °K, all of the observations are well within the ±0.1 percent limit of the net heat capacity of the $BeO \cdot 3Al_2O_3$ sample.

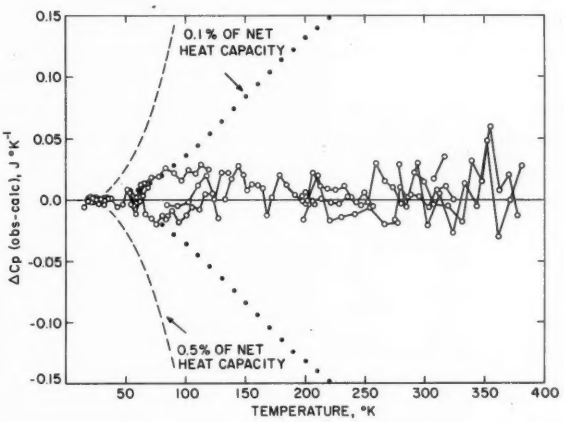

FIGURE 1. *Deviations of the heat-capacity measurements on calorimeter vessel plus beryllium 1:3-aluminate,* $BeO \cdot 3Al_2O_3$.

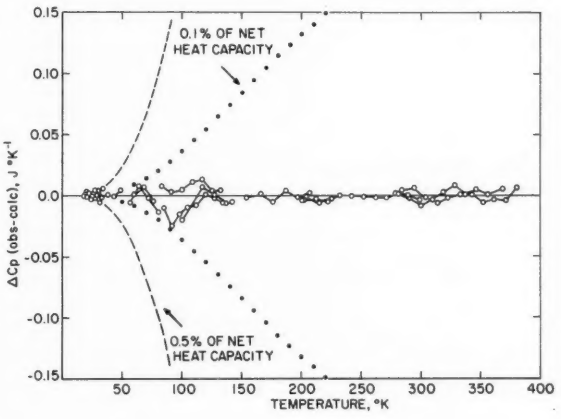

FIGURE 2. *Deviations of the heat-capacity measurements on the empty calorimeter vessel used with beryllium 1:3-aluminate,* $BeO \cdot 3Al_2O_3$.

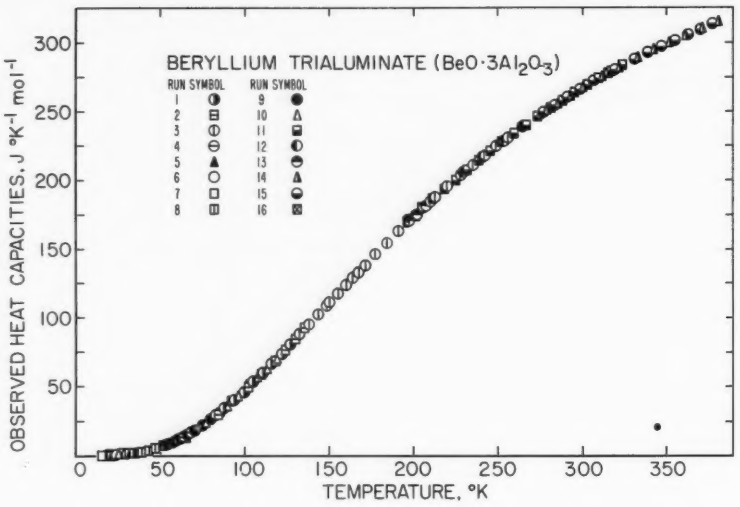

FIGURE 3. *Observed values of the molal heat capacity of beryllium 1:3-aluminate,* $BeO \cdot 3Al_2O_3$, *as a function of the temperature.*
(Numerical values are given in table 3.)

The "observed molal heat capacity" is shown in figure 3 and listed in table 3 in the chronological order of the measurements made. These values were obtained by subtracting the smoothed heat capacity of the empty vessel from that of the calorimeter vessel plus sample at the observed temperatures (mid-temperatures of the heating intervals). The heat-capacity values of the empty vessel at the corresponding observed temperatures were obtained by interpolation in the table of smoothed values described earlier. Corrections were made for the heat capacity of helium gas and for curvature wherever significant and the net heat capacity converted to the molal observed values.

The final smoothed values of heat capacity of $BeO \cdot 3Al_2O_3$ given in table 4 were obtained, however, by differencing at corresponding temperatures the smoothed values described earlier for the two series of measurements and correcting for the contribution of the helium exchange gas wherever significant. The smoothness of the resulting tabular values was checked on the computer and converted to molal values.

The smoothed values at the lower temperatures were plotted as C/T versus T^2 and extrapolated linearly to 0 °K to obtain values below 15 °K, the lower temperature limit of the experimental measurements. The slope of the line used was 4.025×10^{-5} J deg^{-4} mol^{-1}, which corresponds to an effective Debye characteristic temperature of 936 °K (assuming $C_v = C_p$).

5. Reliability of the Results

In addition to the imprecision of the measurements shown in figures 1 and 2, the purity of the sample, the accuracy of calibration of the instruments used, and the possible sources of systematic errors were examined to estimate the uncertainties in the final values of heat capacity of $BeO \cdot 3Al_2O_3$. The estimated uncertainty in the values given in table 4 between 80 and 390 °K is ±0.1 percent. Below about 80 °K, the uncertainty increased, because of the decrease in the contribution of the sample to the gross heat capacity. At 300 °K the heat capacity of the sample was 81 percent of the gross: at 80 °K, 46 percent: at 50 °K, 29 percent; 20 °K, 14 percent; and at 13 °K, only 10 percent. In addition, the sensitivity dR/dT of the platinum resistance thermometer began to decrease significantly below about 40 °K. Considering these factors, the estimated uncertainty is ±0.2 percent at 50 °K, ±1 percent at 20 °K, and ±3 percent at 13 °K.

6. Thermodynamic Functions and Discussion of the Results

The thermodynamic functions for $BeO \cdot 3Al_2O_3$ were derived, using their usual relations with respect to heat capacity, from the smoothed tabular values. The thermodynamic relations were evaluated on the com-

TABLE 3. *Observed heat capacity of beryllium 1:3-aluminate* ($BeO \cdot 3Al_2O_3$)

Gram molecular wt = 330.8952 g 1 cal = 4.1840 J T °K = 273.15 + t °C

T	C_P
RUN 1	
°K	J/deg-mol
82.8203	28.964
88.0822	34.227
93.6560	40.027
99.4640	46.435
105.1819	53.076
110.8937	59.946
116.2799	66.639
121.5671	73.341
126.9319	80.234
RUN 2	
83.4430	29.619
93.1378	39.520
102.3438	49.768
110.0670	58.972
117.2945	67.939
123.8566	76.279
129.9306	84.191
135.6114	91.641
RUN 3	
132.6454	87.716
138.1908	95.032
143.4155	101.938
148.3858	108.477
150.3864	111.090
155.0609	117.220
159.5568	123.071
163.8977	128.677
167.4038	133.143
171.4439	138.297
177.6536	146.111
184.5438	154.587
191.1511	162.544
197.5135	170.039
199.9364	172.860
206.0172	179.794
212.9353	187.490
220.6606	195.831
228.1316	203.644
235.3762	210.991
242.4181	217.892
249.2865	224.433
255.9950	230.597
RUN 4	
54.4277	8.188
57.6286	9.833
60.6838	11.611
64.0585	13.748
68.1789	16.598
RUN 5	
21.9906	0.446
25.3842	0.691
28.5606	1.002
32.1099	1.452
35.5483	2.025
RUN 6	
18.4505	0.250
21.0068	0.381

T	C_P
RUN 6—Con.	
°K	J/deg-mol
23.3504	0.532
26.8876	0.827
30.7964	1.270
RUN 7	
14.7135	0.107
19.0305	0.279
21.4966	0.414
24.9047	0.654
28.9755	1.047
RUN 8	
25.6653	0.718
29.7872	1.147
33.8800	1.737
38.4138	2.618
42.7876	3.715
46.9192	5.045
51.3870	6.817
56.0607	9.017
RUN 9	
53.0258	7.546
57.5249	9.794
61.8323	12.339
66.0923	15.097
70.4018	18.206
74.9699	21.849
79.9109	26.210
85.1544	31.264
RUN 10	
53.4833	7.764
58.9604	10.617
64.5559	14.102
70.6195	18.435
77.0761	23.717
83.3997	29.590
89.8264	36.063
96.1066	42.727
102.1024	49.512
107.8188	56.257
113.3406	63.011
119.0752	70.194
RUN 11	
196.3894	168.737
200.5662	173.578
206.1477	179.973
212.0283	186.512
218.3673	193.399
224.7804	200.188
231.5555	207.161
238.6756	214.253
245.6172	220.957
252.3915	227.307
259.3612	233.673
266.5257	239.939
273.6103	246.048
280.6552	251.690
287.9167	257.439

T	C_P
RUN 11—Con.	
°K	J/deg-mol
295.3757	263.122
302.7188	268.501
309.9404	273.633
317.0493	278.493
324.0556	283.101
RUN 12	
199.6885	172.558
209.5623	183.776
220.4510	195.579
230.4099	205.954
241.5414	217.011
253.8218	228.599
265.6168	239.092
277.0019	248.759
RUN 13	
198.0565	170.655
201.9686	175.189
207.2721	181.202
RUN 14	
275.0636	247.116
278.9339	250.319
285.8983	255.860
293.6534	261.865
301.7499	267.778
311.7800	274.892
322.8485	282.271
333.3522	288.997
343.2091	294.909
352.1076	300.070
361.4226	305.043
371.2744	310.239
380.9849	315.212
RUN 15	
277.8938	249.497
284.1183	254.451
290.9840	259.825
298.9705	265.799
307.2420	271.725
319.3254	279.963
331.2745	287.670
339.1056	292.530
346.9111	297.086
354.6113	301.477
362.3108	305.570
369.8374	309.529
377.2870	313.293
RUN 16	
307.6850	272.065
315.9765	277.803

TABLE 4. *Thermodynamic functions for beryllium 1:3-aluminate* ($BeO \cdot 3Al_2O_3$) *solid phase.*

Gram molecular wt = 330.8952g 1 cal = 4.1840 J
T °K = 273.15 + t °C

T	C_p^o	$(H_T^o - H_0^c)$	$(H_T^o - H_0^c)/T$	$(S_T - S_0^c)$	$-(G_T^o - H_0^c)$	$-(G_T^o - H_0^c)/T$
°K	J/deg-mol	J/mol	J/deg-mol	J/deg-mol	J/mol	J/deg-mol
0.00	0.000	0.000	0.000	0.000	0.000	0.000
5.00	0.005	0.006	0.001	0.002	0.002	0.000
10.00	0.040	0.101	0.010	0.013	0.034	0.003
15.00	0.135	0.509	0.034	0.045	0.170	0.011
20.00	0.326	1.611	0.081	0.107	0.536	0.027
25.00	0.656	4.002	0.160	0.213	1.316	0.053
30.00	1.167	8.470	0.282	0.374	2.757	0.092
35.00	1.919	16.072	0.459	0.607	5.177	0.148
40.00	2.973	28.165	0.704	0.928	8.975	0.224
45.00	4.387	46.405	1.031	1.357	14.639	0.325
50.00	6.208	72.717	1.454	1.909	22.748	0.455
55.00	8.468	109.22	1.986	2.603	33.968	0.618
60.00	11.196	158.18	2.636	3.454	49.043	0.817
65.00	14.358	221.91	3.414	4.472	68.786	1.058
70.00	17.910	302.41	4.320	5.664	94.053	1.344
75.00	21.885	401.72	5.356	7.032	125.72	1.676
80.00	26.294	521.98	6.525	8.583	164.68	2.059
85.00	31.114	665.35	7.828	10.320	211.86	2.492
90.00	36.197	833.56	9.262	12.242	268.19	2.980
95.00	41.483	1027.7	10.817	14.339	334.57	3.522
100.00	47.050	1248.9	12.489	16.607	411.87	4.119
105.00	52.858	1498.5	14.272	19.043	500.92	4.771
110.00	58.859	1777.8	16.161	21.639	602.56	5.478
115.00	65.021	2087.4	18.151	24.391	717.57	6.240
120.00	71.326	2428.2	20.235	27.291	846.72	7.056
125.00	77.740	2800.8	22.407	30.332	990.72	7.926
130.00	84.236	3205.8	24.660	33.508	1150.3	8.848
135.00	90.790	3643.3	26.987	36.810	1326.0	9.822
140.00	97.375	4113.7	29.384	40.230	1518.6	10.847
145.00	103.97	4617.1	31.842	43.763	1728.5	11.921
150.00	110.55	5153.4	34.356	47.398	1956.4	13.042
155.00	117.11	5722.5	36.920	51.130	2202.6	14.211
160.00	123.62	6324.4	39.527	54.951	2467.8	15.424
165.00	130.07	6958.6	42.173	58.854	2752.3	16.681
170.00	136.46	7625.0	44.853	62.832	3056.5	17.979
175.00	142.77	8323.1	47.560	66.879	3380.7	19.318
180.00	148.99	9052.5	50.292	70.988	3725.4	20.696
185.00	155.13	9812.9	53.042	75.154	4090.7	22.112
190.00	161.16	10604.	55.808	79.372	4477.0	23.563
195.00	167.10	11424.	58.586	83.635	4884.5	25.049
200.00	172.93	12274.	61.372	87.939	5313.4	26.567
205.00	178.65	13153.	64.163	92.280	5763.9	28.117
210.00	184.26	14061.	66.956	96.652	6236.3	29.696
215.00	189.75	14996.	69.748	101.05	6730.5	31.305
220.00	195.14	15958.	72.536	105.48	7246.8	32.940
225.00	200.41	16947.	75.320	109.92	7785.3	34.601
230.00	205.57	17962.	78.095	114.38	8346.1	36.287
235.00	210.62	19002.	80.862	118.86	8929.2	37.996
240.00	215.56	20068.	83.616	123.34	9534.7	39.728
245.00	220.38	21158.	86.359	127.84	10163.	41.480
250.00	225.10	22272.	89.086	132.34	10813.	43.252
255.00	229.71	23409.	91.799	136.84	11486.	45.043
260.00	234.21	24568.	94.494	141.35	12181.	46.852
265.00	238.61	25751.	97.172	145.85	12899.	48.677
270.00	242.90	26954.	99.831	150.35	13640.	50.518
273.15	245.55	27724.	101.50	153.18	14118.	51.686
275.00	247.09	28179.	102.47	154.84	14403.	52.374
280.00	251.17	29425.	105.09	159.33	15188.	54.244
285.00	255.16	30691.	107.69	163.81	15996.	56.127
290.00	259.05	31977.	110.26	168.29	16827.	58.023
295.00	262.84	33281.	112.82	172.75	17679.	59.929
298.15	265.19	34113.	114.42	175.55	18228.	61.136
300.00	266.54	34605.	115.35	177.20	18554.	61.847
305.00	270.15	35947.	117.86	181.63	19451.	63.774
310.00	273.67	37306.	120.34	186.05	20370.	65.711
315.00	277.11	38683.	122.80	190.46	21312.	67.656

TABLE 4. *Thermodynamic functions for beryllium 1:3-aluminate ($BeO \cdot 3Al_2O_3$) solid phase.*

Gram Molecular wt = 330.8952 g 1 cal = 4.1840 J
T °K = 273.15 + t °C

T	C_p°	$(H_T^\circ - H_0^\circ)$	$(H_T^\circ - H_0^\circ)/T$	$(S_T - S_0^\circ)$	$-(G_T^\circ - H_0^\circ)$	$-(G_T^\circ - H_0^\circ)/T$
°K	J/deg-mol	J/mol	J/deg-mol	J/deg-mol	J/mol	J/deg-mol
320.00	280.46	40077.	125.24	194.85	22275.	69.609
325.00	283.72	41488.	127.65	199.22	23260.	71.569
330.00	286.90	42914.	130.04	203.58	24267.	73.537
335.00	290.00	44356.	132.41	207.92	25296.	75.510
340.00	293.02	45814.	134.75	212.24	26346.	77.489
345.00	295.96	47287.	137.06	216.54	27418.	79.473
350.00	298.82	48774.	139.35	220.81	28512.	81.461
355.00	301.60	50275.	141.62	225.07	29626.	83.454
360.00	304.32	51789.	143.86	229.31	30762.	85.451
365.00	306.98	53318.	146.08	233.53	31919.	87.450
370.00	309.59	54859.	148.27	237.72	33097.	89.452
373.15	311.21	55837.	149.64	240.35	33850.	90.715
375.00	312.15	56413.	150.44	241.89	34296.	91.457
380.00	314.68	57981.	152.58	246.04	35516.	93.464
385.00	317.19	59560.	154.70	250.17	36757.	95.472
390.00	319.69	61152.	156.80	254.28	38018.	97.482

H_0° and S_0° apply to the reference state of the solid at zero °K.

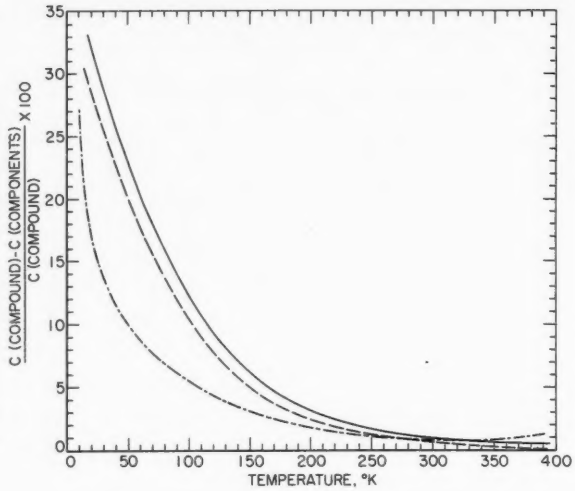

FIGURE 4. *Comparison of the additivity of heat capacities:*
——$BeO \cdot 3Al_2O_3$ *versus* $BeO + 3Al_2O_3$
– – – $BeO \cdot 3Al_2O_3$ *versus* $BeO \cdot Al_2O_3 + 2Al_2O_3$
—— – —— $BeO \cdot Al_2O_3$ *versus* $BeO + Al_2O_3$

puter by numerical integration procedures with four-point Lagrangian integration coefficients [12]. The thermodynamic functions are given in table 4 from 0 to 390 °K.

Although x-ray diffraction measurements on $BeO \cdot 3Al_2O_3$ have been reported [1, 2, 7], no information on the crystal structure of the material has been found. The room temperature density (3.73 g cm^{-3} [2]) of $BeO \cdot 3Al_2O_3$ indicates that the crystal is more loosely bound on the average than the parent oxides, BeO and Al_2O_3. The molal volume, $V(BeO \cdot 3Al_2O_3)$, of $BeO \cdot 3Al_2O_3$ is larger (4.03%) than the sum of the molal volumes, $V(BeO) + 3V(Al_2O_3)$, of BeO and Al_2O_3, respectively. The molal volume of $BeO \cdot 3Al_2O_3$ is also larger (3.56%) than the sum of the molal volumes, $V(BeO \cdot Al_2O_3) + 2V(Al_2O_3)$, of $BeO \cdot Al_2O_3$ and Al_2O_3, respectively. The molal volume of $BeO \cdot Al_2O_3$ is likewise larger (1.21%) than the volume of equimolal mixture of BeO and Al_2O_3.

A comparison (fig. 4) of the heat capacity of $BeO \cdot 3Al_2O_3$ with those of the corresponding molar mixtures of BeO and Al_2O_3 and of $BeO \cdot Al_2O_3$ and Al_2O_3 shows a positive deviation throughout the temperature range (15 to 390 °K), with the deviations increasing with decrease in temperature. A similar positive deviation from "additivity" of the heat capacity was found with $BeO \cdot Al_2O_3$ [6] (fig. 4) and with many mixed metal oxides reported in the literature. Also, with the exception of a few, where the density data may possibly be in error, a positive deviation from the additivity of the molal volumes was found at room temperature for the same mixed metal oxides. For substances at temperatures below the classical heat capacity limit, this correspondence is reasonable since a more open structure yields a "softer" force constant and hence, a lower Debye characteristic temperature. Further comparison of heat capacity and volume over a wide range of temperature is in progress, but unfortunately relatively few thermal expansion data seem to be available for the range below room temperature.

The authors are indebted to a number of staff members at the National Bureau of Standards for their contribution toward the characterization of the $BeO \cdot 3Al_2O_3$ sample investigated. Grateful acknowledgement is made to E. K. Hubbard for the spectrochemical analysis, to A. Van Valkenburg for the petrographic examinations, to H. E. Swanson for the x-ray analysis, and to E. J. Maienthal for the chemical analysis.

7. References

[1] P. P. Budnikov, V. G. Avetikov, E. I. Dudavsky, and A. A. Zvyagilsky, Doklady Akad. Nauk SSSR **68,** 313 (1949).
[2] W. R. Foster and H. F. Royal, J. Am. Ceram. Soc. **32,** 26 (1949).
[3] G. T. Furukawa, T. B. Douglas, R. E. McCoskey, and D. C. Ginnings, J. Res. NBS **57,** 67 (1956) RP2694.
[4] G. T. Furukawa and M. L. Reilly, unpublished measurements.
[5] G. T. Furukawa, M. L. Reilly, and J. H. Piccirelli, J. Res. NBS **68A** (Phys. and Chem.) No. 4, 381 (1964).
[6] G. T. Furukawa and W. G. Saba, J. Res. NBS **69A** (Phys. and Chem.) No. 1, 13 (1965).
[7] F. Ya. Galakov, Izvest. Akad. Nauk SSSR, Otdel. Khim. Nauk, No. 9, 1035 (1957); Bull. Acad. Sci. USSR, Div. Chem. Sci. No. 9, 1062 (1957).
[8] A. E. Cameron and E. Wichers, J. Am. Chem. Soc. **84,** 4192 (1962).
[9] S. M. Lang, C. L. Fillmore, and L. H. Maxwell, J. Res. NBS **48,** 298 (1952) RP2316.
[10] C. Palache, H. Berman, and C. Frondel, The System of Mineralogy, Vol. 1, p. 718 (J. Wiley & Sons, Inc., New York, N.Y., 1944).
[11] R. B. Scott, C. H. Meyers, R. D. Rands, Jr., F. G. Brickwedde, and N. Bekkedahl, J. Res. NBS **35,** 39 (1945) RP1661.
[12] Tables of Lagrangian Interpolation Coefficients (Columbia University Press, New York, N.Y., 1944).
[13] W. A. Young, J. Phys. Chem. **64,** 1003 (1960).

(Paper 71A1–429)

JOURNAL OF RESEARCH of the National Bureau of Standards—A. Physics and Chemistry
Vol. 71A, No. 1, January–February 1967

Dissociation Constant of *m*-Nitrophenol in 50 Wt Percent Methanol-Water Solvent from 25 to 40 °C and Related Medium Effects

Barry J. Steel,[1] R. A. Robinson, and Roger G. Bates

Institute for Materials Research, National Bureau of Standards, Washington, D. C. 20234

(August 15, 1966)

The dissociation constant of *m*-nitrophenol in 50 wt percent methanol-water as solvent has been determined at 25, 30, 35, and 40 °C. A spectrophotometric method was used, together with acidity functions for buffer solutions in 50 percent methanol derived from previous emf measurements. Values of the enthalpy and entropy changes on dissociation of the phenol have been calculated. A comparison with corresponding values for the dissociation of *m*-nitrophenol in aqueous solution affords a measure of the medium effect. The medium effect for *m*-nitrophenol lies intermediate between that for *o*-nitrophenol and that for *p*-nitrophenol.

Key Words: Dissociation, electrolytes, methanol, *m*-nitrophenol, nonaqueous solvents, phenols, thermodynamics.

1. Introduction

The acidic dissociation of ammonium ion is an acid-base process (protolysis) of charge type A^+B°. Ammonium ion dissociates to give an uncharged product, NH_3:

$$NH_4^+ \rightleftharpoons H^+ + NH_3.$$

The dissociation constant for an A^+B° process (expressed as pK) is invariably reduced if, instead of water as solvent, 50 wt percent methanol is used. This is true for the ammonium ion [1][2] and the protonated forms of tris(hydroxymethyl)aminomethane [2], 4-aminopyridine [3], aniline, and methyl- and dimethylaniline [4]. The contrary behavior is found for dissociation processes of charge type $A^\circ B^-$ such as acetic acid,

$$HAc \rightleftharpoons H^+ + Ac^-$$

whose pK values are higher in 50 percent methanol than in water. This has been shown to be true for acetic acid itself [5] and for a number of other acids [4] of the same charge type. Data are now presented for an acid of the phenolic type, *m*-nitrophenol, and it is shown that its pK values follow the same pattern.

[1] On leave from the University of Adelaide, South Australia.

[2] Figures in brackets indicate the literature references at the end of this paper.

2. Method

The principle of the spectrophotometric method used in this work is as follows. Consider three solutions of *m*-nitrophenol, all of the same stoichiometric concentration. Let acid be added to the first solution to convert the phenol entirely into its molecular form, HN. Let alkali be added to the second solution to convert the phenol entirely into its dissociated form, N^-. Let the third solution contain a buffer mixture. The optical densities of the three solutions, each at the same wavelength, are D_1, D_2, and D, respectively. Then $\alpha = (D - D_1)/(D_2 - D_1)$ is the proportion of phenol present in the anionic form, N^-, and the dissociation constant of the phenol is given by:

$$pK = -\log a_{H^+} - \log (D - D_1)/(D_2 - D) - \log \gamma_{N^-}/\gamma_{HN}. \quad (1)$$

This can be written as:

$$pK = p(a_H\gamma_{Cl}) - \log (D - D_1)/(D_2 - D) - \log \gamma_{N^-}/(\gamma_{HN}\gamma_{Cl^-}) \quad (2)$$

where the acidity function $p(a_H\gamma_{Cl})$ designates the quantity $-\log (m_{H^+}\gamma_{H^+}\gamma_{Cl^-})$.

It is advantageous to use a buffer solution whose $p(a_H\gamma_{Cl})$ value is approximately equal to the pK value of the phenol; α is then about 0.5 and the ratio $(D - D_1)/$

D_2-D) can be measured with maximum accuracy. Buffer solutions which are equimolal in tris(hydroxymethyl)aminomethane and its hydrochloride in 50 percent methanol have values of $p(a_H\gamma_{Cl})$ about 8 [6]. *m*-Nitrophenol, however, has a *pK* value nearly 9 in this solvent medium. Some measurements were made (table 1) of the *pK* value of *m*-nitrophenol at 25 °C using this equimolal buffer solution, but it was thought desirable to use solutions with a higher value of the buffer ratio m_2/m_1, where m_2 is the molality of tris(hydroxymethyl)aminomethane and m_1 that of its hydrochloride.

The problem is to obtain $p(a_H\gamma_{Cl})$ values for these buffer solutions, and to do so it is necessary to revert to some earlier work. The *pK* value of tris(hydroxymethyl)aminomethane in its protonated form (designated pK_T in order to distinguish it from the *pK* value of *m*-nitrophenol) is given by:

$$pK_T = p(a_H\gamma_{Cl}) - \log (m_2/m_1) - \log \gamma_T/(\gamma_{TH^+} \cdot \gamma_{Cl^-}) \quad (3)$$

where T designates tris(hydroxymethyl)aminomethane and TH^+ the protonated form. It has been shown [2, 7] that the last term can be represented as:

$$-\log \gamma_T/(\gamma_{TH^+} \cdot \gamma_{Cl^-}) = -2AI^{1/2}/(1 + BaI^{1/2}) + \beta I. \quad (4)$$

Here *A* and *B* are constants of the Debye-Hückel equation and β is the parameter of the term linear in the ionic strength. For tris(hydroxymethyl)aminomethane in 50 percent methanol, it was found that a satisfactory representation of the data could be obtained with $a=0$. Hence,

$$p(a_H\gamma_{Cl}) = pK_T + \log (m_2/m_1) + 2AI^{1/2} - \beta I. \quad (5)$$

Using $p(a_H\gamma_{Cl})$ values already tabulated [6], values of $\beta = 1.22$, 1.26, 1.32, and 1.32 kg mol^{-1} at 25, 30, 35, and 40 °C, respectively, are calculated.

These values of β are valid for solutions in which tris(hydroxymethyl)aminomethane and its hydrochloride are present in equimolal amounts. The assumption is now made that these values also hold for solutions in which the buffer ratio is not unity. Some doubt may be held as to the validity of this assumption. In the determination of the dissociation constant of tris(hydroxymethyl)aminomethane in aqueous solution, Bates and Hetzer [8] found eq (4) was satisfactory with $a=0$. They used solutions containing only tris(hydroxymethyl)aminomethane and its hydrochloride. Datta, Grzybowski, and Weston [9], however, added potassium chloride to their solutions and found that $a=3.2$ Å gave a good representation of their results. Nevertheless, the use of β values independent of the buffer ratio seems to be justified by the fact that it leads to concordant *pK* values (table 1) at 25 °C with buffer ratios of $m_2/m_1 = 1.007$, 4.06, and 5.98.

3. Experimental Procedure

Degrees of dissociation, α, of *m*-nitrophenol were measured spectrophotometrically in the usual manner. A stable single-beam spectrophotometer was used. It had been found in earlier studies to be capable of precise and reproducible measurements of the optical density in the visible and ultraviolet regions of the spectrum.

A thermostated cell block was constructed using the metal cell holder supplied with the spectrophotometer. The holder has provision for four cells, and a heater was placed in each of the outer cell positions (fig. 1). These heaters were formed by winding 7 ft of 26 B and S nichrome wire, insulated with glass spaghetti, on to each of two aluminum blocks. The complete heaters fitted snugly into the cell holder. The heater windings were connected in series.

A thermistor cemented to the cell holder served as a sensor in a temperature-control circuit. A second thermistor, used for temperature measurement, was mounted on a movable metal bracket so that it could be placed in the solution in one of the cells or moved aside when solutions were being changed. Leads from the heaters and thermistors terminate in a six-pin socket mounted on the cell holder; the leads from a corresponding six-pin plug were passed through a hole in the lid of the cell compartment.

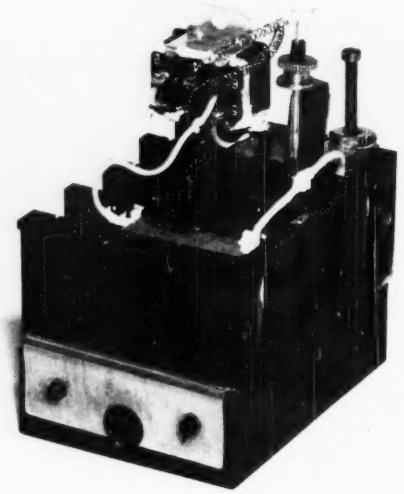

FIGURE 1. *Controlled-temperature cell block for spectrophotometric measurements.*

The resistance of the measuring thermistor was determined using a d-c Wheatstone bridge. The leads from the regulating thermistor were connected to the input of a commercial electronic proportional temperature controller. The heaters constitute the load for this controller. Provision was made for connecting a 100- or 250-Ω ballast load in series with the heaters. Using this apparatus, the temperature of the solutions could be regulated between room temperature and 50 °C with a constancy of 0.01 °C.

The *m*-nitrophenol, of a commercial grade believed to be highly pure, was recrystallized twice from water. Its melting point, found to be 96 °C after crystallization, agreed well with values given in the literature. The buffer solutions were prepared from tris base, standard hydrochloric acid, and purified methanol in the manner described in an earlier publication [2].

TABLE 1. *Dissociation constant of* m-*nitrophenol in 50 wt percent methanol from 25 to 40 °C*

	I	$-2 \log \gamma$	400 mμ		390 mμ	
			D	pK	D	pK
25 °C	$\log m_2/m_1 = 0.003$		$D_1 = 0.051$,	$D_2 = 0.840$	$D_1 = 0.119$,	$D_2 = 0.840$
	0.01988	0.204	0.131	8.977	0.188	8.998
	.03974	.271	.144	8.971	.199	8.995
	.05955	.318	.150	8.989	.205	8.996
	.07921	.354	.157	8.990	.216	8.983
	.09858	.383	.175	8.943	.233	8.930
			Mean pK	8.97_4	Mean pK	8.98_0
	$\log m_2/m_1 = 0.608$		$D_1 = 0.052$,	$D_2 = 0.847$	$D_1 = 0.122$,	$D_2 = 0.840$
	0.00722	0.127	0.264	8.982	0.312	8.987
	.01455	.175	.287	8.973	.333	8.977
	.02178	.209	.297	8.983	.347	8.973
	.02903	.238	.312	8.974	.359	8.968
	.03604	.260	.318	8.983	.365	8.975
			Mean pK	8.97_9	Mean pK	8.97_6
	$\log m_2/m_1 = 0.777$		$D_1 = 0.059$,	$D_2 = 0.930$	$D_1 = 0.135$,	$D_2 = 0.925$
	0.00581	0.115	0.359	8.974	0.405	8.979
	.01159	.159	.387	8.974	.433	8.964
	.01737	.190	.407	8.957	.452	8.954
	.02313	.216	.425	8.947	.467	8.947
	.02880	.237	.441	8.936	.483	8.933
			Mean pK	8.95_6	Mean pK	8.95_5
30 °C	$\log m_2/m_1 = 0.608$		$D_1 = 0.054$,	$D_2 = 0.841$	$D_1 = 0.120$,	$D_2 = 0.831$
	0.00722	0.129	0.235	8.933	0.286	8.924
	.01455	.178	.256	8.924	.300	8.932
	.02178	.213	.266	8.932	.311	8.934
	.02903	.240	.276	8.932	.321	8.930
	.03604	.263	.285	8.932	.327	8.936
			Mean pK	8.93_1	Mean pK	8.93_1
	$\log m_2/m_1 = 0.777$		$D_1 = 0.060$,	$D_2 = 0.919$	$D_1 = 0.131$,	$D_2 = 0.909$
	0.00581	0.117	0.311	8.943	0.361	8.936
	.01159	.160	.338	8.930	.385	8.925
	.01737	.192	.352	8.937	.400	8.922
	.02313	.218	.367	8.927	.411	8.922
	.02880	.240	.373	8.940	.420	8.923
			Mean pK	8.93_4	Mean pK	8.92_6
35 °C	$\log m_2/m_1 = 0.608$		$D_1 = 0.054$,	$D_2 = 0.829$	$D_1 = 0.121$,	$D_2 = 0.819$
	0.00722	0.130	0.207	8.887	0.259	8.886
	.01455	.180	.222	8.896	.273	8.888
	.02178	.215	.236	8.883	.283	8.890
	.02903	.244	.244	8.887	.292	8.888
	.03604	.266	.251	8.889	.297	8.894
			Mean pK	8.88_7	Mean pK	8.88_9

Dissociation constant of m-*nitrophenol in 50 wt percent methanol from 25 to 40 °C*—Continued

	$\log m_2/m_1 = 0.777$		$D_1 = 0.062$, $D_2 = 0.909$		$D_1 = 0.131$, $D_2 = 0.904$	
	0.00581	0.118	0.277	8.897	0.331	8.886
	.01159	.163	.301	8.888	.350	8.885
	.01737	.195	.319	8.878	.369	8.869
	.02313	.221	.329	8.882	.376	8.877
	.02880	.245	.341	8.878	.388	8.872
			Mean pK	8.88_5	Mean pK	8.87_8
40 °C	$\log m_2/m_1 = 0.777$		$D_1 = 0.065$, $D_2 = 0.907$		$D_1 = 0.133$, $D_2 = 0.894$	
	0.00581	0.120	0.250	8.858	0.303	8.848
	.01159	.166	.268	8.859	.320	8.848
	.01737	.198	.284	8.850	.335	8.838
	.02313	.224	.293	8.853	.342	8.845
	.02880	.246	.310	8.833	.359	8.820
			Mean pK	8.85_1	Mean pK	8.84_0

The concentration of *m*-nitrophenol was 5.83×10^{-4}, 5.80×10^{-4}, and 6.34×10^{-4} *m* in the buffer solutions for which $\log (m_2/m_1)$ was 0.003, 0.608, and 0.777, respectively. All optical measurements were made in cells 1 cm in length; m_2 is the molality of tris(hydroxymethyl)aminomethane, $m_1 (= I)$ that of its hydrochloride.

4. Results

Table 1 gives experimental details of the measurements: I, the total ionic strength of the solution, is equal to m_1, the concentration of tris(hydroxymethyl)-aminomethane hydrochloride; 2 log γ is an abbreviation for $\log \gamma_T/(\gamma_{TH^+} \cdot \gamma_{Cl^-})$ and has been calculated using eq (4). Measurements were made at two wavelengths, using 1 cm cells. In calculating values of pK a small correction was made for the effect of *m*-nitrophenol on the $p(a_H\gamma_{Cl})$ value of the buffer solution [10].

Mean values of pK at 25, 30, 35, and 40 °C are given below, where they are compared with corresponding values for the dissociation process in aqueous solution [11].

	pK		
	In 50 percent methanol	In water	ΔpK
°C			
25	8.97_0	8.35_5	0.61_5
30	8.93_0	8.28_4	$.64_6$
35	8.88_4	8.23_2	$.65_2$
40	8.84_6	8.16_7	$.67_9$

The difference, $\Delta pK = pK$ in 50 percent MeOH $- pK$ in H_2O, is a measure of the medium effect. The value of ΔpK at 25 °C for *m*-nitrophenol in 50 wt percent methanol (0.615) falls between the values for *o*-nitrophenol (0.687) and *p*-nitrophenol (0.536) for the same temperature and solvent [12]. The quantity $\Delta G° = 2.3026RT\Delta pK$ is the change in Gibbs free energy for the transfer reaction:

$$HN(s) + H^+(w) + N^-(w) = HN(w) + H^+(s) + N^-(s), \qquad (6)$$

where w stands for water and s for 50 percent methanol. $\Delta G°$ for this reaction increases from 0.84 kcal mol^{-1} at 25 °C to 0.97 kcal mol^{-1} at 40 °C (1 cal = 4.1840 J). This is in marked contrast to what has been observed with protonated tris(hydroxymethyl)aminomethane [2], where the medium effect is almost independent of temperature, ΔpK being −0.251 at 25 °C and −0.248 at 40 °C. The Gibbs free energy change corresponding to the medium effect on tris · H^+ is thus −0.34 kcal mol^{-1} at 25 °C. The different signs of the medium effects for these two acids are a consequence of the difference in charge type of the two dissociation reactions.

The pK values of *m*-nitrophenol in 50 percent methanol can be represented as a function of temperature (T) in °K by the equation

$$pK = 6.352 + 780.8/T \qquad (7)$$

with a maximum error of 0.002 in pK. It follows that the enthalpy change on dissociation in 50 percent methanol is 3.57 kcal mol^{-1} compared with 5.14 kcal mol^{-1} in water, while the entropy change is −29 cal deg^{-1} mol^{-1} compared with −21 cal deg^{-1} mol^{-1} in water. Thus reaction (6), the transfer of hydrogen and phenolate ions from water to 50 percent methanol and of phenol molecules from 50 percent methanol to water is accompanied by an enthalpy change $\Delta H° = -1.57$ kcal mol^{-1} and an entropy change $\Delta S° = -8$ cal deg^{-1} mol^{-1}.

5. References

[1] M. Paabo, R. G. Bates, and R. A. Robinson, J. Phys. Chem. **70,** 247 (1966).
[2] M. Woodhead, M. Paabo, R. A. Robinson, and R. G. Bates, J. Res. NBS **69A** (Phys. and Chem.) No. 3, 263 (1965).
[3] M. Paabo, R. A. Robinson, and R. G. Bates, Anal. Chem. **38,** 1573 (1966).
[4] A. L. Bacarella, E. Grunwald, H. P. Marshall, and E. L. Purlee, J. Org. Chem. **20,** 747 (1955).
[5] T. Shedlovsky and R. L. Kay, J. Phys. Chem. **60,** 151 (1956).
[6] M. Woodhead, M. Paabo, R. A. Robinson, and R. G. Bates, Anal. Chem. **37,** 1291 (1965).
[7] R. G. Bates and G. D. Pinching, J. Res. NBS **42,** 419 (1949).
[8] R. G. Bates and H. B. Hetzer, J. Phys. Chem. **65,** 667 (1961).
[9] S. P. Datta, A. K. Grzybowski, and B. A. Weston, J. Chem. Soc. (London) 792 (1963).
[10] R. A. Robinson and A. K. Kiang, Trans. Faraday Soc. **51,** 1398 (1955).
[11] R. A. Robinson and A. Peiperl, J. Phys. Chem. **67,** 2860 (1963).
[12] R. A. Robinson and R. G. Bates, J. Res. NBS **70A** (Phys. and Chem.) No. 6, 553 (1966).

(Paper 71A1–430)

JOURNAL OF RESEARCH of the National Bureau of Standards—A. Physics and Chemistry
Vol. 71A, No. 1, January–February 1967

On the Calculation of Moments of Molecular Weight Distribution from Sedimentation Equilibrium Data

Irwin H. Billick, Michael Schulz,[1] and George H. Weiss[2]

Institute for Materials Research, National Bureau of Standards, Washington, D.C., 20234

(October 4, 1966)

In this paper we discuss a technique for calculating moments of polydisperse materials in terms of concentration readings along the cell. The proposed method minimizes dependence on data from the end points where they may be unreliable. An analysis is given of the errors involved in the use of the proposed method when the underlying molecular weight distribution is the Schulz distribution or the lognormal.

Key Words: Molecular weight average, molecular weight distributions, moments, polydispersity, polynomial representation, sedimentation equilibrium.

One of the primary functions of a sedimentation equilibrium experiment is to measure the molecular weight of the solute, and in the case of a polydisperse solute, obtain information about the molecular weight distribution. In the latter case, the information is in the form of the first several moments of the distribution. The commonly used methods of data analysis derive these moments from the values of the concentration and its spatial derivatives evaluated at the end points of the solution column [1].[3] Methods of evaluating the moments using a point nearer the center of the solution column have been described by Fujita [2] and Adams [3]. However, these techniques require data over the entire range from zero to infinite centrifugal field. Thus far, no practical test of these latter methods has appeared in the literature.

Recently it has been suggested [4] that improved accuracy could be obtained for the moments and hence the molecular weight averages if measurements were made as a function of centrifugal field as the field approaches zero. This latter method again requires some data to be obtained by extrapolation to the meniscus and other data to be obtained by extrapolation to the cell bottom or from a point near the center of the cell. The purpose of this paper is to present a general method of analyzing experimental data in which the end points play a less important role and advantage is taken of the more accurate data obtainable elsewhere in the cell. It will also be shown that the treatment of Osterhoudt and Williams [4] represents a special case of the general treatment presented below. In addition to presenting the method we shall analyze possible errors in the method when the underlying molecular weight distribution is the Schulz [5] distribution or the lognormal distribution [1].

Method of analysis. In the case of an ideal, noncompressible solution the radial concentration distribution of a single solute species $c_i(\zeta)$ of molecular weight M_i, is given by [2]

$$\frac{c_i(\zeta)}{c_i^0}=\frac{\lambda M_i \exp(-\lambda M_i\zeta)}{1-\exp(-\lambda M_i)}, \tag{1}$$

where c_i^0 is the original concentration before sedimentation and where ζ is the reduced radial variable given by

$$\zeta=\frac{b^2-r^2}{b^2-a^2}. \tag{2}$$

The distance of the meniscus and bottom of the solution column from the center of rotation are given by a and b respectively, and r is any arbitrary intermediate position. The quantity λ, is defined by

$$\lambda=\frac{(1-\bar{v}\rho)(b^2-a^2)\omega^2}{2RT} \tag{3}$$

where the other symbols have their usual definitions [2].

For a solute which is not monodisperse but has a continuous distribution of molecular weights given by some function $f(M)$, the radial distribution of the concentration at sedimentation equilibrium is given by

$$\frac{c(\zeta)}{c_0}=\theta(\zeta)=\int_0^\infty \frac{\lambda M f(M) e^{-\lambda M\zeta} dM}{1-e^{-\lambda M}}, \tag{4}$$

where $\theta(\zeta)$ is defined by this equation.

One observes that the form of the function given by the right-hand side of eq (1) and contained in the integrand of eq (4) is the same as that of the generating function for the Bernoulli polynomials [6], provided

[1] Present address: Department of Physics, M.I.T., Cambridge, Mass.
[2] National Cancer Institute, National Institutes of Health, Bethesda, Md., 20014.
[3] Figures in brackets indicate the literature references at the end of this paper.

that $\lambda M \leq 2\pi$. Thus eq (4) can be rewritten

$$\theta(\zeta)=\sum_{n=0}^{\infty}\frac{(-1)^n}{n!}B_n(\zeta)\lambda^n\nu_n^*+\int_{2\pi/\lambda}^{\infty}\frac{\lambda M e^{-\lambda M\zeta}f(M)dM}{1-e^{-\lambda M}}. \quad (5)$$

where ν_n^* is the truncated moment

$$\nu_n^*=\int_0^{2\pi/\lambda}M^n f(M)dM=\begin{cases}M_w^* & , n=1\\ (M_w M_z M_{z+1}\ldots M_{z+n-2})^*, & n>1\end{cases} \quad (6)$$

M_w^*, the truncated weight average molecular weight and so on. Some properties of the polynomials $B_n(\zeta)$ are given in reference 6.

The basis for the method suggested by Osterhoudt and Williams is the replacement of $\theta(\zeta)$ by $\theta^*(\zeta)$, defined by

$$\theta^*(\zeta)=\sum_{n=0}^{\infty}\frac{(-1)^n}{n!}B_n(\zeta)\lambda^n\nu_n^*. \quad (7)$$

i.e., the integral in eq (5) is assumed to be negligible. With this definition, the identity $dB_n(\zeta)/d\zeta=nB_{n-1}(\zeta)$, and the particular values $B_0(0)=1$, $B_1(0)=-1/2$, $B_2(0)=1/6$, $B_3(0)=0$, $B_4(0)=-1/30$, $B_5(0)=0$, ... we readily obtain the result of Osterhoudt and Williams

$$\left.\frac{d\theta(\zeta)}{d\zeta}\right|_{\zeta=0}=-\lambda\nu_1^*-\frac{1}{2}\lambda^2\nu_2^*-\frac{1}{12}\lambda^3\nu_3^*+\frac{1}{120}\lambda^4\nu_4^*+\ldots \quad (8)$$

The remaining formulas in reference 4 for $\zeta=1/2$ and 1 are derived in similar fashion. However, we can also derive other identities that allow us to use any ζ values between zero and one thus permitting the use of points that obviate extrapolation and are therefore more reliable. For example, we have

$$\theta^*\left(\frac{1}{2}-\alpha\right)-\theta^*\left(\frac{1}{2}+\alpha\right)=2\alpha\lambda\nu_1^*+\left(\alpha^3-\frac{\alpha}{4}\right)\frac{\lambda^3\nu_3^*}{3}+0(\lambda^5\nu_5^*)$$

$$\theta^*\left(\frac{1}{2}-\alpha\right)+\theta^*\left(\frac{1}{2}+\alpha\right)=2+\left(\alpha^2-\frac{1}{12}\right)\lambda^2\nu_2^*+\left(\alpha^4-\frac{\alpha^2}{2}+\frac{7}{120}\right)\frac{\lambda^4\nu_4^*}{12}+0(\lambda^6\nu_6^*). \quad (9)$$

where α can be chosen arbitrarily. By choosing $\alpha=1/4$ we find

$$\theta^*\left(\frac{1}{4}\right)-\theta^*\left(\frac{3}{4}\right)=\frac{\lambda\nu_1^*}{2}-\frac{1}{64}\lambda^3\nu_3^*+\ldots$$

$$\theta^*\left(\frac{1}{4}\right)+\theta^*\left(\frac{3}{4}\right)=2-\frac{\lambda^2\nu_2^*}{48}+\frac{119}{46080}\lambda^4\nu_4^*+\ldots. \quad (10)$$

or choosing $\alpha=0$,

$$\theta^*\left(\frac{1}{2}\right)=1-\frac{\lambda^2\nu_2^*}{24}+\frac{7}{1440}\lambda^4\nu_4^*+\ldots. \quad (11)$$

Values of the moments are derived from these relations by taking measurements at several values of λ and extrapolating to the dependence at $\lambda=0$.

It is possible to extend these considerations so that a series is obtained, the first term of which is proportional to $\lambda^r\nu_r$, and in which any number of terms in $\nu_1^*, \nu_2^*, \ldots, \nu_{r-1}^*, \nu_{r+1}^*, \ldots \nu_{r+m}^*$ have zero coefficients, by properly choosing points $\zeta_1, \zeta_2, \ldots, \zeta_{r+m}$, and coefficients $\alpha_1, \alpha_2, \ldots \alpha_{r+m}$, in linear combination:

$$F^*(\zeta_1, \zeta_2, \ldots, \zeta_{r+m})=\alpha_1\theta^*(\zeta_1)+\alpha_2\theta^*(\zeta_2)+\ldots+\alpha_{r+m}\theta^*(\zeta_{r+m}). \quad (12)$$

Given the set of points $\zeta_1, \zeta_2, \ldots, \zeta_{r+m}$ the α_i are chosen so that

$$\sum_{j=1}^{r+m}\alpha_j B_k(\zeta_j)=0,\ k=1, 2, \ldots, r-1, r+1, \ldots r+m. \quad (13)$$

One of the constants, α_1, can be set equal to 1 and the ratios α_j/α_1, are determined from eq (13). The points ζ_j can be chosen arbitrarily except for the condition

$$\sum_{j=1}^{r+m}\alpha_j B_r(\zeta_j)\neq 0 \quad (14)$$

in order that the coefficient of $\lambda^r\nu_r^*$ be nonzero. As an example we can calculate a formula in which the first nonzero is proportional to $\lambda^3\nu_3^*$, and the second $\lambda^5\nu_5^*$, by choosing

$$\zeta_1=1/5,\ \zeta_2=2/5,\ \zeta_3=3/5,\ \zeta_4=4/5.$$

Using the procedure outlined above we find that

$$-\theta^*\left(\frac{1}{5}\right)+3\theta^*\left(\frac{2}{5}\right)-3\theta^*\left(\frac{3}{5}\right)+\theta^*\left(\frac{4}{5}\right)=\frac{\lambda^3\nu_3^*}{125}-\frac{111\lambda^5\nu_5^*}{375{,}000}+\ldots \quad (15)$$

Error analysis. So far we have made the tacit assumption that the observed value $\theta(\zeta)$ is identical to $\theta^*(\zeta)$ so that ν_n^* can be identified with the desired value ν_n. It clearly is not, so that some error analysis is required to set bounds on the validity of the method. Two types of error require investigation. The first is the error in using the observed $\theta(\zeta)$ rather than the required $\theta^*(\zeta)$, and the second is in the calculation of values of ν_n^* rather than ν_n.

Let us denote by $\epsilon(\zeta)$ the difference

$$\epsilon(\zeta)=\theta(\zeta)-\theta^*(\zeta)=\int_{2\pi/\lambda}^{\infty}\frac{\lambda M e^{-\lambda M\zeta}}{1-e^{-\lambda M}}f(M)dM. \quad (16)$$

The absoulte error incurred by using values of $\theta^*(\zeta)$ rather than $\theta(\zeta)$ can be bounded as follows:

$$|F-F^*|=\left|\sum_{j=1}^{r+m}\alpha_j\epsilon(\zeta_j)\right|$$

$$=\int_{2\pi/\lambda}^{\infty}\frac{\lambda M f(M)}{1-e^{-\lambda M}}\left|\sum_{j=1}^{r+m}\alpha_j e^{-\lambda M\zeta_j}\right|dM$$

$$\leq(1-e^{-2\pi})^{-1}\lambda(\nu_1-\nu_1^*)\sum_{j=1}^{r+m}|\alpha_j|e^{-2\pi\zeta_j}, \quad (17)$$

so that the difference between the observed F and the desired F^* is proportional to $\lambda(\nu_1-\nu_1^*)$. Theoretically one can decrease this bound by choosing the ζ_j close to 1 but this method is limited by observational errors the meniscus. It is interesting to note that if the moments are to be calculated in terms of parameters relating to the derivative $\theta'(\zeta)$, as is the case in Osterhoudt and Williams' paper, the bound corresponding to eq (17) contains $\lambda(\nu_2-\nu_2^*)$ in place of $\lambda(\nu_1-\nu_1^*)$ and is therefore larger.

For the purpose of illustrating errors in terms of physical quantities we will derive explicitly the formulas for $\lambda(\nu_1-\nu_1^*)$ and $J_n=1-(\nu_n^*/\nu_n)$ for two common polymer distributions; the Schulz [5] and the lognormal [1]. We consider first the Schulz distribution

$$f(M)=\frac{a^{\rho+1}M^{\rho}}{\Gamma(\rho+1)}e^{-aM}, \quad (18)$$

where the two adjustable parameters a and ρ can be expressed in terms of M_w and M_z, the weight and z average molecular weights as

$$a=(M_z-M_w)^{-1}$$

$$\rho=\frac{2M_w-M_z}{M_z-M_w}. \quad (19)$$

For this distribution $\lambda(\nu_1-\nu_1^*)$ can be written

$$\lambda(\nu_1-\nu_1^*)=\frac{\lambda}{a\Gamma(\rho+1)}\int_{2\pi a/\lambda}^{\infty}u^{\rho+1}e^{-u}du. \quad (20)$$

We therefore see that the difference depends on the parameters ρ and λ/a where

$$\lambda/a=\lambda(M_z-M_w). \quad (21)$$

Experiments of the type discussed here can be arranged so that $\lambda M_w\approx 1$. Furthermore, the Schulz distribution is a sensible one for polymers only for ρ positive or $2>M_z/M_w$ hence $\lambda M_z\leq 2$ and λ/a is at most equal to 2. For $\rho\lambda/(2\pi a)$ a small number we can approximate the integral in eq (20) by

$$\int_{2\pi a/\lambda}^{\infty}u^{\rho+1}e^{-u}du\sim\left(\frac{2\pi a}{\lambda}\right)^{\rho+1}e^{-\frac{2\pi a}{\lambda}}$$

$$\left[1+(\rho+1)\left(\frac{\lambda}{2\pi a}\right)+\ldots\right] \quad (22)$$

so that

$$\lambda(\nu_1-\nu_1^*)\sim\frac{(2\pi)^{\rho+1}}{\Gamma(\rho+1)}\left(\frac{a}{\lambda}\right)^{\rho}e^{-2\pi a/\lambda}. \quad (23)$$

In figure 1 we have plotted some representative values of $-\log_{10}\lambda(\nu_1-\nu_1^*)$ as a function of λM_w. As can be seen from the figure $\theta(\zeta)$ and $\theta^*(\zeta)$ are experimentally indistinguishable when λM_w is less than 1 except when M_z/M_w is greater than 1.75. Even in that case if λM_w can be set less than 0.5, $\theta(\zeta)$ and $\theta^*(\zeta)$ are experimentally indistinguishable.

To estimate the accuracy with which ν_n^* approximates to ν_n we calculate the ratios

$$J_n=1-\frac{\nu_n^*}{\nu_n}=\frac{1}{\Gamma(n+\rho+1)}\int_{2\pi a/\lambda}^{\infty}u^{\rho+n}e^{-u}du$$

$$\sim\left(\frac{2\pi a}{\lambda}\right)^{\rho+n}\frac{1}{\Gamma(\rho+n+1)}e^{-2\pi a/\lambda}. \quad (24)$$

In figure 2 we have plotted $-\log_{10}J_1$ and $-\log_{10}J_2$ as a function of λM_w for $M_z/M_w=1.75$. It is to be noted that both ν_1 and ν_2 can theoretically be determined to within an error of about 1% with the present method, provided that λM_w is less than 1.

Another distribution useful in polymer work is the lognormal [1]

$$f(M)=\frac{1}{\sigma M\sqrt{2\pi}}\exp\left\{-\frac{1}{2\sigma^2}\ln^2\left(\frac{M}{M_0}\right)\right\}. \quad (25)$$

The two adjustable parameters M_0 and σ, are related to M_w and M_z by

$$M_0=M_w(M_w/M_z)^{1/2}$$

$$\sigma^2=\ln(M_z/M_w). \quad (26)$$

A straightforward calculation suffices to show that

236-431 O-67-2

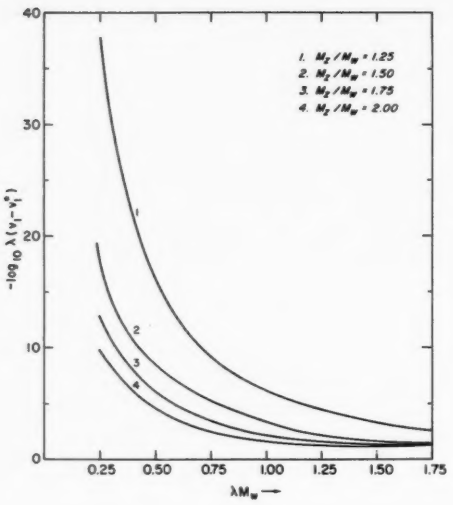

FIGURE 1. *Graphs of* $-\log_{10} \lambda(\nu_1-\nu_1^*)$ *as a function of* λM_w *for different values of* M_z/M_w *for a Schulz distribution.*

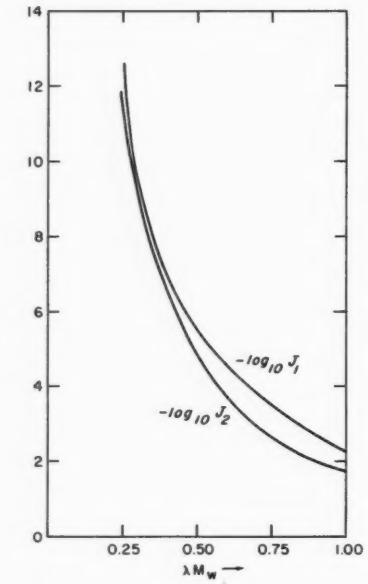

FIGURE 2. *Graphs of* $-\log_{10} J_1$ *and* $-\log_{10} J_2$ *as a function of* λM_w *for Schulz distribution.*

$\lambda^n(\nu_n-\nu_n^*)$ can be expressed as

$$\lambda^n(\nu_n-\nu_n^*)=\frac{(\lambda M_0)^n\sigma^{n-1}}{\sqrt{2\pi}}\int_{\frac{2\pi}{\lambda M_0\sigma}}^{\infty} u^{n-1}e^{-u^2/2}du. \tag{27}$$

For odd n these can be written in terms of complementary error functions and exponentials, while for even n they can be written in terms of exponentials. The J_n defined in eq (24) are expressible in the form

$$J_n=\int_{\frac{2\pi}{\lambda M_0\sigma}}^{\infty} u^{n-1}e^{-u^2/2}du\Big/\int_0^{\infty} u^{n-1}e^{-u^2/2}du. \tag{28}$$

Specifically, the first three J's are

$$J_1=2\ \text{erfc}\left(\frac{2\pi}{\lambda M_0\sigma}\right)$$

$$J_2=\exp\left(-\frac{2\pi^2}{\lambda^2M_0^2\sigma^2}\right) \tag{29}$$

$$J_3=J_1+\sqrt{2\pi}\,J_2,$$

where $\text{erfc}(x)=(2\pi)^{-1/2}\int_x^{\infty}\exp(-u^2/2)\,du.$

These formulas can be simplified by noting that practical values of $\lambda M_0\sigma$ are of the order of 1 or less. As we have already noted, λM_w can be made of the order of 1, and $M_w/M_z<1$ so that $\lambda M_0<\lambda M_w$. Further, for the cases where the ratios (M_z/M_w) are less than approximately 10 and $\sigma<1.6$, the ratio $\dfrac{2\pi}{\lambda M_0\sigma}$ is greater than 3 and we can approximate the complementary error function by

$$\text{erfc}\left(\frac{2\pi}{\lambda M_0\sigma}\right)\sim\frac{\lambda M_0\sigma}{2\pi}\exp\left(-\frac{2\pi^2}{\lambda^2M_0^2\sigma^2}\right) \tag{30}$$

which can be inserted in the expressions for $\lambda(\nu_1-\nu_1^*)$ and J_1, J_2, J_3. This procedure yields

$$\lambda(\nu_1-\nu_1^*)\sim\frac{(\lambda M_0)^2\sigma}{2\pi}\exp\left(-\frac{2\pi^2}{\lambda^2M_0^2\sigma^2}\right)$$

$$J_1\sim\frac{\lambda M_0\sigma}{\pi}\exp\left(-\frac{2\pi^2}{\lambda^2M_0^2\sigma^2}\right)$$

$$J_2\sim\exp\left(-\frac{2\pi^2}{\lambda^2M_0^2\sigma^2}\right). \tag{31}$$

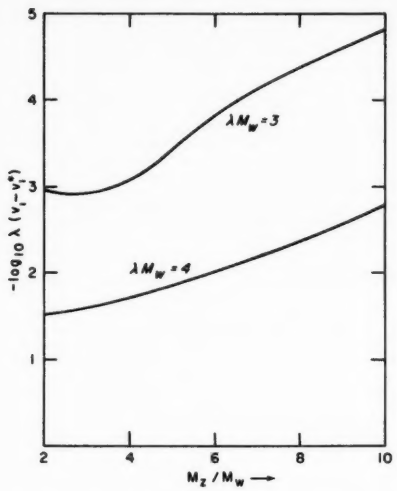

FIGURE 3. *Graphs of* $-log_{10}\ \lambda(\nu_1 - \nu_1^*)$ *as a function of* M_z/M_w *for lognormal distribution.*

Figure 3 shows curves of $-\log_{10}\lambda(\nu_1 - \nu_1^*)$ as a function of M_z/M_w for $\lambda M_w = 3$ and 4. It can be seen that $\lambda\nu_1$ is very close to $\lambda\nu_1^*$ for $\lambda M_w = 3$ and all M_z/M_w. Since λM_w can be kept in the neighborhood of 1 the present technique of deriving moments from the concentration can be justified theoretically for all M_z/M_w provided that the lognormal distribution is a suitable representation of the weight distribution. Calculation of the J's serves only to confirm this observation. It is of some interest to note that in contrast to the results for the Schulz distribution, the J_n decrease when M_z/M_w increases.

The two distributions assumed here are for illustrative purposes only. It is probably safe to say that if $\lambda M_w \leq 1$ the errors made in the mathematical assumptions are negligible compared to the experimental errors.

References

[1] W. D. Lansing and E. O. Kraemer, J. Am. Chem. Soc. **57**, 1369 (1935).
[2] H. Fujita, Mathematical Theory of Sedimentation Analysis, (Academic Press, New York) 1962.
[3] E. T. Adams, Jr., Proc. Nat. Acad. Sci. **51**, 509 (1964).
[4] H. W. Osterhoudt and J. W. Williams, J. Phys. Chem., **69**, 1050 (1965).
[5] G. V. Schulz, Z. Phys. Chem. **A193**, 168 (1944).
[6] M. Abramowitz and I. A. Stegun, Handbook of Mathematical Functions, p. 803, (National Bureau of Standards, Washington, D.C.) 1964.

(Paper 71A1–431)

JOURNAL OF RESEARCH of the National Bureau of Standards—A. Physics and Chemistry
Vol. 71A, No. 1, January–February 1967

The Far Infrared Spectrum of Vulcanized Natural Rubber

James E. Stewart* and Frederic J. Linnig

Institute for Materials Research, National Bureau of Standards, Washington, D.C., 20234

(August 15, 1966)

Earlier studies of the infrared spectra of natural rubber and some vulcanizates of rubber have been extended into the 650 to 33 cm^{-1} far infrared region. Some of the absorption bands originating in the crystalline portion of unvulcanized rubber have been studied by using polarized radiation and samples oriented by stretching. Vulcanization of rubber with sulfur alone produces a general weakening of all absorption bands and no new absorptions. Vulcanization with sulfur and an accelerator also results in a reduction in intensity of the rubber absorptions, but is accompanied by the appearance of new bands. When the accelerator is tetramethylthiuram disulfide (TMTD) the new bands are probably indicative of a thiocarbamate structure. When zinc dibutyldithiocarbamate is used as an accelerator a band probably due to zinc sulfide occurs. Vulcanization with TMTD alone produces only slight changes in the far infrared spectrum. However, when TMTD is used in the presence of zinc oxide a reaction occurs in which zinc dimethyldithiocarbamate (ZnDMDC) is formed. After vulcanization for a short period of time strong TMTD bands remain, but after long vulcanization the TMTD bands are replaced by ZnDMDC bands.

Key Words: Accelerators, far infrared, natural rubber, sulfur, tetramethylthiuram disulfide, vulcanization, zinc dibutyldithiocarbamate, zinc dimethyldithiocarbamate.

1. Introduction

In previous reports [1, 2][1] we discussed the absorption spectra of natural rubber, its vulcanizates, and of squalene as a model compound in the ultraviolet, visible, near infrared, and mid infrared. The far infrared has only recently become available on anything like a routine basis. We have extended our work into this region in order to investigate the usefulness of the far infrared in vulcanization studies. In this article we shall discuss the low-frequency infrared spectra of natural rubber and some of its vulcanizates in the 650 to 33 cm^{-1} region.

2. Experimental Procedure

Unvulcanized samples were prepared from natural rubber by milling it at 70 °C for 15 min and pressing it between sheets of Teflon for 7 min at 100 to 125 °C. Attempts to prepare films of unmilled rubber were not successful.

Vulcanized samples were prepared between sheets of aluminum foil in the manner described previously [1, 2]. The compositions of the vulcanized samples are tabulated in table 1. Except where noted in the figures, all samples were approximately 0.2 mm thick. In every case, natural rubber NBS Standard Sample No. 385a was used, and in addition, Samples I, II, and III were duplicated with high purity natural rubber No. 2103 of the United States Rubber Company. Other compounding materials were Sulfur (NBS Standard Sample 371d), Stearic Acid (NBS Standard Sample 372e), Zinc Oxide (NBS Standard Sample 370B), Tetramethylthiuram Disulfide or TMTD (NBS Standard Sample 374b), and Zinc Dibutyldithiocarbamate or ZnDBDC (R. T. Vanderbilt Co.). In addition, samples of Zinc Dimethyldithiocarbamate or ZnDMDC (R. T. Vanderbilt Co.), Squalene (Eastman Kodak Co.), and a squalene-sulfur reaction product were studied.

TABLE 1. *Compositions of rubber vulcanizates.*

Sample	Vulcanization		Rubber	Sulfur	Stearic acid	Zinc oxide	TMTD	ZnDBDC
	Time	Temp.						
	hr	°C	%	%	%	%	%	%
I	20	150	97.1	2.9	.....	.....	.....	.....
II	1	115	96.6	1.9	0.5	0.5	.....	0.5
III	3/4	125	96.1	.....	.5	.5	2.9	.....
IV	70	125	85.0	15.0	.....	.....	.....	.....
V	43	125	77.5	15.0	.....	.....	7.5	.....
VI	3	125	77.5	15.0	.....	.....	.....	7.5
VII	40	125	85.0	.....	.....	.....	15.0	.....
VIII	3/4	125	78.0	.....	2.0	5.0	15.0	.....
IX	20	125	78.0	.....	2.0	5.0	15.0	.....

* Present address: Beckman Instruments, Inc., Fullerton, Calif., 92634.
[1] Figures in brackets indicate the literature references at the end of this paper.

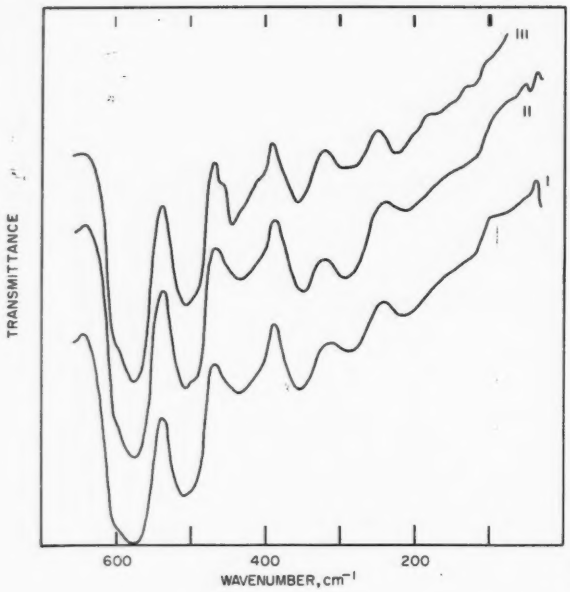

FIGURE 1. *Far infrared spectra of natural rubber vulcanized with (I) sulfur; (II) sulfur, ZnDBDC, zinc oxide, and stearic acid; and (III) TMTD, zinc oxide, and stearic acid.*

See table 1 for composition, times, and temperatures. Width of lines at the top of the figure indicates the spectral slit width.

Spectra in the 650 to 33 cm^{-1} region were recorded with a Beckman IR–11.[2] Spectral slit widths (reciprocal dispersion multiplied by slit width) between 1 and 5 cm^{-1} were used throughout the far infrared region. This is quite adequate resolution for the broad absorption bands of rubber. The change in spectral slit width with frequency for all figures except figure 2 is given in figure 1. Stray radiation amounts to about 4 percent or less at 80 cm^{-1}, 2 to 3 percent between 120 and 150 cm^{-1}, and less than 0.4 percent at frequencies higher than 200 cm^{-1}. Studies of oriented samples using polarized radiation were made with a Beckman IR–7. The latter observations were confined to the 650 to 200 cm^{-1} region by the cesium iodide fore prism. The polarizer consists of ten polyethylene sheets mounted at the Brewster angle. The calculated percentage polarization $(I_p-I_s)/(I_p+I_s)$, is about 60 percent, in satisfactory agreement with observations using crossed polarizers.

3. Far Infrared Spectrum of Natural Rubber

A goal of infrared spectroscopy is to observe and measure absorption bands and to determine the nature of the molecular vibrations which are responsible for them. The low frequency vibrations of hydrocarbons seen in far infrared spectra are skeletal in nature, involving the entire molecule to some extent. They cannot be considered as localized in any small functional group, as is often the case with vibrations of higher frequency. Nevertheless we wish to characterize them as fully as possible. To this end, we employed the technique of polarized infrared spectroscopy. We have also compared the infrared spectra of other compounds whose structures resemble natural rubber.

In one of the previous studies of natural rubber we observed four prominent bands in the infrared spectrum—at 570 with a shoulder at 590, 510 with a shoulder at 490, 430, and 360 cm^{-1}. With the extension of the spectrum to 33 cm^{-1}, additional bands were found at 295, 220, and 120 cm^{-1}. Representative spectra are shown in figure 1. The absorption bands are broad, with half-widths in the neighborhood of 30 cm^{-1}, and show evidence of overlapping structure. The materials used in obtaining these spectra were vulcanized to some extent. The samples were compounded in different ways (see table 1)–(I), with sulfur alone, (II) with sulfur and an accelerator, ZnDBDC, and (III) with TMTD and no sulfur. The spectra are very similar, except for some small differences which will be discussed in later sections. The spectrum of unvulcanized natural rubber is indistinguishable from the spectrum of I. Spectra were obtained using purified rubber because some differences had been observed in the mid infrared, particularly around 1600 cm^{-1}, depending on the rubber used. No differences were seen in the far infrared spectra.

Natural rubber contains amorphous and crystalline regions. The proportion of crystalline structure can be enhanced by lowering the temperature or by mechanical elongation. Certain bands in the mid infrared are known to be sensitive to the degree of crystallinity, and in the case of orientation by stretching, the same bands are most responsive to changes of the plane of polarization of the incident radiation [3, 4]. The polarized infrared spectrum of an oriented film of natural rubber, vulcanized with TMTD and no sulfur, (III) is shown in figure 2. The film was oriented by stretching to about six times its original length. More highly vulcanized samples could not be oriented by stretching, presumably because of the network of cross-links. Unvulcanized rubber on the other hand is difficult to handle. The spectrum of the unstretched sample included in figure 2 is seen to differ somewhat from the spectrum of III in figure 1, notably in the contrast of the shoulders at 462 and 407 cm^{-1}. The two samples were prepared in the same way, but at different times. The spectral differences might reflect differences in extent of vulcanization. A sample of rubber vulcanized with sulfur alone (I) displayed qualitatively similar dichroic behavior, but not as pronounced as the TMTD vulcanizate. The vibrations responsible for the bands at 570 and 295 cm^{-1} are found to have their transition moments predominantly parallel to the direction of stretch and therefore

[2] Certain commercial materials and equipment are identified in this paper in order to adquately specify the experimental procedure. In no case does such identification imply recommendation or endorsement by the National Bureau of Standards, nor does it imply that the material or equipment identified is necessarily the best available for the purpose.

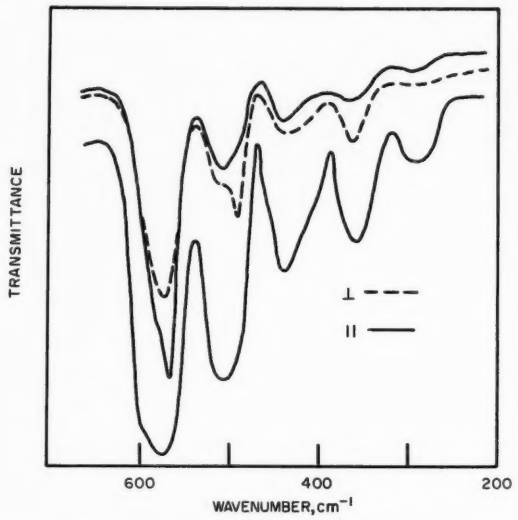

FIGURE 2. *Rubber vulcanized with* TMTD, *zinc oxide and stearic acid (III).*

Upper curves: sample oriented by stretching and polarized incident radiation with E-vector parallel and perpendicular to direction of stretch. Thickness not known. Lower curve: unoriented sample.

parallel to the axis of the polyisoprene chain. The 490 and 360 cm^{-1} vibrations are predominantly perpendicular. The 570 and 490 cm^{-1} bands are known to originate in the crystalline portion of the rubber, as demonstrated by low temperature experiments [4]. The shoulders on the high frequency sides of these bands at roughly 590 and 510 cm^{-1} are not sensitive to polarization and are due to the amorphous portion.

The basic unit of the polyisoprene chain of natural rubber has no symmetry, the conformation of the chain structure is not known, and detailed band assignments of similar molecules are not available. It would be presumptuous to attempt to assign the far infrared absorption bands of rubber to specific vibrations. We can, however, make some observations on the probable nature of some of these bands.

Hydrocarbons containing the $RR'=CHR''$ structure appear to have characteristic strong absorptions at 543 ± 26 and 497 ± 28 cm^{-1} and usually weaker bands at 437 ± 25 cm^{-1} [5]. These vibrations are probably similar in form to those responsible for the 570, 500, and 430 cm^{-1} absorptions in rubber. Hence, it is reasonable to suppose that the 543 cm^{-1} vibrations of hydrocarbons are parellel to the C=C axis and the 497 cm^{-1} vibrations are perpendicular.

Shipman and Golub [6] have recently published spectra of polyisoprene, and the deuterated forms polyisoprene $-3-d_1$ and polyisoprene $-d_8$. In the completely deuterated material the 570 and 490 cm^{-1} bands are shifted to about 500 and 440 cm^{-1}, very nearly in the ratio of the square roots of the masses of CD_3 and CH_3 groups. In the singly deuterated polymer the shift is only about 10 cm^{-1}. This is consistent with a surmise that these vibrations are dominated by the methyl group. The far infrared spectrum of polypropylene displays a sequence of bands progressing from 575 to 104 cm^{-1} and resembling the bands in the rubber spectrum, although weaker by nearly an order of magnitude. The normal coordinate analyses of Miyazawa et al. [7], and of Tadokoro et al. [8], show that $C-C-CH_3$ bending motion *tends* to prevail at the higher frequency end of this range while the $C-C-C$ bending is more important at the lower frequencies.

4. Sulfur Vulcanizates

The far infrared spectrum of a sample of natural rubber vulcanized with a small amount of sulfur (I) is included in figure 1. As previously indicated, it is qualitatively identical to the spectrum of unvulcanized rubber. The spectrum of a sample highly vulcanized with sulfur alone (IV) is shown in figure 3. It may be seen by comparison with (I) of figure 1 that extensive sulfur vulcanization is accompanied by a reduction in intensity of all of the bands of natural rubber and no new bands appear. In our previous work [1] we reported that several new bands appear in the far infrared spectrum of sulfur-vulcanized rubber. It now appears that such is not the case with either high or low sulfur content. The bands observed earlier were probably interference fringes. Interference fringes are also observed in many of the spectra presented here, especially at low wavenumbers. It might seem surprising that bands characteristic of the modified double bond structure do not appear in the far infrared spectrum as they do in the mid infrared. However, the vibrations associated with the most probable structure, trans $-RCH=CHR'$, occur in the same region as the vibrations of the $RR'=CHR''$ structure.

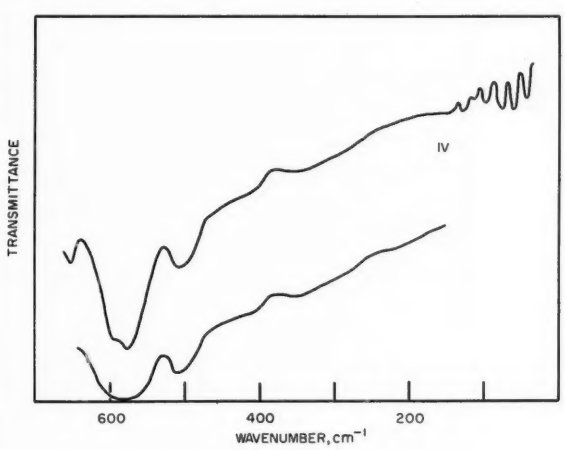

FIGURE 3. *Far infrared spectrum of rubber vulcanized with sulfur (IV).*

Film thickness for upper curve is about 0.2 mm; lower curve about 0.6 mm.

Squalene (hexaisoprene) resembles natural rubber structurally and chemically, and the infrared spectrum of squalene in the rocksalt region is very much like that of rubber because of the similarity of functional groups. Moreover, the rocksalt infrared spectrum of the reaction product formed by squalene and sulfur resembles the spectrum of vulcanized rubber. We have extended the spectrum of squalene into the far infrared. Except for a strong squalene band at 453 cm^{-1} and the lack of absorption at 120 cm^{-1} the resemblance between the squalene and the natural rubber spectra continues into the far infrared. The band at 453 cm^{-1} is very likely associated with the $(CH_3)_2C=C$ end groups of squalene. The far infrared spectrum of squalene, reacted with more than the usual amount of sulfur for 16 hr at 150 °C, shows a general reduction in intensity of all of the squalene bands and, just as in the case of the rubber vulcanizate, no new bands appear.

5. Accelerated Sulfur Vulcanizates

Two compounds frequently used as accelerators in sulfur vulcanization of rubber are TMTD and ZnDBDC. The far infrared spectra of natural rubber vulcanized with sulfur and TMTD and with sulfur and ZnDBDC are shown in figure 4. The absorption bands of natural rubber are reduced in intensity just as in the case of vulcanization with sulfur alone. However, new bands are produced which are related to reaction products of the accelerators.

The spectra of TMTD, ZnDBDC, and the related compound ZnDMDC were recorded. The spectra all have absorption bands near 575 ±9, 446 ±4, 391 ±8, 257 ±23 cm^{-1}. It is likely that these vibrations are associated with the thiocarbamate structure

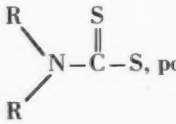

, possessed by all three compounds.

The far infrared spectrum of natural rubber highly vulcanized with sulfur and TMTD (V) has new bands at 448, 395, and 307 cm^{-1} and a change in the contour of the 500 cm^{-1} band which are not seen in the sulfur vulcanizate curve. Two of these bands are close to bands of TMTD at 444 and 398 cm^{-1} but TMTD has a strong band at 279 cm^{-1} and none at 307 cm^{-1}. Thus the absence of a strong band at 279 cm^{-1} and the presence of the band at 307 cm^{-1} in the spectrum of V indicate that the bands present at 448, 395, and 307 cm^{-1} are probably not due to a significant amount of TMTD. However, they do fall not far from the region where similar compounds absorb. Hence, it is reasonable to suppose that they are associated with a thiocarbamate structure formed during the sulfur-TMTD vulcanization process.

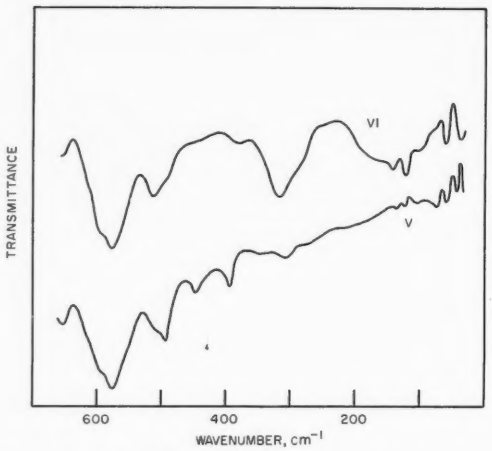

FIGURE 4. *Far infrared spectra of rubber vulcanized with (V) sulfur and* TMTD *and (VI) sulfur and* ZnDBDC.

The spectrum of natural rubber highly vulcanized with sulfur and ZnDBDC (VI) has a new strong band at 310 cm^{-1} and another weaker broad absorption at about 150 cm^{-1}. Notice that increased absorpion at 310 cm^{-1} is already evident with only 0.5 percent ZnDBDC and 1.9 percent sulfur (II) in the spectrum of figure 1. The origin of these bands is not known with certainty, but we have found that the absorption spectrum of zinc sulfide in a mineral oil mull has a strong band at about 310 cm^{-1}.

6. TMTD Vulcanizates

The far infrared spectra of natural rubber vulcanized with TMTD alone (VII) is given in figure 5. Aside from small changes in band contours, the only new feature seen in the spectrum of VII is a weak band at 302 cm^{-1}. The spectrum of a sample identical in composition to VII, but vulcanized for only 20 hr, did not differ significantly from the spectrum of VII.

When rubber is vulcanized with TMTD in the presence of zinc oxide and stearic acid, the spectra shown in figure 6 are quite different from that shown in figure 5. TMTD is known to react with zinc oxide during vulcanization to form ZnDMDC [9]. After vulcanization for a short period there is a considerable concentration of residual TMTD and only slight evidence of the formation of ZnDMDC. The conversion continues as vulcanization progresses for longer periods of time.

The spectrum of a compound vulcanized for 45 min (VIII) has plainly visible TMTD bands at 86, 279 (with a shoulder at 315), 362, 399, and 444 cm^{-1}. The band at 234 cm^{-1} is due to ZnDMDC. Zinc oxide itself has a strong broad absorption at 450 cm^{-1} which accounts for some of the absorption in that region. At the end of 20 hr of vulcanization (IX)

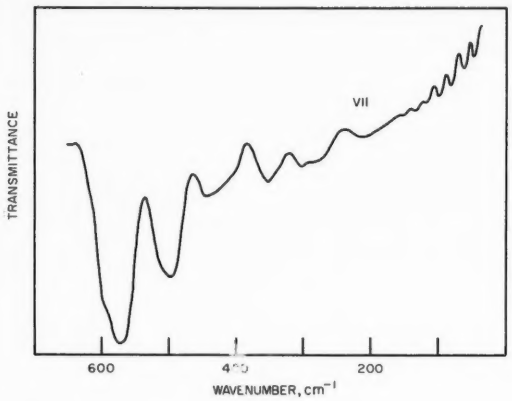

FIGURE 5. *Far infrared spectrum of rubber vulcanized with* TMTD *(VII).*

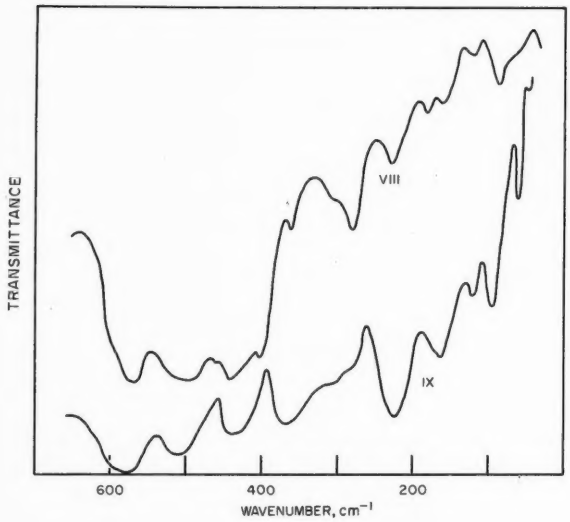

FIGURE 6. *Far infrared spectra of rubber vulcanized with* TMTD, *zinc oxide, and stearic acid for (VIII) 45 min, and (IX) 20 hr.*

the TMTD has been nearly consumed, with only a weak absorption left at 280 cm^{-1}, while pronounced ZnDMDC bands are found at 48, 61.5, 99, 120, 169, 234, 385, and 450 cm^{-1}. Disappearance of TMTD absorptions during the course of vulcanization was also observed in the rocksalt region [1].

Aside from an increased and sharpened absorption at 445 cm^{-1}, the spectrum of rubber vulcanized with less TMTD, zinc oxide, and stearic acid (III, fig. 1) does not display either TMTD or ZnDMDC absorption bands. Rather, it has weak bands at 407 and 462 cm^{-1} which do not correspond to any bands seen in the spectra of VIII or IX.

7. Conclusion

Low frequency vibrations of natural rubber are observed in the far infrared spectrum at 590, 570, 510, 490, 430, 360, 295, 220, and 120 cm^{-1}. Polarized infrared studies of stretched samples show the vibrations at 570 and 295 cm^{-1} to be predominantly parallel to the direction of stretch and vibrations at 490 and 360 cm^{-1} to be perpendicular. These polarization sensitive vibrations occur in the crystalline portion of the rubber. The vibrations at 590 and 510 cm^{-1} originate in the amorphous portion and are insensitive to polarization.

The effect of vulcanization on the far infrared spectrum of natural rubber can be summarized as follows:

(1) Vulcanization with sulfur alone produces no new bands, but an overall weakening of the absorption bands of natural rubber.

(2) Vulcanization with sulfur and an accelerator reduces the intensity of the rubber absorptions and introduces new bands, some of which have been tentatively explained. When the accelerator is TMTD new bands at 458, 395, 307 and perhaps near 500 cm^{-1} probably originate in thiocarbamate structures. When ZnDBDC is used as an accelerator new bands are found at 310 and 150 cm^{-1}. The former might be due to zinc sulfide.

(3) Vulcanization with TMTD in the absence of elemental sulfur and zinc oxide introduces only minor changes in band shapes and a weak band at 302 cm^{-1}.

(4) After brief vulcanization with TMTD in the presence of zinc oxide and stearic acid, bands contributed by unreacted TMTD at 86, 279, 315, 362, 399, and 444 cm^{-1} and zinc oxide at 450 cm^{-1} remain. If the vulcanization is continued for a longer period the reaction of TMTD with zinc oxide produces ZnDMDC which contributes bands at 48, 61.5, 99, 120, 169, 234, 385, and 450 cm^{-1}.

8. References

[1] F. J. Linnig and J. E. Stewart, J. Res. NBS **60,** 9 (1958) RP2816; Rubber Chem. Technol. **31,** 719 (1958).
[2] F. J. Linnig, E. J. Parks, and J. E. Stewart, J. Res. NBS **68A** (Phys. and Chem.) No. 4, 499 (1964).
[3] G. B. B. M. Sutherland and A. V. Jones, Disc. Faraday Soc. **9,** 281 (1950).
[4] R. A. Saunders and D. C. Smith, J. Appl. Phys. **20,** 953 (1949).
[5] J. E. Stewart, Far Infrared Spectroscopy, Interpretive Spectroscopy, S. K. Freeman, ed. (Rheinhold, New York, 1965).
[6] J. J. Shipman and M. A. Golub, J. Polymer Sci. **58,** 1063 (1962).
[7] T. Miyazawa, Y. Ideguchi, and K. Fukushima, J. Chem. Phys. **38,** 2709 (1963).
[8] H. Tadokoro, M. Kobayashi, M. Ukita, K. Yasufuku, S. Murahashi, and T. Torii, J. Chem. Phys. **42,** 1432 (1965).
[9] W. Scheele, O. Lorenz, and W. Dummer, Kautshuk u. Gummi **7, WT 273** (1954); Rubber Chem. Technol. **29,** 1 (1956).

(Paper 71A1–432)

JOURNAL OF RESEARCH of the National Bureau of Standards—A. Physics and Chemistry
Vol. 71A, No. 1, January–February 1967

Irradiation of Dextran and Its Aqueous Solutions With Cobalt-60 Gamma Rays*

Joseph H. Flynn, Leo A. Wall, and William L. Morrow

Institute for Materials Research, National Bureau of Standards, Washington, D.C., 20234

(October 19, 1966)

Cross-linking predominates over chain scission during the irradiation of concentrated aqueous dextran solutions by cobalt-60 gamma rays in the absence of oxygen. An extensive and long-lived postirradiative viscosity decay, which has not been previously reported, is attributed to the agency of hydrogen peroxide formed during the radiolysis of water. Solid dextran primarily degrades upon γ-irradiation while dextran triacetate is borderline between dominant scission and cross-linking. Both exhibit a postirradiative viscosity decrease when irradiated in the presence of water vapor. Electron spin resonance spectra of dextran in the solid state and in aqueous solution are presented and compared. Spin resonance spectral and chemical evidence concerning the mechanism of cross-linking and postirradiative decay reactions is presented. There is conflicting evidence for the presence of oxyradicals. Speculations are made concerning possible mechanisms of oxyradical formation and their role in the production of ether and peroxy linkages.

Key Words: Aqueous solution, cross-linking, dextran, dextran triacetate, gamma irradiation, polymer degradation postirradiative decay.

1. Introduction

The effects of ionizing radiation on dextran have been reported by a number of investigators [1–7][1] and dextran has been classed, along with other polysaccharides such as starch and cellulose as a polymer which primarily degrades upon irradiation. One percent solutions of dextran, irradiated with γ-rays, degraded even more rapidly than dry dextran powder [1] and the irradiation of a concentrated syrupy solution did not produce a gel [1].

Bovey [8] has concluded from the analysis of the effect of high speed electrons on native dextran [2] that the ratio of scissions to cross-links is only slightly greater than two—the critical value above which gel formation will not occur.

This proximity to incipient gelation coupled with the behavior of other polymers suggests that under certain conditions when dextran solutions are irradiated, cross-linking may predominate. For example, solid polyvinyl alcohol, upon irradiation, is degraded in the presence of oxygen [9–10] or in a moderate vacuum [10–12] but is cross-linked in aqueous solution [9] and in the water-swollen state [10].

In this paper, we report the changes in viscosity and osmotic pressure resulting from the γ-irradiation of solid dextran and dextran triacetate and aqueous solutions of dextran under a variety of conditions.

2. Experimental Procedure

The dextran used in these experiments was obtained from Pharmachem Corp. It is a purified dextran from Leuconostoc mesenteroides, NRRL B–512 [viscosity average molecular weight of 109,000; intrinsic viscosity (water at 25 °C), 0.33 dl/g; and a number average molecular weight, 28,100 (osmotic pressure)].

Dextran triacetate was prepared by treatment of a formamide solution of the above dextran with pyridine and acetic anhydride [13]. Its intrinsic viscosity in sym-1,1′,2,2′-tetrachloroethane at 25 °C was 0.32 dl/g.

The solid dextran and dextran triacetate samples were placed in glass ampoules and evacuated to 10^{-5} mm Hg for several days with occasional heating to 60 °C. The dried, evacuated samples were then sealed off. Dried oxygen at 150 mm Hg and/or degassed water vapor were added to other samples before sealing.

The concentrations of dextran and dextran triacetate solutions were calculated from dry weights of these substances by correcting for moisture content.

The dextran solutions were placed in glass ampoules or sealed tube viscometers previously described [14]. The solutions were alternately frozen and refluxed a number of times under vacuum over a period of several days to remove dissolved gases as completely as practicable and then sealed under vacuum. L-shaped pyrex sample tubes were used in the ESR experiments. The empty arm was heated to remove its signal before the sample was transferred to it for the determination of the sample's spectrum.

*Presented at the Division of Cellulose, Wood, and Fiber Chemistry, 148th Am. Chem. Soc. Meeting, Chicago, Ill., September 1964.

[1] Figures in brackets indicate the literature references at the end of this paper.

The samples were irradiated in a cobalt-60 gamma facility at 20 ±2 °C.

The intrinsic viscosity measurements of the dextran in water and of dextran triacetate in 1,1′,2,2′-tetrachloroethane were performed at 25 °C in Ubbelohde viscometers. Flow times of the sealed tube viscometers also were measured at 25 °C. Viscosity average molecular weight was calculated from $[\eta] = 1 \times 10^{-3} M_v^{0.50}$, which has been found to hold for acid-hydrolyzed fractions of NRRL B-512 [15a].

Osmotic pressure determinations were made on water solutions of dextran at 25 °C in a Bull [15b] osmometer with a Visking dialysis tubing membrane. Extrapolation to infinite dilution from 2.0–0.5 g/dl concentration was performed only on data for the unirradiated dextran so values for M_N for irradiated dextrans in tables 3 and 4 were approximated from single points (0.5 g/dl) and are included only for drawing qualitative conclusions from them.

Electron spin resonance spectra were obtained for dry evacuated samples and for a water gel on a Varian apparatus with a 100 kHz field modulation at about 1 mW power and 0.2 G magnetic field modulation.

3. Results

Solid dextran was irradiated with cobalt-60 γ-rays at a dose rate of 0.33 MR/hr for a total dose of 9.16 MR. The storage times between the end of the irradiation and the viscosity determination and the intrinsic viscosities in water at 25 °C are given in table 1.

The dry evacuated samples showed least intrinsic viscosity decrease. A slightly greater decrease occurred when oxygen at 150 mm Hg was present. The greatest decrease occurred in the samples that were exposed to degassed water vapor at 25 °C for 30 min. Postirradiative deterioration also was more rapid and more extensive in the presence of water vapor.

TABLE 1. *γ-Irradiated solid dextran*

Dose rate = 0.33 MR/hr Total dose = 6.19 MR

Conditions	Storage time [a]	$[\eta]$ [b] (dl/g)
Unirradiated	.....	0.33
Dry, vacuum	1 hour	.28
Dry, vacuum	1 day	.26
Dry, vacuum	2 days	.27
Dry, O_2	2 hours	.26
Dry, O_2	3 days	.24
Wet, vacuum	1 hour	.24
Wet, vacuum	1 day	.20
Wet, O_2	1 hour	.25
Wet, O_2	2 days	.19

[a] Time between irradiation and viscosity determination.
[b] In water at 25 °C.

These results in table 1 may be compared with those in table 2 for the irradiation of dextran triacetate. The triacetate was much more resistant to γ-ray degradation than is dextran. Oxygen enhanced the viscosity decrease as it also did in the case of dextran. Again, there was some evidence for a postirradiative viscosity decay.

TABLE 2. *γ-Irradiated dextran triacetate*

Dose rate 0.33 MR/hr

Conditions	Total dose MR	Storage time [a]	$[\eta]$ [b] (dl/g)
Unirradiated	0.00	.....	0.32
Dry, vacuum	7.92	1 day	.34
Dry, vacuum	7.92	8 days	.33
Dry, vacuum	25.6	1 day	.32
Dry, O_2	7.92	1 day	.31
Dry, O_2	7.92	60 days	.27

[a] Time between irradiation and viscosity determination.
[b] In 1,1′,2,2′-tetrachloroethane at 25 °C.

Reduced specific viscosities, $\frac{\eta_{sp}}{C}$, are plotted as a function of time in figure 1 for 10 percent and 2.75 percent aqueous solutions of dextran in air and vacuum. The sealed viscometers received doses of γ-rays at intervals A, B, C, D, and E of 1.73, 1.29, 5.73, 10.00 and 8.25 MR, respectively, at a dose rate of 0.34 MR/hr. Curves similar to the 2.75 percent solutions were obtained for concentrations of 1 percent and 0.3 percent.

All solutions exhibited a considerable viscosity decrease during the first irradiation interval, A. Augmentation of the reduced viscosity occurred during the latter periods of irradiation (D and E) in all cases in vacuum and in the more concentrated solutions in air. However, gel formation occurred only in the 10 percent solution in vacuum during irradiation period D. The gel softened during storage but was rehardened upon further irradiation (E). Further storage resulted in the slow but complete dissolution of the gel $\left(\frac{\eta_{sp}}{C} = 0.317 \text{ dl/g at } 148 \text{ days}\right)$ and continued decay to $\eta_{sp}/C = 0.282$ dl/g at 192 days.

The broken line in figure 1 represents the decay of an unirradiated 7.5 percent solution of dextran containing 1 *M* hydrogen peroxide.

The postirradiative viscosity decreases for 1 percent dextran solutions irradiated in air and vacuum for total doses of 1.73 and 15.3 MR are shown in figure 2. The viscosity decrease concurrent with irradiation was greater in air than in vacuum but the postirradiative decrease was greater in the evacuated systems. Presence of iron salts decreased the amount of postirradiative degradation in vacuum.

A 10.7 percent dextran solution, irradiated at a 28-fold higher dose rate (9.54 MR/hr) for a total dose of 19.08 MR did not form a gel. The intrinsic viscosity of the dextran changed from an initial value of 0.33 to 0.27 dl/g (in air) and to 0.23 in vacuum.

It may be concluded from the above results that the conditions conducive to gelation are high concentration, exclusion of air and a dose rate somewhat less than 10 MR/hr.

Irradiation of an evacuated dextran-water paste at 0.33 MR/hr for a total dose of 9.61 MR resulted in an insoluble material and a sol fraction of 0.23. The material had the same physical appearance as, for

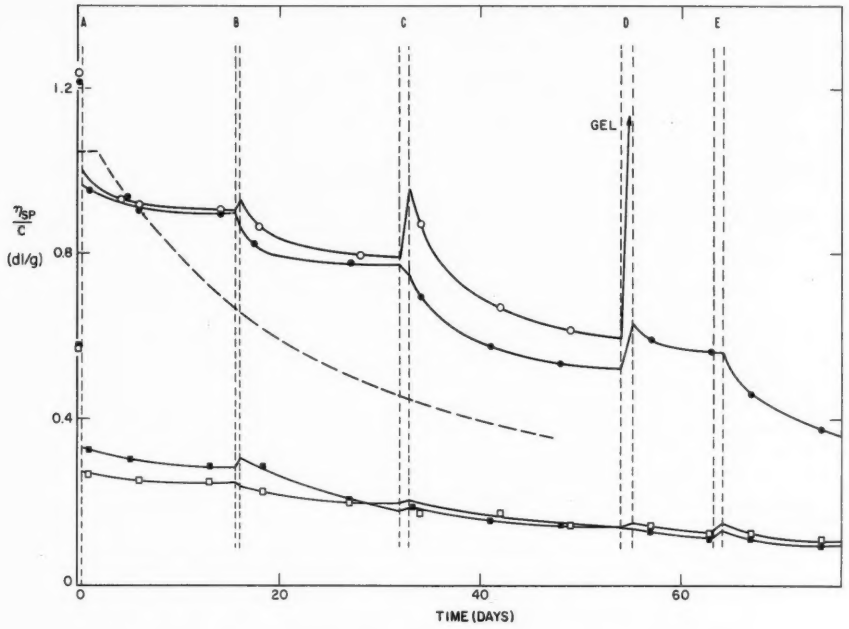

FIGURE 1. *Viscosities of intermittently irradiated aqueous dextran solutions.*

Rate of irradiation, 0.34 MR/hr. Total dose during irradiation intervals A, B, C, D, and E are 1.73, 1.29, 5.73, 10.0, and 8.25 MR, respectively.

○ 9.93%, vacuum
● 9.87%, air
□ 2.75%, vacuum
■ 2.75%, air
——— 7.5%, 1 *M* H_2O_2 (unirradiated).

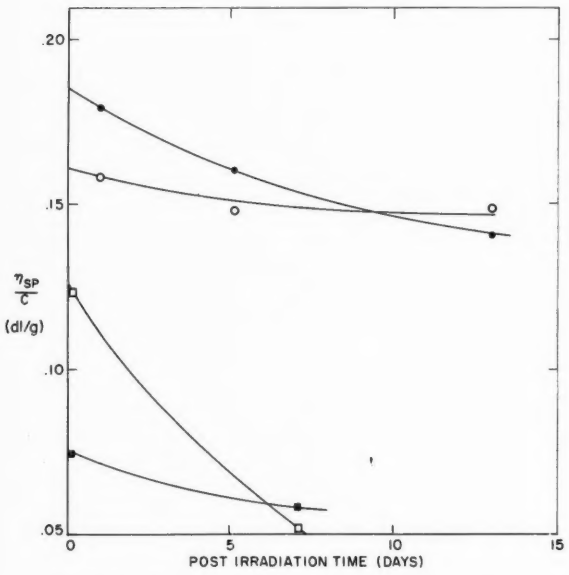

FIGURE 2. *Postirradiative viscosity decay of 1 percent aqueous dextran solutions.*

Rate of irradiation, 0.34 MR/hr. Initial η_{sp}/c, 0.42 dl/g.

○ vacuum, 1.73 MR
● air, 1.73 MR
□ vacuum, 15.3 MR
■ air, 15.3 MR.

example, cross-linked dextran prepared by heating dry dextran swollen in dimethyl formamide with epichlorohydrin and sodium hydroxide. Similar experiments with a glycerine-dextran paste and a 15 percent solution of dextran in glycerine did not produce any gel.

The intrinsic viscosity and number average molecular weight (from osmotic pressure) are given as a function of storage time in table 3 for a 19.1 percent solution of dextran irradiated at a rate of 0.33 MR/hr for a total dose of 21.45 MR. Here, the intrinsic viscosity increased upon irradiation while the number average molecular weight showed a slight decrease.

The number average molecular weights of two of the dextran solutions shown in figure 1 are given in table 4. The overall degradation was less in the more concentrated solution.

TABLE 3. *Number average molecular weight and intrinsic viscosity at 25 °C of 19.1% dextran in water irradiated under vacuum*

Dose rate = 0.33 MR/hr
Total dose = 21.45 MR

	M_N [a]	$[\eta]$ [b] (dl/g)
Before irradiation	28.100	0.33
Immediately after	24.100	.40
4 Days after	14.700	.36
24 Days after	13.200	.31

[a] From osmotic pressure measurement.
[b] In water at 25 °C.

TABLE 4. *Number average molecular weight of irradiated dextran solutions*

(See figure 1 for experimental conditions)
(Storage time, over two months)

Concentration (%)	Conditions	M_N[a]
9.87	air	9,600
2.75	vacuum	5,400

[a] From measurements of osmotic pressure, in water, 25 °C.

The electron spin resonance spectrum for dry dextran irradiated in a vacuum at a dose rate of 9.02 MR/hr for a total dose of 14.58 MR is shown in figure 3b. The general shape of the spectrum did not change upon several months' storage at room temperature. This spectrum may be compared with that in figure 3a obtained from dextran plus hydroxyl radical generated from titanous ion and hydrogen peroxide in an aqueous flow system [16].

A gel, formed by the irradiation of a concentrated dextran solution at a rate of 9.02 MR/hr for 1/2 hr in vacuum, gave no signal a few minutes after irradiation. This indicates that if radicals were present their concentration was less than 10^{-8} mol/liter.

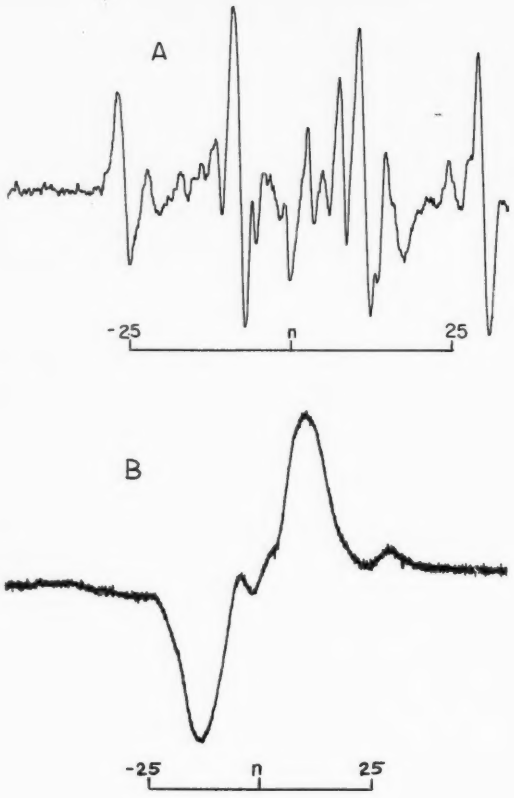

FIGURE 3. *The ESR spectra for γ-irradiated dextran.*
(a) Aqueous flow system—dextran plus hydroxyl radicals (Ti^{3+} and H_2O_2). (Ref. [16]).
(b) Dry-evacuated dextran; field increases to right.

4. Discussion

An increase in polydispersity and branching upon irradiation has been found both for solid dextran [6] and for aqueous solutions [3]; e.g., see table 3, where an increase in $[\eta]$ concurrent with a slight $\overline{M}_N$ decrease for the 19.1 percent solution demonstrates this observation. This suggests a near balance between scission and cross-linking in both cases. Because of these structural changes, no effort was made to convert viscosity values to molecular weights.

The postirradiative decay in solid dextran (table 1) and especially in solution (fig. 1) has not been taken into account by previous investigators and could materially affect many of their results and conclusions.

The calculated radical concentration in solid irradiated dextran [7] is of the same order of magnitude as the calculated chain scissions during the postirradiative decay. Therefore, much of this decay in the dry solid may be attributed to long-lived radicals. This decrease in degree of polymerization with time can result from the slow decay of radicals either by directly causing scission or by the production of water-labile linkages, or from the decrease in concentration of radicals potentially able to cross-link upon solution of the dextran. Hydrogen is evolved during the γ-irradiation of solid dextran [4, 7] so cross-linking-type radicals may be present in a steady-state concentration waiting to be unleashed by dissolution.

The above explanations are all compatible with the enhancement of postdecay by oxygen. Traces of water have little observable effect during irradiation, but cause a marked postirradiative viscosity decrease. This is attributed to the same reaction which causes a similar effect in solution.

The intrinsic viscosities for irradiated solid dextran triacetate in table 2 indicate a greater preponderance of cross-linking than is the case for solid dextran, although gelation did not occur under these conditions. It may be predicted that longer aliphatic esters will further augment cross-linking as the polymer side chains become more polyolefin-like in character.

The differential electron spin resonance spectrum shown in figure 3b for irradiated solid dextran is almost identical with that observed by Kinell at room temperature [7]. It contains mainly a poorly resolved doublet of about 15 G separation. Satellite structure and other complicating features indicate that several radical species are present.

A single fracture of each of the 22 bonds per dextran anhydroglucose unit would produce 44 radical species, viz, 10 H, 3 OH, 7 oxy-radicals ($\geqslant C-O\cdot$), 1 β

hydro-radical $\left(\begin{array}{c} \cdot \quad H \\ -C-C- \\ | \quad | \end{array}\right)$, 1 β,β,β' trihydro-radical $\left(\begin{array}{c} | \quad \cdot \quad H \\ -C-C-C- \\ H \quad | \quad H \end{array}\right)$, 1 α,α' dihydro-radical $\left(\begin{array}{c} H \\ -C\cdot \\ H \end{array}\right)$, 1 α,α,β trihydro-radical $\left(\begin{array}{c} H \quad H \\ -C-C\cdot \\ | \quad H \end{array}\right)$, 3 β,β' dihydro-radicals $\left(\begin{array}{c} | \quad \cdot \quad | \\ -C-C-C- \\ H \quad | \quad H \end{array}\right)$, and 17 α hydro-radicals, 11 of which have a single β hydrogen atom. Radicals formed by disproportionation and from ionic precursors may be added to these possibilities. Therefore, it is not surprising that the spectrum is ill-defined and appears to be a composite.

The "most probable" primary radical, $\left(\begin{array}{c} H \quad \cdot \quad | \\ -C-C-C- \\ | \quad H \quad | \end{array}\right)$, which should produce a four-line hyperfine split doublet, certainly does not dominate the spectrum. Kinell [7] attributes the spectrum to be mainly that of a single hydrogen with negligible interaction with β hydrogen as he interprets the smearing out of the structure at shorter wavelengths to be the result of a direct field effect. The ESR spectrum of γ-irradiated cellulose has many similar features [17]. The greater splitting found in highly oriented ramie cellulose [17] also suggests α hydrogen interaction.

An oxy-radical interacting strongly with a nearby proton would be expected to produce a broad symmetrical doublet and would have the thermal and oxidative stability found experimentally. Other evidence for such a radical is given in the subsequent discussion of irradiation in solution.

The electron spin resonance spectrum for dextran plus hydroxyl radicals in aqueous solution [16] is given in figure 3a. It is considered here because much of the reaction upon irradiation in dilute aqueous solution will be dextran interacting with OH, H, O_2H, etc., produced during the radiolysis of water. The spectrum is quite complicated and the lack of overall symmetry suggests that at least several radicals are present. The four principal lines have approximately 1,2,2,1 intensities and a 19 G splitting compatible with radicals of the type, $\begin{array}{c} | \quad \cdot \quad | \\ -C-C-C- \\ H \quad H \quad H \end{array}$. However, reactions such as, ROH $+ OH \longrightarrow R + H_2O + O$, are not as energetically favored as simple hydrogen abstraction from a secondary carbon atom. There is no good evidence for the spectrum predicted for radicals of the type

$$\begin{array}{c} H \quad \cdot \quad H \\ -C-C-C- \\ | \quad O \quad | \\ \quad H \end{array}.$$

The effect of γ-irradiation on aqueous solutions of polymers such as polyvinyl alcohol, polyethylene oxide, polypyrrolidine, etc., have been investigated in detail by Charlesby [18] and Sakurada [19]. These polymers have a minimum gelation dose at around 1 percent concentration which is not far above the critical concentration for gel formation. Dextran, on the other hand, degrades less rapidly in more concentrated solution. (See table 4.)

This anomalous behavior of γ-irradiated polysaccharide solutions may be explained by two separate effects. The first, a rapid postirradiative depolymerization reaction, will be discussed subsequently. The second concerns differences in the cross-linking process and its explanations are more speculative.

Cross-linking in aqueous solutions of polyvinyl alcohol, for example, is assumed to occur by hydrogen abstraction followed by $2R \longrightarrow R-R$ [18, 19]. (For dry samples of PVA, irradiated in air or vacuum, there is some evidence to the contrary. Periodate oxidation brings all samples to the same limiting DP, irrespective of dose, indicating that scission and cross-linking may occur mainly at 1,2 glycol groups [20].)

For dextran, cross-links of the type,

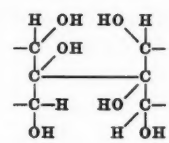

would be prohibitively restrictive sterically, so, unless pendant decyclitized anhydroglucose fragments are involved, the probable modes of connection are ether and/or peroxy linkages.

Thus, if the reaction in eq (1) can not occur, eqs (2–5) produce unstable peroxy links while eqs (6, 7) produce stable ether linkages.

$$R\cdot + R\cdot \longrightarrow R-R \tag{1}$$

$$R + O_2 \longrightarrow RO_2 \tag{2}$$

$$RO_2 + R \longrightarrow ROOR \tag{3}$$

$$RO_2 + RO_2 \longrightarrow ROOR + O_2 \tag{4}$$

$$RO + RO \longrightarrow ROOR \tag{5}$$

$$RO + R \longrightarrow ROR \tag{6}$$

$$RO + RO \longrightarrow ROR + O \tag{7}$$

Therefore, if ether links are formed, oxy-radicals must be present in the solution. If eq (6) represents the cross-linking mechanism, then R · must simultaneously be present. Equation (2) would then explain the inhibition of cross-linking by oxygen which occurs here and in the γ-initiated polymerization of glucose [21].

Possible sources of alkoxy radicals are the dissociation of peroxides [eq (8)] and disproportionation between R and O_2H radicals [eq (9)].

$$ROOR \longrightarrow 2RO \qquad (8)$$

$$R + O_2H \longrightarrow RO + OH \qquad (9)$$

Since cross-linking is dominant only at high concentrations the main source of RO may be the direct radiolysis of dextran. In dilute solutions the RO · concentration should be diminished by the presence of OH which may either combine or disproportionate with it.

$$RO + OH \left\{ \begin{array}{l} \longrightarrow ROOH \\ \longrightarrow ROH + O. \end{array} \right. \qquad (10)$$

Another mechanism of RO formation has been proposed by Grishina [22]. He concludes from the changes in the ESR spectrum of γ-irradiated solid PVA that $HO-\overset{|}{\underset{|}{C}}\cdot \longrightarrow H\overset{|}{\underset{|}{C}}O\cdot$ takes place at room temperature. (Such a rearrangement can explain the formation of deuterium containing hydrocarbon fragments [23] and the absence of D_2 in the evolved gases during the photolysis [23] and radiolysis [24] of cellulose containing OD groups.)

This rearrangement could occur either through an inter- or intra-molecular transfer,

$$H-\overset{\wr\wr}{\underset{\wr\wr}{C}}-OH + \cdot\overset{\wr\wr}{\underset{\wr\wr}{C}}-OH \rightleftharpoons H-\overset{\wr\wr}{\underset{\wr\wr}{C}}-O\cdot H-\overset{\wr\wr}{\underset{\wr\wr}{C}}-OH \rightleftharpoons$$

$$H-\overset{\wr\wr}{\underset{\wr\wr}{C}}-O\cdot + H-\overset{\wr\wr}{\underset{\wr\wr}{C}}-OH \qquad (11)$$

or in acid solution through a proton exchange reaction. Sugar solutions [25] and dextran solutions [5] show a marked increase in acidity ($pH \longrightarrow 3$) upon γ-irradiation.

Bonder et al., [21] find no indication of C–D bond formation from infrared investigation of the polymer formed during the irradiation of 0.1 percent glucose solutions in heavy water. Apparently the transfer reaction in eq (11) does not take place in dilute solution.

Kuri [26] points out the remarkable inertness to air and scavenger gases of radicals formed from polyhydroxy solids. Hydrogen-bonded alkoxy-radicals as in eq (11) should show such inertness. However Kinell [7] can find no evidence of deuteron-electron interaction in the ESR spectrum of γ-irradiated heavy-water-treated dextran.

Although the agency of oxy-radicals certainly has not been established, one of the many possible ether links formed by eq (6), a 3–6 link, is shown below.

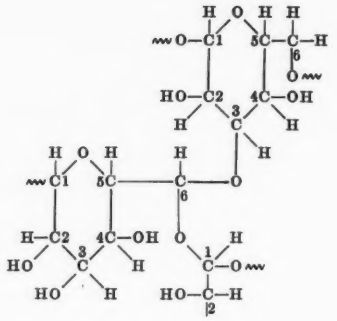

Equations (2–5) result in the formation of peroxy cross-links. The extreme lability of cross-links formed in aqueous solution as seen from the initial rapid viscosity decay in figure 1 and in table 3 suggests such a possibility. Comparison of the postirradiative decay of solutions in air and vacuum in figure 2 again points to the rapid deterioration of the cross-links formed in the evacuated solution. Although the viscosity decreases less in vacuum due, presumably, to concurrent cross-linking, both solutions tend toward the same ultimate viscosity upon storage.

The principle branching points in native dextran are 1,3 and 1,4-like linkages. If similar types of cross-links form in the irradiated dextran then a loose network with one or more anhydroglucose units in the connecting links would result. The 1,3 and 1,4 linkages in native dextran are more susceptible to acid hydrolysis than the normal 1,6 links [27]. However, free radical initiated cross-linking can not have the same formative mechanism as natural branching which is presumably a condensation process.

The production of three carbon atom dihydroxy acetone (from glyceraldehyde), two carbon atom glyoxal and four carbon atom erythrose from the γ-irradiation of glucose or dextran in dilute solution [5] suggests that hydrogen abstraction at the 2, 3, and 4-carbon atoms can result in scission plus carbonyl formation. These pendant side-chains could be the mode of cross-linking. Of the nine carbon-carbon-ether links, primary scission of four produce pendant groups; two, ring opening with greater geometrical flexibility and only the remaining three result directly in chain fracture.

We attribute the postirradiative decay of viscosity to the presence of hydrogen peroxide, the only long-lived product of the radiolysis capable of initiating further degradation. The viscosity decay of a 7.5 percent solution of dextran containing 1 *M* hydrogen peroxide, in figure 1, is similar to the postirradiative decay at comparable reduced viscosities.

Hydrogen peroxide is formed during the radiolysis of water and its production is augmented by the presence of carbohydrates in the solution [4,25]. Hydrogen peroxide is formed at an initial rate corresponding to $G(H_2O_2) = 1.8$ during the γ-irradiation of 0.19 percent aqueous dextran solution in oxygen and a slow postirradiative disappearance of the H_2O_2, not found when pure water has been irradiated, has been observed [5].

The marked lowering of viscosity of dextran and other polysaccharide solutions by very dilute hydrogen peroxide [28] has been classified as a hydrolysis reaction as shorter chain polysaccharides rather than oxidized products are formed [28].

The mechanism by which H_2O_2 catalyzes this nonoxidative cleavage is not established. Hydrogen peroxide is far too weak an acid for the likelyhood of an acid catalyzed hydrolysis. Likewise, it is difficult to envision a direct molecular attack by H_2O_2 which would not produce an oxidized product probably through some hydroperoxy intermediate.

Active species formed during the slow decomposition of H_2O_2 are probably responsible for the dextran cleavage. If OH radicals are formed in the initiation step, then the simplest chain mechanism for H_2O_2 decomposition is [29]

$$OH + H_2O_2 \longrightarrow H_2O + HO_2 \qquad (12)$$

$$HO_2 + H_2O_2 \longrightarrow H_2O + O_2 + OH \qquad (13)$$

eventually followed by second order termination by radical disproportionation or combination [29].

Dextran will compete with H_2O_2 for the OH radicals, eq (14)

$$\text{HCOH} + \text{OH} \longrightarrow \cdot\text{COH} + \text{H}_2\text{O} \qquad (14)$$

but the more sluggish dextran radicals may contribute more to the depropagation reaction as in eq (15),

$$\text{HCO}\cdot \text{ or } \text{HOC}\cdot + \text{H}_2\text{O}_2 \longrightarrow \text{HCOH} + \text{HO}_2 \qquad (15)$$

than to second order termination reactions, thus catalyzing the H_2O_2 decomposition. Also the reaction of dextran radicals with OH will not generally lead to stable chain-terminating products, e.g.,

$$\begin{aligned} RO + OH &\rightleftharpoons ROOH \\ &\rightarrow ROH + O. \end{aligned} \qquad (16)$$

Only estimates of the scission to cross-link ratio may be made as it is impossible to separate completely the viscosity change resulting from the postirradiative decomposition reaction from the scission and cross-linking occurring as a more immediate consequence of the γ-irradiation. However, the initial viscosity decrease for the 10 percent solution in vacuum in figure 1 indicates that the scission to cross-link ratio is greater than one [30] but less than two, the critical value above which gelation will not occur.

The low sol fraction of 0.23 for the evacuated water-dextran paste irradiated for a total dose of 9.61 MR suggests a ratio of scissions to cross-links of less than one for these conditions.

The authors thank R. E. Florin for his assistance in obtaining and advise in interpeting the electron spin resonance spectra.

5. References

[1] C. R. Ricketts and C. E. Rowe, Chem. Ind. (London), 46 (1951).
[2] F. P. Price, W. D. Bellamy, and E. J. Lawton, J. Phys. Chem. **58,** 821 (1954).
[3] R. Lang, E. S. Schmitt, E. J. Henley, and E. L. Gaden, U.S. AEC Rept. NY03320 (Part II) 50 (1956).
[4] G. Binder and A. Vincze, Magyar Tudományos Akad. Központi Fiz. Kutató Intézetének Közle-ményei **5,** 364 (1957).
[5] G. O. Phillips and G. J. Moody, J. Chem. Soc. 3534 (1958).
[6] K. A. Granath and P.-O. Kinell, Acta. Chemica Scandinavica **15,** 141 (1961).
[7] P.-O. Kinell, A. Lund, and T. Vänngård, Arkiv för Kemi **23,** 193 (1965).
[8] F. A. Bovey, The Effects of Ionizing Radiation on Natural and Synthetic High Polymers (Interscience, New York, 1958), pp. 197–203.
[9] P. Alexander and A. Charlesby, J. Chim. Phys. **52,** 691 (1955).
[10] K. Shinohara et al., Dai-2 kai Nippon Isotope Kaigi Hobunshu, p. 142 (1958); Proc. Inter. Conf. Peaceful Uses At. Energy, Geneva **29,** 186 (1958).
[11] A. Danno, J. Phys. Soc. Japan **13,** 614 (1958).
[12] I. Sakurada and S. Matsuzawa, Kobunshi Kagaku **17,** 268 (1960).
[13] A. Jeanes and C. A. Wilham, J. Am. Chem. Soc. **68,** 742 (1946).
[14] L. A. Wall and M. Magat, J. Chim. Phys. **50,** 308 (1953).
[15a] M. Wales, P. A. Marshall, and S. G. Weissberg, J. Polymer Sci. **10,** 229 (1953); F. R. Senti, N. N. Hellman, N. H. Ludwig, G. E. Babcock, R. Tobin, C. A. Glass, and B. L. Lamberts, J. Polymer Sci. **17,** 527 (1955).
[15b] H. B. Bull and B. T. Currie, J. Am. Chem. Soc. **68,** 742 (1946).
[16] F. Sicilio and R. E. Florin, private communication.
[17] R. E. Florin and L. A. Wall, J. Polymer Sci. **1A,** 1163 (1963).
[18] A. Charlesby and P. Alexander, J. Polymer Sci. **23,** 355 (1957).
[19] I. Sakurada and Y. Ikada, Bul. Inst. Chem. Research Kyoto Univ. **39,** 99 (1961); **40,** 1, 16, 25 (1962); **41,** 103, 114, 123 (1963).
[20] Y. Hirano, Bul. Chem. Soc. Japan **34,** 292 (1961).
[21] S. A. Bonder, P. M. Grant, M. Stacey, and R. B. Warder, J. Chem. Soc. 2648 (1959).
[22] A. D. Grishina, Doklady, Akad. Nauk. SSSR **150,** 809 (1963).
[23] J. H. Flynn and W. L. Morrow, J. Polymer Sci. **2A,** 91 (1964).
[24] M. Horio, R. Imamura and H. Mizukami, Bul. Inst. Chem. Research Kyoto Univ. **41,** 17 (1963).
[25] J. Osakabe and H. Yamashita, Radioisotopes **6,** 29 (1957).
[26] Z. Kuri, Y. Fujiwara, H. Ueda, and S. Shida, J. Chem. Phys. **33,** 1885 (1960).
[27] M. A. Swanson and C. F. Cori, J. Biol. Chem. **172,** 797 (1948).
[28] I. Levi and E. Lozinski, Canadian J. Biochem. Physiol. **33,** 448 (1955).
[29] D. J. Currie and F. S. Dainton, Trans. Faraday Soc. **61,** 1156 (1965).
[30] A. R. Shultz, P. J. Roth, and G. B. Rathmann, J. Polymer Sci. **27,** 495 (1956).

(Paper 71A1–433)

236-431 O-67-3

JOURNAL OF RESEARCH of the National Bureau of Standards—A. Physics and Chemistry
Vol. 71A, No. 1, January–February 1967

Synthesis of Poly-*p*-oxyperfluorobenzylene and Related Polymers. A Novel Synthesis of the Monomer 2,3,5,6-Tetrafluoro-4-trifluoromethylphenol*

Joseph M. Antonucci and Leo A. Wall

Institute for Materials Research, National Bureau of Standards, Washington, D.C. 20234

(August 15, 1966)

The synthesis and polymerization of 2,3,5,6-tetrafluoro-4-trifluoromethylphenol (heptafluoro-*p*-cresol) is described. The polymer, poly-*p*-oxyperfluorobenzylene (polyperfluoro-*p*-benzylene oxide), is probably formed through the perfluoro-*p*-quinonemethide intermediate obtained by the intramolecular loss of either hydrogen fluoride or a metal fluoride. The polymer has a structure analogous to that reported for the polymer derived from *p*-trifluoromethylphenol under similar conditions.

In the course of the synthesis of the monomer, heptafluoro-*p*-cresol, a novel synthetic method was discovered. The synthesis consists in the prior preparation of 1-*t*-butoxy-2,3,5,6-tetrafluoro-4-trifluoromethylbenzene and its subsequent thermal decomposition into the isobutylene and the desired cresol. Similarly, *N*-*t*-butyl-2,3,5,6-tetrafluoro-4-trifluoromethylaniline undergoes a similar liquid phase pyrolysis into isobutylene and 2,3,5,6-tetrafluoro-4-trifluoromethylaniline. However, during the course of this pyrolysis, practically all of the aniline undergoes polymerization with the concomitant loss of hydrogen fluoride. The polymer is formed by the same mechanism operative in the thermal polymerization of *p*-heptafluorocresol except that additional quantities of hydrogen fluoride can be eliminated from the $-NHCF_2-$ segments of the polymer chain thereby introducing $-N=CF-$ units into the polymer backbone.

Other *t*-butyl derivatives were synthesized and their thermal decomposition studied. Several possible mechanisms for the decomposition of these *t*-butyl compounds are considered.

Key Words: 1-*t*-Butoxy-2,3,5,6-tetrafluoro-4-trifluoromethylbenzene, perfluoro-*p*-quinonemethide, polymerization, poly-*p*-oxyperfluorobenzylene, pyrolysis, 2,3,5,6-tetrafluoro-4-trifluoromethylphenol.

1. Introduction

The need for new polymers that display both good stability and elasticity at elevated temperatures is well known. Although, at present, there appear to be no theoretical reasons to suppose that this elusive combination of properties can not be realized in a polymer, general experience associates good thermal stability with stiff, high melting, and usually intractable materials.

For example, in an earlier phase of this work [1],[1] it was reported that although perfluorophenylene ether polymers exhibit rubbery characteristics above 90 °C, their thermal stability is not exceptional. Conversely, polymers of the type polyperfluorophenylene show good thermal stability (about 600 °C in vacuo) but poor elasticity [2–7].

Since the ether linkage between polyfluoroaromatic rings resulted in a lowering of the thermal stability of the polyfluorophenylene type polymer, it was thought that the introduction of a different linkage or swivel group into the polymer chain might result in an elastic phenylene polymer of superior thermal stability. Thus such groups as shown below might prove useful as links in polyperfluorophenylene type polymers.

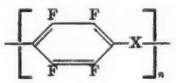

$$X = -CF_2-,\ -CH_2-,\ -\overset{\overset{O}{\|}}{C}-,\ -CH_2CF_2-,$$
$$-OCF_2-,\ -SCF_2-,\ -NCF_2-,$$
$$-CF_2OCF_2-,\ -CH_2OCH_2-,$$
$$-CF_2SCF_2-,\ -CH_2SCH_2-,\ \text{etc.}$$

This paper will deal primarily with the synthesis of poly-*p*-oxyperfluorobenzylene (polyperfluoro-*p*-benzylene oxide), where X is $-OCF_2-$, and the requisite monomer, 2,3,5,6-tetrafluoro-4-trifluoromethylphenol (heptafluoro-*p*-cresol) [2]

*Based on work supported by the Bureau of Naval Weapons, Department of the Navy.

[1] Figures in brackets indicate the literature references at the end of this paper.

[2] During the course of our investigation of the poly-*p*-oxyperfluorobenzylene polymer, V. C. R. McLoughlin and J. Thrower of the Royal Aircraft Establishment, Farnsborough, England informed us that they were engaged in closely related research. They have since published some of their results [8].

2. Historical Data

In 1947 R. G. Jones reported [9] that *p*-trifluoromethylphenol, upon treatment with cold dilute alkali or a trace of hydrogen fluoride, forms a polymer of the structure shown at the right of the following equation,

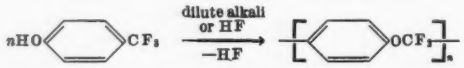

Similarly, *o*-trifluoromethylphenol is found to undergo facile polymerization under similar conditions to give an *ortho*-linked polymer as shown below,

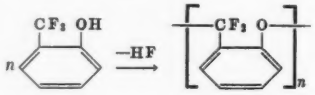

However, the *m*-trifluoromethylphenol, in contrast with the *ortho* and *para* isomers, is stable to aqueous alkali. No polymerization is evident even when the *meta* isomer is heated to 100 °C with 50 percent aqueous sodium hydroxide. The susceptibility of the *ortho* and *para* isomers of trifluoromethylphenol to polymerization by the elimination of a molecule of hydrogen or alkali fluoride seems to suggest the intermediacy in the reaction mechanism of such quasi-quinoidal structures as shown below,

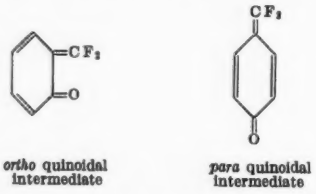

ortho quinoidal intermediate

para quinoidal intermediate

Since the *meta* isomer would be incapable of existing in a similar quinoidal form, its inability to undergo polymerization, at least by this mechanism, is explicable.

3. Synthesis of 2,3,5,6-Tetrafluoro-4-trifluoromethylphenol (Heptafluoro-*p*-cresol)

The facile polymerization of the *ortho* and *para* isomers of trifluoromethylphenol ($CF_3C_6H_4OH$), probably by means of a quasi-quinoidal intermediate, would seem to suggest that an analogous polymerization process would be followed by the *ortho* and *para* isomers of heptafluorocresol ($CF_3C_6F_4OH$).

Accordingly, in order to test this hypothesis and to prepare a *para*-linked polyoxyperfluorobenzylene polymer, a search was undertaken for a convenient synthesis of the monomer, 2,3,5,6 - tetrafluoro - 4 - trifluoromethylphenol (heptafluoro-*p*-cresol).

The successful synthesis of pentafluorophenol from hexafluorobenzene has been effected by several synthetic methods [10–13]. However, early attempts, both here and elsewhere [14], at the synthesis of heptafluoro-*p*-cresol from octafluorotoluene by these same synthetic methods were for the most part unsuccessful. For example, when octafluorotoluene was heated under reflux with a 25 percent aqueous potassium hydroxide solution for 24 hr no cresol was obtained, but instead a complex mixture of solids, some polymeric, was formed. Apparently, both the nuclear and benzylic fluorine atoms are susceptible to attack by the hot alkaline solution. Furthermore, any initially formed *ortho* and/or *para* heptafluorocresol would undergo polymerization under the conditions of the reaction. Finally, the reaction is further complicated by the fact that the poly-*p*-oxyperfluorobenzylene polymer, unlike the analogous poly-*p*-oxy-α,α-difluorobenzylene polymer, is subject to hydrolytic degradation [8]. This method of synthesis therefore, was abandoned.

Less direct methods such as the cleavage of 1-ethoxy-2,3,5,6-tetrafluoro-4-trifluoromethylbenzene with various acidic and basic reagents failed to yield the desired heptafluoro-*p*-cresol [14]. Also, heating octafluorotoluene with an excess of potassium hydroxide in *t*-butanol or in a mixture of pyridine and ethylene glycol was reported to give a complex mixture of products but none of the desired cresol [14]. In our hands, the method of synthesis employing potassium hydroxide in *t*-butanol was partially successful.

In addition to the formation of a polymeric solid (polyoxyperfluorobenzylene), a 57 percent yield of a liquid with a phenolic odor and boiling range of 140 to 155 °C was obtained. Vapor phase chromatographic analysis revealed the presence of three components with rather close retention times. One component comprised about 90 percent of the mixture. The two minor components were present in about equal quantities. Apparently all three of the possible isomers of heptafluorocresol had formed. The polymeric solid had arisen in all likelihood from the polymerization of the *ortho* and *para* isomers of heptafluorocresol. One of the minor components of the crude liquid product was shown to have the same retention time as an authentic sample of heptafluoro-*p*-cresol prepared by the novel synthetic method described below. Presumably, the other minor component is the *ortho* isomer. The major component, by a process of elimination, is then the *meta* isomer. However, although this structural assignment appears likely, it has not yet been confirmed by NMR analysis.

McLoughlin and Thrower [8] have studied this reaction more thoroughly and reported that under carefully controlled conditions (excess potassium hydroxide at 20 °C and long reaction times, or equivalent quantities of potassium hydroxide and octafluorotoluene at reflux temperature for short reaction times) a 70 percent yield of heptafluoro-*p*-cresol is obtained. The *para* cresol is purified by recrystallization of its ether soluble potassium salt using a solvent pair of ether/petroleum ether. The recrystallization procedure is necessary because of several contaminants

(heptafluoro-*o*-cresol and the *t*-butyl ethers of the cresols are mentioned as probable by-products of the reaction).

It was evident, therefore, that the standard methods available for the hydroxylation of polyfluoroaromatic compounds, when applied to octafluorotoluene, either gave polymeric solids and/or impure *para* cresol. A new synthetic reaction was needed that would lead to good yields of the pure *para* isomer of heptafluorocresol with a minimum of polymerization.

The procedure devised simply involves the prior synthesis of the highly branched ether, 1-*t*-butoxy-2,3,5,6-tetrafluoro-4-trifluoromethylbenzene and its subsequent thermal cleavage to 2,3,5,6-tetrafluoro-4-trifluoromethylphenol and isobutylene as shown below,

(1)

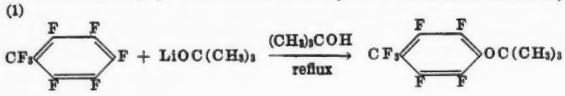

(2)

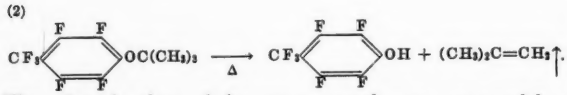

The *t*-butyl ether of the *para* cresol was prepared by refluxing equivalent amounts of lithium *t*-butoxide and octafluorotoluene in a suitable solvent or diluent. Excess *t*-butanol serves this purpose quite well. After all the solvent is removed by careful distillation, the *t*-butyl ether is pyrolyzed either in the liquid phase or in the vapor phase. The overall yield of heptafluoro-*p*-cresol from octafluorotoluene is of the order of 70 to 75 percent. Vapor phase chromatographic analysis indicates that the product is a single substance (no trace of the other two possible isomers of the cresol was found). Both infrared and nuclear magnetic resonance analyses of the compound indicated that the hydroxyl group is *para* to the trifluoromethyl group.

The critical step in this synthesis is the initial preparation of the ether, 1-*t*-butoxy-2,3,5,6-tetrafluoro-4-trifluoromethylbenzene free of two other possible isomeric ethers.

Several factors seem to insure this result. One involves the nature of the substrate molecule, octafluorotoluene. It has been demonstrated that pentafluorophenyl derivatives of the type C_6F_5X undergo nucleophilic displacement reactions predominantly by substitution *para* to X, unless X is a very strong electron-attracting or repelling substituent [10, 15]. Electron-attracting groups, such as the trifluoromethyl group, also should enhance the reactivity of the substrate molecule toward nucleophilic attack. The enhancement of nucleophilic reactivity of octafluorotoluene, however, is slight and appears to be confined to the already activated *para* position rather than being distributed over both the *ortho* and *para* positions as expected [14]. This is borne out by the fact that with the exception of the hydroxylation reactions previously discussed [8], no *ortho* products have been observed in the reported nucleophilic reactions of octafluorotoluene [14]. This lack of *ortho* substitution may arise from the following considerations: (1) A charge repulsion between the highly dense electron cloud provided by the trifluoromethyl group and the attacking nucleophile, and (2) the steric hindrance created by the bulk of the nucleophile and the crowded condition of the *ortho* positions.

The nature of the nucleophile also is an important factor in assuring the formation of highly pure *para* *t*-butyl ether. In general, a more highly basic nucleophile will lead to a higher degree of *para* substitution than a less basic nucleophile. Attack at the *ortho* positions by a highly nucleophilic reagent is much less favored because of the increased charge repulsion existing between the trifluoromethyl group and the nucleophile. Thus, the *t*-butoxy anion should, by reason of its great nucleophilicity, prefer to attack the unhindered *para* position of octafluorotoluene. Even the less nucleophilic ethoxy anion is reported to give only *para* substitution [14]. Moreover, the large bulky nature of the *t*-butoxy anion would further hinder attack at the *ortho* positions.

As mentioned before, it had been found difficult to effect the successful cleavage of the ethoxy ether of heptafluoro-*p*-cresol by chemical means [14]. However, the relative instability of other *t*-butyl ethers to both heat and acid [16–18] suggested that the *t*-butyl ether of heptafluoro-*p*-cresol might possibly undergo facile cleavage to the desired cresol. Indeed, it was found that by either liquid phase or vapor pyrolysis the ether undergoes cleavage to give heptafluoro-*p*-cresol and isobutylene.

4. Mechanism of Ether Cleavage

The formation of heptafluoro-*p*-cresol from its *t*-butyl ether can be accounted for by several different mechanisms.

One possible mechanism is similar to that proposed for the thermal dehydrohalogenation of alkyl halides [19], whereby the decomposition is viewed as a unimolecular process involving a four-membered cyclic-transition state such as that shown below.

Decomposition of Alkyl Halide

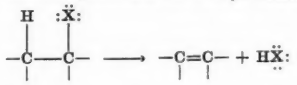

Decomposition of *t*-Butyl Ether

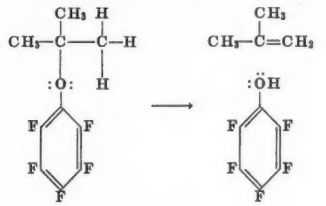

The thermal decomposition of alkyl vinyl ethers should bear at least a formal relationship to that of alkyl aryl ethers. One mechanism proposed for their thermal decomposition is unimolecular in nature and involves a six-membered cyclic transition state formed by a beta hydrogen of the alkyl group and the terminal carbon of the vinyl group [20].

Thermal Decomposition of Alkyl Vinyl Ether

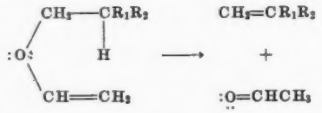

Recently, W. J. Bailey and D. McKenzie [21] proposed an analogous mechanism to explain the thermal decomposition of phenetole into phenol and ethylene.

Thermal Decomposition of Alkyl Aryl Ether

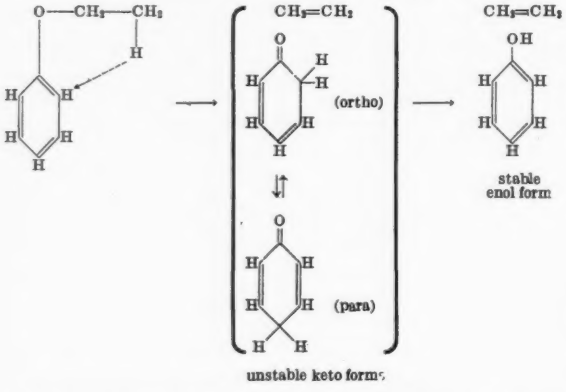

The transient cyclohexadienone intermediate, which can be viewed as the *ortho* and/or *para* tautomer of phenol, spontaneously reverts to the more stable enol form.

It seems likely that the same mechanism would be operative in the gas-phase pyrolysis of 1-*t*-butoxy-2,3,5,6-tetrafluoro-4-trifluoromethylbenzene. Thus the reaction would proceed as follows,

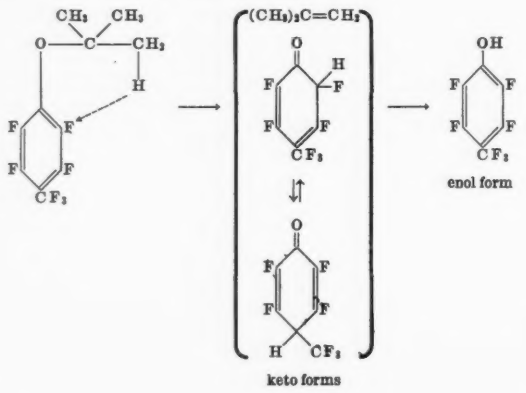

Although the isomerization of an *ortho* fluorine atom or the *para* trifluoromethyl group would seem to be possible, there is no evidence of the presence of either the hypofluorite, $CF_3C_6F_3HOF$, or of the ether, $C_6F_4HOCF_3$. The unfavorable energetics involved in the shifting to the oxygen either a fluorine atom or a trifluoromethyl group compared to that of shifting a hydrogen would seem to support these observations.

A slightly different representation of the transient intermediate would be that of a quasi-zwitterionic intermediate, formed by the protonation of the π-electron system of the phenyl ring by a beta hydrogen, while the oxygen simultaneously is transformed into the phenoxide form as shown,

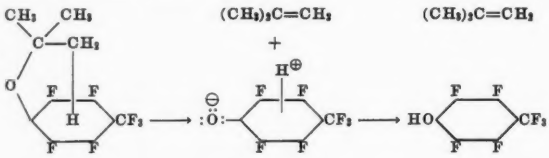

Such a species with disparate charges in close proximity would be expected to undergo instantaneous collapse to the stable cresol. The advantage of this type of representation is that it minimizes the disruption of the aromaticity of the benzene ring.

5. Polymerization of 2,3,5,6-Tetrafluoro-4-trifluoromethylphenol

The polymeric solid obtained from the reaction of potassium hydroxide and octafluorotoluene in *t*-butanol, as previously noted, arises from the polymerization of the potassium salts of the *ortho* and *para* isomers of heptafluorocresol. The polymer is a light-tan crystalline solid, which has a softening range of 65 to 70 °C. It is soluble in common organic solvents such as diethyl ether and acetone. Molecular weight determinations, as made by vapor phase osmometry (VPO), indicated a molecular weight range of 3000 to 4000.

When a pure sample of heptafluoro-*p*-cresol is heated with a 5 percent aqueous solution of sodium bicarbonate, a white solid soon begins to form. In one experiment the mixture was heated under reflux for 17 hr. A white crystalline solid was isolated. The molecular weight of the solid was of the same order of magnitude as that observed for the polymer obtained from the potassium hydroxide-*t*-butanol system. However, the softening range was somewhat higher, 70 to 75 °C. This discrepancy probably arises from the presence of *ortho* cresol units in the polymer obtained from the potassium hydroxide/*t*-butanol system.

The *para* cresol also undergoes polymerization by heating with a 1 percent aqueous potassium fluoride solution. After heating the mixture under reflux for 3 hr, a hard white solid was obtained with a softening range of 70 to 80 °C. The molecular weight (VPO), 4000 to 5000, was somewhat higher than that observed for the earlier polymer samples.

Still another method for the polymerization of the cresol is based on the technique discovered by Szwarc [22, 23] for the preparation of poly-*p*-xylylene. This method consists in the thermal dehydrogenation of the monomer, *p*-xylene, at high temperatures and at reduced pressures to an intermediate quinonedimethide, which on quenching undergoes spontaneous polymerization.

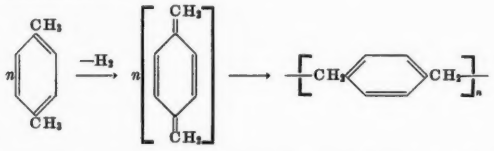

We were able to extend the application of this technique to the polymerization of both *p*-trifluoromethylphenol and heptafluoro-*p*-cresol by thermal dehydrofluorination under reduced pressure. The *p*-trifluoromethylphenol is simply passed through a quartz reactor tube heated in the vicinity of 900 to 950 °C and evacuated to a pressure of 1 to 5 mm. A tough slightly amber film is formed in the first trap held at room temperature. The polymer appears to be of higher molecular weight than that reported by Jones [9]. Infrared analysis of the film revealed little if any absorption in the hydroxyl region of the spectrum. The polymer also showed poor solubility in the common organic solvents (which may be indicative of high molecular weight and/or extensive cross-linking. Further study of the polymer is needed to establish which of these possible explanations is correct.

By analogy with the formation of poly-*p*-xylylene from *p*-xylene, the poly-*p*-oxy-α,α-difluorobenzylene polymer should form in a similar fashion.

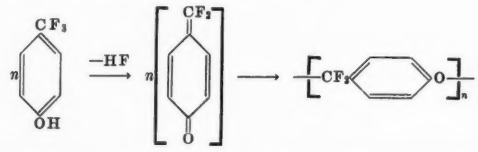

The heptafluoro-*p*-cresol, under similar conditions, also forms a polymer. However, the film produced in the first trap does not appear to be as tough as that which formed from the thermal polymerization of *p*-trifluoromethylphenol. An attempt to remove the film intact by prying it away from the glass trap resulted in its conversion to yellow waxy solid which softened at 110 to 120 °C.

6. Mechanism of Polymerization

The synthesis of the polymer, polyperfluorophenylene ether, proceeds via a nucleophilic attack of a growing phenoxide anion at nuclear carbon-fluorine position of a polyfluoroaromatic moiety capable of continuing the condensation process [1]. The same mechanism might be expected to apply to the polymerization of heptafluoro-*p*-cresol in solvent systems. However, the rather mild conditions that can be employed to effect polymerization would seem to argue for a different mechanism [8]. As in the case of the polymer derived from *p*-trifluoromethylphenol, $CF_3C_6H_4OH$, the polymerization proceeds by some reaction involving the phenoxide anion and the trifluoromethyl group. A likely mechanistic path is the formation of a *p*-quionoidal intermediate by chemical dehydrofluorination. The *p*-quinoidal intermediate, *p*-quinonedifluoromethide, is then the actual monomer which gives rise to the poly-*p*-oxy-α,α-difluorobenzylene polymer (see above). Additional support for the intermediacy of a *p*-quinoid transition state would seem to be offered by the successful polymerization of both *p*-trifluoromethylphenol and heptafluoro-*p*-cresol by thermal dehydrofluorination. However, further study is needed to ascertain conclusively that the same intermediate is involved in the two polymerization processes.

7. Thermal Stability

The thermal volatilization of several samples of poly-*p*-oxyperfluorobenzylene was investigated. Table 1 summarizes a typical experiment in which the polymer (a white crystalline solid, mp 70 to 75 °C, mol wt 4000 to 5000 as determined by vapor phase osmometry) was heated in vacuo successively for 1 hr at the indicated temperatures.

The results of this preliminary thermal analysis of the polymer would seem to suggest only a moderate order of thermal stability for poly-*p*-oxyperfluorobenzylene. However, since the polymer sample has a molecular weight of the order of 4000 to 5000, the possibility of some loss in weight through the evaporation of certain low molecular weight fractions must be considered in the evaluation of the results of this thermal analysis.

TABLE 1. *Thermal volatilization of poly-p-oxyperfluorobenzylene*

Wt	% Wt lost		Treatment	
	Incremental	Total	Time (hr)	Temp °C
18.35	0	0	0	
17.50	4.6	4.6	1	110
13.30	22.8	27.4	1	250
2.00	61.5	88.9	1	350

In their investigations, McLoughlin and Thrower [8] attempted to increase the molecular weight of a sample of poly-*p*-oxyperfluorobenzylene (prepared from a hot aqueous solution of the potassium salt of heptafluoro-*p*-cresol) by first treating the polymer with cold dilute alkali and then heating in vacuo to a temperature of over 200 °C. The original polymer was a pale amber brittle solid, mp 90 to 100 °C, with a reported molecular weight of 1500 to 3000.

The new polymer which displays rudimentary elastomeric properties above 120 °C, was found to undergo a rapid loss of weight above 300 °C in vacuo. Since the molecular weight of the new polymer was not given, the thermal stability reported for poly-*p*-oxyperfluorobenzylene should be considered only tentative. A more accurate determination of the thermal properties of poly-*p*-oxyperfluorobenzylene awaits the preparation of a truly high molecular weight polymer.

8. Synthesis of Related Monomers and Polymers

In order to study the scope of the synthetic method developed for the synthesis of heptafluoro-*p*-cresol, a similar synthetic approach was employed for the preparation of such known compounds as pentafluorophenol, pentafluoroaniline, 2,3,5,6-tetrafluoro-4-trifluoromethylaniline and 2,3,5,6-tetrafluoro-4-trifluoromethylthiophenol. The method of synthesis may be generalized as follows:

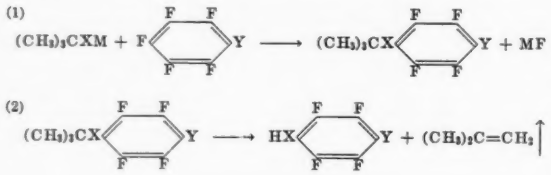

X=—O—, —S—, —NH—, etc.
Y=F, CF_3, etc.
M=H, Li, etc.

In general, derivatives of perfluorotoluene ($Y = CF_3$) can undergo subsequent polymerization by an elimination reaction of the type shown,

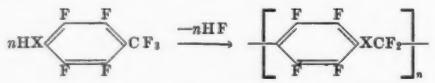

8.1. Attempted Synthesis of 2,3,5,6-Tetrafluoro-4-trifluoromethylaniline

An attempt was made to prepare 2,3,5,6-tetrafluoro-4-trifluoromethylaniline by the scheme outlined above. Octafluorotoluene and excess *t*-butylamine undergo reaction under relatively mild conditions (25 to 50 °C) to give the expected *N*-*t*-butyl derivative of heptafluoro-*p*-toluidine. Unfortunately, after the excess *t*-butylamine was removed, distillation at atmospheric pressure of the yellow liquid led to a vigorous decomposition of the pot residue. A copious evolution of isobutylene and hydrogen fluoride occurred as the temperature of the pot residue was gradually increased. Tatlow and co-workers [14] reported a boiling point of 180 °C for 2,3,5,6-tetrafluoro-4-trifluoromethylaniline. However, from our distillation only a few drops of the aniline were obtained. Most of the product consisted of a brownish-red polymeric mass. Apparently the temperature of the pot had reached the decomposition point of the heptafluoro-*p*-toluidine. Apparently the solid material is the poly-*p*-aminoperfluorobenzylene polymer. It was soluble in most organic solvents. On standing, further emission of hydrogen fluoride gas was evident. The solid had a wide softening range (80 to 135 °C). The polymerization would appear to follow the scheme indicated below,

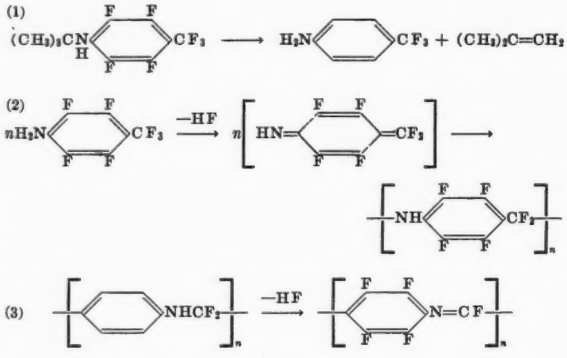

The secondary dehydrofluorination (reaction 3) is not unexpected since the juxtaposition of a $-NH_2$ or $>NH$ group next to a carbon carrying fluorine atoms is known to be an unstable arrangement of atoms.

Not necessarily all of the basic units need undergo this intramolecular secondary dehydrofluorination. Intermolecular secondary dehydrofluorination is also a possibility. However, since the great bulk of the polymer is soluble, this cross-linking reaction would appear to be at minimum.

8.2. Synthesis of Pentafluorophenol and Pentafluoroaniline

As expected, hexafluorobenzene undergoes a similar reaction with lithium *t*-butoxide in *t*-butanol, and the expected *t*-butyl ether of pentafluorophenol, 1-*t*-butoxy-2,3,4,5,6-pentafluorobenzene, is formed in low conversion but good yield after 24 hr of reflux. Presumably higher conversions can be obtained by suitable modifications of the reaction conditions (e.g., longer reaction times and/or higher reaction temperatures.

The *t*-butyl ether of pentafluorophenol is distillable at atmospheric pressure in contrast to that of the heptafluoro-*p*-cresol, which undergoes liquid phase pyrolysis when subjected to atmospheric distillation. However, vapor phase pyrolysis of 1-*t*-butoxy-2,3,4,5,6-pentafluorobenzene does result in its decomposition into the phenol and isobutylene.

A similar result was obtained in the preparation of pentafluoroaniline via its *N*-*t*-butyl derivative. Hexafluorobenzene and excess *t*-butylamine were heated in a bomb at 200 °C for 1 hr. A low conversion but good yield of the expected *N*-*t*-butyl-2,3,4,5,6-pentafluoroaniline was obtained. The same reaction with octafluorotoluene succeeds to higher conversions under considerably milder conditions. Conversely, the product, *N*-*t*-butyl-2,3,4,5,6-pentafluoroaniline, can

be distilled under atmospheric pressure with only slight decomposition. As already noted the *N*-*t*-butyl derivative of heptafluoro-*p*-toluidine undergoes rapid decomposition when distillation under atmospheric pressure is attempted. Vapor phase pyrolysis of the *N*-*t*-butyl derivative of pentafluoroaniline, as expected, leads to the formation of pentafluoroaniline and isobutylene.

8.3. Reaction of Octafluorotoluene With Lithium *t*-Thiobutoxide

An attempt was made to prepare 2,3,5,6-tetrafluoro-4-trifluoromethylthiophenol by the method outlined above. The *t*-butyl derivative of heptafluoro-*p*-thiocresol, *t*-butyl-2,3,5,6-tetrafluoro-4-trifluoromethylphenyl sulfide, was prepared in 75 percent yield by the reaction of lithium *t*-thiobutoxide with octafluorotoluene in excess *t*-butanol. In contrast to the *t*-butyl derivative of heptafluoro-*p*-cresol and heptafluoro-*p*-toluidine, the *t*-butyl derivative of heptafluoro-*p*-thiocresol can be distilled at atmospheric pressure without decomposition. A preliminary study of its behavior when subjected to vapor phase pyrolysis also indicates a greater thermal stability compared to the other *t*-butyl derivatives. Only trace quantities of what appears to be the thiocresol were observed by gas liquid chromatographic analysis of various pyrolyzates obtained in the temperature range 400 to 500 °C. At these temperatures most of the *t*-butyl sulfide was recovered unchanged. However, at higher temperatures extensive decomposition occurred to give a foul-smelling liquid mixture of several components. Again, only trace quantities of the expected thiocresol were present. Apparently the *t*-butyl derivative of heptafluoro-*p*-thiocresol undergoes thermal decomposition by a different mechanism than that observed for the other *t*-butyl derivatives. From the lack of any appreciable quantities of thiocresol present in the pyrolyzates, it would appear that perhaps the initial step in the decomposition involves predominantly scission at the aryl carbon-sulfur bond to give the radicals shown below:

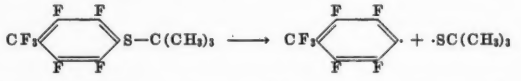

These radicals can then undergo the usual secondary radical reactions such as disproportionation, combination and transfer. However, further study of this decomposition reaction is required to establish the exact mechanistic process involved.

9. Experimental Procedure

9.1. Synthesis of 2,3,5,6-Tetrafluoro-4-trifluoromethylphenol

a. Reaction of Octafluorotoluene With Potassium Hydroxide in *t*-Butanol

A mixture of 6 g (0.021 mole) of octafluorotoluene, 3.8 g (0.068 mole) of potassium hydroxide, and 50 ml of freshly distilled *t*-butanol was heated under reflux for 14 hr under an atmosphere of nitrogen. The *t*-butanol was removed by flash vacuum distillation (1 mm pressure). The residue in the flask consisted of a solid mass. Water was added to this residue and after vigorous agitation, the insoluble portion was separated by filtration. The light tan solid was washed repeatedly with hot water to remove any residual soluble material, such as potassium fluoride and the potassium salts of any phenolic products. The aqueous filtrate was acidified with concentrated hydrochloric acid and then extracted with ether several times (continuous extraction may have been preferable at this point). The ether extracts were combined, dried, and then subjected to atmospheric distillation using a 6-in glass-helix-packed column. After the ether had been removed, the residue was distilled without the column to give 3.4 g (57% yield) of a clear, phenolic-smelling liquid with a wide boiling range (140–155 °C). Vapor phase chromatographic analysis of this liquid, using two 10 ft by 1/4 in columns packed with 20 percent SE 30 on 60–80 mesh acid-washed Chromosorb W and 20 percent neopentyl gylcol succinate on 60–80 mesh acid-washed Chromosorb P, respectively, revealed that the product consisted of three components with close retention times. The principal component comprised about 90 percent of the mixture and appears to be the *meta* isomer of heptafluorocresol (2,3,4,6-tetrafluoro-5-trifluoromethylphenol). One of the minor components had the same retention time as an authentic sample of heptafluoro-*p*-cresol. The filtered solid, after drying, weighed 2.5 g and had a melting range of 65 to 70 °C. It was soluble in ether, acetone, and tetrahydrofuran, and probably is a mixed copolymer of the *para* and *ortho* heptafluorocresols. Molecular weight determinations using vapor phase osmometry indicated a molecular weight range of 3000 to 4000. The solvent used was anhydrous tetrahydrofuran.

b. Reaction of Octafluorotoluene With Lithium *t*-Butoxide in *t*-Butanol

A mixture of 11 g (0.047 mole) of octafluorotoluene and 3.8 g (0.047 mole) of lithium *t*-butoxide in 30 ml of *t*-butanol was heated under reflux for 15 hr. After removal of the insoluble solids (lithium fluoride), the solvent (*t*-butanol) was removed by distillation at atmospheric pressure through a 6-in glass-helix-packed column. After the bulk of the *t*-butanol was removed, the pot temperature was raised to permit distillation of the higher boiling *t*-butyl ether. Shortly thereafter a vigorous reaction ensued and a gas with an olefinic odor (iosbutylene) was emitted through the distillation head. The reaction was allowed to continue while a water-white liquid with a phenolic odor was collected, bp 142 to 144 °C. The yield of liquid product was 8 g (72% yield). The liquid product was shown by vapor phase chromatography (using the two columns mentioned previously) to consist of but one substance. Near-infrared analysis of the type reported for similar halophenols [10] appears to suggest either a *para* or *meta* orientation of the hydroxyl

group with reference to the trifluoromethyl group. Nuclear magnetic resonance analysis confirms the *para* orientation. A solid residue of about 2 g remained in the distillation flask.

9.2. Polymerization of 2,3,5,6-Tetrafluoro-4-trifluoromethylphenol

a. Polymerization With Dilute Aqueous Sodium Bicarbonate

About 1 g of the heptafluoro-*p*-cresol and 15 ml of 5 percent aqueous sodium bicarbonate were heated under reflux for 17 hr. The white polymeric solid was separated by filtration, washed about ten times with large quantities of hot water, and then allowed to suck-dry overnight. The solid was then dissolved in diethyl ether; the solution was filtered and the ether removed under vacuum distillation (15 mm) using moderate heating. The dried crystalline solid, about 1 g, had a softening point of 70 to 75 °C.

b. Polymerization With Dilute Aqueous Potassium Fluoride

About 0.5 g of the heptafluoro-*p*-cresol was added to 10 ml of a 1 percent aqueous solution of potassium fluoride. The mixture was refluxed with stirring (magnetic bar) for 3 hr. A hard, white solid was formed along with a white, tacky substance. The hard, white solid was separated from the tacky material, washed with copious amounts of water, filtered and dried under vacuum.

After this treatment it exhibited a tough crystalline appearance and had a softening range of 70 to 80 °C. The tacky solid had a phenolic odor and probably represented a lower molecular weight fraction.

c. Thermal Polymerization

It was found that the method developed by Szwarc [22, 23] to polymerize *p*-xylene to poly-*p*-xylylene by vacuum pyrolysis could be extended to both *p*-trifluoromethylphenol and heptafluoro-*p*-cresol. By use of the apparatus and technique described below, it was possible to polymerize *p*-trifluoromethylphenol at 820 °C and 1 to 5 mm pressure to a tough, yellowish transparent film. The film was insoluble in common organic solvents (ether, acetone, benzene, etc.) and the infrared analysis showed little, if any, unreacted hydroxyl groups. The same method was employed with heptafluoro-*p*-cresol. About 1 g of heptafluoro-*p*-cresol was allowed to vaporize under a slow strean of nitrogen over a 30 min period through a quartz tube (48 cm by 1.5 cm) heated to 980 °C and evacuated to a pressure of 1 to 5 mm. The quartz reactor was placed vertically in a heated zone of about 25 cm and was connected at the lower end to three traps in a series. The first trap was a 50 ml sidearm, round-bottom flask maintained at room temperature. The other two traps were cooled in a slurry of solid carbon dioxide and acetone. The quartz tube was connected at the upper end through a capillary bore stopcock to a 5 ml sidearm, round-bottom flask with a nitrogen inlet tube attached to its sidearm.

A yellow film was deposited on the sides of the first trap. The second trap contained an acid smelling liquid which appeared to be primarily unconverted cresol. The third trap contained only a trace of volatile material. The yellow film crumbled to a waxy solid when it was removed from the sides of the flask with a spatula. The solid softened over the range 110 to 120 °C and appeared to lose little weight up to 300 °C. The conversion to polymer was of the order of 20 to 30 percent.

The pyrolysis of heptafluoro-*p*-cresol at lower temperatures (below 800 °C) gave little polymer formation. Somewhat higher temperatures (800 to 850 °C) resulted in the formation of a greasy solid in low conversion. Higher temperatures above 950 °C tended to give some carbonization in the tube as well as polymer formation. The optimum conditions for this type of polymerization are still under investigation.

9.3. Synthesis of Other Monomers

a. Attempted Synthesis of 2,3,5,6-Tetrafluoro-4-trifluoromethylaniline

A mixture of 20 g (0.085 mole) of octafluorotoluene and 20 g (0.27 mole) of *t*-butylamine was heated under reflux for 2 hr. After the mixture had cooled, approximately 40 ml of water was added to the mixture to remove the amine salt. The organic layer was separated and dried over anhydrous sodium sulfate. Any unreacted *t*-butylamine was removed by distillation. Further distillation at atmospheric pressure caused the yellow liquid to undergo a vigorous reaction which was accompanied by the evolution of isobutylene and hydrogen fluoride. A brownish-red glassy solid formed in the bath. The heating was continued until the temperature reached about 190 °C. A small amount of pungent liquid was collected and tentatively identified as 2,3,5,6-tetrafluoro-4-trifluoromethylaniline. The material in the etched flask was scraped out to give a hard crystalline brownish red solid. The solid dissolved in ether, acetone and hexafluorobenzene. It melted over a wide range 80 to 135 °C to a viscous yellow liquid. Preliminary studies indicate the polymer has a thermal stability comparable to that observed for the poly-*p*-oxyperfluorobenzylene polymer.

A sample of the polymer was heated under reflux for 45 min with a 5 percent aqueous solution of potassium carbonate. The solid was filtered, washed with copious quantities of hot water and finally dried in vacuo overnight. At this point the solid had a tan crystalline appearance and a softening point of 120 to 140 °C.

b. Reaction of Hexafluorobenzene With Lithium *t*-Butoxide in *t*-Butanol

A mixture of 18.6 g (0.1 mole) of hexafluorobenzene and 8.0 g of lithium *t*-butoxide in 50 ml *t*-butanol was heated under reflux for 24 hr. The mixture was allowed to cool and then diluted with 50 ml of *n*-

pentane. The insoluble lithium fluoride was removed by filtration. The filtrate was washed several times with water and dried over anhydrous sodium sulfate. The pentane was removed by careful distillation through a 10-in glass-helix-packed column. Approximately 10 g of hexafluorobenzene was recovered unchanged along with a few ml of *t*-butanol. The high boiling liquid in the pot was then carefully distilled at atmospheric pressure through a 6-in. glass-helix-packed column to give 6 g of a clear colorless liquid, bp 175 to 177 °C. The *t*-butoxy-2,3,4,5,6-pentafluorobenzene was shown by vapor phase chromatographic analysis (10-ft by 1/4-in 20% SE column) to be better than 99 percent pure. The small amount of lower boiling impurity present had the same retention time as pentafluorophenol. The conversion to product was only 25 percent but the yield of *t*-butyl ether was 55 percent. Vapor phase pyrolysis of the *t*-butyl ether (400 to 550 °C) resulted in the formation of pentafluorophenol and isobutylene, as determined by vapor phase chromatographic and infrared analyses.

c. Reaction of Hexafluorobenzene With *t*-Butylamine

A mixture of 5.8 g (0.08 mole) of *t*-butylamine and 7.4 g (0.04 mole) of hexafluorobenzene was placed in a platinum lined bomb of 80 ml capacity. The bomb was sealed and heated to 200 °C for 1 hr. After the bomb had cooled, the contents were poured into about 50 ml of water. The organic layer was separated, washed several times with water and finally dried over anhydrous sodium sulfate. After the removal by distillation of any excess *t*-butylamine and any unreacted hexafluorobenzene (6 g), 1.6 g of clear, colorless liquid, bp 190 to 193 °C, was obtained. During the final stages of the distillation, the pot residue began to decompose and the odor of isobutylene was prevalent. Vapor phase chromatographic analysis revealed that the liquid product was composed of one component (only a trace pentafluoroaniline was present). The conversion was about 20 percent but the yield based on unrecovered hexafluorobenzene was 70 percent. Vapor phase pyrolysis (400 to 550 °C) resulted in the formation of pentafluoroaniline and isobutylene, as determined by vapor phase chromatographic and infrared analyses.

d. Reaction of Octafluorotoluene With Lithium *t*-Thiobutoxide

A mixture of 60 ml of *t*-butanol and 0.8 g (0.1 mole) of lithium hydride was stirred for 1 hr. To this mixture was added 9.0 g (0.1 mole) of *t*-butylmercaptan. The mixture was heated under reflux for 1 hr. Approximately 23.6 g (0.1 mole) of octafluorotoluene was added to the refluxing mixture. The mixture was then heated under reflux for an additional 7 hr. After the mixture cooled to room temperature, the solids were removed by filtration. The filtrate was fractionated through 10-in glass-helix-packed column to give, after removal of the *t*-butanol and a small amount of octafluorotoluene (0.5 g), 23.0 g of a pale yellow liquid, bp 212 to 214 °C. Vapor phase chromatographic analysis (10-ft by 1/4-in 20% SE 30 column) revealed that the *t*-butyl-2,3,5,6-tetrafluoro-4-trifluoromethylphenylsulfide was of high purity (> 99%).

Vapor phase pyrolysis at relatively low temperatures (400 to 500 °C) resulted in the recovery of the *t*-butylsulfide virtually unchanged. Pyrolysis at higher temperatures (above 500 °C) resulted in a complex mixture of products and some carbonization. Very little, if any, of the heptafluoro-*p*-thiocresol was formed (vapor phase chromatographic analysis indicated that perhaps a small amount—less than 1%—of the thiocresol was formed).

10. References

[1] W. J. Pummer and L. A. Wall, J. Res. NBS **68A** (Phys. and Chem.) No. 3, 277 (1964).
[2] M. Hellmann, A. J. Bilbo, and W. J. Pummer, J. Am. Chem. Soc. **77**, 3650 (1955).
[3] E. J. Fear, J. Thrower, and M. A. White, Intern. Congr. Pure Appl. Chem. 19th, pp. A5–103, London, 1963.
[4] J. Thrower and M. A. White, Abstract Paper 148th Am. Chem. Soc. Meeting, p. 19K (Aug.–Sept. 1964).
[5] G. M. Brooke, R. D. Chambers, J. Heyes, and W. K. R. Musgrave, J. Chem. Soc. 731 (1964).
[6] W. J. Pummer and L. A. Wall, Abstract paper 150th Am. Chem. Soc. Meeting, p. 10K (Sept. 1965).
[7] J. M. Antonucci and L. A. Wall, ibid., p. 11K.
[8] V. C. R. McLoughlin and J. Thrower, Chem. and Ind. (London), 1557 (1964).
[9] R. G. Jones, J. Am. Chem. Soc. **69**, 2346 (1947).
[10] L. A. Wall, W. J. Pummer, J. E. Fearn, and J. M. Antonucci, J. Res. NBS **67A** (Phys. and Chem.) No. 5, 481 (1963).
[11] J. M. Birchall and R. N. Haszeldine, J. Chem. Soc. 13 (1959).
[12] M. Hellmann, E. Peters, W. J. Pummer, and L. A. Wall, J. Am. Chem. Soc. **79**, 5654 (1957).
[13] E. J. Forbes, R. D. Richardson, M. Stacey, and J. C. Tatlow, J. Chem. Soc. 2019 (1959).
[14] D. J. Alsop, J. Burdon, and J. C. Tatlow, J. Chem. Soc. 1801 (1962).
[15] G. M. Brooke, J. Burdon, and J. C. Tatlow, J. Chem. Soc. 802 (1961).
[16] J. T. Barr, K. E. Rapp, R. L. Pruett, C. T. Bahner, J. D. Gibson, and R. H. Lafferty, J. Am. Chem. Soc. **72**, 4480 (1950).
[17] H. C. Brown and P. Tarrant, J. Am. Chem. Soc. **73**, 1781 (1951).
[18] D. C. England, L. R. Melby, M. A. Dietrich, and R. V. Lindsey, J. Am. Chem. Soc. **82**, 5116 (1960).
[19] A. Maccoll, Theoretical Organic Chemistry, Kekulé Symp., p. 24 (Butterworth Scientific Publications, London 1959).
[20] W. J. Bailey and J. DiPietro, Abstract Paper 134th Am. Chem. Soc. Meeting, p. 41T (Sept. 1958).
[21] W. J. Bailey, private communication.
[22] M. Szwarc, J. Chem. Phys. **16**, 128 (1948).
[23] M. Szwarc, J. Polymer Sci. **6**, 319 (1951).

(Paper 71A1–434)

JOURNAL OF RESEARCH of the National Bureau of Standards—A. Physics and Chemistry
Vol. 71A, No. 1, January–February 1967

Preparation, Purity, and Homogeneity of NBS Standard Samples 705 and 706, Polystyrene

D. McIntyre*

Institute for Materials Research, National Bureau of Standards, Washington, D.C. 20234

(September 14, 1966)

The state-of-art in the measurement of the molecular weights of macromolecules is discussed. The preparation of polystyrene standard samples 705 and 706 is described. The results and the description of the carbon-hydrogen microanalysis, the ash determination, the lithium analysis, and the volatiles determination are given. The sampling methods for determining the homogeneity of 705 and 706 are presented. Some evidence of heterogeneity appeared to be present, particularly for lot 705, but the experiment did not provide conclusive evidence of heterogeneity of the material.

Key Words: Ash content, elemental analysis, homogeneity, lithium content, molecular weights, polymer, preparation, purity, sampling, standard sample, volatile content.

1. Introduction

For some time there has been a need for standard samples of polymers beyond the usual scientist-to-scientist exchange of interesting and/or well-characterized polymers. This need has been met by several undertakings in recent years. The Commission on Macromolecules of the International Union of Pure and Applied Chemistry in 1950 undertook the distribution of four samples of polystyrene with a request that recipient laboratories report their data on the characterization of the molecular weight. The polystyrene samples were fractions from two polymers obtained by the thermal polymerization of bulk styrene. One fraction was taken from a polymer formed at 15 percent conversion of the monomer; the other three fractions were from a polymer prepared by a bulk polymerization carried to a very high conversion. The characterization results, reported by H. P. Frank and H. Mark [1],[1] are summarized in table 1. The weight-average molecular weights (M_w) of the three fractions reported are approximately 1×10^5, 3.5×10^5 and 10×10^5. The distribution of the molecular weights in the respective fractions are all relatively large; the M_w/M_n ratio is approximately 1.4, where M_n is the number-average molecular weight. For all of the fractions the range of reported M_n's determined by osmotic pressure measurements in the same solvent is always greater than 30 percent of the mean value, comparing only the results from more than four laboratories using the same conditions of measurement. The M_w's, where there are more than four results under the same conditions, give a range that is always greater than 20 percent of the mean value. The intrinsic viscosities show much less variance in general, although the results in methyl ethyl ketone (MEK) are often more scattered than those in toluene. The viscosities of the MEK solutions have an average range which is 14 percent of the mean, whereas the range in toluene is 9 percent. Some of the measurement problems were attributed to the large polydispersity of the polymers.

TABLE 1. *Summary of the IUPAC molecular weight intercomparison* [1]

Fraction	Solvent	No. of reports	Average	Range	Range as a % of average
Osmotic pressure measurements: M_n					
I	Toluene	6	1,000,000	790,000–1,110,000	32
II	MEK	4	235,000	199,000–280,000	34
III	MEK	5	680,000	474,000–852 000	55
IV	MEK	5	86,000	77,500–100,000	38
Viscosity measurements: $[\eta]$ml/g					
I	MEK	6	103.5	90–111	16
I	Benzene	4	221	211–230	9
I	Toluene	13	204	174–216	21
II	Toluene	4	104	102–106	4
II	MEK	5	61.7	54–69	23
III	Toluene	4	228	223–234	5
III	MEK	5	115	110–122	10
IV	Toluene	4	48	47–49.5	5
IV	MEK	5	30.2	29–31.5	8
Light scattering measurements: M_w					
II	MEK	5	328,000	288,000–360,000	21
III	MEK	5	960,000	840,000–1,050,000	22
IV	MEK	4	110,300	96,000–124,000	25

*Present address: Department of Chemistry, The University of Akron, Akron, Ohio.

[1] Figures in brackets indicate the literature references at the end of this paper.

In 1956 Milkovich, Szwarc, and Levy [2] pointed out a new kinetic mechanism that could lead to narrowly dispersed molecular weights in polymers. McCormick, Brower, and Kin [3] scaled up the above laboratory preparation to produce 300-g quantities of polystyrene. This group was later able to produce several pounds of narrowly dispersed polystyrene by a similar technique. On behalf of the Commission on Macromolecules of the IUPAC, H. Mark in 1960 undertook to distribute three new polystyrene samples of narrow molecular weight distribution prepared by the polymerization technique described in [3]. The M_w's of the samples to be intercompared were nominally described as 8.2×10^4, 2.39×10^5, and 3.56×10^6. The polydispersity (M_w/M_n) was stated to be 1.05, 1.08, and 1.24. In all cases the polydispersity of the test samples is much less than in the previous intercomparison. The final results of the exchange program are not yet published, but the results of the characterization of the lowest two molecular weights have been reported to the Commission and are to be published [4]. In order to assess in a cursory fashion the development of the measurement techniques, selected data from one solvent or one wavelength are presented in table 2. The reported values for the viscosity, osmotic pressure, and light-scattering measurements are in much better agreement than in the previous intercomparison (table 1), although the range of the viscosity, $[\eta]$, and light-scattering measurements is not much different in the two intercomparisons. The standard deviation calculated for all of the reported results is smaller in the second IUPAC intercomparison. There is a marked improvement in the standard deviation of the osmotic pressure measurements; however, the results do indicate that the determination of these parameters is beset by considerable uncertainty even in laboratories specializing in macromolecular research.

TABLE 2. *Preliminary results on second IUPAC molecular weight intercomparison [4]*

Sample	Property	No. results	Average	Range	Range % of average
S_{102}	$[\eta]$, toluene	14	39 ml/g	38.3 − 40.5	5
	M_n	8	78,000	$75 - 82.3 \times 10^3$	9
	M_w	8	88,000	79 − 114	40
S_{111}	$[\eta]$, toluene	12	78 ml/g	76.5 − 80.3	5
	M_n	8	210,000	$196 - 225 \times 10^3$	14
	M_w	8	233,000	196 − 270	32

Early in 1963 the National Bureau of Standards issued two standard polystyrene samples to help standardize the measurement of certain macromolecular properties. Over the course of several years the NBS improved the capability of measuring the molecular weights of high polymers. With the cooperation of H. W. McCormick and his group at Dow Chemical Company in Midland, it became possible to obtain in 1961 a sufficient quantity of narrowly dispersed polystyrene to justify an effort to certify molecular measurements on a polymer sample that could be issued to all scientists. It was decided that two polystyrene samples would be certified and made available through the NBS Standard Sample program, one sample with a narrow molecular weight distribution, and the other with a broad molecular weight distribution. The first sample, being a new and laboratory scale preparation, would be distributed in limited quantities; the latter sample, being a pilot plant or commercial preparation, would be available in larger quantities.

Both samples were intended for instrument calibrations, but the narrow molecular weight distribution sample could eliminate certain experimental difficulties connected with the presence of appreciable amounts of low molecular weight polymer like the unavoidable diffusion of low molecular weight molecules across the semipermeable membrane during osmotic pressure measurements. The dispersion of molecular weights about the mean is sufficiently small so that most molecular properties are almost those of a monodisperse high polymer. In contrast, the polymer sample of broad molecular weight distribution would much more closely be related to commercially available polymers. The use of such samples would help control laboratory uses and also serve to define the properties of polydisperse materials.

The determination of molecular weights and molecular weight distribution can be roughly separated into three classes based on the existing experimental techniques and their limitations of measurement. Some of these limitations have been discussed earlier [5]. There is a low molecular weight range ($\sim 10^4$), a moderate molecular weight range $(0.4\text{–}40) \times 10^5$, and a high molecular weight range ($> 4 \times 10^6$). The middle of the moderate range is experimentally very favorable, compared to the other ranges. In consideration of the known measurement techniques in 1958, the measurement program at the NBS was aimed at the improvement of technqiues to determine accurate molecular weights in the molecular weight range of 50,000 to 500,000 [5]. Later emphasis was to be given to the development of special techniques for M_n determinations in the low molecular weight range. It was felt that though the high molecular weight range had tremendous importance for biological systems, it would be deferred until the low molecular weight range could be measured accurately. The commercial importance of both the low and moderate molecular weight range polymers implied that both broad and narrow molecular weight polymer standards should ultimately be available for both ranges of molecular weight.

The choice of the polymer to be issued as a standard is dictated by two simple questions: (1) Is there a polymer in the correct molecular weight range which can be supplied in a narrowly dispersed and also a broad dispersed sample, and (2) is this polymer reasonably stable and soluble in ordinarily used organic solvents? Polystyrene satisfies both of these requirements. A water-soluble polymer would have many additional advantages for those scientists interested in studying naturally occurring polymers. However many syn-

thetic polymers, though not water soluble, are easily dissolved and stable in simple organic solvents. Polystyrene is not crystalline when it is derived from the usual free-radical or homogeneous anionic polymerization of styrene, yet it can be dissolved and handled in solution at high temperatures. Thus it can serve to standardize high temperature molecular weight measurements for crystalline polymers which are not soluble at lower temperatures as well. The unknown stereo-regularity of polystyrene is its only serious disadvantage for a macromolecular standard. Nevertheless, unknown stereo-regularity should not affect any molecular weight measurements, although fractionation efficiencies and transport properties could, to some small extent, be affected.

The results of the envisioned program to measure some of the molecular properties of a narrow and broad MWD polystyrene samples at moderate molecular weights will be presented in a series of papers. This first paper deals with the preparation, purity, and homogeneity of the samples referred to as NBS Polystyrene Standard Sample 705 and 706, respectively. Successive papers will discuss other aspects of the solution properties of these samples, such as the extinction coefficient, the partial specific volume, the osmotic pressures, turbidities, viscosities, and concentration gradients in a centrifugal field, measured at various initial concentrations in different solvents, as well as the phase diagrams and fractionation curves determined by separations from two coexisting liquid phases.

2. Preparation of Samples

2.1. Polystyrene Standard Sample 705

The styrene was polymerized in benzene solution using butyl lithium by McCormick and co-workers [3]. The polymer was precipitated from the benzene solution by adding methanol. The precipitate was then dried in a vacuum oven for 15 to 20 hr at 75 °C. The fibrous precipitate was then densified by calendering momentarily at 175 °C. The polymer was then ground, injection molded at a high temperature, and cut into pellets weighing approximately 10 mg.

2.2. Polystrene Standard Sample 706

Pure styrene was thermally polymerized at 140 °C to a conversion of 37.2 percent. The polymer was carefully heated and the residual monomer was pumped off at an elevated temperature. The polymer was then injection molded and cut into pellets weighing approximately 80 mg.

3. Sampling of Polymers

Polystrene 705—The entire original sample, shipped in a carton, was placed in three amber jars. From each of these three jars, two 2-g samples were removed, one about one-fourth the distance from the top of the jar, and the other about one-fourth the distance from the bottom of the jar. These six samples from six different locations constituted the samples for the study of the heterogeneity of the polymer, referred to later as heterogeneity samples. After the study of heterogeneity was concluded, two 50-g representative samples of the entire supply of polymer were formed by emptying and rebottling the entire sample while retaining one scoop from every twenty scoops, each scoopful weighing 10 g. These pooled and homogenized samples were called final samples. Measurements of the molecular properties were then made on these final samples.

Polystyreme 706—Six 10-g samples were taken from the barrel of material to test the homogeneity of the sample. Each sample was taken from a different level of the barrel and at a different angular position with respect to the center of the barrel. The first sample was taken near the top center and the other samples from positions which formed a spiral path of constant descent. Two 500-g final samples were formed by collecting alternately 20 g of polymer from 250-g scoopfuls, while emptying the barrel. These pooled samples were then thoroughly mixed and called final samples. The measurements of the molecular properties were made on these final samples.

4. Heterogeneity of Samples

Polystyrene 705—Since the polymer standards were initially planned for molecular weight calibrations, the tests for homogeneity of the sample were based on the simplest measurements related to molecular weight, namely, the measurement of the intrinsic viscosities in a good solvent and the osmotic pressures in an ideal solvent. The percent of volatiles in the samples also was measured for samples taken from the top and the center of the barrel of Polystyrene 706; however, the differences in volatile content were not significant compared to the experimental error in the determination.

Cyclohexane at 35 °C was considered to be an ideal solvent for these samples, and the number-average molecular weight was therefore determined simply by the van't Hoff relation ($M_n = RTc/\pi$) using a single, fixed concentration, where π is the osmotic pressure, c is the concentration, T is the absolute temperature, and R is the gas constant. The osmotic pressures of two independently made solutions of each heterogeneity sample were determined in cyclohexane at 35 °C. The osmotic pressure measurements were made with 600 gel cellophane in osmometers described in reference [7]. Previous work [8] had established the fact that the variation of ideality with molecular weight was very small, unless the end groups were quite different chemically from the backbone.

The intrinsic viscosities of the heterogeneity samples were determined in benzene at 25 °C with an Ubbelohde viscometer having a flow time of approximately 200 sec, and a maximum shear rate of ~ 1700

sec^{-1}. The intrinsic viscosities were calculated by an extrapolation to zero concentration of the reduced specific viscosities for one initial concentration, ~ 0.3 g/dl, and two serial dilutions.

Table 3 reports the M_n from osmotic pressure measurements and the intrinsic viscosities of the heterogeniety samples. The sample numbers, (1, 2, 3), refer to the storage bottles and top (T) and bottom (B) to the location of the sample. The intrinsic viscosity of B–1 was determined three times because the average of the first two values was so much higher than the other averages, and an error in weighing was suspected. The third value also is high. An analysis of variance was performed to evaluate the variances within and between samples. For both the viscosity and the osmotic pressure measurements, the variability between different locations was found to be somewhat larger than that between duplicate measurements carried out on the same sample. However, the ratio of the between-to-within variability failed to reach significance at the 5-percent level. Thus, the experiment did not show conclusive evidence of heterogeneity of the material.

TABLE 3. *Tests for homogeneity of polystyrene 705**

Sample	M_n	[η]. (ml/g) benzene at 25 °C
T-1	170,000; 171,200	75.1, 74.2
T-2	170,800; 170,800	74.3, 74.3
T-3	171,300; 171,400	74.6, 74.3
B-1	172,500; 171,900	74.8, 75.1, 76.0
B-2	172,200; 174,800	74.4, 74.0
B-3	172,700; 175,600	73.8, 73.6

*These values do not represent the values listed on the certificate. The certificate value was determined from a larger number of determinations on a pooled sample.

Polystyrene 706—The intrinsic viscosities were measured in an Ubbelohde viscometer, having a flow time of 200 sec for benzene and a maximum rate of shear of 1700 sec^{-1}, respectively. The intrinsic viscosities were determined by extrapolations of the reduced specific viscosity measured on a solution of polymer in benzene made by weight (~ 0.3 g/dl), and two other solutions made by serial dilutions of the original concentration in the viscometer. The intrinsic viscosities for different heterogeneity samples in benzene at 25 °C are reported in table 4. An analysis of variance was performed and indicated no conclusive evidence of heterogeneity. This may be due to the fact that the error in the determination of the molecular weight by the simple intrinsic viscosity measurements is large enough to obscure any small heterogeneity in the lot of material. No further attempts at heterogeneity corrections were made. A number-average determination probably would have been revealing, but at the time of the measurements no suitable combination of membrane and osmometer was capable of measuring the osmotic pressure in a way that would give meaningful information on the low molecular weight species that are present.

TABLE 4. *Test for homogeneity of polystyrene 706**

Sample (in sequence)	[η]. (ml/g) benzene at 25 °C
1	94.2, 94.6
2	92.6, 94.4
3	94.7, 93.2
4	92.5, 93.8
5	94.2, 92.8
6	93.1, 94.1

*These values do not represent the values listed on the certificate. The certificate value was determined from a larger number of determinations on a pooled sample.

5. Chemical Analysis

The styrene used in the polymerization of both 705 and 706 was commercial feedstock styrene. Five-milligram portions of polystyrene from the final sample of both 705 and 706 were analyzed for carbon and hydrogen. The lithium content of sample 705 was determined on the ash by flame photometry. The values are close to the limit of detection. Table 5 lists the average experimental values and the assumed carbon and hydrogen percentages calculated from the formula C_8H_8. The total percent of carbon, hydrogen, and ash accounts for all of the material within experimental error. The carbon and hydrogen analyses are in good agreement with the formula C_8H_8. (The actual value in both cases is very close: 705 is $C_8H_{7.86}$ and 706 is $C_8H_{7.97}$.)

The ash content was independently determined by firing in a muffle, using a 1-g and 2-g sample of 705, and a 2.5-g and 4.7-g sample of 706. Only 10 and 20 μg of ash were found in the samples of 706. The ash content is very low for 706. The ash content of the 705 is surprisingly high, considering the care necessary to carry out such polymerizations. The lithium content of ~ 0.005 percent is approximately what is expected for a polymerization involving one lithium atom for every growing chain, i.e., 6.94/170,900 ~ .004 percent.

TABLE 5. *Chemical analyses of 705 and 706*

	Theoretical	705	706
% Carbon	92,257	92,2 {92,07, 92,23, 92,22}	92,0$_5$ {92,0$_5$, 92,0$_5$}
% Hydrogen	7.743	7.7 {7.75, 7.69, 7.74}	7.7 {7.75, 7.63}
% Ash		0.036 {0.034, 0.037}	< 0.001
% Lithium		0.005 {0.004, 0.005}	
Total		99.9	99.8

6. Volatiles

The percent by weight of volatiles in the two standard samples was more difficult to determine than might

be expected. Since both samples were prepared in their final form in the same manner, namely, devolatilization at high temperatures and reduced pressure, followed by extrusion, it is not surprising that both samples contain appreciable amounts of volatiles. For 705 the volatiles would primarily be benzene, for 706 the volatiles would be styrene. Both volatile contaminants are good solvents for the polymer and both have the same molecular size as the polymer repeating unit so that the diffusion of the last traces of the residual volatiles might be very difficult below the glass temperature of polystyrene (90 to 100 °C).

A drying apparatus had been constructed which allowed relatively large samples (~ 100 mg) to be dried under a high vacuum (~ 10^{-6} mm Hg) for long times at various temperatures. One difficulty with any simple drying technique is the necessity of crushing the pellets in air to allow better diffusion of the trapped solvent out of the polymer into the cold trap. Table 6 reports the results of drying the polymer several times under different conditions of time and temperature. Neither the length of time (greater than 18 hr), nor the temperature (greater than 100 °C), made much difference in the weight loss. The average value is calculated for the weight loss at 100 °C over approximately 20 hr. If the crushing of 706 is continued vigorously for a long time, the weight loss is found to be less than 0.8 percent.

TABLE 6. *Volatiles in 705 and 706 by weight loss measurements*

Run	% Loss	Time (hr)	Temp. °C
Sample 705			
1	0.49*	18	100
	.49	42	100
	.51	24	115
2	.37*	24	100
3	.69*	22	100
(Ave)*	0.52		
Sample 706			
1	0.68*	18	100
	.67	42	100
	.73	24	115
2	1.01*	24	100
3	0.67*	18	100
4	.91*	18	100
(Ave)*	0.82		

Samples of both 705 and 706 were heated to 100 °C in separate closed containers for 8 hr. The containers were then cooled in liquid nitrogen in order to pump off the residual air. The containers were then warmed to room temperature, and the volatilized material was analyzed mass spectrometrically. Under these conditions the weight loss was very small (~ 0% for 705 and 0.01% for 706). The analysis of the volatiles produced in the above treatment showed mainly water (92 mole percent in 705, 97 in 706) with traces of benzene in 705 (8 mole percent) and styrene in 706 (3 mole percent). The major contaminants, benzene and styrene, are those volatiles to be expected from the sample preparation, although the adsorbed water is the predominant species pumped off at room temperature. The determination of the residual styrene by a spectrophotometric analysis is discussed in a succeeding paper.

An analysis of the thermal degradation of both 705 and 706 appears in reference [9]. The weight loss in achieving the lowest temperatures reported for the kinetic studies (~ 350 °C) was about 0.5 percent for 705 and 1 percent for 706.

7. Packaging

The packaging was carried out to avoid those pellets which had some gross physical imperfections, such as occluded foreign matter. Sample 705 is packaged in 2-g lots in amber bottles to minimize degradation. Sample 706 is packaged in 20-g amounts. A small quantity has been stored in a freezer and will be compared in a few years with samples stored at room temperature.

The author thanks the following scientists both in and outside of the NBS who have helped in this standards effort: H. McCormick and R. Boyer of the Dow Chemical Company, who arranged to make the polymers available to the NBS program; G. M. Kline and N. Bekkedahl for initiating the program; J. Mandel for the statistical analysis of some of the data; R. A. Paulson for the chemical analyses; and J. H. O'Mara, D. E. Roberts, J. McElwain, and D. Starr for many of the measurements and the detailed handling procedures.

8. References

[1] H. P. Frank and H. Mark, J. Polymer Sci. **10,** 129 (1953).
[2] R. Milkovich, M. Szwarc, and M. Levy, J. Am. Chem. Soc., **78,** 2656 (1956).
[3] H. W. McCormick, F. M. Brower, and L. Kin, J. Polymer Sci. **39,** 87 (1959).
[4] Private communication, Dr. Mark.
[5] D. McIntyre, Unsolved Problems in Polymer Science, NAS–NRS Publication No. 995 (1962).
[6] Donald McIntyre, Symposium on Plastics Testing and Standardization, ASTM Special Technical Publication No. 247 (1958).
[7] Donald McIntyre, J. Res. NBS **62,** 63 (1959) (RP 2931).
[8] Donald McIntyre, J. H. O'Mara, and B. C. Konouck, J. Am. Chem. Soc. **81,** 3498 (1959).
[9] L. A. Wall, S. Straus, J. H. Flynn, D. McIntyre, and R. Simha, J. Phys. Chem. **70,** 53 (1966).

(Paper 71A1–435)

236–431 O–67–4

JOURNAL OF RESEARCH of the National Bureau of Standards—A. Physics and Chemistry
Vol. 71A, No. 1, January–February 1967

Large-Scale, Preparative Paper Chromatography

Harriet L. Frush

Institute for Materials Research, National Bureau of Standards, Washington, D.C. 20234

(September 8, 1966)

Simplified techniques are described for the use of heavy papers in large-scale, preparative chromatography. A new technique is illustrated for nondestructively locating bands of compounds on wet chromatograms. Capacities and behavior characteristics of Whatman seed-test paper and Whatman No. 17 paper are illustrated.

Key Words: Chromatography on seed-test paper, large-scale paper chromatography, radioactive carbohydrates, use of heavy papers in preparative chromatography.

1. Introduction

Most of the techniques that have been described for large-scale, preparative paper chromatography depend on an increase in bulk through the use of many closely pressed layers of a thin paper [1].[1] Some of these methods require the tedious loading of each sheet, and others tend to suffer from a lack of uniformity in the movement of compounds throughout the bulk. The latter disadvantage has been overcome in one commercial apparatus by empirically regulating the pressure [2].

In 1957, Brownell and co-workers [3] described a large-scale, heavy-paper technique for preparative chromatography in which, after a preliminary treatment, the paper is used in essentially the customary manner. The authors stated that the dense paper (Whatman seed-test paper, 1.5 mm thick) is capable of separating 0.5 to 3.0 g of material per large sheet (18×22 in), depending on the spread in R_f values.[2] They also described a method for nondestructively locating the separated bands by staining a "print" obtained by pressing a sheet of thin paper against the wet chromatogram.

However, despite the unusually high capacity of the heavy paper, and the inherent advantages of paper chromatography over column chromatography, the techniques described by Brownell et al. have not been widely adopted, presumably because of several difficulties encountered in using the heavy paper. Thus, (a) the edge of the paper must be provided with a machine-stitched stirrup or loop (for supporting the paper on a rod) and with a stitched wick of a thinner paper.[3] (b) Because the seed-test paper is not pure cellulose, it must be chromatographically washed with dilute acid and with water; this treatment requires several days. Finally, (c) the movement of the bands through the paper is not as uniform as that in papers made of pure cellulose.

Despite these disadvantages, heavy-paper chromatography has found extensive application in this laboratory in the large-scale separation of mixtures of carbohydrates and related compounds, both radioactive and nonradioactive. Certain simplified techniques, described below, have facilitated application of the paper to problems of separation and may prove useful in other laboratories. Chief among these techniques is a more precise method for nondestructively locating the bands of compounds on the developed chromatograms.

The techniques described are equally applicable to Whatman No. 17 paper, and, on this paper, afford satisfactory separations of 0.2 to 0.6 g per large sheet. The No. 17, like the seed-test paper, is a "fast" paper whose properties are also improved by use of a thinner wick.

2. Preparation of the Heavy Paper

A strip of Whatman No. 3MM paper (7×18 in) is loosely machine-stitched with white, mercerized, heavy-duty thread along each short side, about 2 in

[1] Figures in brackets indicate the literature references at the end of this paper.

[2] The use of this paper for chromatography had been suggested earlier [4].

[3] The use of a wick of a thinner paper to retard the movement of a solvent through a "fast," thick paper had been described [5]. Slower movement of a solvent affords more complete equilibration and sharper separation.

A patent [6] describes the use of a seed-test paper, *without* a wick, for rapid, large-scale purifications; for example, 100 sheets (3 mm thick) were used in purifying 220 g of aniline in 6 hr. It appears doubtful that compounds having similar R_f values can be separated by such rapid chromatography.

from the edge. The strip is then folded as shown in figure 1, to form both a stirrup and a wick. The 18-in edge of the seed-test paper is softened by momentarily dipping it in water, and the excess is thoroughly blotted. The dampened edge is inserted about ¾-in into the folded strip, and the two papers are twice machine-stitched together. During washing of the paper (and, occasionally, during development of a chromatogram), it is desirable to use an auxiliary wick to facilitate flow of solvent. However, the second wick need not be sewn, but may be added as shown in figure 2. The additional wick is inserted near the base of the stirrup, and functions as well as if it had been sewn in place. To facilitate dripping of the solvent, the lower edge of the heavy paper is conveniently serrated by dampening it as described above and tearing off small pieces of the paper so as to form an irregular edge.

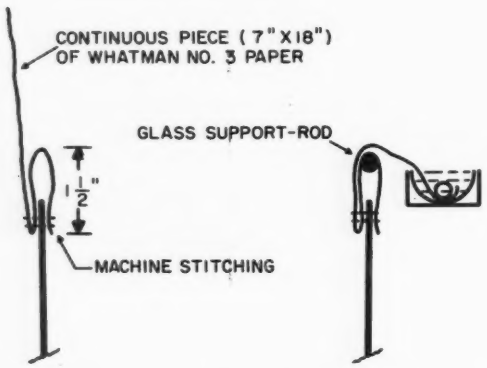

FIGURE 1. *Preparation of stirrup and wick (cross section).*

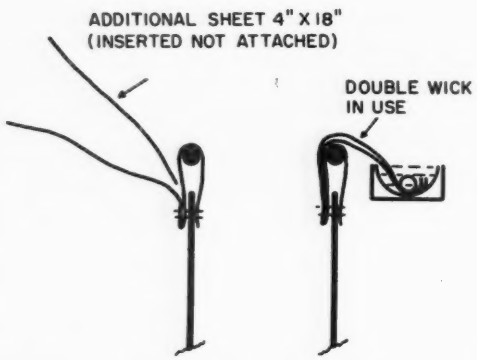

FIGURE 2. *Addition of auxiliary wick in order to increase flow of solvent.*

Papers are usually prepared in groups of eight, and simultaneously washed in a commercial chromatography cabinet having four troughs, each of which holds the wicks from two papers. Four external, 500-ml, leveling bulbs supply the solvent through four holes in the cabinet lid, each hole being situated above the middle of a trough. The papers are washed, with 0.01 *N* hydrochloric acid and then with water, as described by Brownell et al., except that the total time of washing is reduced from seven to four days (two for each solvent). The sheets are air-dried, and strips (1 in or more in width) are cut from each long edge that appears to be thin; the stirrups and wicks are trimmed to match. If the papers are used within two or three weeks after preparation, no further washing is necessary. If they are kept for longer periods, an additional washing is given, before use, with the solvent to be employed in elution of the bands (frequently, 50% aqueous methanol). This washing removes some color that develops in the paper on standing.

Before application of the sample, a narrow band (< 0.5 cm wide) is drawn with a pencil about 2 cm below the stirrup and on *both* sides of the paper. Aqueous or alcoholic solutions of mixtures (as much as 2 ml) are applied to this band by means of a commercial loading pipet having a 1-ml bulb and a short tip of capillary tubing. The pipet affords excellent control of the solution, which flows only on contact of the tip with the paper. The band is loaded from both sides of the paper, which is then air-dried for several hours.

Development with the solvent of choice is carried out in the chromatography cabinet with the aid of the leveling bulbs, and the use of either one or two wicks per sheet. Two wicks are employed with a slow-moving solvent, such as one containing *tert*-pentyl alcohol; only one wick is necessary with less viscous solvents, such as ethyl acetate or 2-butanone.

Preparation of the No. 17 or similar paper is simpler. The same stirrup and wick are stitched to the paper (which need not be previously moistened), but the addition of the auxiliary wick is unnecessary. The paper is used without prior purification or trimming.

3. Nondestructive Location of Bands on the Developed Chromatogram

When development is judged to be satisfactory, the wet chromatogram is laid on a glass plate in a well ventilated hood, and is overlaid with a sheet of thin paper (such as Whatman No. 1) carefully positioned at the origin. A small, plastic wheel[4] is then drawn down the paper in a series of straight lines (see fig. 3). By pressing the thin paper into the wet chromatogram, the wheel causes good (and fairly uniform) absorption of the solvent in narrow, vertical lines (about 3 mm wide). The chromatogram is temporarily returned to the cabinet, and the tracing may be sprayed with a suitable color reagent. Because the color is intense

[4] This is a pastry wheel, available in stores selling kitchenware.

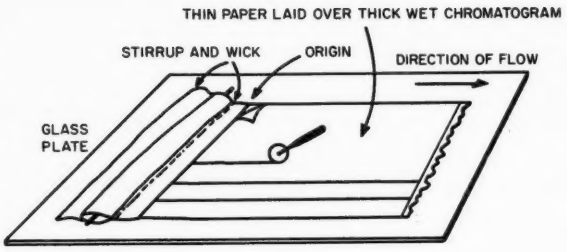

FIGURE 3. *Preparation of tracing.*

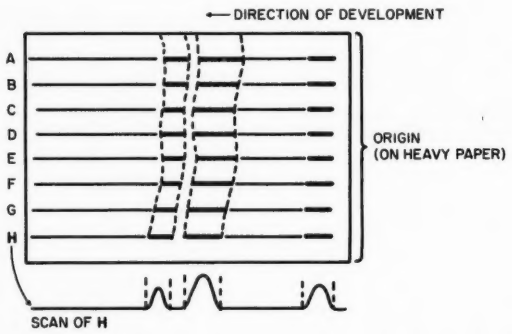

FIGURE 4. *Use of tracing in chromatography of tritiated compounds.*

in the lines of absorption, limits of the bands are more clearly defined than in a "print" [3] of the entire chromatogram. Spraying of alternate strips, or of two different tracings, with different color reagents sometimes gives additional information concerning the compounds. (If it is desired only to ascertain the progress of a development approximately, a single line, drawn by the wheel on a strip of thin paper placed lengthwise on the middle of the wet chromatogram, will suffice.)[5] When the separation of bands has become satisfactory, and a tracing has clearly indicated their limits, the chromatogram is air-dried.

For compounds labeled with carbon-14, a radioautograph is the most accurate means of locating bands on a chromatogram. However, the *progress* of the completeness of separation may be quickly ascertained by use, on a strip of thin paper, of the tracing technique described above. The strip is then scanned for radioactivity in a paper-chromatogram scanner having a 1 : 1 correspondence of chromatogram and chart.

For tritium-labeled compounds, the tracing technique has a further advantage. Tritium does not produce a good radioautograph of a chromatogram, because of the weakness of its radiation. If the compounds are not present in sufficient quantity to be clearly defined on the tracing by means of a color reagent, the technique illustrated in figure 4 is employed. In this, the individual lines produced by the plastic wheel are scanned for radioactivity, and the positions recorded for the peaks are used to locate the bands. This technique has been employed in the separation of high-activity tritium-labeled compounds on the lower capacity papers (such as Whatman No. 3MM).

4. Removal and Treatment of Bands of the Developed Chromatogram

Bands sketched on a tracing may be outlined on the heavy chromatogram merely by positioning the tracing and using a sharp pencil or stylus. Band outlines from a radioautograph are conveniently transferred to the chromatogram by (a) puncturing the film to form series of small holes outlining the bands, (b) positioning the film on the chromatogram,[6] and (c) dusting the film with charcoal. The series of black dots produced on the chromatogram adequately and accurately outline the bands, and the intact film may be saved for reference. Seed-test paper is extremely difficult to cut with scissors, and it tends to crumble when cut with a sharp knife. However, the bands are conveniently removed by means of tinners' shears.

For elution of a band, the stirrup and wick are attached to one narrow edge, not by sewing, but by use of a series of vertically-placed, stainless-steel staples. The auxiliary wick is added as shown in figure 2, and the band, trimmed to a point at the lower end, is eluted in the chromatography cabinet, usually with 50 percent aqueous methanol. Subsequent treatment of the eluant usually includes the use of small amounts of a decolorizing carbon, and, in some instances, of ion-exchange resins.

5. Capacity of the Heavy Papers

Figures 5 and 6 show some results of a study made of the capacity of the seed-test and the No. 17 paper, respectively. Obviously, the ease of separation depends on the spread in R_f values and on the quantities separated. At most indicated levels of loading, L-rhamnose was satisfactorily separated from both D-glucose and D-fructose. Separation of the last two from each other by further development or by a second development is feasible on the seed-test paper at the 1-g level, and on the No. 17 paper at the 400-mg level. It is possible to increase the capacities of the heavy papers somewhat (if the decrease in length is unimportant) by attaching the stirrup and wick to the

[5] In a recently described technique for ascertaining the progress of a development [7], the chromatogram is *dried*, and a strip of pressure-sensitive tape is applied lengthwise, peeled off with the adhering fibers, and sprayed with a color reagent. The technique described in the present paper permits monitoring of the *wet* chromatogram. If the separation of bands is insufficient, the development can be continued immediately.

[6] In this laboratory, film is *stapled* to the chromatogram for the preparation of a radioautograph, and the puncture marks from the staples subsequently afford a convenient means for precisely positioning the developed radioautograph on the chromatogram.

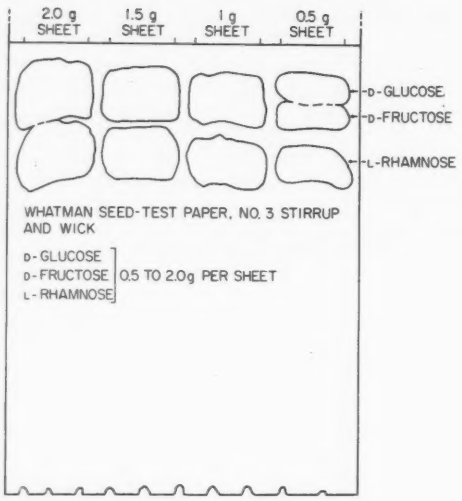

FIGURE 5. *Illustration of capacity of seed-test paper (solvent: 1-butanol—acetic acid—water 4 : 1 : 5, upper layer).*

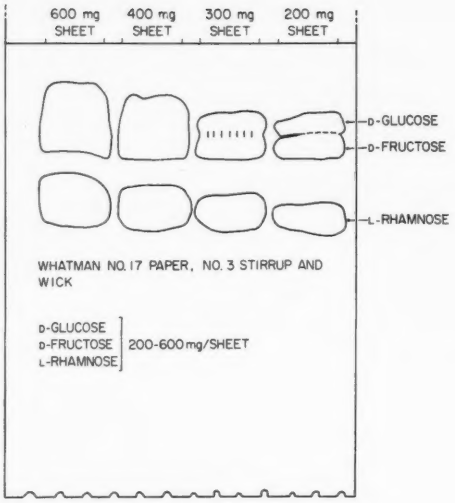

FIGURE 6. *Illustration of capacity of No. 17 paper.*

long (22-in) edge of the paper. In the two directions, the chromatographic properties of the seed-test paper are the same. The R_f values for the seed-test paper are about 0.7 of those for Whatman paper No. 1.

6. Summary

Simplified techniques are described for the use of heavy papers in large-scale, preparative chromatography. Bands of compounds on the developed chromatogram are nondestructively located by laying the wet chromatogram on glass, overlaying it with a thin paper, and pressing a series of lines down the length of the upper paper by means of a small, plastic wheel. When this tracing is stained, limits of the bands are clearly defined. Capacities and behavior characteristics of Whatman seed-test paper and Whatman No. 17 paper are illustrated. The R_f values for Whatman seed-test paper are about 0.7 of those for Whatman paper No. 1.

7. References

[1] H. K. Mitchell and F. A. Haskins, Science **110,** 278 (1949); W. L. Porter, Anal. Chem. **23,** 412 (1951); A. Fischer and M. Behrens, Z. Physiol. Chem. **291,** 14 (1952); L. Zechmeister, Science **113,** 35 (1951); L. Hagdahl and C. E. Danielson, Nature **174,** 1062 (1954); L. B. Rockland, J. Chromatog. **16,** 547 (1964).

[2] Instructions for LKB "Chromax" Pressurized Paper Chromatography Column System, LKB-Produkter, Stockholm 12, Sweden.

[3] H. H. Brownell, J. G. Hamilton, and A. A. Casselman, Anal. Chem. **29,** 550 (1957).

[4] J. N. Balston and B. E. Talbot, A Guide to Filter Paper and Cellulose Powder Chromatography (H. Reeve Angel & Co., Ltd., London, and W. & R. Balston Ltd., Maidstone, England, 1952, p. 21).

[5] J. H. Mueller, Science **112,** 405 (1950).

[6] Australian Patent No. 233,713, Imperial Chemical Industries of Australia and New Zealand, Ltd., May 1961.

[7] D. J. MacLaurin, J. K. Crossman, and J. W. Green, Chemist-Analyst **10,** No. 4, 118 (1965).

(Paper 71A1–436)

JOURNAL OF RESEARCH of the National Bureau of Standards—A. Physics and Chemistry
Vol. 71A, No. 1, January–February 1967

Infrared Absorption Spectra of Some Aldofuranoid, Aldopyranoid, and Acyclic 1-Acylamido Derivatives of Sugars

R. Stuart Tipson, Alberto S. Cerezo,[1] Venancio Deulofeu,[1] and Alex Cohen

Institute for Materials Research, National Bureau of Standards, Washington, D.C. 20234

(October 17, 1966)

The infrared absorption spectra of two glycofuranosylacetamides and their perbenzoates, and of eleven glycopyranosylacylamides and eight esters thereof, are presented and discussed. For comparison, the spectra of thirteen 1,1-bis(acylamido)-1-deoxyalditols and eight esters thereof are also given and discussed.

The useful correlations between structure and infrared absorption made by Barker and co-workers for certain carbohydrates, and by Nanasi and co-workers for some *N*-arylglycosylamines, cannot be extended to the 1-acylamido compounds we have studied. Certain of Verstraeten's correlations may have some diagnostic value.

Key Words: Absorption spectra, acyclic sugars, 1-acylamido sugars, aldofuranoid sugars, aldopyranoid sugars, infrared spectra.

1. Purpose and Scope of the Project

The main object of the present project was to record the infrared absorption spectra of a variety of 1-acylamido derivatives of sugars (having furanoid, pyranoid, or acyclic structures), in order to find whether previously reported correlations between the structure and specific bands in the infrared spectra of certain derivatives of sugars are also applicable to this group of compounds. In essence, the study consisted of answering two questions: (a) Do compounds having certain structural features show, in their infrared spectra, the bands previously described as characteristic of such features, and (b) do compounds that lack these structural features show or fail to show these bands in their infrared spectra? No infrared band can be regarded as unique for any feature, of course; and interpretation must be substantiated by other evidence.

The spectra have been recorded for two glycofuranosylacetamides and their perbenzoates; eleven glycopyranosylacylamides and eight esters thereof; and thirteen 1,1-bis(acylamido)-1-deoxyalditols and eight esters thereof. For this purpose, we used one of the small instruments now commercially obtainable, because such low-cost instruments are now customarily employed routinely as an analytical tool in practical organic chemistry.

2. Compounds Investigated

Table 1 gives a list of the compounds, their code numbers [1],[2] and an index to the spectrograms; the serial number of a compound is the same as the number of its spectrogram.

In addition, a discussion is given of the spectra previously published [2] for five *N*-glycopyranosylacetamides and six acetates thereof, and for a 1,1-bis(acetamido)-1-deoxyalditol and its tetraacetate; the serial number given each of these compounds is that originally assigned [2], with the letter A suffixed thereto. Also, the spectra previously published [3] for three derivatives of D-ribosylamine have received consideration; the serial numbers for them are those originally given [3], with the letter B added.

The spectra were measured in the region of 4000 to 667 cm^{-1}. The spectrograms of compounds 1 to 44 are given (see fig. 1), together with a discussion of (a) the structure of the compounds and (b) some of the outstanding features of their spectra.

[1] Departamento de Química Orgánica, Facultad de Ciencias Exactas y Naturales, Universidad de Buenos Aires, Perú 222, Buenos Aires, Argentina.

[2] Figures in brackets indicate the literature references at the end of this paper. The references for table 1 are given at the end of the table.

TABLE 1. *Compounds measured and index to spectrograms*

Code [a]	Compound	mp (°C)	$[\alpha]_D$, degrees	References	Spectrogram
	A. *N*-GLYCOFURANOSYLACETAMIDES				
	1. Unsubstituted				
	N-Acetyl-				
10.116(82)	α-D-xylosylamine	147–148	+100.0(H_2O)	1	1
10.216(82)	α-D-glucosylamine	195–197	+87.6(H_2O)	2	2
	2. Esters				
	N-Acetyl-				
15.116(82)	2,3,5-tri-*O*-benzoyl-α-D-xylosylamine	139–141	+31.8($CHCl_3$)	1	3
15.216(82)	2,3,5,6-tetra-*O*-benzoyl-α-D-glucosylamine	153–155	−20.1($CHCl_3$)	3	4
	B. *N*-GLYCOPYRANOSYLACYLAMIDES				
	1. Unsubstituted				
	N-Acetyl-				
10.11?(82)	β-D-xylosylamine	213–214	−0.7(H_2O)	[b] 4, 5	(1A)
10.21?(82)	β-D-glucosylamine	230–260(dec.)	−22.8(H_2O)	[b] 4, 5	(2A)
10.12?(82)	β-D-lyxosylamine	166–167	−47.0(H_2O)	6	5
10.22?(82)(99)	β-D-mannosylamine, monohydrate	203–204	−47.4(H_2O)	[b] 4	(3A)
10.22?(80)(82)	6-deoxy-β-L-mannosylamine	210–211	+65.7(H_2O)	6	6
10.13?(82)	α-L-arabinosylamine	222–224	+69.1(H_2O)	[b] 7	(4A)
10.23?(82)	α-D-galactosylamine	179–180	+194.9(H_2O)	6,8	7
10.23?(82)	β anomer	233	+9.8(H_2O)	[b] 8	(5A), 8
		236–238	+10.2(H_2O)		
10.14?(82)	α-D-ribosylamine	198–200	+17.8(H_2O)	[c] 9	(5B)
10.14?(82)	β anomer	195–197	−23.4(H_2O)	[c] 9	(6B)
10.21?(83)	*N*-Propionyl-β-D-glucosylamine	193–194	−23.2(H_2O)	3	9
	N-Benzoyl-				
10.12?(84)	β-D-lyxosylamine	234–235	−22.0(H_2O)	6	10
10.13?(84)	α-D-arabinosylamine	209–211	−53.2(H_2O)	6	11
10.21?(84)	β-D-glucosylamine	231–233	−12.2(H_2O)	3	12
10.22?(84)	β-D-mannosylamine	251–252	+5.8(py)	10	13
10.22?(80)(84)	6-deoxy-β-L-mannosylamine	235–237	+18.9(H_2O)	11	14
10.23?(84)	β-D-galactosylamine	188–190	+17.3(H_2O)	6	15
	2. Esters				
	N-Acetyl-				
12.11?(82)	2,3,4-tri-*O*-acetyl-β-D-xylosylamine	172–173	+28.5($CHCl_3$)	[b] 4	(6A)
12.21?(82)	2,3,4,6-tetra-*O*-acetyl-β-D-glucosylamine	163–164	+17.4($CHCl_3$)	[b] 4	(7A)
12.22?(82)	2,3,4,6-tetra-*O*-acetyl-β-D-mannosylamine	188–189	−16.5($CHCl_3$)	[b] 4	(8A)
12.22?(80)(82)	2,3,4-tri-*O*-acetyl-6-deoxy-β-L-mannosylamine	135–137	+6.2($CHCl_3$)	6	16
12.13?(82)	2,3,4-tri-*O*-acetyl-α-L-arabinosylamine	177–178	+89.6($CHCl_3$)	[b] 7	(9A)
15.13?(82)	2,3,4-tri-*O*-benzoyl-α-D-arabinosylamine	121–123	−270.6($CHCl_3$)	[d]	17
12.23?(82)	2,3,4,6-tetra-*O*-acetyl-α-D-galactosylamine	172–173	+117.4($CHCl_3$)	[b] 8	(10A)
12.23?(82)	β anomer	173	+34.7($CHCl_3$)	[b] 8	(11A)
12.14?(82)	2,3,4-tri-*O*-acetyl-β-D-ribosylamine	128–130	+35.3($CHCl_3$)	[c] 9	(4B)
	N-Propionyl-				
14.21?(83)	2,3,4,6-tetra-*O*-propionyl-β-D-glucosylamine	103–104	+19.3($CHCl_3$)	3	18
15.21?(83)	2,3,4,6-tetra-*O*-benzoyl-β-D-glucosylamine	151–152	+68.7($CHCl_3$)	3	19
	N-Benzoyl-				
12.13?(84)	2,3,4-tri-*O*-acetyl-α-D-arabinosylamine	162–163	−40.1($CHCl_3$)	[d]	20
15.11?(84)	2,3,4-tri-*O*-benzoyl-β-D-xylosylamine	173–175	+1.9($CHCl_3$)	6	21
15.13?(84)	2,3,4-tri-*O*-benzoyl-α-D-arabinosylamine	214	−174.2($CHCl_3$)	[d]	22
15.21?(84)	2,3,4,6-tetra-*O*-benzoyl-β-D-glucosylamine	113–115	+23.0($CHCl_3$)	3	23
15.21?(84)	ditto	184	+22.9($CHCl_3$)	3	23a
	C. 1,1-BIS(ACYLAMIDO)-1-DEOXYALDITOLS				
	1. Unsubstituted				
	1,1-Bis(acetamido)-				
10.027(52)(82)	1-deoxy-D-erythritol	210–211	+8.7(H_2O)	12	24
10.137(52)(82)	1-deoxy-L-arabinitol	189–191	+9.8(H_2O)	[b] 13	(15A)
10.217(52)(82)	1-deoxy-D-glucitol	165–167	+4.0(H_2O)	3	25
10.227(52)(80)(82)	1,6-dideoxy-L-mannitol	238–240	+22.7(H_2O)	11	26
10.237(52)(82)	1-deoxy-D-galactitol	194–196	+8.4(H_2O)	14	27
10.217(56)(83)	1-Deoxy-1,1-bis(propionamido)-D-glucitol	154–156	+6.6(H_2O)	3	28
	1,1-Bis(benzamido)-				
10.027(57)(84)	1-deoxy-L-erythritol	217–219	+13.5(py)	15	29
10.137(57)(84)	1-deoxy-L-arabinitol	194–196	−5.3(py)	15	30
10.147(57)(84)	1-deoxy-D-ribitol	190–192	−8.1(py)	15	31
10.217(57)(84)	1-deoxy-D-glucitol	199–201	+1.3(py)	10	32
10.217(57)(80)(84)	1,2-dideoxy-D-*arabino*-hexitol	208–210	+12.0(py)	[e]	33
10.227(57)(84)	1-deoxy-D-mannitol	222–224	+2.9(py)	10, 16	34
10.227(57)(80)(84)	1,6-dideoxy-L-mannitol	220–222	+14.1(py)	11	35
10.237(57)(84)	1-deoxy-D-galactitol	207–208	−6.8(py)	14	36

	2. Esters				
	1,1-Bis(acetamido)-1-deoxy-				
12.137(52)(82)	2,3,4,5-tetra-*O*-acetyl-L-arabinitol	218–219	−72.5(CHCl$_3$)	[b] 5	(16A)
12.217(52)(82)	2,3,4,5,6-penta-*O*-acetyl-D-glucitol	188–190	+22.3(CHCl$_3$)	3	37
	1,1-Bis(benzamido)-1-deoxy-				
10.217(22)(57)(84)	6-*O*-benzoyl-D-glucitol	208–209	+5.2(py)	17	38
12.127(22)(57)(84)	2,3,4-tri-*O*-acetyl-5-*O*-benzoyl-D-lyxitol	184–186	+35.1(CHCl$_3$)	18	39
12.137(22)(57)(84)	2,3,4-tri-*O*-acetyl-5-*O*-benzoyl-D-arabinitol	192–193	+68.1(CHCl$_3$)	18	40
15.137(57)(84)	2,3,4,5-tetra-*O*-benzoyl-D-arabinitol	134–136	+62.0(CHCl$_3$)	15	41
12.027(57)(84)	2,3,4-tri-*O*-acetyl-L-erythritol	181–183	+9.2(CHCl$_3$)	15	42
12.147(57)(84)	2,3,4,5-tetra-*O*-acetyl-D-ribitol	175–176	−10.2(CHCl$_3$)	15	43
12.217(57)(84)	2,3,4,5,6-penta-*O*-acetyl-D-glucitol	189–191 (needles) 199–200 (plates)	−39.4(CHCl$_3$)	19	44

[a] In the coding system [1], certain numbers were left blank to permit later assignment to structural features as the need arose. The following additions have now been made: table 1, column 2, code No. 4, propionated; column 2, code No. 5, benzoylated; table 2, code No. 56, propionamido; code No. 57, benzamido; code No. 83, deoxypropionamido; code No. 84, benzamidodeoxy. [b] Spectrum given in reference 5. [c] Spectrum given in reference 9. [d] Prepared by A. S. Cerezo. [e] We thank J. O. Deferrari and I. Mastronardi (Buenos Aires) for providing a sample of this compound.

References for Table 1

1. A. S. Cerezo and V. Deulofeu, Carbohydrate Res. **2**, 35 (1966).
2. R. C. Hockett and L. B. Chandler, J. Am. Chem. Soc. **66**, 957 (1944).
3. A. S. Cerezo, S. Delpy, and V. Deulofeu, paper in preparation.
4. H. S. Isbell and H. L. Frush, J. Org. Chem. **23**, 1309 (1958).
5. R. S. Tipson and H. S. Isbell, J. Res. NBS **65A** (Phys. and Chem.) No. 1, 31 (1961).
6. S. Delpy, Ph.D. thesis, Buenos Aires, Argentina, 1962.
7. H. S. Isbell and H. L. Frush, J. Res. NBS **46**, 132 (1951) RP2186.
8. H. L. Frush and H. S. Isbell, J. Res. NBS **47**, 239 (1951) RP2248.
9. R. S. Tipson, J. Org. Chem. **26**, 2462 (1961).
10. P. Brigl, H. Mühlschlegel, and R. Schinle, Ber. **64**, 2921 (1931).
11. J. O. Deferrari and V. Deulofeu, J. Org. Chem. **22**, 802 (1957).
12. V. Deulofeu and J. O. Deferrari, Anales Assoc. Quim. Arg. **38**, 241 (1950).
13. H. S. Isbell and H. L. Frush, J. Am. Chem. Soc. **71**, 1579 (1949).
14. J. O. Deferrari and V. Deulofeu, J. Org. Chem. **17**, 1097 (1952).
15. J. O. Deferrari, M. A. Ondetti, and V. Deulofeu, J. Org. Chem. **24**, 183 (1959).
16. J. O. Deferrari and V. Deulofeu, J. Org. Chem. **17**, 1093 (1952).
17. E. Gros, A. Lezerovich, E. F. Recondo, V. Deulofeu, and J. O. Deferrari, Anales Asoc. Quim. Arg. **50**, 185 (1962).
18. E. R. de Labriola and V. Deulofeu, J. Org. Chem. **12**, 726 (1947).
19. V. Deulofeu and J. O. Deferrari, J. Org. Chem. **17**, 1087 (1952).

3. Correlations Made by Barker and Co-workers

3.1. Description of the Correlations for Certain Aldopyranose Derivatives

In a series of articles [4, 5, 6], Barker and co-workers sought to identify, in the range of 960 to 730 cm^{-1}, infrared bands characteristic of several aldopyranoses and their derivatives.

They expressed the frequency of a band as the mean and the standard deviation; although indication of a range is customary, their expression was used for *defining* the probable frequency of an absorption band shown by each of a set of compounds. However, it is not practical in the reverse process, namely, in *searching* for this band within a range of wavelengths in the spectrum of a single compound. For example, the value given for the type 1a band was 917 ± 13 cm^{-1}; this *includes* the interval of 930 to 904 cm^{-1}, but it does not *exclude* the possibility that, for any one compound of this kind, the band might occur above 930 cm^{-1} or below 904 cm^{-1}. Therefore, for each band sought in an individual spectrum, subsequent authors have, for practical purposes, apparently confined their attention to the interval obtained by adding the standard deviation to, and subtracting it from, the mean value as given by these workers [4, 5, 6].

a. (D or L)-*gluco* Group Configuration

In their first article [4], they recorded (in tables) the frequencies of various types of bands shown by D-glucopyranose derivatives; these bands are listed in table 2. From these results, they identified [4] "three principal sets of bands, for which the average values (cm.$^{-1}$) and standard deviations" were (for α anomers) type 1a, 917 ± 13; type 2a, 844 ± 8; and type 3a, 766 ± 10; (for β anomers) type 1b, 920 ± 5; type 2b, 891 ± 7; and type 3b, 774 ± 9. They found that the type 2a band can be used with considerable confidence for diagnosing the α anomeric form, particularly in polymers of glucopyranose. The type 2b band was not found useful for diagnosing the β anomeric form, but the *absence* of the type 2a band was considered very useful for diagnosing the β anomeric form. They regarded the bands of types 1 and 3 as only useful for determining points of linkage in polymers of α-glucopyranose.

TABLE 2. *Frequencies* [a] *(cm^{-1}) of various types of bands for* D-*glucopyranose derivatives, as recorded in the tables in Ref. [4]*

Linkage	Type 1	Type 2a	Type 2b	Type 3
α Anomeric				
Monosaccharides	915 ± 5	847 ± 6		767 ± 8
	900 ± 8	842 ± 7		751 ± 8
Higher saccharides	930 ± 9	843 ± 10		761 ± 8
	917 ± 2	839 ± 1		768 ± 1
β Anomeric				
Monosaccharides	914 ± 6		896 ± 6	
	[b] 918 ± 5		891 ± 8	[c] 772 ± 9
Higher saccharides	921 ± 4		890 ± 5	[d] 774 ± 9

[a] Mean and standard deviation. [b] Six of ten compounds did not show this band. [c] Eleven of sixteen compounds did not show this band. [d] Five of sixteen compounds did not show this band.

In a review, Neely [7] summarized this and related work; without explanation, he arrived at further conclusions, presumably in the following way. It would seem that, as the range for type 1a encompasses that for type 1b, the range 917 ± 13 cm^{-1} may be simply referred to as type 1 (as shown in table 3). Also, as there is an overlap (from 776 to 765 cm^{-1}) of 11 cm^{-1} for the ranges of types 3a (766 ± 10) and 3b (774 ± 9), only extreme values of each range will have diagnostic value for these respective types, and so, they were combined (as 770 ± 14 cm^{-1}) and referred to as type 3 (see table 3).

TABLE 3. *Summary of the results of Barker and co-workers [4,5] for infrared bands characteristic of five* (D *or* L)*-aldopyranoses and their derivatives*

Type	Bands (cm^{-1}; mean and standard deviation, or range)				
	Xylose	Arabinose	Glucose	Mannose	Galactose
	Both anomers				
1	?	?	[a] 917 ± 13	?	?
2c	–	–	[b] –	[b] 876 ± 9	[b] 871 ± 7
3		[c] 781–744	[a] 770 ± 14 [b] 753 ± 17	[b] 791 ± 18	[b] 752 ± 20
	α anomers only				
2a	[d] –	[c] –	[a, c] 844 ± 8 843 ± 4	[b] 833 ± 8	[b] 825 ± 11
3	[d] 749 ± 10				
	β anomers only				
2a	[d] –	[d] 855–830 [c] 854–836			
2b			[a, c] 891 ± 7 [b] 890 ± 8	[b] 893 ± 6	[b] 895 ± 9

[a] Given in table 2 of ref. [7]; see present text for probable derivation. [b] Given in table 5 of ref. [5]. [c] Given in table 4 of ref. [5]. [d] Given in the text of ref. [5]. [e] Given in the text of ref. [4].

In summary, in the correlations of Barker and co-workers [4], the infrared spectra of α- and β-(D or L)-glucopyranose derivatives should show type 1 absorption (917 ± 13 cm^{-1}) and type 3 absorption (770 ± 14 cm^{-1}). In addition, the spectra of the α anomers should show type 2a absorption (844 ± 8 cm^{-1}), and the spectra of the β anomers should show type 2b absorption (891 ± 7 cm^{-1}). These values were given by Neely [7], in an article which will be discussed in section 3.2.

If the bands are to have diagnostic value for glucopyranose derivatives, α anomers should not show type 2b absorption, and β anomers should not show type 2a absorption. However, these workers [4] found that (a) some α anomers exhibited type 1 absorption in the range of type 2b bands, and (b) some β anomers showed "weak peaks of type 2a" which they believed were due to traces of the α anomers.

Barker and co-workers [4] then made tentative assignments for these glucopyranose derivatives. They suggested that: (1) type 1 bands might be due to a ring vibration including ring C-O-C antisymmetrical stretching; (2) type 2 bands might be connected with "one of the C-H deformation modes in which the hydrogen on C-1 is involved intimately"; and (3) type 3 bands might be correlated with ring breathing.

In a second article, Barker and co-workers [5] examined the infrared spectra of some more glucopyranose derivatives, and found slightly different positions for bands of type 2a and type 3 (see table 3). As before, some of the α anomers were found to show type 1 absorption in the range of type 2b bands. Also, they pointed out that derivatives containing a benzene ring may show absorption in the region of the type 2a band, and that acetates absorb in the region of the type 2b band.

b. Other Group Configurations

The results of Barker and co-workers [5] for infrared bands characteristic of four other pyranoid aldoses and their derivatives are also summarized in table 3.

No decision was made as to the presence or absence of bands of *type 1* in the spectra of these other compounds. It was found that, for manno- and galactopyranose, the *type 2a* band can be used for diagnosing the α anomeric form, although with slightly less confidence than for α-glucopyranose derivatives. Absence of the type 2a band was useful for diagnosing the β anomeric form.

These authors [5] also found that a band at 876 ± 9 cm^{-1}, designated *type 2c*, was characteristic of mannopyranose derivatives; and that a band of type 2c, at 871 ± 7 cm^{-1}, was characteristic of galactopyranose derivatives.

From these results (see table 3), it may be seen that the mean frequency for a given type of absorption may change with the group configuration; for example, the mean frequency for type 3 absorption is at 791 cm^{-1} for the *manno* configuration, but at 752 to 753 cm^{-1} for the *gluco* and *galacto* configurations. Furthermore, β-(D or L)-xylopyranose derivatives are not characterizable by any of the bands listed in table 3. In connection with the present study, it should be noted that many derivatives containing a benzene ring absorb [8] in the region of the type 3 band of the glucopyranose, galactopyranose, and α-xylopyranose derivatives.

Barker and co-workers suggested that *type 2a* bands may be associated with an equatorial C-1—H grouping, because the favored conformation [3] (CA) of the α-(D or L) anomers having the *gluco*, *manno*, and *galacto* configurations has an equatorially attached hydrogen atom on C-1. (However, for both the *manno* and *galacto* configurations, some β anomers showed type 2a absorption.) The type 2a absorption for β-(D or L)-arabinopyranose (see table 3) was related to the same structural feature, because the CE conformation (having an equatorially attached hydrogen atom on C-1 of the β anomer) is favored for the *arabino* configuration. Similarly, *type 2b* bands, shown by the β-(D or L) anomers of gluco-, manno-, and galactopyranose, were associated with the presence of an axial C-1—H grouping.

[3] In the conformational nomenclature of Isbell and Tipson [9], the β anomer of a pyranoid aldose in the CA conformation has an *axial* C-1—H bond; in the CE conformation, it has an *equatorial* C-1—H bond.

Barker and co-workers [5] again made assignments for these bands. They suggested that the *type 2c* bands are due to deformations of the equatorial C—H bond at C-2 of (D or L)-mannopyranose-CA and at C-4 of (D or L)-galactopyranose-CA. In agreement with this conclusion, Ellis [10] has found that derivatives of (D or L)-arabinopyranose-CE show type 2c absorption. However, according to Ellis, "an equatorial C—H bond at C-3 may also give rise to the type 2c absorption," as in derivatives of (D or L)-ribopyranose-CA. Barker and co-workers indicated that β-(D or L)-xylopyranose derivatives show no absorption of *type 3*, and that, in the CA conformation, these derivatives have *all* of the exocyclic C—O bonds equatorial; β-(D or L)-glucopyranose derivatives showed weak absorption of type 3, and their CA conformation has an equatorial hydroxymethyl group on C-5. If type 3 absorption is a symmetrical ring-breathing frequency, such a band would not be expected to be strong for the more symmetrical molecules, such as β-D-xylo- and β-D-gluco-pyranose, but would be expected to be stronger for the corresponding α anomers (having a bulky group attached axially at C-1). Their *assignments* for the bands of *types 2a and 2b* have since been disproved [11], but the *correlations*, already mentioned, remain unaffected. It was "concluded that a vibration of the whole grouping at C-1 is responsible for type 2a and type 2b absorption. The frequency exhibited is dependent on the stereochemical configuration at C-1 (i.e., α or β)."

Barker and co-workers [6] next found that 2-deoxy and 3-deoxy derivatives of gluco-, manno-, and galactopyranose show absorption at 867 ± 2 cm^{-1}, attributed to a CH_2 rocking mode of a ring-methylene grouping *not* adjacent to the ring-oxygen atom (because xylopyranose derivatives, having a methylene grouping at C-5 do not show this band). In addition, they noted that seven 6-deoxy derivatives of mannopyranose or galactopyranose show a band near 967 cm^{-1}, tentatively attributed to a *C*-methyl (terminal) rocking mode, but they cautioned that this band might not have diagnostic value.

Application of the correlations of Barker and co-workers [4, 5, 6] has proved useful in the study of many related compounds, including oligo- and poly-saccharides; and, for the compounds they studied, none of their correlations are questioned in the present article.

TABLE 4. *Ranges*[a] *(cm^{-1}) for the bands of types 2a and 2b, as given by Spedding* [13] *from the work of Barker and co-workers* [12]

Type	Anomer	Glucopyranose	Mannopyranose	Galactopyranose
2a	α	[b]855–833 (844)	[b]843–818 (831)	[b]839–810 (825)
2b	β	[c]905–876 (891)	[d]898–888 (893)	[d]914–886 (900)

[a] The mean is given in parentheses. [b] Derivatives containing a benzene ring absorb here. [c] Must be confirmed by absence of absorption at 855–833 cm^{-1}. [d] But other types of vibration also occur here.

These results were collated by Barker and co-workers [12]. Some of them were summarized by Spedding [13], who gave slightly different figures for the ranges of absorption for the bands of types 2a and 2b, as shown in table 4. He also stated that β-arabinopyranose derivatives show a type 2a band at 855 to 830 cm^{-1} (mean, 843 cm^{-1}); and that α-xylopyranose derivatives show a band at 760 to 740 cm^{-1} (mean, 750 cm^{-1}), but that many derivatives containing a benzene ring absorb here.

3.2. Neely's Summation

In a review [7], Neely correctly described the results of Barker and co-workers in the text of his article, and he attempted to condense this information in his table II (reproduced in table 5) entitled "Frequencies Characteristic of the Sugar Pyranose Ring." Study of this table reveals that, of the seven vibrations listed in column 1, only the first two could be described as possibly being "frequencies characteristic of the sugar pyranose ring." The other bands are those indicated by Barker and co-workers [4, 5, 6] to be characteristic of certain structural features possessed by some compounds that have a pyranoid ring. Unfortunately, Neely's table II has since been copied in articles and books [14].

TABLE 5. *Frequencies characteristic of the sugar pyranose ring*[a]

Group	Frequency	References [b]
	cm^{-1}	
Antisymmetrical ring vibration	917 ± 13	[4]
Symmetrical ring breathing vibration	770 ± 14	[4]
α-Anomeric C—H deformational vibration	844 ± 8	[4]
β-Anomeric C—H deformational vibration	891 ± 7	[4]
Equatorial C—H deformational vibration, other than anomeric C—H	880 ± 8	[5]
Ring methylene rocking vibration	867 ± 2	[6]
Terminal methyl group rocking vibration	967 ± 6	[6]

[a] According to W. B. Neeley [7]. [b] The reference numbers have been changed to those used in the present article.

The 2a band was described in table 5 as due to an "α-anomeric C—H deformational vibration"; however, Spedding more correctly described it as caused by an "anomeric C—H equatorial deformation" [15], because Barker and co-workers [12] had indicated that, in the favored chair conformation (CE) of (D or L)-arabinopyranose derivatives, the β anomers have an equatorial C-1—H bond. As already mentioned, further work [11] has shown that all that can at present be said is that type 2a bands are in some way associated with structures having an equatorial C-1—H bond, and type 2b bands with those having an axial C-1—H bond.

It is evident that the bands of types *2a and 2b*, listed in table 5 as occurring at 844 ± 8 cm^{-1} and at 891 ± 7 cm^{-1}, were taken from the paper [4] which had been restricted to study of D-glucopyranose and its derivatives. However, Neely may have considered that these values also applied fairly well to other pyranoses; because, for the gluco-, manno-, and galacto-pyranose derivatives (see table 3), the ranges of 852 to 814 cm^{-1} (mean, 833 cm^{-1}) and 904 to 882 cm^{-1} (mean, 893 cm^{-1}) encompass the values given [5] for the 2a and 2b bands, respectively, of these three groups of sugars. Moreover, as pointed out by Barker

and co-workers [5], the range of 855 to 830 cm^{-1} (mean, 843 cm^{-1}) for the β-arabinopyranose derivatives (see table 3) fits the value for the 2a band.

As regards the bands of *types 1 and 3*, we have already discussed (in sec. 3.1a) how Neely [7] must have derived the values that he lists as occurring at 917 $\pm$13 cm^{-1} and at 770 $\pm$14 cm^{-1}—namely, from the values given [4] for D-glucopyranose derivatives. Barker and co-workers [5] had reached no firm conclusion as to the presence of *type 1* bands in the spectra of any pyranoid sugar derivatives other than those of (D or L)-glucopyranose. However, it would appear that, without comment, Neely may have intended to include bands of mannopyranose and galactopyranose derivatives in these values. Inspection of columns 2 and 3 of table 3 in Ref. [5] reveals that all of the mannopyranose compounds show a type 1 band in the range of 947 to 905 cm^{-1} (mean, 926 cm^{-1}); similarly, twelve of the 14 galactopyranose compounds (columns 1, 2, and 3 of table 2 in Ref. [5]) show a band in the range of 943 to 905 cm^{-1} (mean, 924 cm^{-1}). For the *type 3* bands listed for these three hexopyranoses in our table 3, the range is 809 to 732 cm^{-1} (mean, 771 cm^{-1}); Neely [7] listed 770 $\pm$14 cm^{-1}, and presumably concluded that this value should serve for derivatives of the three hexopyranoses. As derivatives of β-(D or L)-xylopyranose do not show type 3 absorption [5], this band cannot be ascribed to the pyranoid ring *per se*.

The band of *type 2c*, given in table 5 as lying at 880 $\pm$8 cm^{-1}, was presumably derived by Neely [7] from the values given by Barker and co-workers [5] for manno- and galacto-pyranose derivatives, namely, 876 $\pm$9 cm^{-1} and 871 $\pm$7 cm^{-1}; it was indicated that this band is shown by conformers having an equatorial C—H bond (other than an equatorial, anomeric C—H bond).

Finally, Neely [7] indicated that the last two bands listed in his table II were taken from a paper by Barker and co-workers [6]. The band at 867 $\pm$2 cm^{-1} had been found for 2-deoxy derivatives of gluco- and galacto-pryanoses and for a 3-deoxy derivative of mannopyranose. The band at 967 $\pm$6 cm^{-1} had been found for 6-deoxy derivatives of manno- and galactopyranoses.

3.3. Description of the Correlations for Aldo- and Keto-furanose Derivatives

For aldo- and keto-furanose derivatives, Barker and Stephens [16] noted absorption bands as follows: type A, 924 $\pm$13 cm^{-1} ("not distinguished from types 1 or 2b" of aldopyranoses); and type D, 799 $\pm$17 $cm.^{-1}$. "In addition, most of these compounds also showed type B absorption at 879 $\pm$7 $cm.^{-1}$ and type C at 858 $\pm$7 $cm.^{-1}$." Type A absorption was assigned to the symmetrical ring-breathing frequency. The following tentative assignments were also made: type D, to a carbon-hydrogen deformation mode where the hydrogen atom is on a carbon atom directly attached to the ring-oxygen atom; and types B and C, to modes of vibration involving the skeletal stretching of the substituents, with type B possibly concerned with side chains and type C "with the OH group."

3.4. Attempted Application of These Correlations to 1-Acylamido Derivatives

In this part of our study, the objective was not to make assignments for the bands observed in the spectra, but to determine whether the bands of the types reported by Barker and co-workers [4, 5, 6, 16] have *diagnostic value* for sugar derivatives other than those studied by these investigators. That is, we wished to find out if, when a 1-acylamido group is present in the molecule, the presence or absence of these bands can still be correlated with those structural features mentioned by Barker and co-workers.

For example, absorption of type A has been assigned to the symmetrical ring-breathing frequency of the furanoid ring. Consequently, it is to be expected that the spectrum of every furanoid compound having ring-breathing should show a band of type A. If the spectrum of a furanoid compound does *not* show a band of type A, either the ring-breathing is disturbed (or suppressed) or the correlation is faulty. However, if the spectrum of a *non*furanoid compound *shows* a band of type A, the correlation is still valid, but its diagnostic value is impaired because it is no longer exclusive, but merely indicative of a possibility that must then be checked by some other test.

To make this study, we examined, in turn, the spectra of those cyclic 1-acylamido derivatives having the five configurations given in table 3, because these were the only configurations discussed by Barker and co-workers for pyranoid derivatives. For comparison, we also examined the spectra of related acyclic derivatives, where available.

Table 6 lists the bands for compounds having the *xylo* configuration, from which it may be seen that the furanoid compounds 1 and 3 show some bands that have been associated [16] with the furanoid (*f*) structure, but they also show some bands that have been ascribed to the pyranoid (*p*) structure. The type 3(α) band of compound 3 might be due to the benzene ring. The pyranoid compounds show some *p* bands, and also some *f* bands. Pyranoid compound 1A shows one *f* and one *p* band. The β compounds 1A and 21 lack type 2(β) absorption, and the β compound 6A shows type 3(α) absorption. The type 2(β) band shown by compound 6A (the only acetate ester) might be due to the acetate ester groups. The pyranoid compound 21 shows all of the *f* bands, and also a band in the 855 to 830 cm^{-1} region (a region where the xylopyranose compounds studied by Barker and co-workers [5] show no absorption) which could be due to the benzene ring. The three pyranoid compounds (1A, 6A, and 21) show type 1 absorption; this was not specifically recognized by Barker and co-workers [5] for xylopyranose compounds, although they recorded bands in this region (in table 4 of ref. [5]) for such compounds.

TABLE 6. *Bands* (cm^{-1})[a] *in the spectra of compounds having the* xylo *configuration*

Serial No.	Anomer	*f* bands				*p* bands			
		A	B	C	D	1	2(β)	No band	3(α)
		Range							
		937–911	886–872	865–851	816–782	930–904	896–886	855–830	759–739
Furanoid									
1	α	(938)	883	–	803	(903)	–	831	–
3	α	–	(887, 871)	860	810	–	[b][887]	–	749
Pyranoid									
1A	β	(939)	–	–	–	(903)	–	–	–
6A	β	934	877	–	–	904	895	–	(738)
21	β	(939)[913]	(870)	[853]	805	913	–	853	–

[a] Enclosure of a wavenumber in parentheses indicates that it is located somewhat (usually not more than 3 cm^{-1}) beyond the upper or lower limit of the wavenumber range under consideration. [b] Enclosure of a wavenumber in brackets indicates that, from other evidence, an alternative and more likely assignment can be made. The wavenumber for the latter is not enclosed in brackets.

Table 7 lists six pyranoid compounds and five acyclic compounds having the *arabino* configuration. Four of the α anomers show type 2(β) absorption, and these four compounds have a benzene ring. All of the pyranoid compounds show type 1 absorption; this was not specifically recognized by Barker and co-workers [5] for arabinopyranose compounds, although they recorded bands in this region (in table 4 of ref. [5]) for such compounds. However, the pyranoid compounds also show some *f* bands; indeed, compounds 11, 20, and 22 show all of the *f* bands (as well as the *p* bands). The *acyclic* compounds show some *f* and *p* bands. Compounds 16A and 40 show all of the *f* and *p* bands; and compounds 30 and 41 show all of the *p* bands. Like many furanoid compounds studied by Barker and co-workers [16], the acyclic compounds 30 and 41 show types A and D absorption, but lack type B (compound 41) or type C (compound 30) absorption.

TABLE 7. *Bands* (cm^{-1})[a] *in the spectra of compounds having the* arabino *configuration*

Serial No.	Anomer	*f* bands				*p* bands		
		A	B	C	D	1	2(β)	3(α; β)
		Range						
		937–911	886–872	865–851	816–782	930–904	855–830	781–744
Pyranoid								
4A	α	936[913]	–	864	–	913	–	771
11	α	934[928]	880	[856]	803	928	(856)	780
9A	α	933	(870)	–	–	907	–	(741)
17	α	935[931]	–	862[851]	806	(931)	851 (828)	774, 758
20	α	[931, 917]	876	[851]	808	(931) 917	851	746
22	α	937	877	[851]	804	(901)	851	772, 752
Acyclic								
15A	–	–	877	–	–	904	–	775 (742)
30	–	919	(870)	–	800	919	845	770
16A	–	931, 922	873	856	784	(931) 922	(856)	(784)
40	–	(939) 932, 921, 911	873	855	808, 800	(932) 921, 911	855 (829)	772 (?)
41	–	(938) 933, 911	–	(867) 851	805, 801	(933) 911	851, 846, 840	(743)

[a] See footnotes to table 6.

In table 8 are listed the bands of furanoid and pyranoid compounds having the *gluco* configuration, together with those of seven related acyclic compounds. The *furanoid* compounds show the *f* bands, although the type B band could be interpreted as being a *p* band of type 2(β); hence, *these compounds fit the correlations of Barker and co-workers* [16]. With the possible exception of compound 2A, the *pyranoid* compounds do not show a type 3 band, but all of them show a type 1 band. Although all of the pyranoid compounds are β anomers, four of them do not show type 2 (β) absorption, and three show type 2(α) absorption; compound 18 shows both. Compound 23a, which is formed on melting compound 23 at 117–120° and allowing the melt to crystallize, shows only one *p* band, at 922 cm^{-1}; this could equally well be interpreted as being an *f* band of type A, in which case the compound shows no *p* bands, but all of the *f* bands; this could suggest the possibility that it is the furanoid isomer of compound 23, which shows the ease with which such bands could be misinterpreted. The pyranoid compound 2A shows no *f* bands, and compound 9 shows an *f* band of type 2A which might well be a *p* band of type 1; these are in agreement with the correlations. The rest of the pyranoid compounds show two or more *f* bands, and compounds 18 and 23a show all of them. The *acyclic* compounds show *f* and *p* bands. Compounds 32 and 38 show all of the bands of both sorts; compounds 33 and 44 show all of the *f* bands; and compound 37 shows all of the *p* bands.

For *pyranoid* compounds having the *manno* configuration (see table 9), all of the β anomers show type 1 and 2(β) bands. The β anomers 13 and 14 show a type 2(α) band at the extremes of the range, which could be due to the benzene ring (not present in the four others). Also, the pyranoid compounds show some *f* bands; however, some of the ranges given by Barker and co-workers [16] for *f* bands could also be interpreted as being *p* bands in the case of manno-

TABLE 8. *Bands (cm^{-1})[a] in the spectra of compounds having the* gluco *configuration*

Serial No.	Anomer	*f* bands				*p* bands				
		A	B	C	D	1(α; β)	2(β)	2(α)	3(α; β) or 3(α; β)	
		Range								
		937–911	886–872	865–851	816–782	930–904	898–882	852–836	784–756	770–736
Furanoid										
2	α	(942)	886	(867)	810, 794	–	[886]	–	–	–
4	α	(939)	885	857	803, 800	–	[885]	–	776	–
Pyranoid										
2A	β	–	–	–	–	(902)	–	–	(758?)	(758?)
9	β	[922]	–	–	–	922, 908	896	–	–	–
12	β	[917]	[(889)]	(866)	811	917	889	–	–	–
7A	β	[917]	(871)	–	–	917, 909	897	–	–	–
18	β	934	[886]	864	810	905	886	836	–	–
19	β	(940) [(910)]	–	858	803	910	–	847	–	–
23	β	(940) [(907)]	–	858	804	907	–	845	–	–
23a	β	(940) 922	874	855	806	[922]	–	–	–	–
Acyclic										
25	–	930	882	–	787	930, 909	882	–	756	756
28	–	926	–	864	795	926, 909	894	847	–	–
32	–	923	878	862	800	923	892	851	775	–
33	–	930	877	863, 853	810, 804	930	889	(853)	–	–
37	–	937, 925, 917	–	862 (850)	–	925, 917	897	850	760	760
38	–	929	(870)	(849)	810, 801	929	(901)	849, 842	760	760
44	–	935, 917	(887)	(868)	808	917	887	–	772	(772)

[a] See footnotes to table 6.

TABLE 9. *Bands (cm^{-1})[a] in the spectra of compounds having the* manno *configuration*

Serial No.	Anomer	*f* bands				*p* bands					
		A	B	C	D	5-*C*-CH_3	1	2(β)	2c(α; β)	2(α)	3(α; β)
		Range									
		937–911	886–872	865–851	816–782	973–961	930–904	899–887	885–867	841–825	809–773
Pyranoid											
3A	β	–	[876]	–	[808]	–	907	(900)	876	–	808
6	β	–	–	[(867)]	[(781)]	(958)	(902)	(902)	867	–	781
13	β	(938) [917 (909)]	–	[(866)] 856	[803]	(958)	917, 909	898	(866)	826	803, 776
14	β	937 [917]	–	–	[806]	(975, 957)	917	898	–	(845)	806, 773
8A	β	(940)	[880]	–	–	972, 965	905	(900)	880	–	–
16	β	[924, 914]	–	861	–	(978)	924, 914, 904	893	–	–	–
Acyclic											
26	–	919	–	856	–	(975) 966	919	899	–	–	–
34	–	935	884, 875	–	803, 784	966	928(?)	896	884, 875	–	803, 784
35	–	930	877	–	803	(958)	930	895	877	–	803 (772)

[a] See footnotes to table 6.

pyranose derivatives. Thus, for compounds 13, 14, and 16, some of the *f* bands of type A could be interpreted as being *p* bands of type 1. Similarly, for compound 3A, the type B and D bands, and, for compound 6, the type C and D bands, could be interpreted as being bands of types 2c and 3. The three 5-*C*-methyl compounds (6, 14, and 16) show a band in the range of 978 to 957 cm^{-1}, but compounds 13 and 8A, which lack this grouping, also show a band in this range. The *acyclic* compounds show *f* and *p* bands.

Table 10 lists the bands of five pyranoid compounds having the *galacto* configuration. All of them show type 2c absorption. None of the unsubstituted compounds show type 3 absorption. The α anomers 7 and 10A show type 2(α) absorption, and the β anomers do not. The α anomer 10A also shows type 2(β) absorption. All of the β anomers show type 2(β) absorption. All of the pyranoid compounds show some *f* bands, but some of these bands could equally well be interpreted as being *p* bands. For example,

TABLE 10. *Bands (cm^{-1})[a] in the spectra of compounds having the* galacto *configuration*

Serial No.	Anomer	*f* bands				*p* bands				
		A	B	C	D	1	2(β)	2c(α; β)	2(α)	3(α; β)
		Range								
		937–911	886–872	865–851	816–782	930–904	904–886	878–864	836–814	772–732
Pyranoid										
7	α	[930]	[873]	–	791	930	–	873	833	–
5A: 8	β	–	–	[(868)]	786	–	896	868	–	–
		–	–	[(867)]	786	–	895	867	–	–
15	β	(939)	[(888)876]	858	808, 784	–	896, 888	876	–	–
10A	α	[921]	–	[862]	–	921, 907	(907) 899	(862)	834	757
11A	β	[914]	[(870)]	–	–	914, 907	(907) 894	870	–	734
Acyclic										
27	–	–	879	(867) 856	–	–	–	(879) 867	–	759
36	–	929	875	–	803	929	894	875	–	745

[a] See footnotes to table 6.

for compound 11A, the bands of types A and B could be types 1 and 2c bands, respectively; the bands for this compound then *show complete agreement* with the *p* bands for a β-galactopyranose. Similarly, for compound 10A, if the *f* bands of types A and C are actually *p* bands of types 1 and 2c, the bands *agree with those for a galactopyranose*, but the presence of types 2(α) and 2(β) bands does not permit a conclusion as to the anomeric configuration. The *acyclic* compounds listed show *f* and *p* bands. The bands for compound 36 correspond with those for a β-galactopyranose, which shows that use of these bands without other evidence could give an erroneous conclusion.

To be of general usefulness in structural analysis, the correlations made by Barker and co-workers [12] should be applicable to the furanoid and pyranoid forms, respectively, of sugar derivatives of all kinds, provided that allowance is made for bands attributable to such other features as benzene rings or acetate ester groups present in the molecule. However, from the above study, it is apparent that the correlations made by Barker and co-workers [12] are, in most instances, restricted to the compounds they studied, and that the correlations cannot be extended to have a wider diagnostic applicability to related compounds. This conclusion confirms our previous reports that, for cyclic acetals of sugars, "distinctive absorption bands are not apparent for pyranose or furanose rings" [17], and that, for 1-acetamido derivatives of sugars, "no bands were noted which could be correlated with the absence or presence of the pyranoid ring" [2].

4. Correlations Made by Verstraeten for Furanoid and Pyranoid Forms of Aldoses and Ketoses

In 1962, the infrared spectra of most of the readily available aldo- and keto-pentoses and aldo- and keto-hexoses were published [18], but no correlations of bands according to the type-system of Barker and co-workers [4, 5, 6, 16] were given.

However, in 1964, Verstraeten [19] made a study of these spectra, together with those of some additional 2-ketoses, and obtained evidence that "all of the common sugars having a cyclic structure, and their derivatives, display" absorption at 929 ± 15 cm^{-1} (which he designated "type 1"). Exceptions noted were α-D-lyxose, showing a band at 965 cm^{-1}, and α-D-galactose, at 960 cm^{-1}. He assigned "type 1" absorption to a symmetrical ring-stretching frequency, and apparently regarded his "type 1" absorption as being the same as the type 1 absorption described by Barker and co-workers [4] for glucopyranose derivatives.

Verstraeten found that only furanoses give "type 2" absorption at 850 ± 6 cm^{-1} (provided that the ring is free to vibrate). He stated that his type 2 absorption is the same as the type C absorption of Barker and Stephens [16].

The same author observed that some ketoses, as well as aldoses, show a band at 781 ± 5 cm^{-1}. He designated this band "type 3" and regarded it as being the same as the type 3 absorption mentioned, for several aldoses, by Barker and co-workers [4, 5]. He indicated that type 3 absorption was shown provided that two conditions were met: (a) the sugar must have a pyranoid ring, and (b) this pyranoid form must assume a conformation having at least one axial hydroxyl group. He noted that, if the number of axial hydroxyl groups is increased (thereby decreasing the conformational stability), type 3 absorption becomes manifest. For example, β-(D or L)-xylopyranose-CA, which shows no type 3 absorption, is devoid of axial hydroxyl groups, whereas the α anomer in the CA conformation, which has an axial hydroxyl group at C-1, shows absorption at 760 cm^{-1}. Type 3 absorption was tentatively ascribed to ring-breathing. It was concluded that, if the total structure was suitable, as with compounds having the β-*xylo* or β-*ribo* configuration in the CA conformation, intramolecular

TABLE 11. *Summary of the results of Verstraeten [19] for infrared bands characteristic of various kinds of sugars and derivatives*

Type	Aldoses and ketoses			Ketoses	
	Furanoid	Certain pyranoid [a]	Furanoid and pyranoid	Furanoid [b]	Furanoid and pyranoid
1 [c]	850 ± 6 (856–844)	——	929 ± 15 (944–914)		
2 [d]	——	781 ± 5 (786–776)			
3 [e]					874 ± 9 (883–865)
I [f]					817 ± 7 (824–810)
IIA [g]				834 ± 4 (838–830)	
IIB					

[a] See text.
[b] Substituted, or joined to a pyranoid ring.
[c] Equated with Barker's type 1 for glucopyranose derivatives (917 ± 13 cm^{-1}); Barker and Stephens [16] had pointed out that this is in the same range as their type A for aldo- and keto-furanose derivatives (924 ± 13 cm^{-1}).
[d] Equated with Barker's type C (858 ± 7 cm^{-1}) for aldo- and keto-furanose derivatives.
[e] Equated with Barker's type 3 for certain aldopyranose derivatives.
[f] In the same range as Barker's type B for aldo- and keto-furanose derivatives (879 ± 7 cm^{-1}).
[g] In about the same range as Barker's type D for aldo- and keto-furanose derivatives (799 ± 17 cm^{-1}).

TABLE 12. *Types of bands shown by aldoses and ketoses [19]*

Aldoses		Ketoses	
Furanose	Pyranose	Furanose	Pyranose
1	1	1	1
2	—	2	—
—	[a] 3	—	[a] 3
—	—	I	I
—	—	IIA	IIA
—	—	[b] IIB	—

[a] Not shown if the favored conformation has no axial groups.
[b] Shown if the hydroxyl groups of the ketofuranose are substituted (or if C–2 of the ketofuranose is joined to a pyranoid or furanoid structure).

linkages (such as van der Waals contact or hydrogen bonds) might be formed, resulting in modification of the ring-breathing, so that absorption at this frequency would not be shown.

Verstraeten also found that 2-ketoses display "type I" bands at 874 ± 9 cm^{-1} and "type IIA" bands at 817 ± 7 cm^{-1}, regardless of whether the sugars are pyranose or furanose. These bands were ascribed to the presence of the following structural feature:

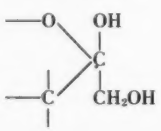

and tentatively assigned to a skeletal vibration. He pointed out that α- and β-D-lyxose, α- and β-D-talose, α-D-mannose, and α-L-fucose (which are not ketoses) also show these bands.

He found that if the ketofuranose ring is substituted, or joined to a pyranoid ring, a type IIB band appears at 834 ± 4 cm^{-1}, in addition to or instead of the type IIA band. Verstraeten's results are summarized in tables 11 and 12.

4.1. Attempted Application of These Correlations to 1-Acylamido Derivatives

None of the compounds in table 1 are derivatives of ketoses. Hence, we wished to find out (a) whether the spectra of our furanoid compounds showed Verstraeten's *f*-band of type 2 and the band of type 1; and (b) whether the pyranoid compounds showed Verstraeten's *p*-band of type 3 and the band of type 1. If the bands of types I, IIA, and IIB are usefully diagnostic of *ketoses*, they should *not* be shown by the compounds in table 1.

a. Unsubstituted Derivatives

The bands in the spectra of 13 unsubstituted furanoid and pyranoid 1-acetamido derivatives are listed in table 13. The *furanoid* compounds 1 and 2 do not show an *f* band of type 2, but both show a type 1 band. Both show the *ketose* band of type I. Compound 1 shows the ketofuranose band of type IIB and the *p* band of type 3; and compound 2 shows the ketose band of type IIA.

Of the 11 *pyranoid* compounds, seven do not show the *p* band of type 3; for the five compounds (1A, 5B, 6B, 2A, and 9) having the *xylo*, *ribo*, or *gluco* configuration, this is in agreement with Verstraeten's correlations. Six do not show the type 1 band. None of them show a type IIA band, so this band may be characteristic of ketoses. Only one of the pyranoid compounds shows a type 2 band, but the two furanoid compounds do not show the band, either. Only two of the eleven pyranoid compounds show a type IIB band, so this band, also, may have some value for diagnosis of ketoses. However, eight of these aldose derivatives show the "type I band of ketoses." Except for the type IIB band shown by compound 7, none of the *N*-acetylaldohexopyranosylamines show bands of types 2, IIA, and IIB, in agreement with Verstraeten's correlations. The β-xylopyranose com-

pound 1A and the β-glucopyranose compounds (2A and 9) show no bands of types 2, I, IIA, or IIB, in agreement with Verstraeten's correlations.

TABLE 13. *Bands (cm^{-1}) in the spectra of unsubstituted, furanoid and pyranoid, 1-acetamido derivatives*

Serial No.	Bands of aldoses (and ketoses)			Bands of ketoses		
	1(*f*, *p*)	2(*f*)	3(*p*)	I	IIA	IIB
	Range					
	944–914	856–844	786–776	883–865	824–810	838–830
Furanoses						
1	938	–	778	883	–	831
2	942	–	–	867	810	–
Pentopyranoses						
1A	939	–	[a]–	–	–	–
5	–	856	776	881	–	–
4A	936 (913)	–	(771)	(864)	–	–
5B	–	–	[b]–	882	–	838
6B	–	–	[b]–	880	–	–
Hexopyranoses						
2A	–	–	[c]–	–	–	–
[9 [d]	922	–	[c]–	–	–	–]
3A	–	–	–	876	–	–
6	–	–	781	867	–	–
7	930	–	–	873	–	833
5A,8	942	–	786	867	–	–

[a] *xylo.* [b] *ribo.* [c] *gluco.* [d] 1-Propionamido derivative.

Table 14 lists the bands in the spectra of six unsubstituted, pyranoid, 1-benzamido derivatives. Only two do not show the *p* band of type 3, and for one of these (compound 12), this agrees with Verstraeten's correlations. All of them show the band of type 1. Four of these pyranoid compounds show the *f* band of type 2; this impairs the diagnostic value of the band. Only one of the compounds shows a type IIA band and only one shows a type IIB band; this strengthens the possibility that these bands have some diagnostic value for ketoses. All but one of the compounds show a "type I band of ketoses," as do ten aldose derivatives listed in table 13; hence, the type I band has no value for diagnosing the presence of the 2-ketose structure.

TABLE 14. *Bands (cm^{-1}) in the spectra of unsubstituted, pyranoid, 1-benzamido derivatives*

Serial No.	Bands of aldoses (and ketoses)			Bands of ketoses		
	1(*f*, *p*)	2(*f*)	3(*p*)	I	IIA	IIB
	Range					
	944–914	856–844	786–776	883–865	824–810	838–830
Pentopyranoses						
10	933, 918	–	–	870	–	830
11	934, 928	856	780	880	–	–
Hexopyranoses						
12	917	–	[a]–	866	811	–
13	938, 917	856	776	866	–	–
14	937, 917	845	(773)	–	–	–
15	939	(858)	784	876	–	–

[a] *gluco.*

From a study of tables 13 and 14, it may be seen that only two of these aldose derivatives show the type IIA band of ketoses, and only four of them show the type IIB band of ketofuranoses. Of the five compounds showing the type 2 absorption of furanoses, four are 1-benzamido pyranoid derivatives. Also, from a comparison of the spectra of the β-glycopyranose compounds 2A and 12, it would seem that, for compound 12, the 1-benzamido group must, in some way, be responsible for the bands of types 1, I, and IIA.

Table 15 lists bands in the spectra of five unsubstituted 1,1-bis(acetamido)-1-deoxyalditols. None of them show the types IIA and IIB bands of ketoses, indicating that these bands may have some diagnostic value. All of these acyclic compounds show the type 1 band of aldoses and ketoses, and all but one show the type I band of ketoses. Two of the five compounds show the type 2 band of furanoses, and two of the five show the type 3 band of certain pyranoid aldoses and ketoses.

TABLE 15. *Bands (cm^{-1}) in the spectra of unsubstituted 1,1-bis(acylamido)-1-deoxyalditols*

Serial No.	Bands of aldoses (and ketoses)			Bands of ketoses		
	1(*f*, *p*)	2(*f*)	3(*p*)	I	IIA	IIB
	Range					
	944–914	856–844	786–776	883–865	824–810	838–830
1,1-Bis(acetamido)						
24	936	–	–	882	–	–
15A	(947)	–	(775)	877	–	–
25	930	–	(787)	882	–	–
26	919	856	–	–	–	–
27	943	856	–	879, 867	–	–
1,1-Bis(propionamido)						
28	926	847	–	(864)	–	–
1,1-Bis(benzamido)						
29	937, 926	(843)	–	880	–	–
30	919	845	–	870	–	–
31	932, 916	–	–	881	–	838
32	923	851	(775)	878	–	–
33	930	853	–	877	810	–
34	935	–	784	(884)875	–	–
35	930	846	(772)	877	–	–
36	929	847	–	875	–	–

In table 15 are also listed the bands of unsubstituted 1,1-bis(benzamido)-1-deoxyalditols. Only one compound (33) shows type IIA absorption, and only one compound (31) shows type IIB absorption, confirming that these bands have some diagnostic value. However, like the compounds shown in table 14, all of these acyclic compounds show the type 1 band of aldoses and ketoses, and all show the type I band of ketoses. Only two of the eight acyclic compounds do not show the type 2 band of furanoses, and three show the type 3 band of certain pyranoid aldoses and ketoses.

b. Esters

Verstraeten did not study the infrared spectra of esters. The bands in the spectra of esters of furanoid and pyranoid 1-acetamido derivatives are listed in

236-431 O-67-5

table 16. The *furanoid* compounds 3 and 4 show the *f* band of type 2 and the band of type 1, in agreement with Verstraeten's correlations. However, they both show the ketose band of type I. In agreement with Verstraeten's correlations, compound 3 does not show the *p* band of type 3; however, compound 4 shows this band. Compound 3 shows the type IIA band of ketoses, and compound 4 shows the type IIB band of ketoses.

TABLE 16. *Bands (cm^{-1}) in the spectra of esters of (pyranoid) 1-propionamido and (furanoid and pyranoid) 1-acetamido derivatives*

Serial No.	Ester	Bands of aldoses (and ketoses)			Bands of ketoses		
		1(*f*, *p*)	2(*f*)	3(*p*)	I	IIA	IIB
		Range					
		944–914	856–844	786–776	883–865	824–810	838–830
		1-PROPIONAMIDO					
18	*O*-Pr	934	–	[a]–	(886, 864)	810	836
19	*O*-Bz	940	(858)847	[a]–	–	–	830
		1-ACETAMIDO					
Furanoses							
3	*O*-Bz	943	(860)	–	(887)871	824, 810	–
4	*O*-Bz	939	(857)	776	(885)	–	830
Pentopyranoses							
17	*O*-Bz	944, 935	851	774	(862)	–	(828)
6A	*O*-Ac	934	–	[b]–	877	–	–
9A	*O*-Ac	944, 933	–	–	870	–	–
4B	*O*-Ac	936	–	[c]–	870	–	–
Hexopyranoses							
7A	*O*-Ac	917	–	[a]–	871	–	–
8A	*O*-Ac	940	–	–	880	–	–
16	*O*-Ac	(945)	–	–	(861)	–	–
10A	*O*-Ac	924, 914 943, 921	–	–	(862)	–	834
11A	*O*-Ac	914	–	–	870	–	–

[a] *gluco.* [b] *xylo.* [c] *ribo.*

Of the eight *pyranoid* acetates, none show the *f* band of type 2, and all show the band of type 1, in agreement with Verstraeten's correlations. However, none of them show the type 3 band, although only three (compounds 6A, 4B, and 7A) would be expected not to show it. In agreement with Verstraeten's correlations, none of them show the type IIA band, and all but one (compound 10A) do not show the type IIB band. However, all of them show the type I band of ketoses.

The *pyranoid* benzoates (compounds 17 and 19) show the band of type 1 and do not show the type IIA band, in agreement with Verstraeten's correlations. However, they both show the *f* band of type 2 and the ketose band of type IIB. Compound 17 shows the *p* band of type 3, but compound 19 does not, in agreement with Verstraeten's correlations. Like the acetates in table 16, the propionate (18) and the benzoate (17) show the type I absorption of ketoses, but benzoate 19 does not. The 1-propionamido compounds (18 and 19) show absorption of type 1 but not type 3 absorption, in agreement with Verstraeten's correlations; however, they both show the type IIB absorption of ketofuranoses. Of the pyranoid compounds in table 16, compounds 6A, 4B, 7A, 18, and 19 would be expected not to show type 3 absorption and they do not, in agreement with Verstraeten's correlations. However, compounds 9A, 17, 8A, 10A, and 11A would be expected to show type 3 absorption, but only compound 17 shows it.

Table 17 lists the bands of esters of pyranoid 1-benzamido derivatives. All of them show the type 1 band, in agreement with Verstraeten's correlations. However, they all show the *f* band of type 2 and the type I band of ketoses. Compounds 21, 23, and 23a do not show the *p* band of type 3, whereas compound 22 does, in agreement with Verstraeten's correlations. However, compound 20 does not show this band. Three of the five compounds show the type IIA band of ketoses, and two show the type IIB band of ketofuranoses.

TABLE 17. *Bands (cm^{-1}) in the spectra of esters of pyranoid, 1-benzamido derivatives*

Serial No.	Bands of aldoses (and ketoses)			Bands of ketoses		
	1(*f*, *p*)	2(*f*)	3(*p*)	I	IIA	IIB
	Range					
	944–914	856–844	786–776	883–865	824–810	838–830
***O*-Acetyl**						
20	(947)931, 917	851	–	876	(808)	–
***O*-Benzoyl**						
21	939(913)	853	[a]–	870	824	–
22	(945)937	851	(772)	877	824	–
23	940	(858)845	[b]–	870	–	831
23a	940, 922	855	[b]–	874	–	830

[a] *xylo.* [b] *gluco.*

In table 18 are listed the bands of nine esters of 1,1-bis(acylamido)-1-deoxyalditols. All of these acyclic compounds show types 1 and I bands. All of the acetates, but none of the benzoates or acetate-benzoates, show a band of type 3. All of the benzamido compounds show a band of type IIA. Only two of the compounds do *not* show an *f* band of type 2. Three of the compounds show the type IIB band of ketofuranoses, and they possess both *O*-benzoyl and 1,1-bis(benzamido) groups.

c. Summation

The results are summarized in table 19, which lists, by the categories in tables 13 to 18, the compounds in this study that fit Verstraeten's correlations. For this purpose, an agreement score of unity is given if the spectrum of a compound (a) shows a predicted band or (b) does not show a band predicted to be absent; a score of zero is given if the spectrum (a) does not show a predicted band or (b) shows a band

TABLE 18. *Bands (cm^{-1}) in the spectra of esters of 1,1-bis(acylamido)-1-deoxyalditols*

Serial No.	Bands of aldoses (and ketoses)			Bands of ketoses		
	1(*f*, *p*)	2(*f*)	3(*p*)	I	IIA	IIB
	Range					
	944–914	856–844	786–776	883–865	824–810	838–830
	ACETATES					
Acetamido						
16A	929, 921	855	784	871	–	–
37	937, 925, 917	850	778(?)	(862)	–	–
Benzamido						
42	941, 935	847	778(?)	879	821	–
43	935	847	(775)	870	820(?)	–
44	935, 917	–	(772)	868	824	–
	BENZOATES					
Benzamido						
38	940, 929	849	–	870	810	–
41	938, 933, (911)	851, 846	–	867	822	(840)
	ACETATE–BENZOATES					
39	926, 917	–	–	871	(809)	837
40	939, 932, 921	855	–	873	(808)	(829)

TABLE 19. *Number of compounds of each category that fit Verstraeten's correlations*

Compounds studied			No. of compounds fitting band of type					
In table No.	Structural type	No.	1	2	3	I	IIA	IIB
Furanoses								
13	*N*-Ac	2	2	0	1	0	1	1
16	*N*-Ac, *O*-Bz	2	2	2	1	0	1	1
	Total	4	4	2	2	0	2	2
Pyranoses								
13	*N*-Ac	10	4	9	8	2	10	8
	N-Pr	1	1	1	1	1	1	1
14	*N*-Bz	6	6	2	5	1	5	5
16	*N*-Ac, *O*-Ac	8	8	8	3	0	8	7
	N-Pr, *O*-Pr	1	1	1	1	0	0	0
	N-Ac, *O*-Bz	1	1	0	1	0	1	0
	N-Pr, *O*-Bz	1	1	0	1	1	1	0
17	*N*-Bz, *O*-Ac	1	1	0	0	0	0	1
	N-Bz, *O*-Bz	4	4	0	4	0	2	2
	Total	33	27	21	24	5	28	24
Acyclic								
15	*N*-Ac	5	0	3	3	1	5	5
	N-Pr	1	0	0	1	0	1	1
	N-Bz	8	0	2	5	0	7	7
18	*N*-Ac, *O*-Ac	2	0	0	0	0	2	2
	N-Bz, *O*-Ac	3	0	1	0	0	0	3
	N-Bz, *O*-Bz	2	0	0	2	0	0	1
	N-Bz, *O*-Ac, *O*-Bz	2	0	1	2	0	0	0
	Total	23	0	7	13	1	15	19
	Grand total	60	31	30	39	6	45	45

predicted to be absent. From these results, an estimate of diagnostic value (see table 20) of each type of band was made, on the assumption that an agreement of 50 percent or less has no diagnostic value, but an agreement near 100 percent has diagnostic value. An agreement lying between 50 and 100 percent may have some value as being indicative of a possibility that must be further explored. Table 21 lists the results for six separate compounds, for comparison.

Verstraeten [19] pointed out that the *type 1* band is shown by the cyclic aldoses *and* ketoses that he studied; as may be seen from tables 20 and 21, this is now confirmed, except for some of the 1-acetamido pyranoses (see table 13). Consequently, to have diagnostic value, the band should *not* be shown by the acyclic derivatives; however, the type 1 band is shown by them (see tables 15 and 18). As may be seen from tables 20 and 21, the type 1 band has no diagnostic value for the acyclic derivatives. Hence, it has no diagnostic value at all in distinguishing between cyclic and acyclic structures for the compounds in this study.

TABLE 20. *Diagnostic value of Verstraeten's correlations for the various categories of compounds*

Compounds studied			Diagnostic value [a] of band of type					
In table No.	Structural type	No.	1	2	3	I	IIA	IIB
Aldofuranoses								
13	*N*-Ac	2	[++]	0	0	0	0	0
16	*N*-Ac, *O*-Bz	2	[++]	++	0	0	0	0
Aldopyranoses								
13	*N*-Ac	10	[0]	+	+	0	++	+
14	*N*-Bz	6	[++]	0	+	0	+	+
16	*N*-Ac, *O*-Ac	8	[++]	++	0	0	++	+
17	*N*-Bz, *O*-Bz	4	[++]	0	++	0	0	0
Acyclic								
15	*N*-Ac	5	0	+?	+?	0	++	++
	N-Bz	8	0	0	+?	0	+	+
18	*N*-Ac, *O*-Ac	2	0	0	0	0	++	++
	N-Bz, *O*-Ac	3	0	0	0	0	0	++
	N-Bz, *O*-Bz	2	0	0	++	0	0	0
	N-Bz, *O*-Ac, *O*-Bz	2	0	0	++	0	0	0

[a] Key: ++, 100% agreement; +, nearly 100% agreement; +?, above 50%, but much less than 100% agreement; 0, agreement of 50% or less.

TABLE 21. *Diagnostic value of Verstraeten's correlations applied to single compounds of various categories*

Compounds studied			Diagnostic value [a] of band of type					
In table No.	Serial No.	Structural type	1	2	3	I	IIA	IIB
Pyranoses								
13	9	*N*-Pr	[+]	+	+	+	+	+
16	18	*N*-Pr, *O*-Pr	[+]	+	+	0	0	0
	19	*N*-Pr, *O*-Bz	[+]	0	+	+	+	0
	17	*N*-Ac, *O*-Bz	[+]	0	+	0	+	0
17	20	*N*-Bz, *O*-Ac	[+]	0	0	0	0	+
Acyclic								
15	28	*N*-Pr	0	0	+	0	+	+

[a] Key: +, agrees with correlation; 0, does not agree with correlation.

From line 1 of table 20, it may be seen that none of the bands (including type 1, for the reasons just given) have diagnostic value for the two aldofuranoses studied (table 13); but, on benzoylation (table 16), the *f* band of *type 2* becomes manifest. Similarly, the diagnostic value of the type 2 band for the 1-acetamido pyranoses (table 13) is increased by acetylation (table 16); but the band has no diagnostic value for the 1-benzamido pyranoses (table 14), and benzoylation (table 17) has no effect on the value. The type 2 band has no diagnostic value for distinguishing furanoses from the acyclic compounds (tables 15 and 18).

Except for the furanoses (tables 13 and 16), the *type 3* band has diagnostic value for all of the benzoates (tables 16, 17, and 18), but not for the acetates (tables 16, 17, and 18); it may have value for the unesterified compounds (tables 13, 14, and 15).

From table 20, it may be seen that the band of *type I* has no diagnostic value for any of the compounds; for this band, the results in table 21 have no statistical significance.

Except for the furanoses (tables 13 and 16) and the esters of 1-benzamido compounds (tables 17 and 18), the *type IIA* band has excellent diagnostic value. The same is true for the *type IIB* band, which also has diagnostic value for the acetylated 1,1-bis(acetamido) alditols.

Consequently, for the compounds discussed in this study, the bands of types 1 and I have no diagnostic value. Secondly, before a spectrum is checked for the presence or absence of bands of types 2, 3, IIA, and IIB, it should be examined for the presence or absence of the group frequencies characteristic of the *O*-acetyl and *O*-benzoyl groups. *If no ester group is present*, the spectrum should be examined for the group frequencies characteristic of the *N*-acetyl and *N*-benzoyl groups. (a) If the *N*-acetyl group is present, the Verstraeten bands have no diagnostic value for the furanoid compounds 1 and 2. If these structures are eliminated from consideration by the results of some other kind of test, the bands of types 2, 3, IA, and IIA *may* have diagnostic value. (b) Should the *N*-benzoyl group be present, the type 2 band has no diagnostic value, but the bands of types 3, IA, and IIA should be useful.

If an ester group is present, it may be seen (from table 20) that, for the *N*-acetyl-*O*-acetyl compounds, the bands of types IIA and IIB differentiate between Verstraeten's ketoses and our nonketoses, but cyclic compounds cannot be distinguished from acyclic compounds. Insufficient evidence is available for the *N*-acetyl-*O*-benzoyl compounds; compounds 3 and 4 show the *f* band of type 2, but this band has no diagnostic value for compound 17. As regards the *N*-benzoyl-*O*-acetyl compounds, only the type IIB band has diagnostic value. For the *N*-benzoyl-*O*-benzoyl compounds, only the type 3 band has diagnostic value.

5. Correlations Made by Nanasi and Co-workers

Nanasi and co-workers [20] have made some correlations for infrared spectra of *N*-*p*-tolyl-α-and-β-D-glucopyranosylamines and their tetraacetates, and for tetramethyl ethers of the *N*-*p*-tolylglycosylamines having the α-D-glucofuranosyl, α-D-glucopyranosyl, and β-D-galactopyranosyl structures. They also made correlations for the *N*-*p*-bromophenylglycosylamines having the 2-deoxy-β-D-*arabino*-hexopyranosyl, β-D-glucopyranosyl, and β-D-galactopyranosyl structures, and for the tetraacetates of the last two. In the range of wavelengths we have discussed, most of their correlations agreed with those of Barker and co-workers [12], and so, detailed comment is not necessary. We have found that their correlations cannot be extended to the compounds described in the present article.

6. Other Absorption Bands

All of the compounds in this study are secondary amides, and all of them show at least one band at 3460 to 3226 cm^{-1} (N-H stretching); in this region, the completely esterified compounds (group 1a, table 22) could not be distinguished from those having free hydroxyl groups (group 1b) that would show O-H stretching in the same region. All of the compounds show a band at 1681–1626 cm^{-1} (amide I) and at 1575 to 1504 cm^{-1} (amide II). The bis(acylamido) compounds (group 1d) show two amide II bands, suggesting that the two acylamido groups on C-1 of these compounds are not equivalent. They may have a hydrogen-bonded structure, possibly of the following type.

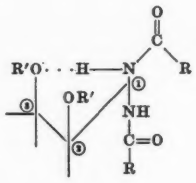

where R is Me, Et, or Ph; and R′ is H, Ac, EtCO, or Bz.

TABLE 22. *Structural groups studied*

Group	Structural feature	Compounds (serial numbers) in group
1	Amide, secondary	
a	no hydroxyl group	3, 4, 16–23a, 37, 39–44, 6A–11A, 16A, 4B
b	free hydroxyl groups	1, 2, 5–15, 24–36, 38, 1A–5A, 15A, 5B, 6B
c	mono(acylamido)	1–23a, 1A–11A, 4B–6B
d	bis(acylamido)	24–44, 15A, 16A
2	Esters	
a	acetates	16, 20, 37, 42–44, 6A–11A, 16A, 4B
b	propionate	18
c	benzoates	3, 4, 17, 19, 21–23a, 38, 41
d	mixed acetate-benzoates	39, 40
3	Phenyl group	
a	*N*-benzoyl, *O*-benzoyl, or both	3, 4, 10–15, 17, 19–23a, 29–36, 38–44
b	no phenyl group	1, 2, 5–9, 16, 18, 24–28, 37, 1A–11A, 15A, 16A, 4B–6B

All of the compounds show a band at 1311 to 1258 cm^{-1} ("amide III"). All of the acyclic compounds having a benzoyl group show the amide V band at 712 to 689 cm^{-1}, and this band is shown by many of the other compounds in this study.

The acetates and the tetrapropionate (groups 2a and 2b) show a band at 1761 to 1742 cm^{-1} (C=O stretching), except for compound 4B, which shows a band at 1718 cm^{-1}. The benzoates (group 2c) show a band at 1745 to 1727 cm^{-1}, except for the monobenzoate (compound 38) which shows a band at 1698 cm^{-1}. The mixed esters (group 2d) show two bands in this region: compound 39 at 1742 and 1715 cm^{-1}, and compound 40 at 1761 and 1745 cm^{-1}.

All of the compounds containing a phenyl group (group 3a) show bands at 1613 to 1600 cm^{-1}, 1587 to 1567 cm^{-1}, and 1506 to 1477 cm^{-1}. All of the compounds containing a phenyl group also show a band at 811 to 798 cm^{-1}; a band (*f* band of type D) in this region is also shown by the furanoid compounds 1 and 2, which lack a phenyl group. Consequently, this band has no diagnostic value for the furanoid ring if benzoyl groups are present. The propionate (compound 18) shows a band at 810 cm^{-1}, and the bis(propionamido) compound 28 shows a band at 807 cm^{-1}, but the propionamido compound 9 shows no band in this region. Compounds 38, 39, and 40, which are 1,1-bis(benzamido) compounds having a lone, terminal, *O*-benzoyl group, show two distinct bands in this region (810 to 798 cm^{-1}).

7. Experimental Procedures

7.1. Preparation and Purification of the Compounds

The compounds listed in table 1 were prepared by the methods given in the references cited. Each compound was recrystallized from an appropriate solvent until further recrystallization caused no change in melting point or optical rotation.

7.2. Measurement of Infrared Absorption

The spectrograms were recorded with a Perkin-Elmer Model 137 spectrophotometer[4] which was calibrated against a polystyrene standard (found value and deviation in parentheses): 3030 (3096; +66), 2924 (2976; +52), 2849 (2865; +16), 1946 (1953; +7), 1802 (1808 to 1805; +6 to +3), 1603 (1605 to 1600; +2 to −3), 1495 (1495 to 1493; 0 to −2), 1155 (1155 to 1153; 0 to −2), 1029 (1029 to 1028; 0 to −1), and 906 (907; +1) cm^{-1}, and against polyethylene: 720 (720 to 719; 0 to −1) cm^{-1}.

The spectrograms (see fig. 1) were recorded for Nujol mulls of the samples, and the bands of Nujol were used as an internal reference standard. In this study, the bands in the range of 4000 to 1800 cm^{-1} were of little interest, and the bands observed were corrected by reference to the above calibration and to the Nujol band at 2861 cm^{-1}. For bands in the range of 1800 to 667 cm^{-1}, the observed bands were not corrected. As, in some instances, the bands of interest occurred inside a range of as much as 26 cm^{-1}, and as (in the range of 1000 to 730 cm^{-1}) this instrument gave results to ± 2 cm^{-1}, the instrument was considered to be sufficiently accurate for our purposes. For example, for compound 15A, the bands in the region of 1000 to 730 cm^{-1} were compared with those recorded for the same specimen with a Beckman Model IR4 (double beam) spectrophotometer[4] (latter results in parentheses) as follows: 966 (964), 948 (947), 906 (904), 879 (877), 775 (775), 741 (742), and 714 (714) cm^{-1}. For compound 5A, the bands were compared with those obtained with a Perkin-Elmer Model 21 (double beam) spectrophotometer[4] (latter results in parentheses): *ca.* 995 (*ca.* 995), 968 (967), 948 (947), 943 (942), 896 (895), 868 (867), and 786 (786) cm^{-1}.

[4] Certain commercial instruments are identified in this paper in order to specify adequately the experimental procedure. In no case does such identification imply recommendation or endorsement by the National Bureau of Standards, nor does it imply that the equipment identified is necessarily the best available for the purpose.

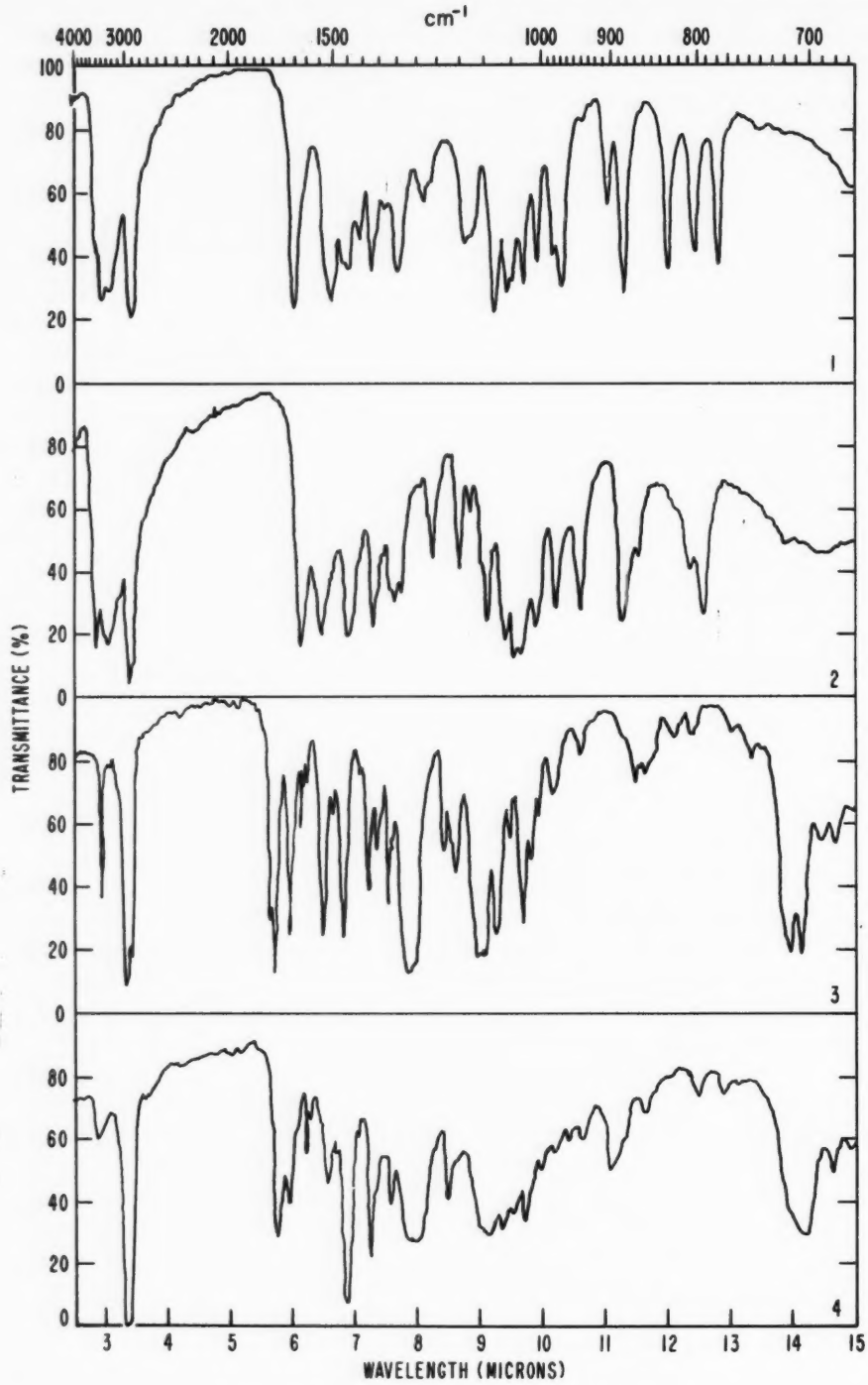

FIGURE 1. *Spectrograms of compounds in Nujol mulls.*

1, *N*-Acetyl-α-D-xylofuranosylamine; **2**, *N*-acetyl-α-D-glucofuranosylamine; **3**, *N*-acetyl-2,3,5-tri-*O*-benzoyl-α-D-xylofuranosylamine; **4**, *N*-acetyl-2,3,5,6-tetra-*O*-benzoyl-α-D-glucofuranosylamine.

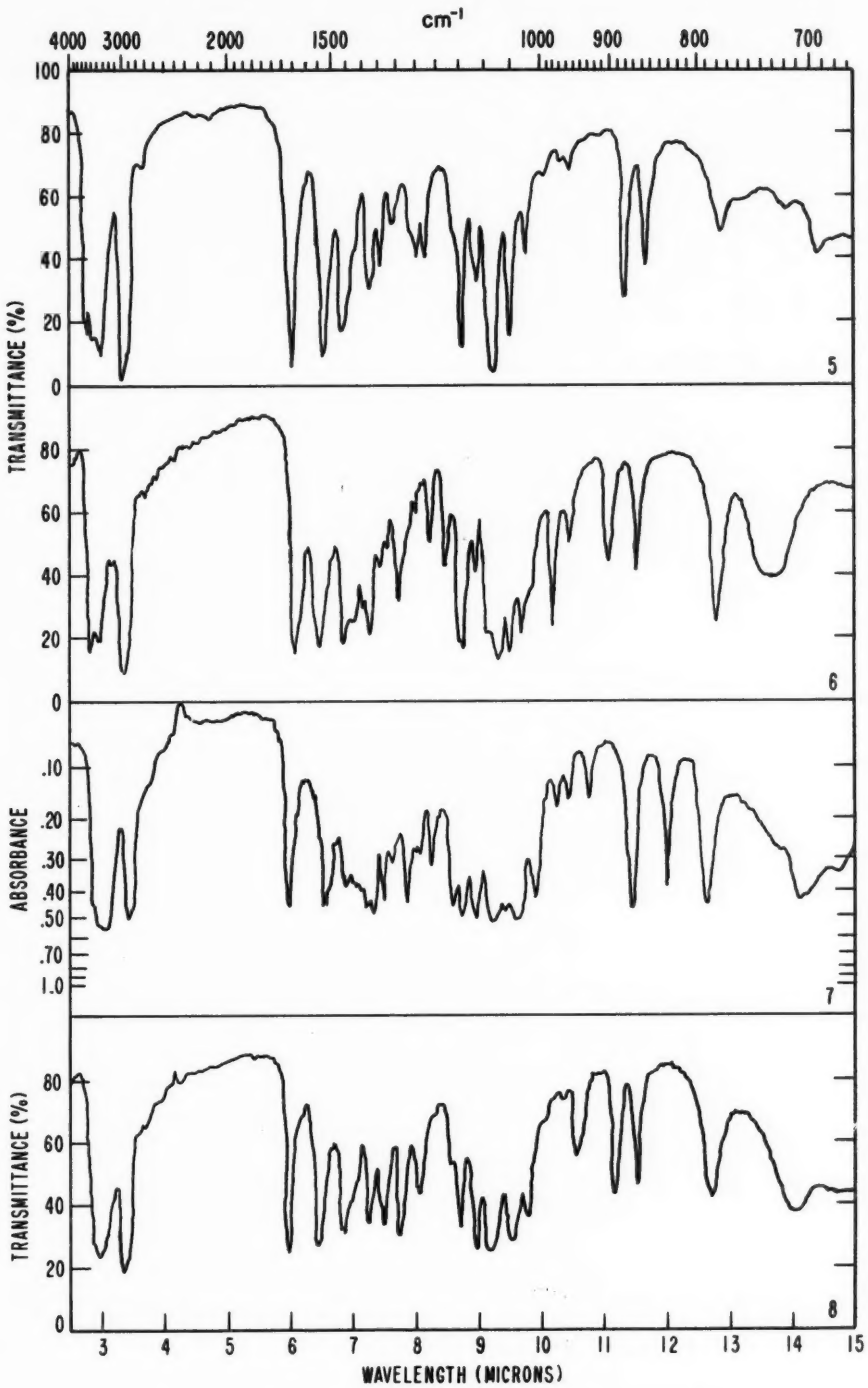

FIGURE 1. *Spectrograms of compounds in Nujol mulls.*—Continued

5, *N*-acetyl-β-D-lyxopyranosylamine; **6**, *N*-acetyl-6-deoxy-β-L-mannopyranosylamine; **7**, *N*-acetyl-α-D-galactopyranosylamine; **8**, *N*-acetyl-β-D-galactopyranosylamine.

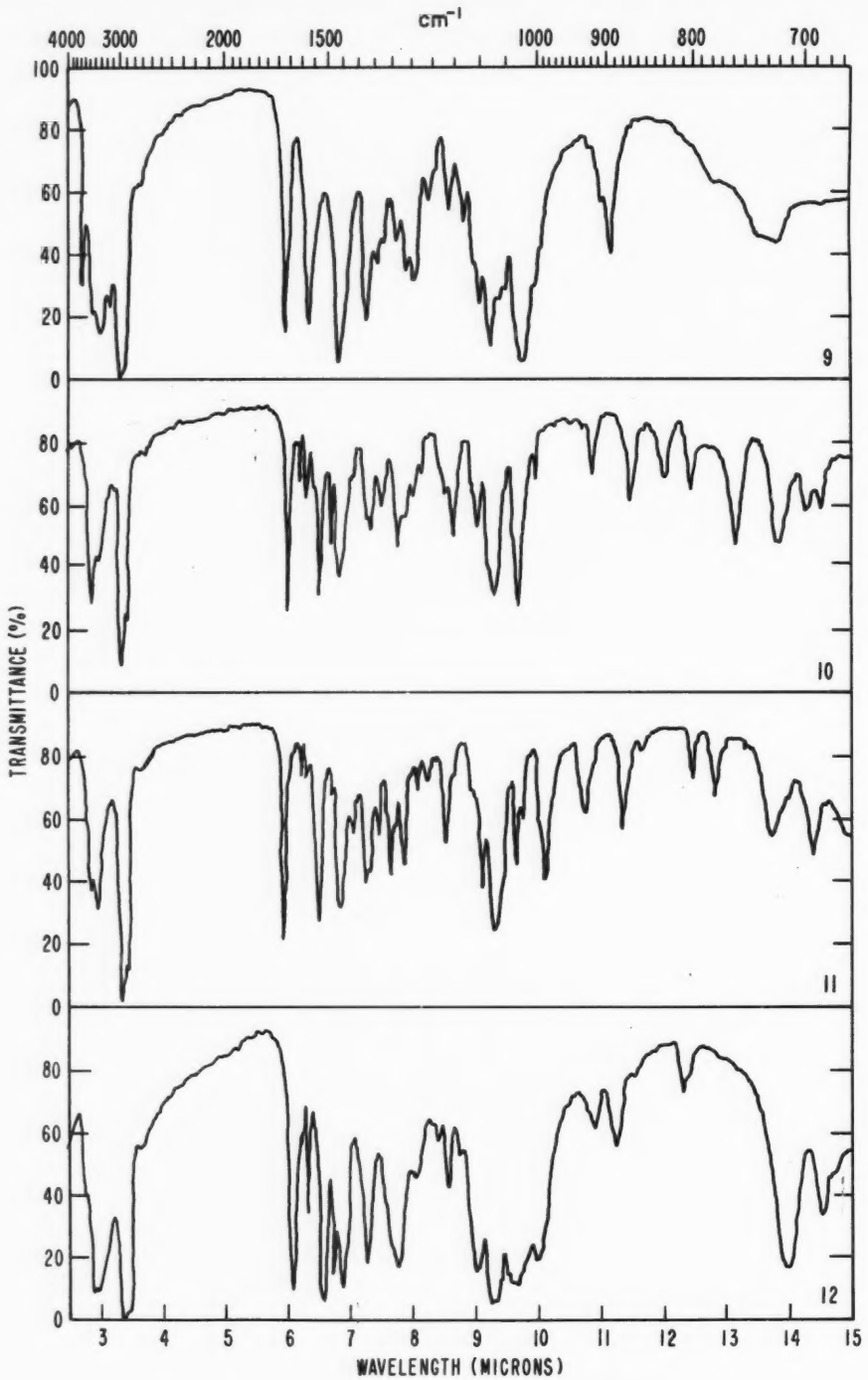

FIGURE 1. *Spectrograms of compounds in Nujol mulls.*—Continued

9, *N*-propionyl-β-D-glucopyranosylamine; **10**, *N*-benzoyl-β-D-lyxopyranosylamine; **11**, *N*-benzoyl-α-D-arabinopyranosylamine; **12**, *N*-benzoyl-β-D-glucopyranosylamine.

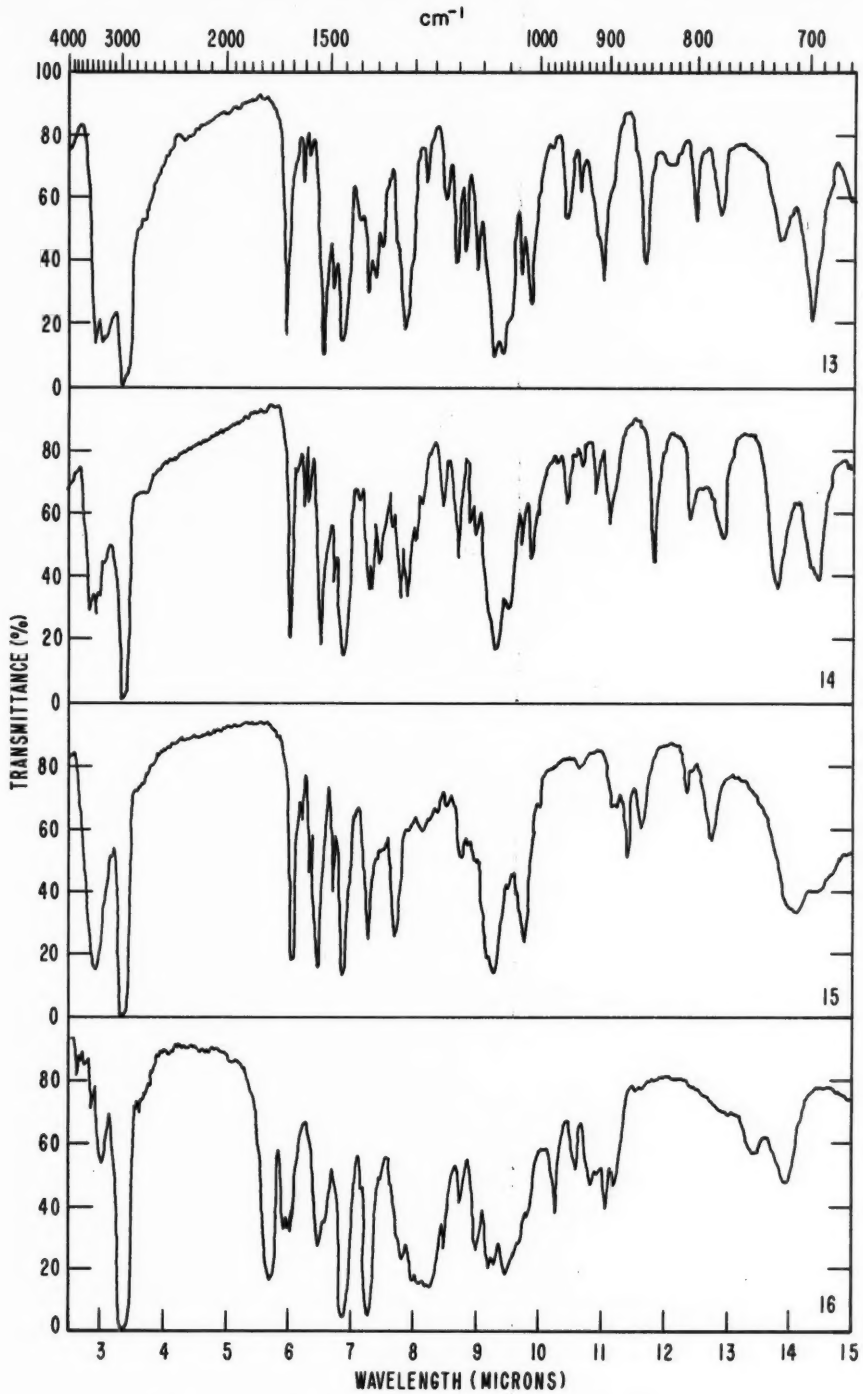

FIGURE 1. *Spectrograms of compounds in Nujol mulls.*—Continued

13, *N*-benzoyl-β-D-mannopyranosylamine; **14**, *N*-benzoyl-6-deoxy-β-L-mannopyranosylamine; **15**, *N*-benzoyl-β-D-galactopyranosylamine; **16**, *N*-acetyl-2,3,4-tri-*O*-acetyl-6-deoxy-β-L-mannosylamine.

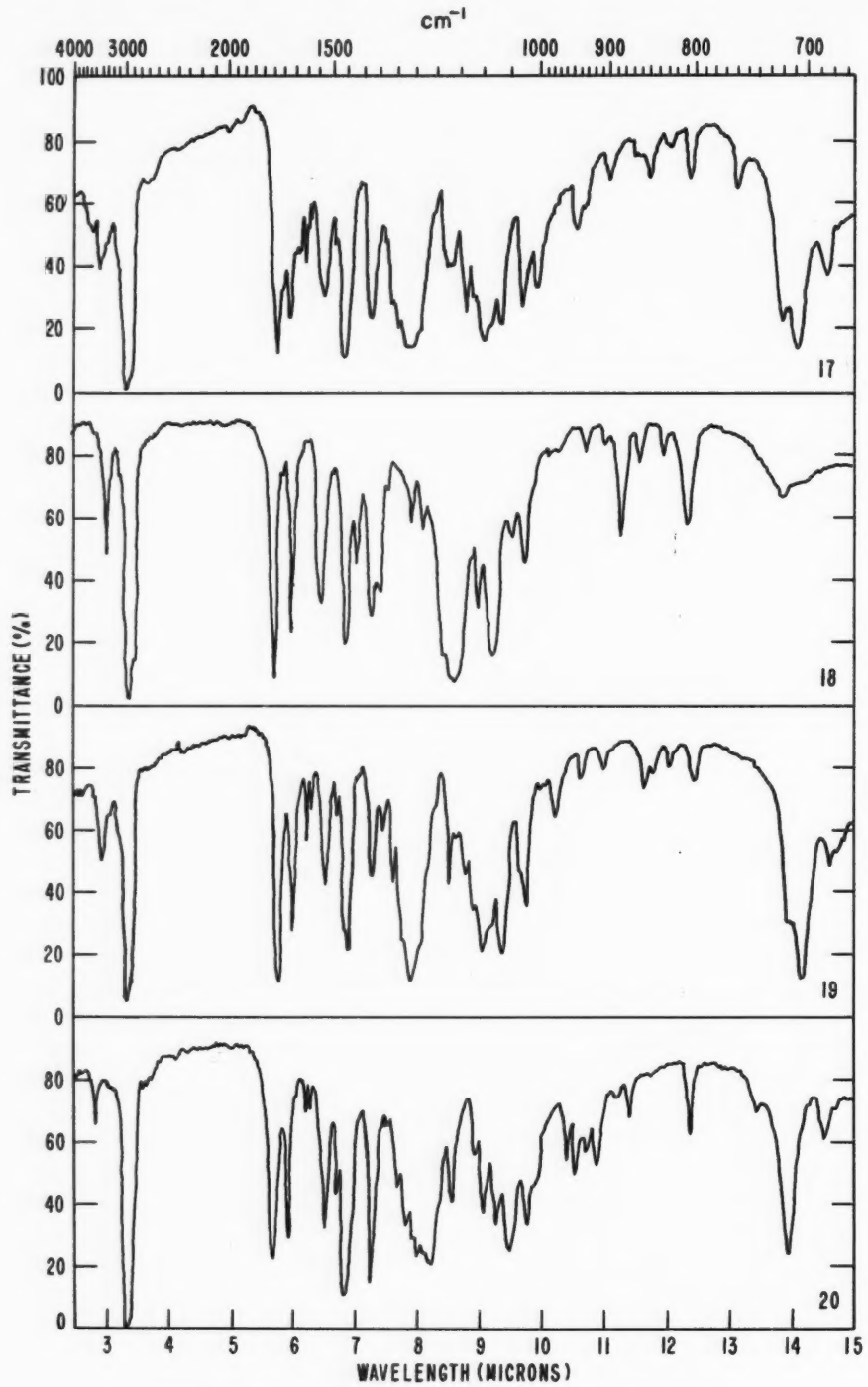

FIGURE 1. *Spectrograms of compounds in Nujol mulls.*—Continued

17, *N*-acetyl-2,3,4-tri-*O*-benzoyl-α-D-arabinosylamine; **18**, *N*-propionyl-2,3,4,6-tetra-*O*-propionyl-β-D-glucosylamine; **19**, 2,3,4,6-tetra-*O*-benzoyl-*N*-propionyl-β-D-glucosylamine; **20**, 2,3,4-tri-*O*-acetyl-*N*-benzoyl-α-D-arabinosylamine.

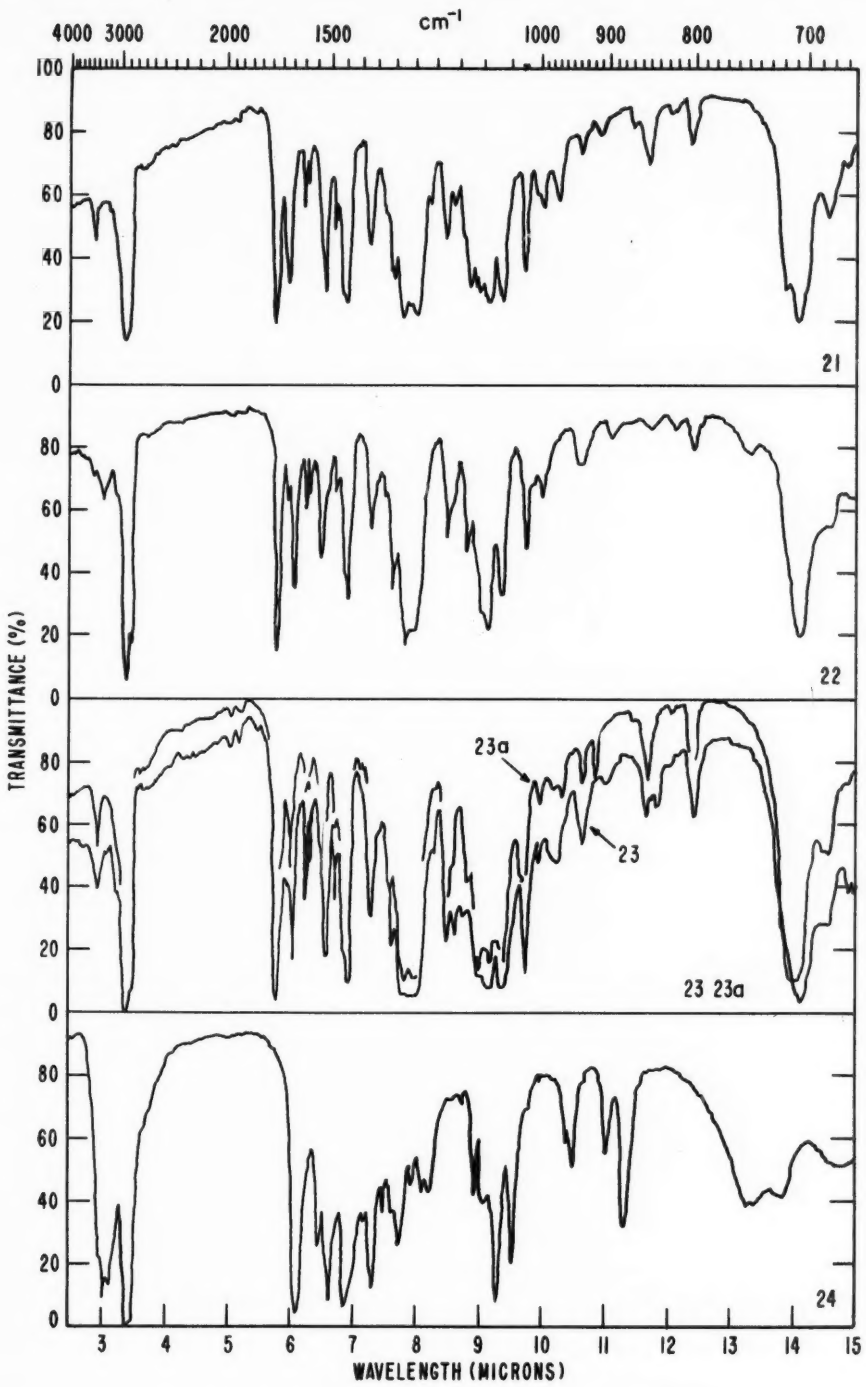

FIGURE 1. *Spectrograms of compounds in Nujol mulls.*—Continued

21, *N*-benzoyl-2,3,4-tri-*O*-benzoyl-β-D-xylosylamine: **22**, *N*-benzoyl-2,3,4-tri-*O*-benzoyl-α-D-arabinosylamine: **23**, *N*-benzoyl-2,3,4,6-tetra-*O*-benzoyl-β-D-glucosylamine (mp 113–115°): **23a**, *N*-benzoyl-2,3,4,6-tetra-*O*-benzoyl-β-D-glucosylamine (mp 184°): **24**, 1,1-bis(acetamido)-1-deoxy-D-erythritol.

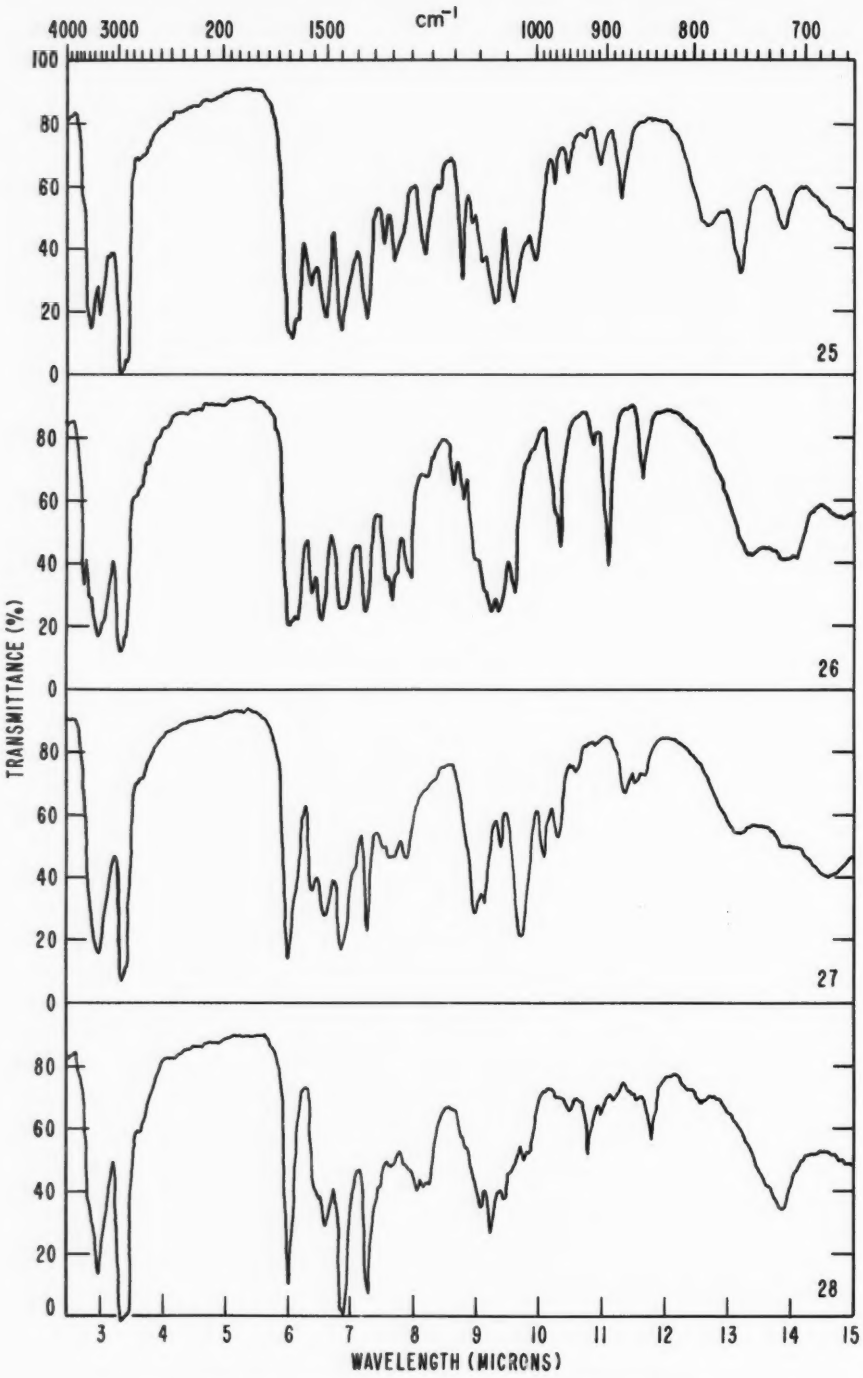

FIGURE 1. *Spectrograms of compounds in Nujol mulls.*—Continued

25, 1,1-bis(acetamido)-1-deoxy-D-glucitol; **26**, 1,1-bis(acetamido)-1,6-dideoxy-L-mannitol; **27**, 1,1-bis(acetamido)-1-deoxy-D-galactitol; **28**, 1-deoxy-1,1-bis(propionamido)-D-glucitol.

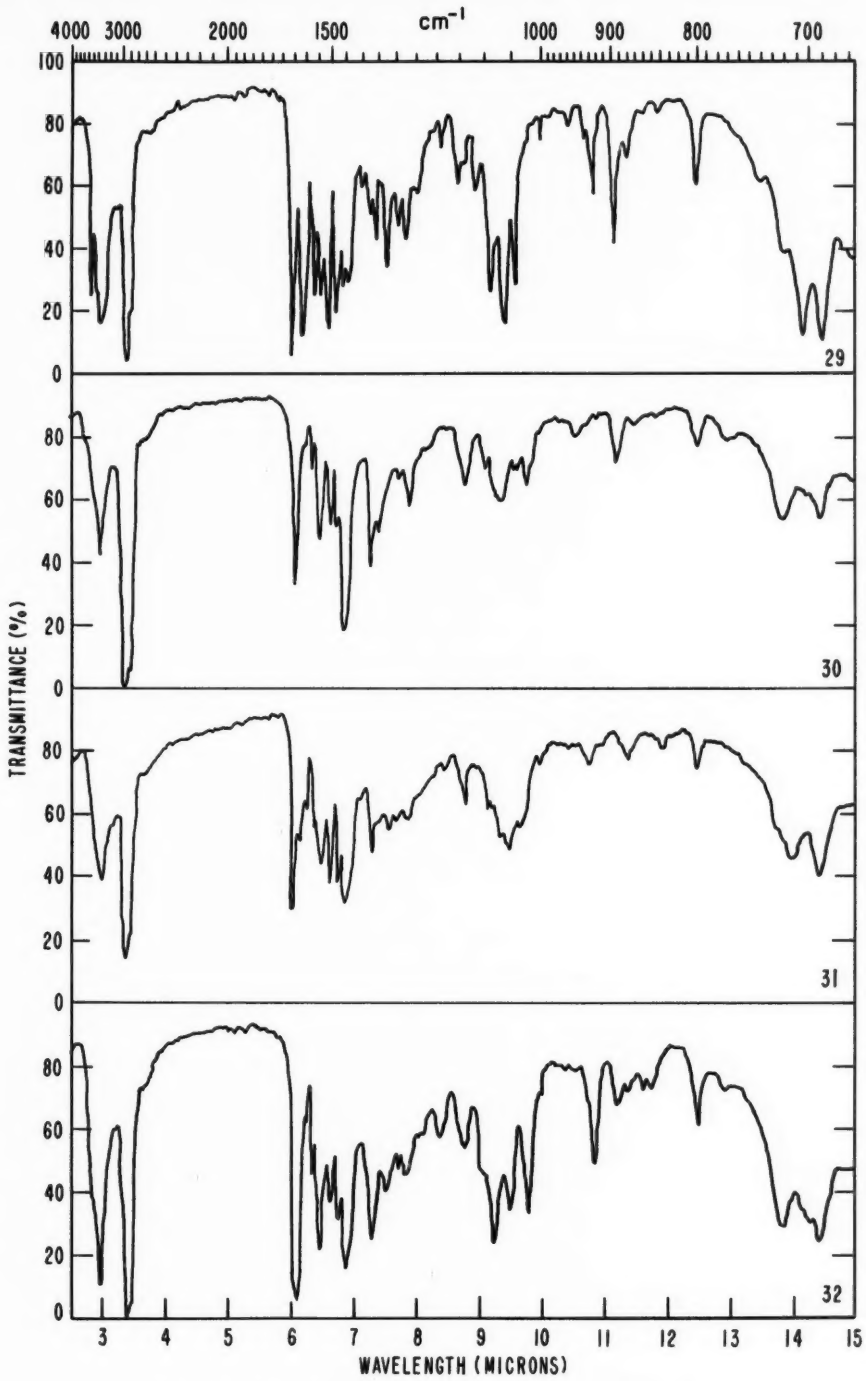

FIGURE 1. *Spectrograms of compounds in Nujol mulls.*—Continued

29, 1,1-bis(benzamido)-1-deoxy-L-erythritol; **30,** 1,1-bis(benzamido)-1-deoxy-L-arabinitol; **31,** 1,1-bis(benzamido)-1-deoxy-D-ribitol; **32,** 1,1-bis(benzamido)-1-deoxy-D-glucitol.

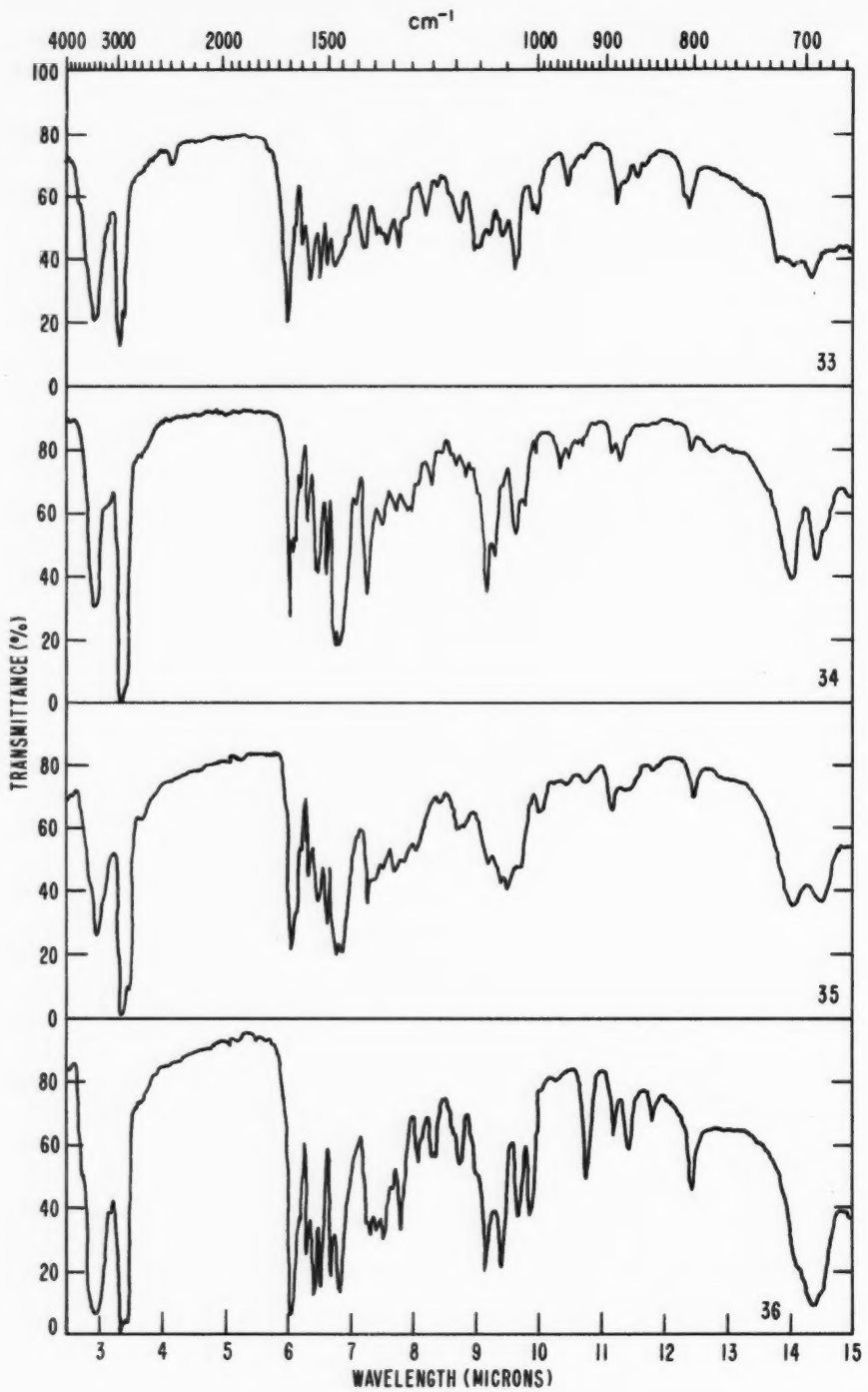

FIGURE 1. *Spectrograms of compounds in Nujol mulls.*—Continued

33, 1,1-bis(benzamido)-1,2-dideoxy-D-*arabino*-hexitol; **34**, 1,1-bis(benzamido)-1-deoxy-D-mannitol; **35**, 1,1-bis(benzamido)-1,6-dideoxy-L-mannitol; **36**, 1,1-bis(benzamido)-1-deoxy-D-galactitol.

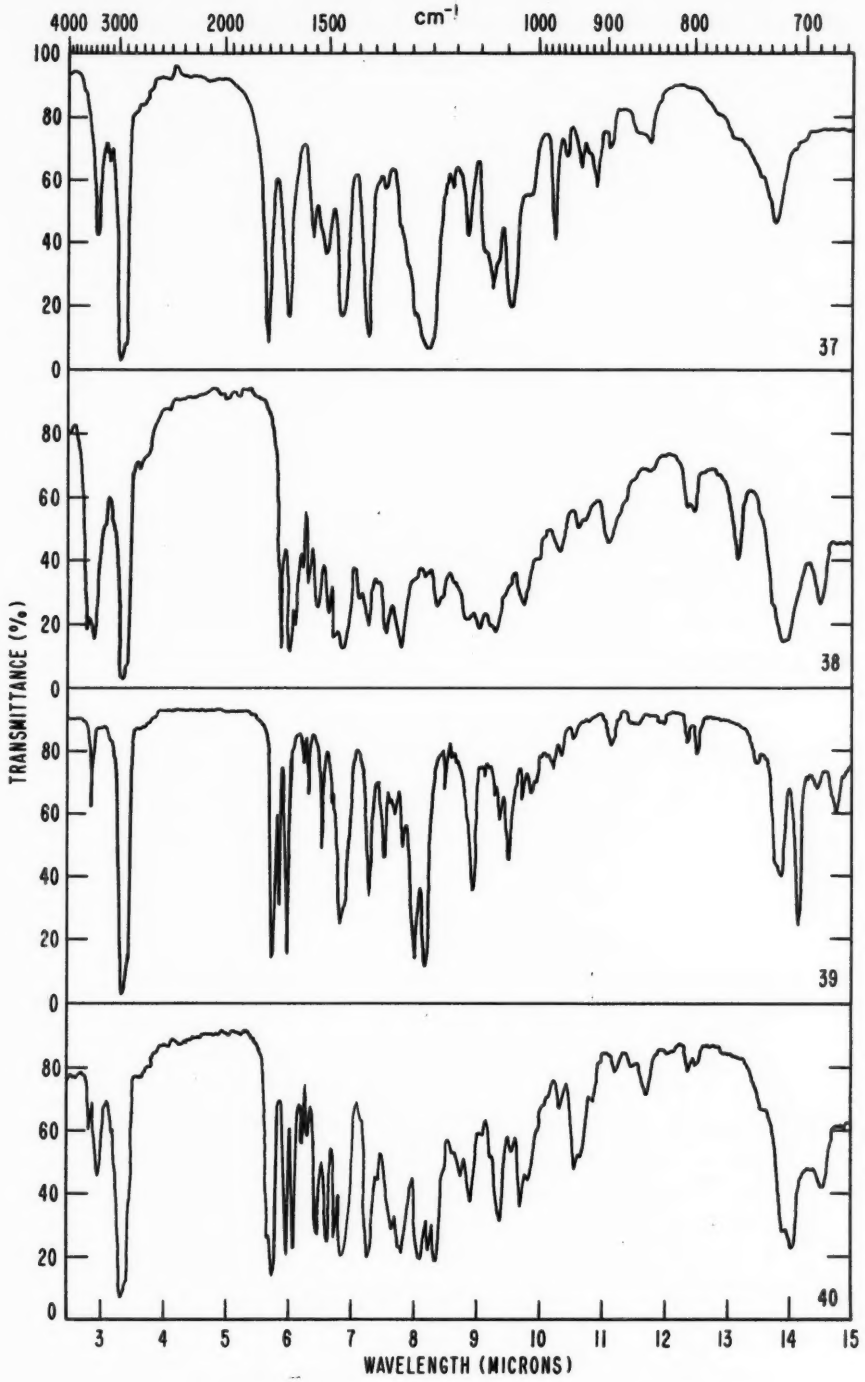

FIGURE 1. *Spectrograms of compounds in Nujol mulls.*—Continued

37, 1,1-bis(acetamido)-2,3,4,5,6-penta-*O*-acetyl-1-deoxy-D-glucitol; **38**, 1,1-bis(benzamido)-6-*O*-benzoyl-1-deoxy-D-glucitol; **39**, 2,3,4-tri-*O*-acetyl-1,1-bis(benzamido)-5-*O*-benzoyl-1-deoxy-D-lyxitol; **40**, 2,3,4-tri-*O*-acetyl-1,1-bis(benzamido)-5-*O*-benzoyl-1-deoxy-D-arabinitol.

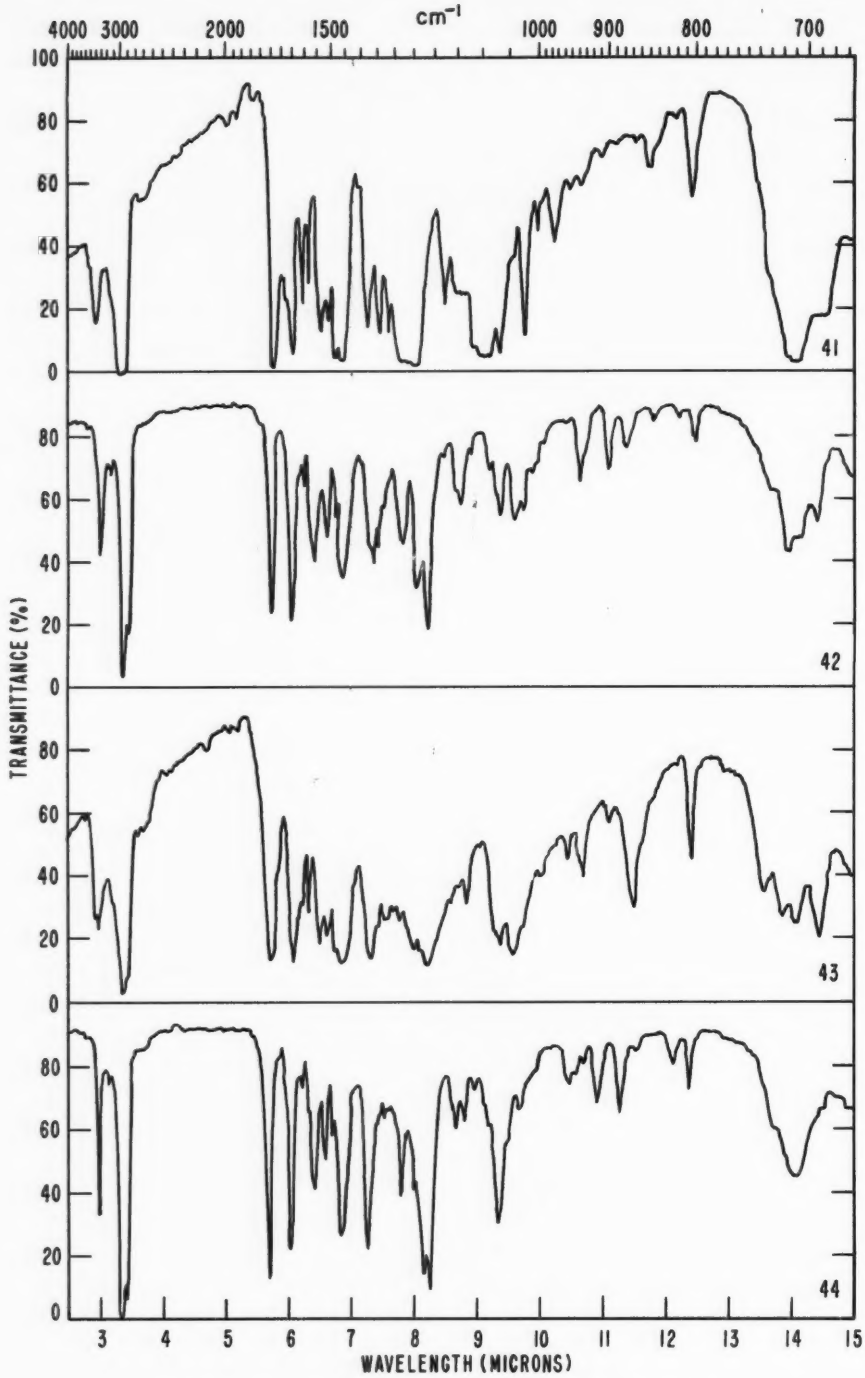

FIGURE 1. *Spectrograms of compounds in Nujol mulls.*—Continued

41, 1,1-bis(benzamido)-2,3,4,5-tetra-*O*-benzoyl-1-deoxy-D-arabinitol; **42**, 2,3,4-tri-*O*-acetyl-1,1-bis(benzamido)-1-deoxy-L-erythritol; **43**, 2,3,4,5-tetra-*O*-acetyl-1,1-bis(benzamido)-1-deoxy-D-ribitol; **44**, 2,3,4,5,6-penta-*O*-acetyl-1,1-bis(benzamido)-1-deoxy-D-glucitol.

8. References

[1] H. S. Isbell, J. Res. NBS **57,** 171 (1956) RP2707.
[2] R. S. Tipson and H. S. Isbell, J. Res. NBS **65A** (Phys. and chem.) No. 1, 31 (1961).
[3] R. S. Tipson, J. Org. Chem. **26,** 2462 (1961).
[4] S. A. Barker, E. J. Bourne, M. Stacey, and D. H. Whiffen, J. Chem. Soc. **1954,** 171.
[5] S. A. Barker, E. J. Bourne, R. Stephens, and D. H. Whiffen, J. Chem. Soc. **1954,** 3468.
[6] S. A. Barker, E. J. Bourne, R. Stephens, and D. H. Whiffen, J. Chem. Soc. **1954,** 4211.
[7] W. B. Neely, Advan. Carbohydrate Chem. **12,** 13 (1957); see table II on p. 27 thereof.
[8] L. J. Bellamy, The infra-red spectra of complex molecules, 2d ed. p. 76 (John Wiley & Sons, New York, N.Y.).
[9] H. S. Isbell and R. S. Tipson, J. Res. NBS **64A** (Phys. and Chem.) No. 2, 171 (1960).
[10] G. P. Ellis, J. Chem. Soc. (B) **1966,** 572.
[11] M. Stacey, R. H. Moore, S. A. Barker, H. Weigel, E. J. Bourne, and D. H. Whiffen, Proc. U.N. Intern. Conf. Peaceful Uses At. Energy, 2d, Geneva, 1958, Vol. 20, p. 251.
[12] S. A. Barker, E. J. Bourne, and D. H. Whiffen, Methods Biochem. Anal. **3,** 213 (1956).
[13] H. Spedding, Methods Carbohydrate Chem. **1,** 548 (1962).
[14] See, for example, C. N. R. Rao, Chemical applications of infrared spectroscopy, Academic Press Inc., New York, N.Y., 1963.
[15] H. Spedding, Advan. Carbohydrate Chem. **19,** 23 (see p. 31) (1964).
[16] S. A. Barker and R. Stephens, J. Chem. Soc. **1954,** 4550.
[17] R. S. Tipson, H. S. Isbell, and J. E. Stewart, J. Res. NBS **62,** 257 (1959) RP2960.
[18] R. S. Tipson and H. S. Isbell, J. Res. NBS **66A** (Phys. and Chem.) No. 1, 31 (1962).
[19] L. M. J. Verstraeten, Anal. Chem. **36,** 1040 (1964); Carbohydrate Res. **1,** 481 (1966).
[20] P. Nanasi and P. Cerletti, Gazz. Chim. Ital. **92,** 576 (1962); P. Nanasi, E. Nemes-Nanasi, and P. Cerletti, ibid. **95,** 966, 975 (1965).

(Paper 71A1–437)

236–431 O–67–6

JOURNAL OF RESEARCH of the National Bureau of Standards—A. Physics and Chemistry
Vol. 71A, No. 1, January–February 1967

Publications of the National Bureau of Standards*

Selected Abstracts

Experimental and theoretical studies of photoionization efficiency curves for C_2H_2 and C_2D_2, R. Botter, V. H. Dibeler, J. A. Walker, and H. M. Rosenstock, *J. Chem. Phys.* **44,** *No. 3, 1271–1278 (Feb. 1966).*

Photoionization efficiency curves for C_2H_2 and C_2D_2 have been remeasured in the wavelength region from onset of ionization to 600Å, using a gold-coated grating and the Hopfield continuum as a photon source. The curve shapes of the molecule ions near threshold are compared with calculations of the Franck-Condon factors. Nearly exact agreement between experiment and calculation is obtained when taking into account hot bands. A general discussion is given for the shape of the molecule ion curve and for that of the fragment ions, C_2H^+ and C_2D^+. The observed onsets of ionization for the latter ions are 17.2_2 eV and 17.3_4 eV, respectively.

Gas-phase radiolysis and photolysis of neopentane, S. G. Lias and P. Ausloos, *J. Chem. Phys.* **43,** *No. 8, 2748–2759 (Oct. 1965).*

The photolysis of neo-C_5H_{12}-neo-C_5D_{12} mixtures has been investigated at 1470 and 1236Å. From the products formed in the absence and presence of NO or H_2S, the occurrence of the following fragmentation processes could be derived:

$$\text{neo-}C_5H_{12}^* \rightarrow CH_4 + \text{iso-}C_4H_8 \quad 1$$
$$CH_3 + H + \text{iso-}C_4H_8 \quad 2$$
$$CH_3 + CH_3 + C_3H_6 \quad 3$$

These modes of decomposition also prevail when neopentane is excited by collision with electrons accelerated by an electrical field applied during radiolysis. At 1236 Å, the relative probabilities of occurrence of processes 1, 2, and 3 are approximately 1.0, 4.5, and 1.1.

From the isotopic analysis of the products formed in the direct and inert gas sensitized radiolysis of neo-C_5H_{12}-neo-C_5B_{12} mixtures in the presence of NO, O_2, or I_2 as free radical scavengers, it could be derived that the fragment ions $C_2H_3^+$, $C_2H_5^+$, $C_3H_5^+$, and $C_3H_7^+$ are formed.

Key Words: Free radicals, ion-molecules reactions, neopentane, photolysis, radiolysis.

Intramolecular insertion of isobutylidene in the vacuum ultraviolet photolysis of isobutane, E. Tschuikow-Roux and J. R. McNesby, *Trans. Faraday Soc.* **62,** *No. 524, 2158–2163 (Aug. 1966).*

The direct photolysis of isobutane was carried out at the Xe resonance line (1470 Å) at 25 °C over the pressure range 5.3 to 410 torr, with and without added nitrogen. Specifically, evidence for the intromolecular insertion of isobutylidene resulting from the carbene elimination of H_2 was sought and found. From the C_4 product distribution at the highest pressure it was deduced that the ratio of isomerization of isobutylidene to intramolecular cyclization is 19:1.

Key Words: Isobutane, isobutylidene, insertion, photolysis, vacuum ultraviolet.

Phenylhydrazono-phenylazo tautomerism. Part I. *xylo*-4,5,6-trihydroxy-2-oxo-1,3-bis(phenylhydrazono) cyclohexane and 4-oxo-1-phenyl-5-phenylazo-3-pyridazine derivatives, H. S. Isbell and A. J. Fatiadi, *Carbohydrate Res.* **2,** *No. 2, 204–215 (June 1966).*

The positions of the phenylhydrazono groups in *xylo*-4,5,6-trihydroxy-oxo-1,3-bis(phenylhydrazono)cyclohexane were established by degradation of the compound with sodium metaperiodate and identification of the reaction product. The dialdehyde initially formed by periodate oxidation (but not isolated) cyclized to 4-oxo-1-phenyl-5-phenylazo-3-pyridazinecarboxaldehyde, which gave a crystalline methyl hemiacetal, an oxime, a semicarbazone, and, by oxidation, the corresponding monocarboxylic acid and sodium salt. Upon treatment with phenylhydrazine at 50°, the carboxaldehyde gave a red crystalline phenylhydrazone which, with phenylhydrazine at 130°, gave a product that appears to be 4-oxo-1-phenyl-5-(phenylhydrazo)-3-pyridazine-carboxaldehyde phenylhydrazone.

The reactions provide a route to a series of new pyridazine derivatives which may prove valuable for the synthesis of unusual compounds for biological and medical research.

Key words: Absorption spectra of pyridazine derivatives, cyclic polyhydroxy ketones, inositol, triketo-, nuclear magnetic resonance of pyridazine derivatives, 4-oxo-1-phenyl-5-phenylazo-3-pyridazine-carboxaldehyde derivatives, phenylhydrazono-phenylazo tautomerism; pyridazine derivatives, *xylo*-trihydroxycyclohexenediolic acid preparation of bis-phenylhydrazone of-, *xylo*-4,5,6-trihydroxy-2-oxo-1,3-bis(phenylhydrazono)cyclohexane.

Solid-vapor equilibrium in the system helium-methane, M. J. Hiza and A. J. Kidnay, *(Proc. 1965 Cryogenic Engineering Conf., University of Pennsylvania, Philadelphia, Pa., Aug. 18–24, 1964), Book, Advances in Cryogenic Engineering 11, 338–348 (Plenum Press Inc. New York, N.Y., 1966).*

Gas phase compositions in the solid-vapor region for the neon-methane system were measured at eight integral temperatures from 50.00° to 87.00 °K up to 100 atmospheres pressure. A flow system was used in which methane was evaporated into a stream of pure neon gas. The equilibrium methane content of the gas phase leaving the equilibrium cell was analyzed continuously with a hydrogen flame-ionization detector. A comparison of these data at 76.00 °K with data for the hydrogen-methane and helium-methane systems is made to show the relative non-ideality of the neon system. Theoretical calculations of the concentration minima for this system are in poor agreement with experimental values.

Key Words: Low-temperature phase-equilibrium, methane, minimum gas phase equilibrium concentration, neon, neon-methane binary system, solid-vapor equilibrium.

The crystal and molecular structure of dichloro (1–10-phenanthroline) zinc, C. W. Reimann, S. Block, and A. Perloff, *Inorg. Chem.* **5,** *No. 7, 1185–1189 (July 1966).*

Crystals of dichloro (1,10 phenanthroline) zinc are monoclinic with four molecules in a unit cell of dimensions $a = 9.73$ Å, $b = 15.67$ Å, $c = 7.97$ Å, $\beta = 101°5'$, space group $P2_1/n$. Three dimensional data were used and the structure solved as a heavy atom problem. The coordination about the zinc atom is distorted tetrahedral. The 1,10 phenanthroline molecule itself is essentially planar and the zinc atom departs 0.13 Å from this plane. The chlorine atoms are nearly equidistant from the zinc atom. The plane of the zinc and two chlorine atoms makes an angle of 79° with the plane of the 1,10 phenanthroline molecule.

Key Words: Crystal structure, dichloro (1,10 phenanthroline) zinc molecular structure, tetrahedral.

The crystal structure of the high temperature form of barium borate, $BaO \cdot B_2O_3$, A. D. Mighell, A. Perloff, and S. Block, *Acta Cryst.* **20,** *Pt. 6, 819–823 (June 1966).*

The crystal structure of the high temperature form of $BaO \cdot B_2O_3$ (M.P. = 1095° ± 5 °C) was determined by conventional three-dimensional Patterson and electron-density syntheses. The heavy atom technique was used to establish the initial phases. $BaO \cdot B_2O_3$ crystallizes in the rhombohedral space group $R\bar{3}c$ with 18 formula units per hexagonal cell. Unit-cell dimensions, referred to hexagonal axes, are $a = b = 7.235$ Å, $c = 39.192$ Å. Least-squares refinement with 498 independent reflections yielded a reliability index of 5.7%, based on the observed data only. The anion in the structure is a nearly planar $(B_3O_6)^{-3}$ group constructed of three BO_3-triangles each of which shares two of the three corners. The structure contains two crystallographically distinct barium atoms located in positions having point symmetries 32 and 3. About the barium in the 32 symmetry position the oxygens are arranged in a

trigonal prism. About the barium which lies in the three-symmetry position the oxygen coordination is 9-fold.

Key Words: $BaO \cdot B_2O_3$, barium borate, borate, crystal, structure, x-ray.

Thermal decomposition of hexamethylethane, 2,2,3-trimethylbutane and neopentane in a single pulse shock tube, W. Tsang, *J. Chem. Phys.* **44,** *No. 11, 4283–4295 (June 1, 1966).*
Hexamethylethane, 2,2,3-trimethylbutane and neopentane have been pyrolyzed in a single pulse shock tube. The initial steps of the main reactions involve the breaking of carbon-carbon bonds. The rate parameters of the following reactions

$$C_4H_9{-}C_4H_9 \longrightarrow 2\ t\text{-}C_4H_9\cdot,$$

$$C_4H_9{-}C_3H_7 \xrightarrow{k_{II}} t{-}C_4H_9\cdot + i{-}C_3H_7\cdot$$

and $$C_4H_9{-}CH_3 \xrightarrow{k_{III}} t{-}C_4H_9\cdot + CH_3\cdot$$

have been found to be

$$k_I = 10^{16.3} \exp(-68{,}500/RT)\ \text{sec}^{-1},$$

$$k_{II} = 10^{16.2} \exp(-73{,}000/RT)\ \text{sec}^{-1}\quad (1100\ ^\circ\text{K and 4 atm.})$$

and $$k_{III} = 10^{16.1} \exp(-78{,}200/RT)\ \text{sec}^{-1}.$$

Key Words: Bond energies, decomposition, hexamethylethane, isopropyl radical, methyl radicals, neopentane, pyrolysis, shock tubes, *t*-butyl radicals, 2,2,3-trimethylbutane.

New standard for the calibration of microphones, W. Koidan, *Mag. Std.* **37,** *No. 5, 141–144 (May 1966).*
This article discusses the background, contents and use of a new American Standard, Calibration of Microphones, S1.10–1966, published by the American Standards Association, Incorporated.

Key Words: Calibration, microphones, standard.

Survey of infrared measurement techniques and computational methods in radiant heat transfer, S. T. Dunn, J. C. Richmond, and J. F. Parmer, *J. Spacecraft Rockets* **3,** *No. 7, 961–975 (July 1966).*
This paper is an analysis of 133 replies to a questionnaire sent to all known workers in the field of thermal radiation property measurements and radiant heat transfer computations. The questions were designed to obtain information on the current state of the art in these fields. In addition, the authors have supplemented the information obtained from the questionnaire to give a broad overall picture of the current status and future needs in each area covered. A brief summary of Russian literature in the field of thermal radiation property measurements is also included.

Key Words: Computational methods, emissivity, emittance measurements, radiant heat transfer, reflectance measurements, thermal radiation.

Atomic timekeeping and the statistics of precision signal generators, J. A. Barnes, *Proc. IEEE* **54,** *No. 2, 207–220 (Feb. 1966).*
Since most systems that generate atomic time employ quartz crystal oscillators to improve reliability, it is essential to determine the effect on the precision of time measurements that these oscillators introduce. A detailed analysis of the calibration procedure shows that the third finite difference of the phase is closely related to the clock errors. It was also found, in agreement with others, that quartz crystal oscillators exhibit a "flicker" or $|\omega|^{-1}$ type of noise modulating the frequency of the oscillator.
The method of finite differences of the phase is shown to be a powerful means of classifying the statistical fluctuations of the phase and frequency for signal generators in general. By employing finite differences it is possible to avoid divergences normally associated with flicker noise spectra. Analysis of several cesium beam frequency standards have shown a complete lack of the $|\omega|^{-1}$ type of noise modulation but an unexplained noise with a spectral variation proportional to $|\omega|^{-1/3}$ for frequency fluctuations was observed for $|\omega|$ less than 10^{-3} to 10^{-4} sec.$^{-1}$ depending on the particular standard.

Key Words: Atomic time, atomic frequency standards, statistics, stability.

Evaluation of a thallium atomic beam frequency standard at the National Bureau of Standards, R. E. Beehler and D. J. Glaze, *IEEE Trans. Instr. Meas.* **IM-15,** *No. 1 & 2, 55–58 (Mar.–June 1966).*
The original NBS cesium standard (NBS. I) has been converted to a thallium standard and was operated for 1½ years with a typical precision of 2×10^{-12} and an accuracy of 1×10^{-11}. Experiments are described which were performed to establish these precision and accuracy estimates. These results, which are comparable to those obtained with longer cesium standards, are considered sufficiently encouraging to justify the conversion of a longer cesium standard to thallium for a more thorough evaluation.

Key Words: Cesium standard, frequency standard, thallium standard.

Optical methods of temperature measurement, G. A. Hornbeck, *J. Appl. Opt. Lead Article* **5,** *No. 2, 179 (Feb. 1966).*
The history of the laws of thermal radiation is briefly reviewed, and the theoretical relations basic to some of the optical methods of temperature measurement are given. Comments on a number of optical methods are presented, as well as a selected reference with each method where more detail is available. In conclusion, several problems, in areas of uncertainty in the field of optical methods of temperature measurement, are suggested in the belief that a solution to these problems will greatly enhance the technical value of this field.

Key Words: Boltzmann, Draper, Jeans, Kirchhoff, optical, Planck, pyrometry, radiance, Rayleigh, Stefan, temperature, Wien.

The performance and capability of cesium beam frequency standards at the National Bureau of Standards, R. E. Beehler and D. J. Glaze, *IEEE Trans. Instr. Meas.* **IM-15,** *No. 1 & 2, 48–55 (Mar.–June 1966).*
NBS. II, the older of the two cesium atomic beam frequency standards which are used alternatively as the United States Frequency Standard, has been operating for more than five years. The contribution to inaccuracy produced by uncertainties in the C field has been reduced by a factor of 30 to $\pm 2 \times 10^{-13}$. The average precision of measurement (standard deviation of the mean) has been demonstrated to be 1×10^{-12} for averaging times of 1 hour and $\times 10^{-13}$ for 12 hours. The overall accuracy is considered to be $\pm 8 \times 10^{-12}$. A new cesium standard, NBS. III, with an interaction length of 3.66 meters is in operation and has demonstrated an improved average precision of 5×10^{-13} over 1 hour and an accuracy of $\pm 5 \times 10^{-12}$. The C field contributions to inaccuracy in this machine have been reduced to $\pm 1 \times 10^{-13}$. Considerable effort has been devoted to the detection and elimination of small frequency shifts produced by various electronic components of the excitation systems. In spite of the various improvements effected, a small unexplained difference in frequency of 1×10^{-12} continues to exist between the standards. The extremely high stability of the difference frequency, however, suggests that resolution of the difficulties should result in an accuracy capability of perhaps $\pm 1 \times 10^{-12}$.

Key Words: Atomic beam, cesium, frequency standard, U.S. frequency standard.

Time resolved microwave interferometry on diagnostic tool for decaying plasma afterglows, A. J. Estin and M. M. Anderson, *Rev. Sci. Instr.* **37,** *No. 4, 468–470 (Apr. 1966).*
Two laboratory techniques are described for making time resolved microwave interferometry measurements of electron density in a decaying plasma afterglow. The time resolution is of the order of 10 microseconds and thus permits at least several hundred sampling periods in the decay of a typical helium afterglow. A simple criterion is given for the error introduced in phase on account of the time-varying medium.

Key Words: Density, diagnostic, electron, interferometry, microwave, plasma, time-resolution.

Calculated line strengths for the transition array for d^2s-d^2p: application to Ni II, H. Mendlowitz, *Astrophys. J.* **143,** *No. 2, 573–590 (Feb. 1966).*
Transition arrays for the square root of the strengths of the transitions relative to a radial integral parameter are presented for $d^2s \rightarrow d^2p$ ($d^8s \rightarrow d^8p$) in *LS* coupling. The relative strengths in Ni II for the transitions between the configurations $3d^84s \rightarrow 3d^84p$ are calculated in intermediate coupling and are compared with earlier calculations by Gruzdev (1962) and with experiments of Bell, Paquette, and Wise (1965).

Comments on the mechanism of the 377-micron CN laser, H. P. Broida, K. M. Evenson, and T. T. Kikuchi, *J. Appl. Phys.* **36,** *No. 10, 3355 (Oct. 1965).*
Very intense laser radiation at 337 μ has been observed by Gebbie et al. [1, 2], when a pulsed electrical discharge is passed through various organic compounds such as HCN, CH_3CN and C_2H_5CN. Chantry et al. [3], suggest a laser transition in the vibrational state $v=2$ of the ground electronic state $X^2\Sigma$ of CN from the rotational level $K=8$ to K=7.
If the proposed explanation is correct, then a number of other transitions should occur, some with considerably higher probability than the observed emission.

Comparison of the Lennard-Jones, Exp: 6, and Kihara potential functions from viscosity data of dilute argon, H. J. M. Halney, *J. Chem. Phys.* **44,** *No. 11, 4219–4222 (June 1966).*
Experimental viscosity coefficients of argon were used to illustrate how the variation of the parameters of the Lennard-Jones, Exp: 6 and Kihara functions effect the correlation of the Chapman-Enskog transport theory with experimental data. By rationalizing the choice of the parameters, better correlations were possible than obtained by previous workers and it was shown that the Kihara function gave the best results.

Key Words: Chapman-Enskog theory, correlation, exp: 6, Kihara, Lennard-Jones, potential parameters, viscosity coefficient.

Electron impact ionization cross section data for atoms, Atomic ions, and diatomic molecules: I. Experimental data, L. J. Kieffer and G. H. Dunn, *Rev. Mod. Phys.* **38,** *No. 1, 1–33 (Jan. 1966).*
This review includes a compilation and critical evaluation of absolute cross sections for ionization of atoms and diatomic molecules by electron impact. Experimental techniques used for ionization are surveyed. Selected relative cross sections for production of multiply charged ions and a brief discussion of relative cross section data near threshold are presented. Absolute limits are not set on the size of probable systematic errors in the various experiments.

Key Words: Absolute cross sections, critical review, electron impact, multiply charged ions, relative cross sections.

Franck-Condon factors for the ionization of H_2 and D_2, G. H. Dunn, *J. Chem. Phys.* **44,** *No. 7, 2592–2594 (Apr. 1966).*
Franck-Condon factors for ionization of $H_2(^1\Sigma_g^+)$ and $D_2(^1\Sigma_g^+)$ are presented for 19 levels in H_2^+ $(^2\Sigma_g^+)$ and 27 levels in D_2^+ $(^2\Sigma_g^+)$. Comparisons are made with calculations, using less accurate potential functions for the molecular ion. Vibrational eigenenergies are given for D_2^+.

Key Words: Franck-Condon factors $H_2(^1\Sigma_g^+)$, ionization $D_2(^1\Sigma_g^+)$, vibrational eigenenergies D_2^+.

Impact broadening of microwave spectra, A. Ben-Reuven, *Phys. Rev.* **145,** *No. 1, 7–22 (May 1966).*
A unified treatment of pressure-broadening phenomena in the microwave spectra of gases is worked out by adaptation of the theories of Baranger and Fano, in which the effects of inelastic collisions are properly taken into account. The rate of relaxation in non-resonant spectra (Debye relaxation) is expressed in terms of collision cross sections. Small deviations from the Debye shape are related to a second moment of the relaxation matrix. Damping in resonance lines is studied, taking into account the coupling of the positive and negative resonance transitions by collisions. A general expression of the line shape as a function of frequency and pressure is given in the impact approximation. The ammonia inversion spectrum serves to demonstrate its applicability.

Key Words: Absorption, dielectric loss, gases, impact, line shape, microwave, permeability, permittivity, pressure broadening, relaxation, spectra.

Infrared spectra of HCl, DCl, HBr, and DBr in solid rare-gas matrices, D. C. Mann, N. Acquista, and D. White, *J. Chem. Phys.* **44,** *No. 9, 3453–3467 (May 1966).*
The infrared absorption spectra of HCl, DCl, HBr, and DBr, trapped in solid rare-gas matrices at liquid hydrogen and liquid helium temperatures, are reported. In the region of their fundamentals, the spectra of all these diatomic molecules consist of a number of bands; some which exhibit reversible changes in intensity and line width with temperature and others which are temperature independent.
The temperature dependent features have been identified as rotation-vibration bands of the matrix isolated diatomic molecule. The spacings of these bands are appreciably less than the separations of corresponding bands in the free molecule spectrum indicating a hindrance to rotation due to lattice-molecule interactions. Two different types of lattice-molecule couplings are examined in the interpretation of the results.
It is shown that the temperature independent bands, identified as vibrational transitions owe their existence to the presence of trace nitrogen impurities in the solidified rare-gas matrices, or concentration effects.

Key Words: Infrared, hydrogen bromide, hydrogen chloride, rare gas matrix, spectrum.

Low temperature speed of sound in single crystal ice, T. M. Proctor, Jr., *J. Acoust. Soc. Am.* **39,** *No. 5, 972–977 (May 1966).*
Only one of the previous measurements of the elastic constants and speed of sound in single-crystal ice-I had been extended below −30 °C. All of the five independent elastic constants have now been measured down to 65 °K. Elastic constant data have been fitted to second-degree polynomials. From these polynomials a 0 °K value for the c_{ij}'s is extracted and a Debye characteristic temperature of 224 °K is calculated. This Debye temperature compares favorably with that previously computed from heat capacity data. No sudden changes in the pseudo-elastic anisotropic factor c_{33}/c_{11} are found to take place at 190 °K as had been previously reported.

Key Words: Elastic constants, lattice dynamics, lattice parameter, single crystal ice, speed of sound, thermodynamic properties.

Measurements of collisional energy transfer between rotational energy levels in CN, K. M. Evenson and H. P. Broida, *J. Chem. Phys.* **44,** *No. 4, 1637–1641 (Feb. 15, 1966).*
A novel microwave optical technique which selectively populated a single rotational level of CN and permits the observation of the redistribution of this population was utilized to measure the rates of collisional energy transfer between rotational energy levels of the $B^2\Sigma$ state of CN.
CN was formed in the $A^2\pi$ state by the addition of CH_2Cl_2 to the afterglow of a nitrogen discharge. The near coincidence of the $K'=4$, $v^2=10$ level of the $A^2\pi$ state with the $K=4$, $v=0$ level of the $B^2\Sigma$ state permits microwave transitions near 10 GHz from the more populated π level to the Σ level. The increased population in the rotational levels neighboring the $K'=4$ level of the $B^2\Sigma$ state was detected by measuring the increased optical emission due to the $B^2\Sigma$ transitions near 3875 Å. Collisional energy transfer was measured over a pressure range from 0.1 to 5 Torr. Rates of energy transfer were measured for rotational level separations from one to ten. It was shown that rotational transitions having changes in the rotation quantum number greater than unity take place with high probability, contrary to the optical selection rule $\Delta K=\pm 1$, and that approximately every collision produces a change in the rotational energy level. The relaxation time for the 4th rotational level was found to be 1.2×10^{-7} (±30%) seconds at pressure of 1 Torr.

Key Words: CN, collisional energy transfer, microwave-optical spectroscopy, rotational levels.

Nonlinear diffusion with recombination in an electron beam excited plasma, E. R. Mosburg, Jr., *Phys. Fluids* **9,** *No. 4, 824–826 (Apr. 1966).*

The radial distributions of electron density and light intensity are calculated from the nonlinear diffusion equations with a recombination term added. Two-body and three-body recombination mechanisms are considered in addition to the intermediate case of collisional-radiative recombination.

Nuclear spin relaxation in liquid hydrogen, C. E. Miller, T. M. Flynn, T. K. Grady, and J. S. Waugh, *Physica* **32,** *No. 2, 244–251 (Feb. 1966).*
The proton longitudinal relaxation time, T_1, has been measured in dilute liquid solutions of *ortho*hydrogen in *para*hydrogen over a range of temperature and composition. Below 1.75% orthohydrogen the temperature dependence of T_1 observed at higher concentration is reversed. This fact is interpreted in terms of an anisotropic intermolecular force which is of longer range for *ortho-ortho* than for *ortho-para* pairs, in keeping with previous interpretations of T_1 in the gaseous state.

Key Words: Cryogenic, liquid hydrogen, nuclear magnetic resonance, nuclear relaxation.

One dimensional solution of the Ginzburg-Landau equations for thin superconducting films, V. D. Arp, R. S. Collier, R. A. Kamper, and H. Meissner, *Phys. Rev.* **145,** *No. 1, 231–236 (May 6, 1966).*
Solutions to the Ginzburg-Landau equations have been obtained for plane films in a longitudinal magnetic field. Only symmetrical one-dimensional solutions were generated, but without restrictive assumptions on κ or ψ. The critical field has been calculated from these solutions as a function of κ and d/λ. Curves are given to show how the behavior of films at the critical field depends on the various parameters involved.
The computer solutions join smoothly onto those derived in the limit $\psi \rightarrow 0$. The limit of validity of these solutions in the face of the vortex solutions of Abrikosov and the asymmetrical solutions of Saint-James and deGennes is determined, and a "phase diagram" in the κ, d plane for all types of solutions is suggested.

Key Words: Ginzburg-Landau theory, magnetic field, superconductor, thin film.

Polycrystalline spin wave theory of ferromagnetic resonance compared with the tilting experiment, A. S. Risley, E. G. Johnson, Jr., and H. E. Bussey, *J. Appl. Phys.* **37,** *No. 2, 656–668 (Feb. 1966).*
Schlömann's spin wave theory of polycrystalline ferromagnetic resonance has been tested in detail using the tilting method reported earlier. Among the quantities measured were the linewdith ΔH, and the maximum value of the imaginary part of the effective susceptibility $(\chi_m'')^{\text{eff}}$. The measurement method is equivalent to measuring asymmetric ($N_x \neq N_y$) ellipsoids and thus, introduces another shape dependence in addition to that due to spin waves. Direct comparison with the symmetric ($N_x = N_y$) form of the theory is inaccurate. A proper comparison can be made in two ways: (1) generalizing the theory to include the $N_x \neq N_y$ case and then using the data directly, (2) transforming the data and then comparing with the $N_x = N_y$ theory. Both comparisons are reported and their equivalence is demonstrated.
It is concluded that Schlömann's theory does not fit the data within the spin wave (SW) manifold. It is suggested that the theory of Sparks may provide a better fit. The difference between coupling models seems to be the basic difference between the two theories. Experimentally and theoretically, ΔH and $(\chi_m'')^{\text{eff}}$ are different quantities. The dispersive effects of spin wave coupling are shown to be the cause of the difference between the theoretical ΔH and $(\chi_m'')^{\text{eff}}$.

Radiation lifetime of the first $^2P_{3/2}$ state of ionized calcium and magnesium by the Hanle effect, W. W. Smith and A. C. Gallagher, *Phys. Rev.* **145,** *No. 1, 26–35 (May 6, 1966).*
The lifetimes of the $Ca^+ 4^2P_{3/2}$ state and $Mg^+ 3^2P_{3/2}$ state have been measured by the Hanle-effect method with optical excitation from the ground states of the ions. The lifetimes are, respectively, $6.72 \pm 0.20 \times 10^{-9}$ sec. and $3.67 \pm 0.18 \times 10^{-9}$ sec. The ions were produced by introducing traces of calcium or magnesium into an argon discharge. Alignment depolarization cross sections, σ, were obtained for the collisional depolarization of the following states of calcium and magnesium due to collisions with argon.

$$\sigma(Ca\,4^1P_1 \text{ state}) = 1.9 \pm 0.3 \times 10^{-14} \text{ cm}^2$$
$$\sigma(Mg\,3^1P_1 \text{ state}) = 1.9 \pm 0.3 \times 10^{-14} \text{ cm}^2$$
$$\sigma(Ca^+ 4^2P_{3/2} \text{ state}) = 1.4 \pm 0.2 \times 10^{-14} \text{ cm}^2$$
$$\sigma(Mg^+ 3^2P_{3/2} \text{ state}) = 1.3 \pm 0.25 \times 10^{-14} \text{ cm}^2.$$

Key Words: $Ca^+ 4^2P_{3/2}$ state, collisional depolarization, Hanle effect, $Mg^+ 3^2P_{3/2}$ state, radiative lifetime.

The soft x-ray spectrum of Ni and comparison with photoemission and ion neutralization results, J. R. Cuthill, A. J. McAlister, and M. L. Williams, *Phys. Letters* **16,** *No. 22, 993–995 (May 30, 1966).*
The soft x-ray $M_{2,3}$ spectrum of Ni has been observed, and now features found. The spectrum agrees well with ion neutralization results on Ni, but disagrees sharply with the density of states deduced from photoemission spectrum of Ni. A double electron photoexcitation process which removes this discrepancy is suggested and shown to fit the available photoemission data on Ni and Cu and Ag as well.

Key Words: Ag, Cu, double electron photoexcitation, Ni, photoemission, soft x-ray spectrum.

Some properties of the long-time values of the probability densities for moderately dense gases, R. A. Piccirelli, *J. Math. Phys.* **7,** *922 (1966).*
It has been argued that for sufficiently large times the n-particle probability densities of a moderately dense, simple gas become time-independent functionals of the one-particle probability densities. Proofs are given for several properties of the power series representation of these functionals. In particular, it is shown that the equilibrium value of the n-particle functional is identical to the usual equilibrium probability density term by term and that the corresponding generalized Boltzmann collision integral vanishes as it should. The two forms of the functional, one due to Bogoliubov and one due to Green and Cohen are shown to be formally identical. It is argued that the higher terms of these two series probably diverge *together.*
In the course of the discussion several new properties of the coefficient operators of the power series for the functional are derived. Moreover, an integral equation for the n-particle functional is derived which may have solutions not representable as functional power series in the one-particle probability density.

Key Words: Long-time-values, moderately dense gases, probability densities.

The Chapman-Enskog solution of the generalized Boltzmann equation, M. S. Green, L. S. Garcia-Colin, and F. Chaos, *Physica* **32,** *450 (1966).*
The generalization of the Chapman-Enskog method is applied to systems of equations which are obtained when Bogolyubov functional assumption is introduced into the BBGKY hierachy. A system of inhomogeneous equations is derived from the solution of which the transport coefficients may be determined.
The kernel of these equations is shown to have different left and right eigen functions with zero eigen values. The method while dependent the Bogolyubov assumption is independent of the assumption of a power series expansion for the transport coefficients.

Key Words: Bogolyubov functional assumption, Chapman-Enskog method, dense gases, equation, generalized Boltzmann, kinetic theory, plasmas, transport properties.

The flow field of a body-stabilized two-dimensional V-flame, F. W. Ruegg and W. W. Dorsey, *Combustion and Flame* **10,** *No. 1, 1–10 (Dec. 1966).*
A two-dimensional, V-shaped flame is simulated by a combination of source and sink sheets of fluid in a general stream. Complex variable theory is used to determine the flow field of the simulated flame. Adjustment of the strength of the sink sheet on the interior symmetry flame axis yields a flame speed that is constant within about one percent along the front. Two 22-degree half-angle flames are calculated. In both cases a portion of the flame front near the

apex of the flame and the sink are found to be enclosed within a body shaped as a flameholder. Actual flames in the calculated approach fields would generate appreciable vorticity in the flame gas, but the calculated field downstream from the simulated flame is irrotational.

Thermodynamics of the rigid-rotor at high temperature, J. E. Kilpatrick, Y. Fukuda, and S. Y. Larsen, *J. Chem. Phys.* **43,** *No. 2, 430–432 (July 1965).*
It is shown that Q_e, the partition function for a rigid-rotor summed over even levels and Q_0, summed over odd levels, have exactly the same asymptotic (power series in $\sigma = h^2/21kT$) expansion. No information as to differences in thermodynamic properties due to spin and statistics can be obtained from this expansion. The exchange partition function, $Q_e - Q_0$, is calculated directly and used to give simple expressions for the differences in thermodynamic properties between the *para*, *ortho*, and equilibrium cases.

Thermophysical properties of metals at cryogenic temperatures, R. L. Powell, *Behavior of Materials at Cryogenic Temperatures, Am. Soc. Testing Mater. Spec. Tech. Publ. No. 387, pp. 134–148 (1966).*
The low temperature thermophysical properties of metals can only be fully understood by utilizing the fundamental concepts of electrons, lattice vibrations, and their interactions. After the introduction, the properties of specific heat and thermal conductivity, are each discussed with the emphasis on understanding the various contributions to the total observed effect. Based on the above discussions, temperature dependencies for each property are given for various representative metals and alloys. The importance of inter-relations between the various thermophysical properties is also noted. With an understanding of basic concepts, inter-relations, and effects of different contributions, one can often make reasonable estimates for the values of the thermophysical properties of new materials or of known materials with different chemical impurities or mechanical or metallurgical treatments. References are given to several good books, review articles and compilations of numerical values. Information is also given on sources of specialized or up-to-date bibliographies and data collections.

Spectral distribution of solar radiation at the earth's surface, D. M. Gates, *Science* **151,** *No. 3710, 523–529 (July 1965).*
The spectral distribution of direct sunlight at the earth's surface at sea level is calculated as a function of the air mass and of aerosol, ozone, and water vapor concentration. A solar constant of 2.0 cal cm^{-2} min^{-1} is used for these calculations. The spectral distribution of sunlight is presented on a wavelength basis and also on a wavenumber basis. For sea level the spectral distributions of skylight and of global radiation incident on a horizontal surface are given. Finally, the variation with altitude of the spectral distribution of direct sunlight incident on a surface perpendicular to the sun's rays is presented.

Other NBS Publications

J. Res. NBS 70B. (Math. and Math. Phys.), No. 4 (Oct.–Dec. 1966), 75 cents.
Dedication of the new NBS laboratories.
A random walk model of chain polymer adsorption at a surface. III. Mean square end-to-end distance. R. J. Rubin.
Abscissas and weights for Gaussian quadrature for $N = 2$ to 100, and $N = 125$, 150, 175, and 200. C. H. Love.
Transverse impact of a linear three-element spring and dashpot model filament: theory. J. C. Smith.
Functions for thermal stress calculation near a transient heat source on a flat surface. S. Jarvis, Jr., and G. Hardy.

Observed phase-front distortion in simulated earth-to-space microwave transmissions, H. B. Janes and M. C. Thompson, Jr., Tech. Note 339 (May 12, 1966), 50 cents. (Formerly Central Radio Propagation Laboratory of the National Bureau of Standards, now Environmental Science Services Administration, Boulder, Colo.)
Hydromagnetic wave propagation near 1c/s in the upper atmosphere and the properties and interpretation of Pc 1 micropulsations, J. A. Dawson, Tech. Note 342 (June 30, 1966), 40 cents. (Formerly Central Radio Propagation Laboratory of the National Bureau of Standards, now Environmental Science Services Administration, Boulder, Colo.)
Analysis of lanolin in soap, F. J. Linnig, Soap Chem. Specialties **XVLL,** No. 7, 55–57 (July 1966).
Analytical applications of microwave spectroscopy, D. R. Lide, Jr., Book, Advances in Analytical Chemistry and Instrumentation **5,** 235–277 (Interscience Publ., New York, N.Y., 1966).
Chemical substructure searching with linear notations, B. A. Marron, G. R. Boltsky, and S. J. Tauber, J. Chem. Doc. **6,** 92–95 (May 1966).
Determination of glycerol in paper, E. L. Graminski and B. W. Forshee, Tappi **49,** No. 7, 324–326 (July 1966).
Electron spin resonance studies of the reaction of water-soluble polymers with hydroxyl radicals, F. Sicilio, M. Dousset, R. E. Florin, and L. A. Wall (Proc. 150th American Chemical Society Meeting, Atlantic City, N.J., Sept. 12–17, 1965), Polymer Preprint **6,** No. 2, 958–964 (Sept. 1965).
Identification of inclusions with the electron probe microanalyzer, K. F. J. Heinrich, Am. Soc. Testing Mater. Spec. Tech. Publ. 393 (Jan. 1966).
Investigation of polymer pyrolysis with thermogravimetry, J. H. Flynn and L. W. Wall (Proc. 150th American Chemical Society Meeting, Atlantic City, N.J., Sept. 12–17, 1965), Polymer Preprint **6,** No. 2, 945–955 (Sept. 1965).
Mass spectrometric study of the reactions of O atoms with NO and NO_2, Erratum, J. T. Herron, J. Chem. Phys. **44,** No. 9, 3645 (May 1966).
Oxidation of asphalt flux with oxides of nitrogen, P. G. Campbell and J. R. Wright, Am. Chem. Soc. Div. Petroleum Chem. **10,** No. 1, 79–89 (Mar. 1965).
Polymerization and pyrolysis of poly-1,2-dihydronaphthalene, L. A. Wall, L. J. Fetters, and S. Straus (Proc. 150th American Chemical Society Meeting, Atlantic City, N.J., Sept. 12–17, 1965), Polymer Preprint **6,** No. 2, 930–939 (Sept. 1965).
Radiation-induced polymerization at high pressure of 3,3,3-trifluoropropene; 4,4,4,3,3-pentafluorobutene-1; and 5,5,5,4,4,3,3-heptafluoropentene-1, D. W. Brown (Proc. 150th American Chemical Society Meeting, Atlantic City, N.J., Sept. 12–17, 1965), Polymer Preprint **6,** No. 2, 965–976 (Sept. 1965).
Status of light-element heat-capacity calorimetry at the National Bureau of Standards: a review of the high-temperature thermodynamics of the $BeO - H_2O$ system, T. B. Douglas, Proc. 4th Meeting Interagency Chemical Rocket Propulsion Group, Working Group on Thermochemistry, Kennedy Space Flight Center, Florida, Mar. 16–17, 1966, I, No. 108, 27 (Chemistry Propulsion Information Agency, Silver Spring, Md., June 1966).
The determination of bound styrene in soluble high styrene-butadiene resins, M. A. Post, J. Paint Tech. Eng. Official Digest **38,** No. 497, 335–342 (June 1966).
The determination of heats of formation of refractory compounds, G. T. Armstrong and E. S. Domalski, Proc. 4th Meeting Interagency Chemical Rocket Propulsion Group, Working Group on Thermochemistry, Kennedy Space Flight Center, Florida, March 16–18, 1966, I, No. 108, 15 (Chemistry Propulsion Information Agency, Silver Spring, Md., June 1966).
The determination of mercury in latex paints and paint films containing mercury fungicides, H. W. Berger, J. Paint Technol. **38,** No. 498, 371–376 (July 1966).
The evolution of the accuracy of isotopic analysis by thermal ionization from 2% to 0.2%, W. R. Shields (Proc. Symp. Nuclear Materials Management, IAEA, Vienna, Austria, Aug. 30–Sept. 3, 1965), Book, Nuclear Materials Management, pp. 737–746 (Intern. Atomic Energy Agency, Vienna, Austria, Feb. 1966).
The monomer-polymer equilibrium of alpha-trideuteromethyl-beta, beta-dideuterostyrene, L. J. Fetters and L. A. Wall (Proc. 150th American Chemical Society Meeting, Atlantic City, N.J., Sept. 12–17, 1965), Polymer Preprint **6,** No. 2, 899–903 (Sept. 1965).
The radiation induced polymerization of hexafluoropropylene at high temperature and pressure, R. E. Lowry, D. W. Brown, and L. A. Wall (Proc. 150th American Chemical Society Meeting, Atlantic City, N.J., Sept. 12–17, 1965), Polymer Preprint **6,** No. 2, 977–984 (Sept. 1965).
Thermolytic chain scission of linear polyethylene and an ethylene-propylene copolymer, H. Yu and L. A. Wall (Proc. 150th American Chemical Society Meeting, Atlantic City, N.J., Sept. 12–17, 1965), Polymer Preprint **6,** No. 2, 940–944 (Sept. 1965).
Vacuum-ultraviolet photolysis of paraffin hydrocarbons, J. R. McNesby, Book, Chemical and Biological Actions of Radiation **IX,** ch. 2, 39–67 (Masson and Co., Editors and Publ., Paris, France, 1966).

Advances in cryogenic engineering, Book, K. D. Timmerhaus, editor, Proc. 1964 Cryogenic Engineering Conf., University of Pennsylvania, Philadelphia, Pa., Aug. 18–21, 1964, 10, Pt. 1 (Plenum Press, Inc., New York, N.Y., 1965).

A cold moderator refrigerator incorporating a high-speed turbine expander, R. O. Voth, M. T. Norton, and W. A. Wilson (Proc. 1965 Cryogenic Engineering Conf., University of Pennsylvania, Philadelphia, Pa., Aug. 18–24, 1964), Book, Advances in Cryogenic Engineering **11**, 126–138 (Plenum Press Inc., New York, N.Y., 1966).

A new near-zone electric field-strength meter, F. M. Greene (Proc. 8th IEEE Symp. Electromagnetic Compatibility, San Francisco, Calif., July 11–13, 1966), Symposium Digest New Ideas for Electromagnetic Compatibility, 1966.

A proposal for a supplement to the patent system, S. Henig, Design News Mag. **21**, No. 1, 84–89 (Jan. 5, 1966).

Bond with reinforcing steel, D. Watstein, ASTM Significance of Tests of Concrete and Concrete Making Materials, Am. Soc. Testing Mater. Spec. Tech. Publ. **169A**, pp. 239–245 (July 1966).

Chemical admixtures, B. E. Foster, ASTM Significance of Tests of Concrete and Concrete Making Materials, Am. Soc. Testing Mater. Spec. Tech. Publ. **169A**, pp. 556–564 (July 1966).

Comparative study of forced convection boiling heat transfer correlations for cryogenic fluids, P. J. Giarratano and R. V. Smith (Proc. 1965 Cryogenic Eng. Conf., University of Pennsylvania, Philadelphia, Pa., Aug. 18–24, 1964), Book, Advances in Cryogenic Engineering **11**, 492–506 (Plenum Press Inc., New York, N.Y., 1966).

Floor coverings, T. H. Boone, Book, Building Construction Handbook, 2d edition, ed. F. S. Merritt, Sec. 13, pp. 13–1 – 13–8 (1965).

Free radical microwave absorption meter, H. E. Radford, Rev. Sci. Instr. **37**, No. 6, 790–792 (June 1966).

Instrumentation and measurements, H. E. Bussey and J. E. Gray, Digest of Literature on Dielectrics **28**, ch. I., 1–31 (1964); Natl. Acad. Sci.–Natl. Res. Council Publ. 1324 (Natl. Acad. Sci.–Natl. Res. Council, Washington, D.C., 1965).

International advances in cryogenic engineering, Book, K. D. Timmerhaus, Editor, Proc. 1964 Cryogenic Engineering Conf., Univ. Pennsylvania, Philadelphia, Pa., Aug. 18–21, 1964, 10, Pt. 2 (Plenum Press, Inc., New York, N.Y., 1965).

Liquid-solid mixtures of hydrogen near the triple point, D. B. Mann, P. R. Ludtke, C. F. Sindt, and D. B. Chelton, (Proc. 1965 Cryogenic Engineering Conf., University of Pennsylvania, Philadelphia, Pa., Aug. 18–24, 1964), Book, Advances in Cryogenic Engineering 11, 207–217 (Plenum Press Inc., New York, N.Y., 1966).

Message from outgoing editor, R. W. Beatty, IEEE Trans. Microwave Theory Tech. **MTT-14**, No. 4, 170 (Apr. 1966).

Metals for use in orthopedics, S. J. Rosenberg, Book, Orothotics Etcetra, ed. S. Licht, 9, 77–94 (E. Licht Publ., New Haven, Conn., 1966).

Resistance to weathering, H. T. Arni, ASTM Significance of Tests of Concrete and Concrete Making Materials, Am. Soc. Testing Mater. Spec. Tech. Publ. 169A, pp. 261–274 (1966).

Voluntary product standards – what they mean to the consumer, M. Lonie, J. Home Econ. **58**, No. 1, 22 (Jan. 1966).

New method and problems in combinatorial optimization, A. J. Goldman, Washington Oper. Res. Council Newsletter **5**, No. 8, 4–8 (Apr. 1966).

On the complex structure of the universe, E. H. Brown, J. Math. Phys. **7**, No. 3, 417–425 (Mar. 1966).

A superconducting liquid-level sensor for slush hydrogen use, B. L. Knight, K. D. Timmerhaus, and T. M. Flynn, (Proc. 1965 Cryogenic Engineering Conf., University of Pennsylvania, Philadelphia, Pa., Aug. 18–24, 1964), Book, Advances in Cryogenic Engineering 11, 218–222 (Plenum Press Inc., New York, N.Y., 1966).

Effects of long-term stability on the definition and measurement of short-term stability, J. A. Barnes and D. W. Allan, Proc. IEEE–NASA Symp. Definition and Measurement of Short-Term Frequency Stability, NASA Spec. Publ. No. 80, pp. 119–123 (Nov. 23–24, 1964).

LF–VLF frequency and time services of the National Bureau of Standards, D. H. Andrews, IEEE Trans. Instr. Meas. **IM-14**, No. 4, 233–237 (Dec. 1965).

Quantity control – A tool of industry, and arm of government, M. W. Jensen, Proc. Annual Conf. Society for the Advancement of Food Service Research, Washington, D.C. (Apr. 18, 1966).

Remote positioner for rotary switches, S. B. Lang, and A. M. Gray, Rev. Sci. Instr. **37**, No. 6, 799–801 (June 1966).

Analyzing liquid H_2 with NMR, C. E. Miller, W. J. Alspach, and T. M. Flynn, Cryogenic Engr. News **1**, No. 8, 66 (June 1966).

Angular dependence of the one-phonon-nuclear quadrupole interactions, R. J. Mahler, J. Phys. Chem. Solids **27**, 871–879 (1966).

A suggested experiment to measure part of the transverse electromagnetic mass of the electron, E. A. Power, Proc. Roy. Soc. (London) **292**, No. 1430, 424–432 (May 31, 1966).

Brillouin scattering in liquids at 4880Å, S. L. Shapiro, M. McClintock, D. A. Jennings, and R. L. Barger, IEEE Quantum Electronics **QE-2**, No. 5, 89–93 (May 1966).

Calculated slant-path absorption and distribution of atmospheric water vapor, R. F. Calfee and D. M. Gates, Appl. Opt. **5**, No. 2, 287–292 (Feb. 1966).

Comparison of the Lennard-Jones, Exp: 6, and Kihara potential functions from viscosity data of dilute argon, H. J. M. Halney, J. Chem. Phys. **44**, No. 11, 4219–4222 (June 1966).

Direct ratio readings from a universal ratio set, D. Ramaley and J. F. Schafer, Instr. Control Systems **39**, 73–74 (Jan. 1966).

Dielectric relaxation in molecular crystals: multiple site models, J. D. Hoffman, Book, Molecular relaxation processes, Chemical Society Spec. Publ. **20**, 47–60 (The Chemical Society and Academic Press, New York, N.Y., 1966).

Electric quadrupole transition in the $A^1\pi \leftarrow X^1\Sigma^+$ system of CO, J. D. Simmons and S. G. Tilford, J. Chem. Phys. **44**, No. 11, 4145–4147 (June 1966).

Fundamentals of ultrasonics, M. Greenspan, J. Acoust. Soc. Am. **37**, No. 1, 158–159 (July 1965).

Infrasonic waves from aurorae, K. Maeda and J. M. Young, Nature **207**, No. 4994, 279–281 (July 1965).

Ion movilities in helium, E. C. Beaty, J. C. Browne, and A. Dalgarno, Phys. Rev. Letters **16**, No. 17, 723–724 (Apr. 1966).

Low-temperature phase transformations, R. P. Reed and J. F. Breedis, Behavior of Materials at Cryogenic Temperatures, Am. Soc. Testing Mater. Spec. Tech. Publ. No. 387, pp. 60–132 (1966).

Magnetic core permeability measurement techniques, R. D. Harrington and A. L. Rasmussen, Proc. Magnetic Core Conf., 7, 11–24 (1965).

Measurements of the viscosity of parahydrogen, D. E. Diller, (Proc. IXth Intern. Conf. Low Temperature Physics, Columbus, Ohio, Aug. 31-Sept. 4, 1964), Book, Low Temperature Physics, LT9, pt. B, pp. 1227–1229 (Plenum Press Inc., New York, N.Y., 1965).

Physics of the *D* region at high latitudes, G. C. Reid, (Proc. NATO Advanced Study Institute, Finse, Norway, April 1965), Book, Electron Density Profiles in Ionosphere and Exosphere, ed. J. Frihagen, pp. 17–26 (North Holland Publ. Co., Amsterdam, The Netherlands, 1966).

Saturation effects in the sensitized fluorescence of CaF_2(Ce, Mn), B. L. Danielson, Phys. Rev. **142**, No. 1, 228–230 (Feb. 4, 1966).

Summary of recent determinations of the ultrasonic velocity in fluid parahydrogen, B. A. Younglove, (Proc. IXth Intern. Conf. Low Temperature Physics, Columbus, Ohio, Aug. 31-Sept. 4, 1964), Book, Low Temperature Physics LT9, pt. B., pp. 1223–1226 (Plenum Press Inc., New York, N.Y., 1965).

The role of hydrogen in the stress-corrosion cracking of low carbon steel in a nitrate solution, H. L. Logan and H. T. Yolken, Proc. 2d Intern. Congress Metallic Corrosion, New York, N.Y., March 1963, pp. 109 (Natl. Assoc. Corrosion Engr., Houston, Texas, 1966).

The spheroidal method in the theory of the orbit of an artificial satellite, J. P. Vinti, Proc. Symp. Celestial Mechanics, Mathematische Forschungsinstitut, Oberwolfach, Germany, March 1964, pp. 97–111 (1964).

The theory of chromospheric spectrum, J. T. Jefferies, Book, The Solar Spectrum, ed. C. DeJager, pp. 131–150 (D. Reidel Publ. Co., Dordrecht, The Netherlands, 1965).

Vacuum ultraviolet spectrum of neutral silicon, V. Kaufman, L. J. Radziemski, Jr., and K. L. Andres, J. Opt. Soc. Am. 56, No. 7, 911–915 (July 1966).

Zero-point energy and Lamb shift, E. A. Power, Am. J. Phys. **34**, No. 6, 516–518 (June 1966).

Computed performance of moderate size, super-gain, end-fire antenna arrays, C. O. Stearns, IEEE Trans. Ant. Prop. **AP-14**, No. 2, 241–242 (Mar. 1966).

Electron precipitation and ionospheric radio absorption in the auroral zones, K. L. Hargreaves and R. D. Sharp, Planetary Space Sci. **13**, 1171–1183 (Dec. 1965).

Evidence of long-period acoustic-gravity waves launched into the *F* region by the Alaskan earthquake of March 28, 1964, R. V. Row, J. Geophys. Res. Letter **71**, 343–345 (Jan. 1966).

International URSIGRAM and world days service "report on activities in 1964," A. H. Shapley, URSI Info. Bull. No. 150, pp. 43–55 (May 1965).

Ionospheric effects of particles, G. C. Reid, Proc. COSPAR Polar Cap Panel Symp., Alpach, Austria, 1964, pp. 221–231 (Academic Press Inc., New York, N.Y., 1965).

Linear tuning of a microwave cavity, M. J. Vetter, IEEE Trans. Microwave Theory Tech. **MTT-13,** No. 6, 880 (Nov. 1965).

Observations of ionospheric irregularities and plasma resonances by the fixed-frequency topside sounder satellite, W. Calvert, (Proc. NATO Advanced Study Institute, Finse, Norway, April 1965), Book, Electron Density Profiles in Ionosphere and Exosphere, ed. J. Frihagen, pp. 281–298 (North Holland Publ. Co., Amsterdam, The Netherlands, 1966).

Observations of the equatorial ionosphere using incoherent backscatter, D. T. Farley, (Proc. NATO Advanced Study Institute, Finse, Norway, April 1965), Book, Electron Density Profiles in Ionosphere and Exosphere, ed. J. Frihagen, pp. 446–469 (North Holland Publ. Co., Amsterdam, The Netherlands, 1966).

Slow fluctuations between conjugate points in the auroral absorption of cosmic noise, H. J. A. Chivers and J. K. Hargreaves, J. Atmos. Terrest. Phys. **28,** 337–342 (1966).

SPACEWARN—an international mechanism for rapid distribution of information on satellites and space probes, A. H. Shapley, COSPAR Info. Bull. No. 24, pp. 30–55 (July 1965).

Statistics of atomic frequency standards, D. W. Allan, Proc. **IEEE 54,** No. 2, 221–230 (Feb. 1966).

Swept-frequency antenna gain measurements, R. G. FitzGerrell, IEEE Trans. Ant. Prop. **AP-14,** No. 2, 173–178 (Mar. 1966).

The important atmospheric processes in the *D* region, G. C. Reid, Proc. COSPAR Polar Cap Panel, Alpach, Austria, 1964, pp. 15–19 (Academic Press Inc., New York, N.Y., 1965).

"Winter anomaly" in ionospheric absorption and stratospheric warnings, A. H. Shapley and W. J. G. Beymon, Nature **206,** 1242–1243 (*June* 1965)..

**Publications for which a price is indicated are available by purchase from the Superintendent of Documents, U.S. Government Printing Office, Washington, D.C. 20402 (Foreign postage, one-fourth additional). The NBS non-periodical series are also available from the Clearinghouse for Federal Scientific and Technical Information, Springfield, Va. 22151. Reprints from outside journals and the NBS Journal of Research may often be obtained directly from the authors.*

U.S. GOVERNMENT PRINTING OFFICE : 1967 OL—236-431

UNITED STATES
GOVERNMENT PRINTING OFFICE
DIVISION OF PUBLIC DOCUMENTS
WASHINGTON, D.C. 20402

OFFICIAL BUSINESS

POSTAGE AND FEES PAID
U.S. GOVERNMENT PRINTING OFFICE

JOURNAL OF RESEARCH of the National Bureau of Standards
A. Physics and Chemistry

Vol. 71A, No. 1 January–February 1967

Contents

	Page
Dedication of the new NBS laboratories.	i
Electric fields produced in cubic crystals by point defects. A. D. Franklin and D. J. Sparks.	1
Heat capacity and thermodynamic properties of beryllium 1:3-aluminate, $BeO \cdot 3Al_2O_3$, from 15 to 390 °K. George T. Furukawa and William G. Saba.	3
Dissociation constant of m-nitrophenol in 50 wt percent methanol-water solvent from 25 to 40 °C and related medium effects. Barry J. Steel, R. A. Robinson, and Roger G. Bates.	9
On the calculation of moments of molecular weight distribution from sedimentation equilibrium data. Irwin H. Billick, Michael Schulz, and George H. Weiss.	13
The far infrared spectrum of vulcanized natural rubber. James E. Stewart and Frederic J. Linnig.	19
Irradiation of dextran and its aqueous solutions with cobalt-60 gamma rays. Joseph H. Flynn, Leo A. Wall, and William L. Morrow.	25
Synthesis of poly-p-oxyperfluorobenzylene and related polymers. A novel synthesis of the monomer 2,3,5,6-tetrafluoro-4-trifluoromethylphenol Joseph M. Antonucci and Leo A. Wall	33
Preparation, purity, and homogeneity of NBS standard samples 705 and 706, polystyrene. D. McIntyre.	43
Large-scale, preparative paper chromatography. Harriet L. Frush.	49
Infrared absorption spectra of some aldofuranoid, aldopyranoid, and acyclic 1-acylamido derivatives of sugars. R. Stuart Tipson, Alberto S. Cerezo, Venancio Deulofeu, and Alex Cohen.	53
Publications of the National Bureau of Standards.	81

Library of Congress Catalog Card Number: 62–37059

For sale by the Superintendent of Documents, U.S. Government Printing Office, Washington, D.C. 20402. Price $1.00 (single copy).
Subscription price: $5 a year; $1.00 additional for foreign mailing.
UNITED STATES GOVERNMENT PRINTING OFFICE, WASHINGTON : 1967